

## Durham E-Theses

---

*Some studies of the interactions of aromatic  
nitro-compounds with nucleophiles*

Michael J. Willison

### How to cite:

---

Willison, Michael J. (1975) Some studies of the interactions of aromatic nitro-compounds with nucleophiles. Doctoral thesis, Durham University.

### Use policy

---

The full-text may be used and/or reproduced, and given to third parties in any format or medium, without prior permission or charge, for personal research or study, educational, or not-for-profit purposes provided that:

- a full bibliographic reference is made to the original source
- a <https://etheses.durham.ac.uk/id/eprint/8283/> is made to the metadata record in Durham E-Theses
- the full-text is not changed in any way

The full-text must not be sold in any format or medium without the formal permission of the copyright holders.

Please consult the [full Durham E-Theses policy](#) for further details.

SOME STUDIES OF THE INTERACTIONS  
OF AROMATIC NITRO-COMPOUNDS WITH NUCLEOPHILES

by

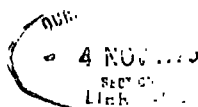
MICHAEL J. WILLISON

B.Sc. (Dunelm)

Van Mildert College

A thesis submitted for the degree of Doctor of  
Philosophy in the University of Durham

September 1975



### ACKNOWLEDGEMENTS

I would like to express sincere thanks to my supervisor, Dr. M.R. Crampton, for his constant enthusiasm and inspiration throughout the course of the research and in preparing this thesis.

My thanks are also due to many of the technical staff of the department without whose help some of the work would not have been possible.

I wish also to thank the Science Research Council for the provision of a studentship.

Finally, may I thank Mrs. Edna McGauley for typing this thesis.

MEMORANDUM

The work in this thesis was carried out in the Chemistry Laboratories of the University of Durham between October 1972 and September 1975. This work has not been submitted for any other degree and is the original work of the author except where acknowledged by reference.

## ABSTRACT

The interactions of some aromatic nitro-compounds with nucleophiles in protic solvents and in protic-dipolar aprotic solvent mixtures have been investigated using the techniques of proton magnetic resonance and visible spectroscopy and stopped-flow spectrophotometry.

The rates of reaction (nucleophilic reactivities) of a series of substituted thiophenoxide ions with 1-chloro-2,4-dinitrobenzene in 95/5 (v/v) ethanol-water, determined by a stopped-flow spectrophotometric method, correlate better with their carbon basicities than with their proton basicities.

In methanol 4-methoxy-3,5-dinitrobenzaldehyde is in equilibrium with its hemiacetal formed by solvent addition to the carbonyl function of the aldehyde group, the equilibrium constant for hemiacetal formation (= 8) being obtained from p.m.r. measurements. In the presence of methoxide ions Meisenheimer complex formation occurs by base addition to the parent aldehyde. Kinetic and equilibrium data are reported for complex formation in methanol. In dimethyl sulphoxide there is straightforward formation of Meisenheimer complex.

The formation of 1:2 adducts from 1-X-2,4,6-trinitrobenzenes (X = OMe, OH, NH<sub>2</sub>, NHMe, NMe<sub>2</sub>) and sodium sulphite in water is characterised by only one relaxation time. P.m.r. measurements also indicate the existence of one isomer of the 1:2 adduct at equilibrium. However when X = H such measurements reveal the presence of both cis- and trans-isomers.

Ring-activated glycol ethers cyclise in the presence of aqueous base to give spiro-complexes. Equilibrium and kinetic parameters for complex formation and decomposition are much higher than the corresponding values for their non-cyclic analogues. The spiro-complexes derived from 1-(2-hydroxyethoxy)-2,4,6-trinitrobenzene and -2,4-dinitronaphthalene undergo general acid catalysed decomposition. On going from spiro-complexes which contain 5- to those which contain 6- and 7-membered dioxolan rings there is a dramatic decrease in complex stability.

Equilibrium and kinetic data have been obtained for the spiro-complex derived from 1-(2-mercaptothioethoxy)-2,4,6-trinitrobenzene and are compared with data for the corresponding di-oxy complex. P.m.r. spectroscopic and stopped-flow spectrophotometric evidence has been obtained for the cyclisation in basic media of 1-(2-hydroxythioethoxy)-2,4,6-trinitrobenzene which subsequently decomposes to picrate and ethylene sulphide.

## PUBLICATIONS

Some parts of the work described in this thesis have been the subject of the following publications:

1.  $^1\text{H}$  Nuclear Magnetic Resonance Evidence for cis-trans-Isomers in the  $\text{C}_6\text{H}_3(\text{NO}_2)_3 \cdot (\text{SO}_3^{2-})_2$  Adduct by M.R. Crampton and M.J. Willison, Chem. Commun., 1973, 215.
2. Some Studies of Substituent Effects on the Nucleophilic Reactivities of Thiophenoxide Ions by M.R. Crampton and M.J. Willison, J.C.S. Perkin II, 1974, 238.
3. The Stabilities of Meisenheimer Complexes. Part VII. Adducts from 4-Methoxy-3,5-dinitrobenzaldehyde by M.R. Crampton, M.A. El Ghariani and M.J. Willison, J.C.S. Perkin II, 1974, 441.
4. The Stabilities of Meisenheimer Complexes. Part VIII. Equilibrium and Kinetic Data for Spiro-complex Formation in Water by M.R. Crampton and M.J. Willison, J.C.S. Perkin II, 1974, 1681.
5. The Stabilities of Meisenheimer Complexes. Part IX. The General Acid Catalysed Ring Opening of Spiro-complexes by M.R. Crampton and M.J. Willison, J.C.S. Perkin II, 1974, 1686
6. The Stabilities of Meisenheimer Complexes. Part XI. The Effects of Ring-size on Spiro-complex Formation by M.R. Crampton and M.J. Willison, J.C.S. Perkin II, in the press.

## CONTENTS

	<u>Page</u>
 <u>CHAPTER 1 - A SURVEY OF THE INTERACTION OF ELECTRON-DEFICIENT</u> <u>AROMATICS WITH BASES</u>	
General Introduction	1
Structural Studies of Meisenheimer Complexes	5
Experimental techniques	5
Complexes derived from oxygen bases	5
(i) Alkoxide ions	5
(ii) Hydroxide ions	17
Complexes derived from carbon bases	19
Complexes derived from nitrogen bases	24
Complexes derived from sulphur bases	26
The Stability of Meisenheimer Complexes	28
(i) Nature of the parent compound	29
(ii) Variation of reactivity with attacking nucleophile	33
(iii) Solvent effects	35
(iv) Micellar and cation effects	37
 <u>CHAPTER 2 - EXPERIMENTAL</u>	
Solution and Preparation of Substrates	39
Spectroscopic Techniques	47
 <u>CHAPTER 3 - A STOPPED-FLOW KINETIC STUDY OF THE REACTION OF SUBSTITUTED</u> <u>THIOPHENOXIDE IONS WITH 1-CHLORO-2,4-DINITROBENZENE -</u> <u>CORRELATION OF THE RATES WITH PROTON AND CARBON BASICITIES</u>	
Introduction	53
Experimental	55
Results and Discussion	56

	<u>Page</u>
<u>CHAPTER 4 - AN EQUILIBRIUM AND KINETIC STUDY OF METHOXIDE ADDITION</u>	
<u>TO AN ACTIVATED ANISOLE CONTAINING AN ALDEHYDE GROUP</u>	
Introduction	63
Experimental	
P.m.r. measurements	64
Visible spectral measurements	64
Results and Discussion	
P.m.r. spectra	66
Visible spectra	68
Equilibrium constants	70
Kinetic measurements	78
<u>CHAPTER 5 - A KINETIC AND P.M.R. STUDY OF THE INTERACTION OF 1-X-2,4,6-</u>	
<u>TRINITROBENZENES WITH SODIUM SULPHITE IN WATER</u>	
Introduction	81
Experimental	
P.m.r. measurements	82
Kinetic measurements	83
Results and Discussion	
P.m.r. spectra	83
(i) 1,3,5-Trinitrobenzene	83
(ii) 2,4,6-Trinitroanisole	85
(iii) N,N-Dimethylpicramide	86
(iv) N-Methylpicramide	86
(v) Picramide	86
(vi) Picric acid	87
Kinetic measurements	87

	<u>Page</u>
<u>CHAPTER 6 - EQUILIBRIUM AND KINETIC STUDIES ON SPIRO-COMPLEX</u>	
<u>FORMATION IN WATER</u>	
Introduction	99
Experimental	100
Results	101
Spiro-complex formation	101
Formation of hydroxide adducts from spiro-complex	102
(i) 1-(2-Hydroxyethoxy)-2,4-dinitronaphthalene	103
(ii) 1-(2-Hydroxyethoxy)-2,4,6-trinitrobenzene	106
(iii) 1-(2-Hydroxyethoxy)-2,6-dinitrobenzene	110
(iv) 1-(2-Hydroxyethoxy)-2,4-dinitrobenzene	114
Discussion	116
Formation of higher complexes	119
<u>CHAPTER 7 - THE GENERAL ACID CATALYSED RING OPENING OF SPIRO-COMPLEXES</u>	
Introduction	122
Experimental	123
Results	123
Discussion	128
Comparison with dialkoxy-Meisenheimer complexes	131
<u>CHAPTER 8 - THE EFFECT OF RING-SIZE ON SPIRO-COMPLEX FORMATION</u>	
Introduction	135
Experimental	135

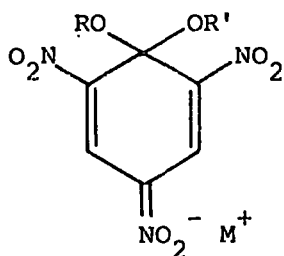
	<u>Page</u>
Results and Discussion	136
P.m.r. spectra	137
Kinetic and equilibrium data	140
Evidence for spiro-complex formation in water	147
Effect of ring-size on spiro-complex formation	149
 <u>CHAPTER 9 - THIO-ANALOGUES OF SPIRO-COMPLEXES</u>	
Introduction	151
A. 1-(2-Mercapthoethoxy)-2,4,6-trinitrobenzene	152
Experimental	152
Results and discussion	152
Comparison with dioxygen analogue	157
B. 1-(2-Hydroxythioethoxy)-2,4,6-trinitrobenzene	160
Experimental	160
Results and discussion	161
1-(2-Hydroxythioethoxy)-2,4-dinitrobenzene	171
 <u>REFERENCES</u>	 176

CHAPTER 1

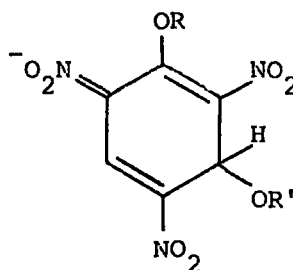
A SURVEY OF THE INTERACTION OF ELECTRON-DEFICIENT AROMATICS WITH BASES

GENERAL INTRODUCTION

The production of brightly coloured solutions by electron-deficient aromatics in basic media was noticed as early as 1882.<sup>1</sup> It was the work of Jackson and Gazzolo<sup>2</sup> in 1900 which resulted in the postulation of the quinoid structure (1.1)



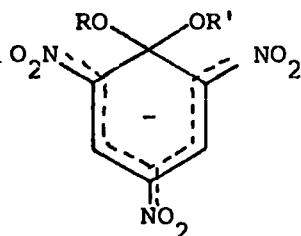
(1.1)



(1.2)

for the products obtained from the reaction of picryl ethers with alkoxide ions. Shortly afterwards chemical evidence for this was presented by Meisenheimer<sup>3</sup> when he obtained the same product from reaction of 2,4,6-trinitroanisole with potassium ethoxide and 2,4,6-trinitrophenetole with potassium methoxide. Thus the possible alternatives of addition at a nitro group or at an unsubstituted ring carbon atom to give (1.2) were discounted.

Considerable evidence has been advanced over recent years in support of the original assignment though it is often now represented as (1.3) with the negative

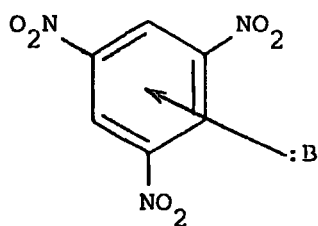


(1.3)

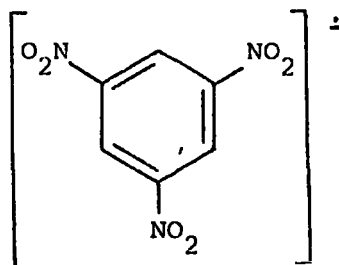
charge delocalised. However the nitro group para to the site of addition, as will be seen later, has been shown to be important with respect to charge delocalisation.

Since the early work of Jackson and Gazzolo, 'Meisenheimer complexes', or  $\sigma$ -complexes as they are now generally known, have been the subject of intensive research especially over the last ten-fifteen years. Aspects such as structure, stability and their role as intermediates in nucleophilic aromatic substitution reactions have been widely studied. Thus a wealth of literature now exists on the subject and a number of excellent reviews have been written.<sup>4-10</sup> It is therefore unnecessary to give a comprehensive survey of the literature in this introduction. However salient features and points of interest in the field will be mentioned. The discussion will be divided into two main sections: structural investigations and adduct stability.

Before beginning, perhaps a brief mention should be made of other possible interactions,<sup>5</sup> apart from  $\sigma$ -complex formation, of activated aromatic compounds with bases. One possibility is either partial electron transfer from the base to the aromatic nucleus giving a  $\pi$ -complex (1.4) (sometimes referred to as a 'charge-transfer' complex<sup>11</sup>) or complete transfer of an electron giving a radical

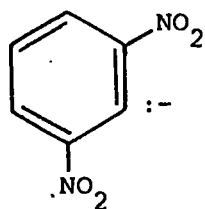


(1.4)

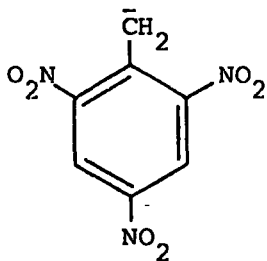


(1.5)

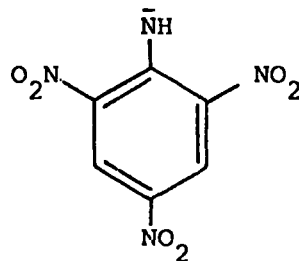
anion (1.5). Alternatively proton abstraction from the ring may occur yielding an aryl carbanion (1.6) or from the side chain as in 2,4,6-trinitrotoluene or



(1.6)



(1.7)

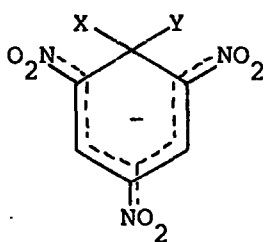


(1.8)

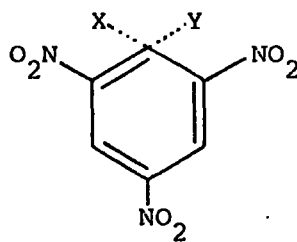
2,4,6-trinitroaniline giving anions (1.7) and (1.8). However evidence suggests<sup>12,13</sup>

that the concentrations of species (1.4), (1.5) and (1.6) are small compared with the concentration of complex (1.3).

Nucleophilic aromatic substitution will occur if the parent compound contains a labile substituent, such as a halogen. Many studies have been made and the subject has been extensively reviewed.<sup>14-19</sup> It has been clearly established that substitutions in suitably activated aromatic substrates proceed via a two-stage addition-elimination mechanism involving a discrete intermediate<sup>14,15</sup> (1.9) as opposed to a synchronous  $S_N2$ -type mechanism involving a transition



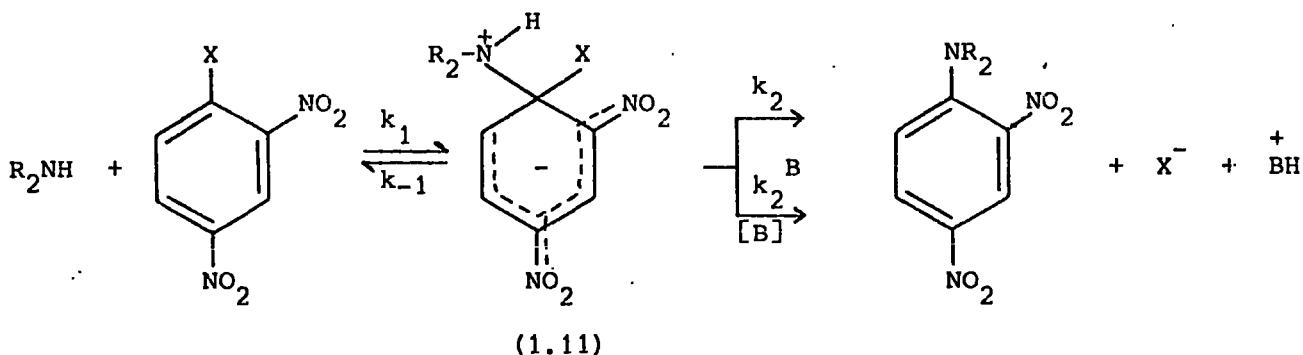
(1.9)



(1.10)

state (1.10) where aromaticity in the ring is retained.<sup>20-22</sup>

The existence of the two-step mechanism has been demonstrated in the reaction



(1.11)

of 1-X-2,4-dinitrobenzenes with secondary amines. Evidence in support of the above scheme is as follows:

(i) For a series of substituents ( $X = \text{Cl, Br, SO}_2\text{Ph, OC}_6\text{H}_4\text{NO}_2(\text{p})$ ) the observed rates are all within a factor of five of one another.<sup>15</sup> This cannot be rationalised by a one-step mechanism but can be explained in terms of the two stage mechanism if  $k_2 \gg k_{-1}$ .

(ii) General base catalysis is often observed especially in the case where  $X = \text{F}$  (poor leaving group). Removal of the amino proton from (1.11) renders it

more likely to decompose to products rather than revert to reactants since  $R_2\bar{N}$  is a poorer leaving group than  $R_2NH$ .

## STRUCTURAL STUDIES OF MEISENHEIMER COMPLEXES

### Experimental techniques

Several spectroscopic and crystallographic techniques have been used in the study of anionic  $\sigma$ -complexes.

The infrared spectra of the crystalline salts obtained from 2,4,6-trinitroanisole and various alkoxides were extensively studied by Foster and Hammick<sup>23</sup> and later by Dyall.<sup>24</sup> The spectra indicated a lowering of the N-O stretching frequencies and this is consistent with increased negative charge on the nitro groups. Also bands were observed, not present in the spectra of the parent ethers, which corresponded with the spectra of ketals,<sup>25</sup> as would be expected from the fully covalent structure (1.3) but not from the charge-transfer complex (1.4).

As a result of the intense colours produced by nitro-aromatics in basic solution, visible spectroscopy has proved a useful and convenient tool in both kinetic and equilibrium measurements. Foster<sup>26</sup> obtained the visible spectrum of the product from potassium methoxide and 2,4,6-trinitrophenetole. The same spectrum was produced from 2,4,6-trinitroanisole and potassium ethoxide. This result was used as evidence<sup>26,27</sup> for the presence of the same species. However, more extensive studies<sup>28</sup> later revealed that the visible spectra of a variety of dialkoxy complexes (1.3;  $R = R'$  and  $R \neq R'$ ) have virtually identical spectra with two maxima in the 400-800 nm region.

Crystallographic studies by Destro<sup>29-31</sup> and Ueda<sup>32</sup> independently have been more conclusive. Using picryl ether-alkoxide complexes (1.3;  $R = R' = \text{Me}$ ,  $R = R' = \text{Et}$ ) they showed that alkoxy groups in the complex were equivalent and that the  $\text{RO-C}_1\text{-OR}'$  plane is orthogonal to the benzene ring. The  $\text{C}_6\text{-C}_1\text{-C}_2$  bond angle was found to be  $109^\circ$ , very close to the tetrahedral bond angle required for  $\text{sp}^3$  hybridisation. Despite this, the benzene ring was very nearly planar. In addition, the measurements revealed that the  $\text{C}_4\text{-N}$  bond distance is significantly shorter than the  $\text{C}_1\text{-N}$  and  $\text{C}_6\text{-N}$  bond lengths, indicating that most

of the negative charge resides on the nitro group para to the site of alkoxide group addition. Thus Meisenheimer's original postulation of (1.1) is possibly a close representation of the charge distribution.

Perhaps the most convincing spectroscopic technique which has been used in the study of Meisenheimer complexes is n.m.r. spectroscopy. Ever since Crampton and Gold<sup>33</sup> obtained the <sup>1</sup>H n.m.r. (p.m.r.) spectra of solutions of 2,4,6-trinitroanisole and 1,3,5-trinitrobenzene with potassium methoxide, the technique has been extensively used to provide the most direct and often unambiguous evidence for the existence and structure of anionic  $\sigma$ -complexes.

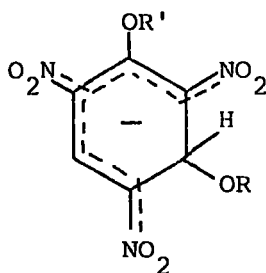
The remainder of this section will be devoted to some examples of the use of spectroscopic methods in the structural studies of activated aromatic compounds with a variety of nucleophiles, most attention being given to complexes derived from alkoxides.

#### Complexes derived from oxygen bases

##### (i) Alkoxide ions

Crampton and Gold<sup>33</sup> obtained the p.m.r. spectrum of the complex produced from 2,4,6-trinitroanisole and potassium methoxide. The parent ether dissolved in dimethyl sulphoxide (DMSO) showed two bands (relative intensity 2:3) at  $\delta$ 9.07 (ring protons) and 4.07 p.p.m. (methoxyl protons) relative to internal tetramethylsilane (TMS). The solid complex dissolved in DMSO again showed two bands but shifted upfield from the parent anisole at  $\delta$ 8.64 and 3.03 p.p.m. (relative intensity 2:6). The singlet due to the methoxyl protons indicates their equivalence in the complex and is evidence for structure (1.3; R = R' = Me). The upfield shift of ring proton bands is generally observed on complexation, and would be expected, a priori, to result from the delocalised negative charge in the adduct. However it has been ascribed to a reduction in the ring current since the electron density in the ring has been shown<sup>34</sup> to be less in the complex than in the substrate, a conclusion also reached by Destro et al<sup>31</sup> from the structural parameters of the ethyl picrate-ethoxide complex. More sophisticated calculations<sup>35</sup> have in fact predicted a negative charge density in the ring.

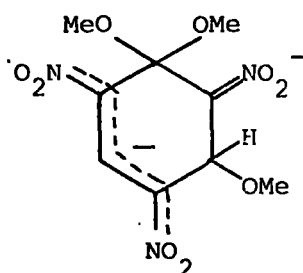
The formation of stable 1,1-dimethoxy-complexes may in some cases be preceded by the formation of transient species resulting from addition at unsubstituted ring positions. Thus using a concentrated methoxide solution in DMSO, Servis<sup>36</sup> obtained a spectrum immediately after mixing the solutions showing new bands (doublets at  $\delta$ 8.4 and 6.2 p.p.m. of equal intensity) which were evidence for attack at C<sub>3</sub> to give (1.12; R = R' = Me). With time a



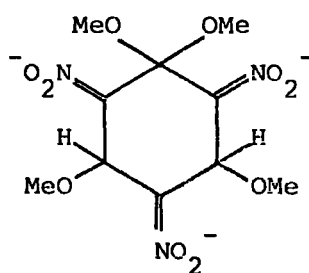
(1.12)

spectrum resulted corresponding to the 1,1-adduct (1.3; R = R' = Me). These observations were substantiated by Foster and Fyfe.<sup>37</sup> In the light of these results, it seems likely that the initial fast reaction observed by Ainscough and Caldin<sup>38</sup> in the reaction of 2,4,6-trinitroanisole with ethoxide ions at low temperature, and attributed to  $\pi$ -complex formation, resulted from (1.12; R' = Me, R = Et). Crampton and Gold found that increasing the proportion of methanol in the solvent resulted in a more rapid conversion to the C<sub>1</sub> isomer.<sup>39</sup> However kinetic evidence for (1.12; R = R' = Me) in methanol has been obtained by Bernasconi<sup>40</sup> using a temperature-jump stopped-flow method.

In methanolic solution, changes in the visible spectrum with base concentration were attributed to the formation of higher adducts.<sup>28,41</sup> The two maxima at 410 and 490 nm (1:1-complex) were replaced by a single band at 480 nm (1:2-complex) as the methoxide concentration was increased. These results were confirmed by Servis<sup>42</sup> when he obtained p.m.r. measurements consistent with (1.13).



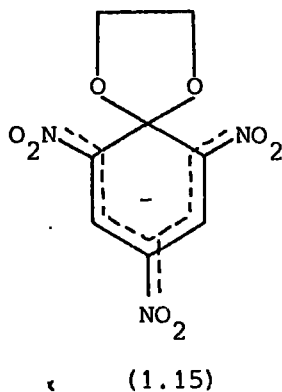
(1.13)



(1.14)

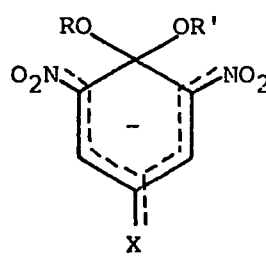
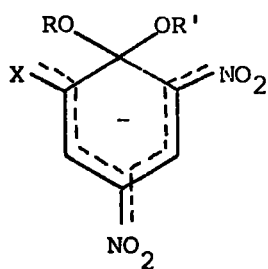
A colourless species was produced at very high base concentrations which was postulated as the tri-adduct<sup>43,44</sup> (1.14). The observed changes in the spectrum of the 1,1-adduct as the sodium methoxide concentration increases are in accord with Abe's calculations.<sup>44</sup> He predicted that the mono-, di- and tri-adducts should show two, one and no absorptions respectively in the visible region.

The spiro-Meisenheimer complex (1.15) has been prepared by Murto,<sup>45</sup> and

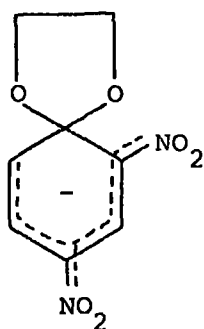


Foster et al<sup>46</sup> showed that it had spectral properties characteristic of complexes of the type (1.3). Thus the p.m.r. spectrum<sup>46</sup> confirmed the structure (1.15) and showed the equivalence of the methylene groups in the dioxolan ring.

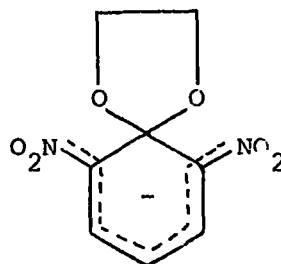
The interactions of 2,4-dinitro-6X-anisoles and 2,6-dinitro-4X-anisoles (X = OMe, H, Cl, CO<sub>2</sub><sup>-</sup>, CONH<sub>2</sub>, CO<sub>2</sub>Me, CN) with methoxide ion have been investigated. Pollitt and Saunders<sup>47</sup> obtained the visible spectra in methanol and dimethylformamide. In general two bands were observed; the band between 350 and 400 nm was present in the complexes from both types of anisole. The adducts from the 2,4-dinitro series had the longer wavelength band in the region 480-530 nm and it occurred between 535 and 612 nm for the 2,6-dinitro compounds. Both series converged to the spectrum shown by complex (1.3; R = R' = Me), and thus structures (1.16) and (1.17) were favoured for the adducts.



For the series  $X = H$ ,  $R = R' = \text{alkyl}$ , p.m.r. spectroscopy<sup>4,48,49</sup> has confirmed the structures suggested by Pollitt and Saunders. Close correspondence of the visible<sup>50</sup> and p.m.r.<sup>51,52</sup> spectral data of adducts (1.16) and (1.17) with those of the spiro-complexes (1.18) and (1.19) has helped confirm the structures.



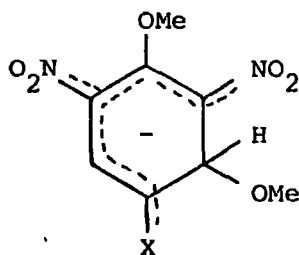
(1.18)



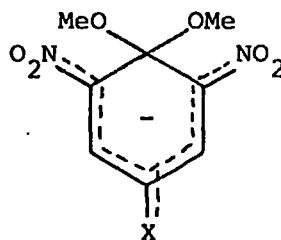
(1.19)

It is interesting to note that the p.m.r. spectrum<sup>51</sup> of (1.18) shows an  $A_2B_2$  pattern for the methylene protons, indicative of the  $sp^3$  hybridisation of  $C_1$  and the dioxolan and benzene rings being orthogonal.

Terrier and coworkers<sup>53-61</sup> have performed extensive stopped-flow kinetic and p.m.r. studies of the reaction of various substituted dinitroanisoles with sodium methoxide. Thus using the stopped-flow method<sup>55</sup> they were able to obtain the initial spectra of methoxide adducts of 4-X-2,6-dinitroanisoles in methanol-DMSO mixtures which were consistent with (1.20). The spectrum rapidly



(1.20)

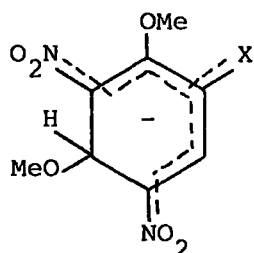


(1.21)

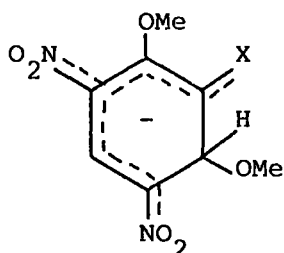
changed to that of the thermodynamically stable adduct (1.21). The rates of conversion of (1.20) to (1.21) depended on X and the solvent composition.

Complex (1.20) appeared to be the most stable with  $X = \text{SO}_2\text{CF}_3$ .<sup>59</sup>

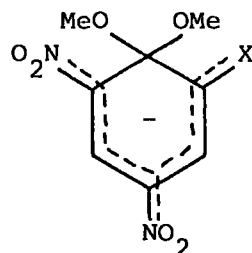
In the case of 2-X-4,6-dinitroanisoles, the initial formation of (1.22) and (1.23) has been observed;<sup>57,58,60</sup> the adduct resulting from addition at the 3-position, (1.23), being the more stable. For X = Cl, (1.22) was observed in a DMSO-methanol solvent mixture containing >85% DMSO.<sup>60</sup>



(1.22)



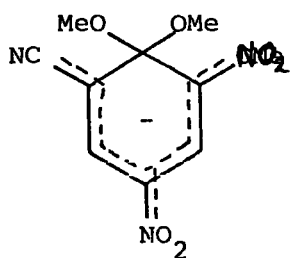
(1.23)



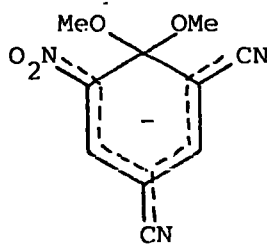
(1.24)

Visible<sup>34,47,62</sup> and p.m.r.<sup>34,62</sup> spectra, consistent with adducts (1.21) and 1.24; X = CN) have been obtained. The prior formation of adducts (1.20) and 1.23; X = CN) in methanolic DMSO has been detected<sup>63,64</sup> and in the case of 2-cyano-4,6-dinitroanisole, Terrier<sup>54</sup> has found both 1,3- (1.23) and 1,5- adducts (1.22).

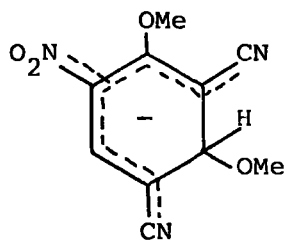
Using the isomeric dicyanonitroanisoles, Fendler *et al*<sup>65</sup> have established the structures (1.25) and (1.26) for methoxide addition. The initial formation



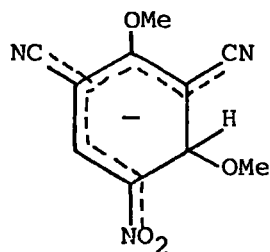
(1.25)



(1.26)



(1.27)

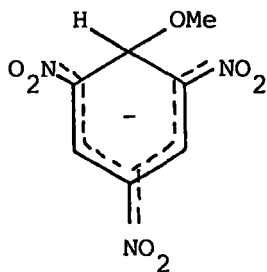


(1.28)

of the 1,3-complex (1.27) was observed by p.m.r. spectroscopy of solutions in DMSO and also by calorimetric studies. However the isomer (1.28) was not detected. The 1,1-dimethoxy-complex of the tricyano derivative has been

reported.<sup>66</sup>

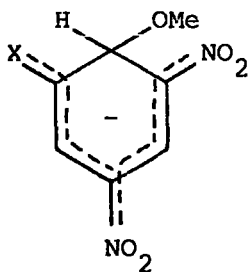
1,3,5-Trinitrobenzene gives a red solution in methanolic sodium methoxide, the visible spectrum<sup>13,41</sup> being similar to that of complex (1.3; R = R' = Me). The p.m.r. spectrum<sup>33,37</sup> of the adduct (1.29) in DMSO showed two sets of bands



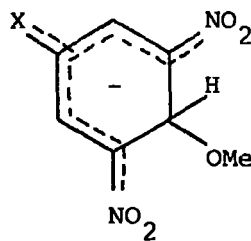
(1.29)

at  $\delta$ 8.4 and 6.1 p.p.m.; the position of the high field band (triplet; J = 1.5 Hz), corresponding to the ring proton at the site of addition, is compatible with a change in hybridisation from  $sp^2$  to  $sp^3$  of the ring carbon.

Adducts from 1-X-3,5-dinitrobenzenes have received some attention. Pollitt and Saunders<sup>67</sup> collected visible spectral data for a series of substituents (X = NMe<sub>2</sub>, OMe, Cl, CO<sub>2</sub><sup>-</sup>, CO<sub>2</sub>Me, CN, CONH<sub>2</sub>). The spectra showed two maxima (351-392 and 498-594 nm depending on X) and it was originally suggested that each band was a contribution from (1.30) and (1.31). However comparison with



(1.30)



(1.31)

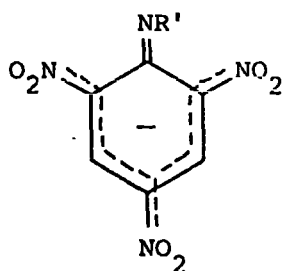
the spectrum of complex (1.29) did not support this.

Foster and Foreman<sup>68</sup> obtained conclusive n.m.r. evidence in DMSO solution for methoxide addition at C<sub>2</sub> to give (1.30; X = CN, CF<sub>3</sub>). Using stopped-flow spectrophotometry, Terrier *et al*<sup>69</sup> found that in methanol-DMSO solution containing >35% DMSO, (1.31; X = CN) was formed rapidly and slowly isomerised to (1.30).

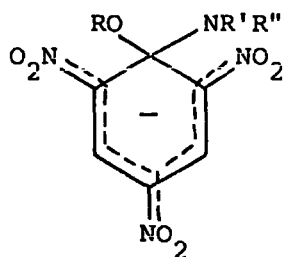
With  $X = \text{CO}_2\text{Me}$ ,<sup>70</sup> methoxide ions appeared to show very little discrimination for the three unsubstituted ring positions, the equilibrium mixture of isomers being ca. 7:3 in DMSO-rich media. Comparison with the spectral changes observed with sulphite and acetate ions as nucleophiles indicated that methoxide ions attacked at  $C_4$  initially prior to equilibrium.

Recently, Fyfe et al<sup>71</sup> have developed a rapid-flow n.m.r. technique and used it to observe the methoxide adducts produced by 1-cyano-3,5-dinitrobenzene in methanolic DMSO. Adduct (1.30;  $X = \text{CN}$ ) appeared to be the thermodynamically stable species, from spectra recorded on a stationary solution. Using flowing solutions bands were observed which corresponded to both  $C_2$ - and  $C_4$ -adducts. A limiting flow rate was achieved when there were approximately equal concentrations of adducts (1.30 and 1.31;  $X = \text{CN}$ ) suggesting that methoxide ions showed little kinetic preference for the ring positions. As a result of these findings, it seems likely that mixtures of isomers may be produced initially prior to rearrangement to the thermodynamically stable  $C_2$ -adduct.<sup>69,70,72</sup>

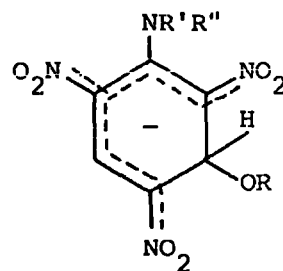
The initial interaction of picramide with base can result in two possibilities, either proton loss from the amino group or complex formation. The conjugate base (1.32) was suggested by Green and Rowe<sup>73</sup> and (1.33) was



(1.32)



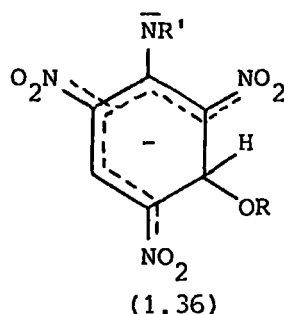
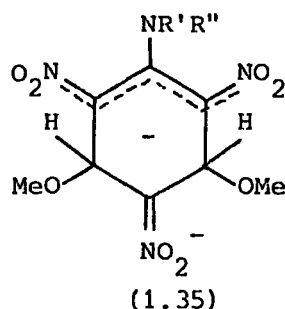
(1.33)



(1.34)

postulated as the structure of the product of the interaction.<sup>74,75</sup> Gold and Rochester<sup>76</sup> found evidence in a visible spectroscopic study, in the case of picramide, for both adduct formation and proton loss and concluded that the adduct was in fact (1.34;  $R' = R'' = \text{H}$ ,  $R = \text{Me}$ ). In the case of *N,N*-dimethylpicramide, where proton transfer is unlikely, there was evidence for the

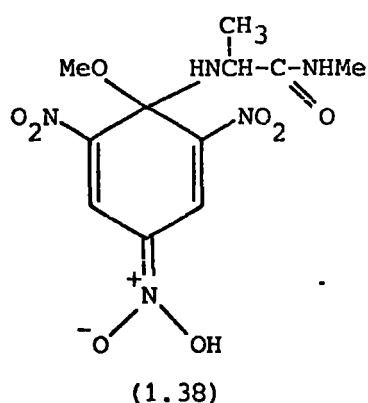
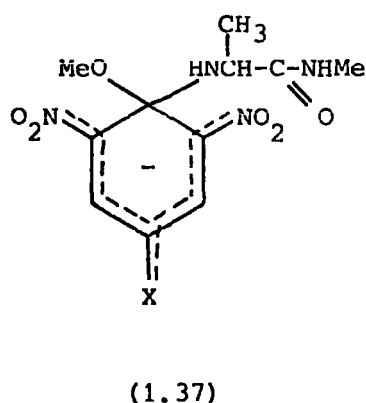
formation of the adduct (1.34;  $R' = R'' = R = \text{Me}$ ) and also for a di-adduct (1.35;  $R' = R'' = \text{Me}$ ).



The proportion of conjugate base formed appears to increase in the series picramide < N-methylpicramide < N-phenylpicramide. In some cases addition to the conjugate base has been observed at higher methoxide concentrations to give (1.36;  $R = \text{Me}$ ,  $R' = \text{Ph}$ ). These findings have been well substantiated by p.m.r. measurements.<sup>36,39,42,48,77</sup>

For dinitroanilines the dominant interaction appears to be proton loss.<sup>39</sup>

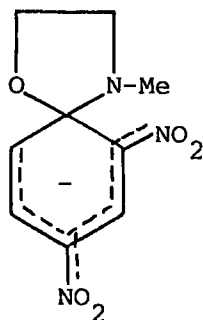
In contrast to the observations on simple picramides, the existence of  $\sigma$ -complexes (1.37) bonded at  $C_1$ , derived from the interaction of 2,6-dinitro-4-X-anilinopropionamides and potassium methoxide in methanol, has been reported.<sup>78,79</sup> The relatively stable neutral complex (1.38) was isolated. It was postulated



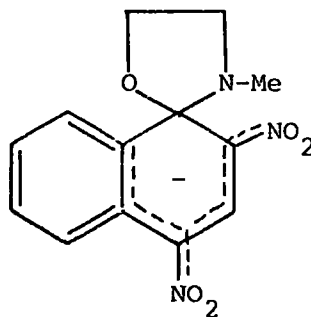
that hydrogen bonding occurred between the amido group and an ortho nitro group in the conformation adopted by the complex. Alkylation of the amido group removed any possibility of hydrogen bonding and amino proton loss resulted. Alkylation of the amino group caused complexation to occur at the 3-position,

steric effects preventing 1,1-complex formation.

1,1  $\sigma$ -Complexes involving amines have been isolated and their stabilities investigated.<sup>80-82</sup> N-2-hydroxyethyl-N-methyl-2,4-dinitroaniline and related compounds in basic solutions cyclise to give complexes (1.39) and (1.40). The ammonium salts of 2-(methylamino)ethylnitroaryl ethers could be trapped out by acidification of (1.39) under controlled conditions since aryl ethers of this



(1.39)

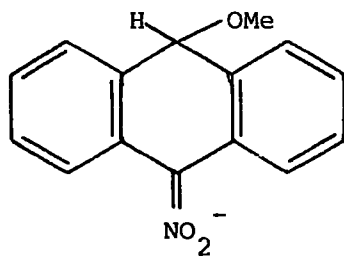


(1.40)

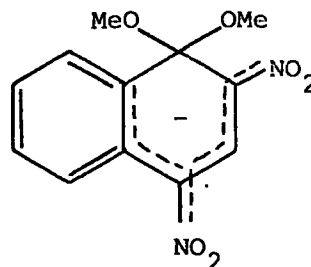
type readily rearrange to arylamines.

More recently<sup>83,84</sup> n.m.r. spectroscopic evidence has been presented for the existence of 1,1-complexes derived from 1-sec-amino-2,4-dinitronaphthalenes and sodium ethoxide. They are preceded by formation of the less stable 1,3-adducts.

A number of Meisenheimer-type adducts from a variety of activated aromatics have been isolated and their structures elucidated by n.m.r. spectroscopy.

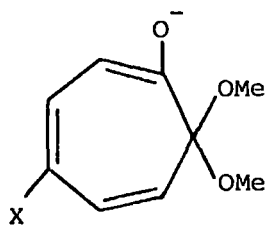


(1.41)

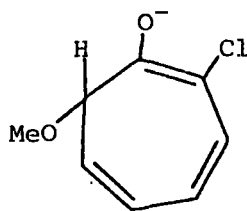


(1.42)

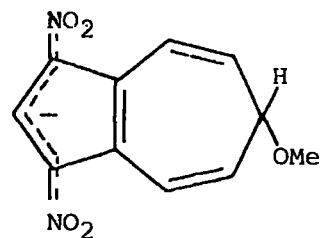
Foster *et al*<sup>49</sup> have confirmed structures (1.41) and (1.42), (1.40) having originally being prepared and its structure suggested by Meisenheimer.<sup>3</sup>



(1.43)



(1.44)

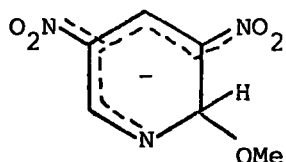


(1.45)

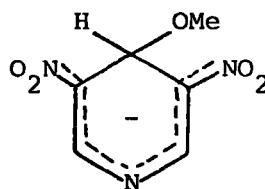
Complexes (1.43) from substituted tropones have been assigned by Pietra<sup>85</sup> (X = H) and Abe<sup>86</sup> (X = NO<sub>2</sub>). With 2-chlorotropone, Pietra<sup>87</sup> observed initial attack at an unsubstituted ring position (C<sub>7</sub>) to give (1.44) before the substitution of the chlorine. 3-X-1-nitroazulenes<sup>88</sup> (X electron withdrawing group) form  $\sigma$ -complexes with methoxide in methanol. When X = NO<sub>2</sub> the adduct (1.45) is formed. In contrast, when X = CF<sub>3</sub>CO addition of base at the carbonyl group occurs.

Considerable interest has been shown recently in adducts formed from activated heterocyclic aromatics with bases and their role as intermediates in nucleophilic heteroaromatic substitution. The aza group has a similar activating effect to the nitro group but is somewhat less sterically demanding.<sup>89</sup> Consequently a number of adducts from substituted nitro-pyridines and -pyrimidines have been reported.

Some twenty years ago, Mariella<sup>90</sup> observed coloured solutions produced in nucleophilic substitution reactions by chloronitropyridines with sodium methoxide. Fyfe<sup>91</sup> obtained p.m.r. and visible spectroscopic evidence for the 3,5-dinitropyridine-methoxide adduct in DMSO solutions. The visible spectrum of the



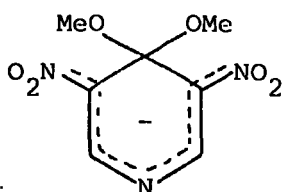
(1.46)



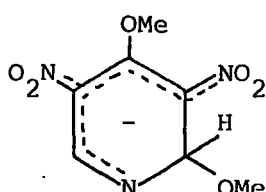
(1.47)

complex shows a band at ca. 487 nm and the bands at  $\delta$ 9.73 and 9.14 p.p.m. in

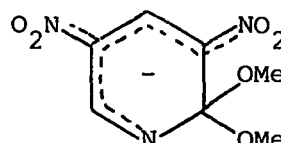
the p.m.r. spectrum of the parent heterocycle were replaced by bands of equal intensity at  $\delta$ 8.62, 8.30 and 6.08 p.p.m. on addition of sodium methoxide. Fyfe found no evidence for the formation of adduct (1.47). However this isomer was later identified by Miller *et al*<sup>92</sup> who also confirmed Fyfe's assignment of the C<sub>2</sub>-adduct (1.46).



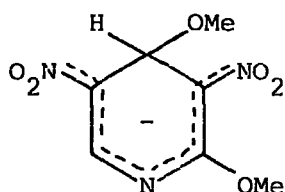
(1.48)



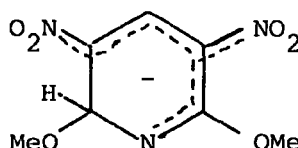
(1.49)



(1.50)



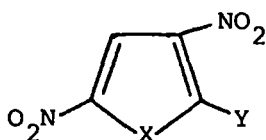
(1.51)<sub>k</sub>



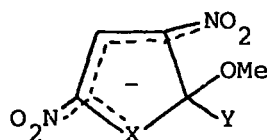
(1.52)

Meisenheimer complexes from the pyridine analogues of 2,4,6-trinitroanisole have been characterised. Thus the crystalline solid adduct (1.48) has been isolated and spectral data obtained.<sup>62,93</sup> The kinetically favoured methine adduct (1.49) has been detected by p.m.r. measurements<sup>94</sup> in methanol-DMSO solutions and by stopped-flow spectrophotometry<sup>95</sup> in methanol and methanolic DMSO prior to its isomerisation to the thermodynamically stable adduct (1.48). With 2-methoxy-3,5-dinitropyridine only one species (1.52) was observed<sup>94,96</sup> with no evidence of either (1.50) or (1.51). Studies on pyrimidines have also been performed.<sup>97</sup>

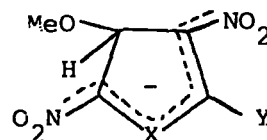
Recent interest has been shown in complexes derived from suitably activated 5-membered ring heterocycles. Thus Illuminati *et al*<sup>98</sup> have prepared complex



(1.53)

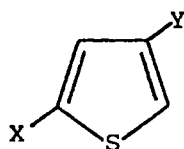


(1.54)

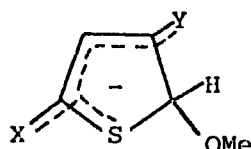


(1.55)

(1.54; X = S, Y = OMe) from 2-methoxy-3,5-dinitrothiophene, (1.53; X = S, Y = OMe) in methanolic sodium methoxide. 3,5-Dinitrothiophene<sup>99</sup> (1.53; X = S, Y = H) is reported to give complex (1.54; X = S, Y = H) rather than (1.55; X = S, Y = H). This conclusion was reached by use of the 2-deuterated compound. However a later investigation by Terrier<sup>100</sup> revealed that deuterium exchange at the 2-position is rapid and that substrates (1.53; Y = D) could not be used to determine structures with any certainty. But Illuminati's postulation of (1.54) for the adduct was supported by using the C<sub>4</sub>-deuterated compound where isotopic exchange was found to be slow.<sup>100</sup> The complex produced from 3,5-dinitroselenophene proved to be (1.54; X = Se, Y = H) on the basis of the magnitude of the  $J_{77}^{\text{Se-H}}$  coupling constant.<sup>100</sup> The substrate (1.56;



(1.56)



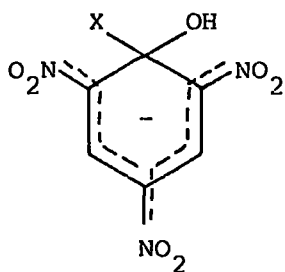
(1.57)

X = NO<sub>2</sub>, Y = CN) gave adduct (1.57; X = NO<sub>2</sub>, Y = CN) with methoxide in both DMSO-rich media<sup>101</sup> and in methanol.<sup>102</sup> However (1.56; X = CN, Y = NO<sub>2</sub>) gave (1.57; X = CN, Y = NO<sub>2</sub>) in DMSO but was found to undergo methoxide addition at the cyano function in methanol,<sup>102</sup> A recent report<sup>103</sup> indicates that 2- and 3-nitrothiophenes (1.56; X = NO<sub>2</sub>, Y = H and X = H, Y = NO<sub>2</sub>) give complexes (1.57; X = NO<sub>2</sub>, Y = H and X = H, Y = NO<sub>2</sub>) with methoxide in DMSO and are believed to represent the first examples of mono-nitro compounds containing no other activating groups which give Meisenheimer-type adducts.

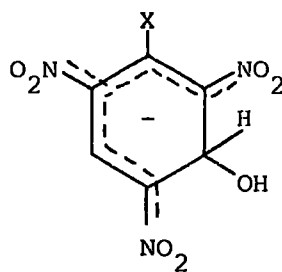
#### (ii) Hydroxide ions

The fairly rapid formation of substitution products has resulted in hydroxide ions being used less extensively than alkoxides in the study of Meisenheimer complexes. For example 2,4,6-trinitroanisole<sup>104</sup> readily gives picrate ions in aqueous alkaline solution. It seems likely that the reaction

proceeds via an intermediate of the type (1.58; X = OMe) although there is no



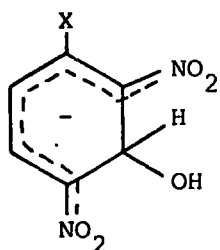
(1.58)



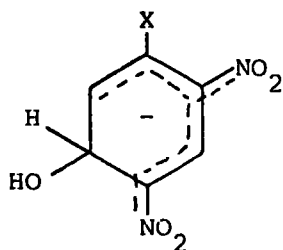
(1.59)

evidence for the build up of such an intermediate in water. However utilising recently developed rapid mixing and recording techniques, adducts derived from hydroxide ions have been detected and studied. Gaboriaud and Schaal,<sup>105</sup> using a stopped-flow technique, investigated a series of 1-X-2,4,6-trinitrobenzenes in fairly concentrated sodium hydroxide solutions. They obtained the visible spectra of transient species and assigned them to structure (1.58; X = H, Cl, OMe). However later work by Bowden and Cook<sup>106</sup> and Crampton et al<sup>107</sup> seems to indicate that the observable intermediate is (1.59). The possibility of a di-adduct formed by hydroxide addition at two unsubstituted ring positions cannot be excluded. When X = NO<sub>2</sub><sup>108</sup> a comparatively stable adduct of type (1.59) is formed. Decomposition of the substrate to give picrate (t<sub>1/2</sub> ca. 2 min. at pH 10) presumably occurs by direct displacement involving the intermediate (1.58; X = NO<sub>2</sub>).

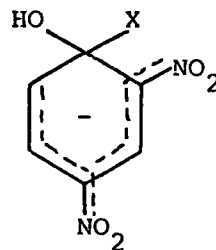
More recently Abe and Hasegawa<sup>109,110</sup> have used a rapid scan recording technique to observe the visible spectra at various times shortly after mixing of a series of 1-X-2,4-dinitrobenzenes (X = H, OMe, Cl, F, OC<sub>6</sub>H<sub>5</sub>, OC<sub>6</sub>H<sub>4</sub>NO<sub>2</sub> (p), CO<sub>2</sub><sup>-</sup>, SCN) in aqueous DMSO containing sodium hydroxide. Two species were



(1.60)



(1.61)

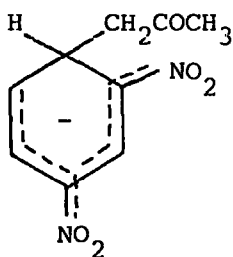


(1.62)

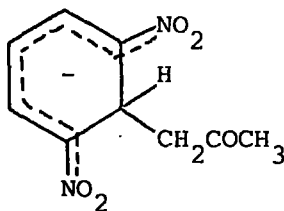
were observed, the first having  $\lambda_{\max}$  between 565 and 650 nm and consistent with (1.60), the second with  $\lambda_{\max}$  480-550 nm is consistent with either (1.61) or (1.62) since both contain the 1,3-dinitropentadienyl  $\pi$ -electron system. Except for X = H, the final spectrum corresponded to that of the 2,4-dinitrophenoxide ion.

#### Complexes derived from carbon bases

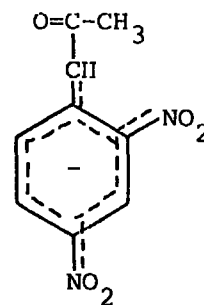
The intense purple-coloured solution produced by 1,3-dinitrobenzene in alkaline acetone was first noted by Janovsky and Erb<sup>111</sup> in 1886. Since then large numbers of compounds containing active methylene groups have been observed to give coloured solutions with nitro-aromatics in basic media. Now generally known as the Janovsky reaction it has been widely applied as a test for such groups.



(1.63)



(1.64)

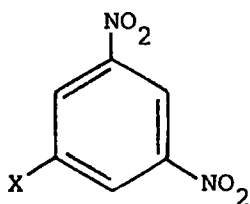


(1.65)

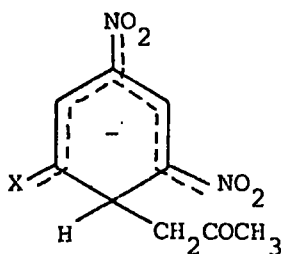
Canback<sup>112</sup> originally suggested (1.63) as being the adduct on the basis of the electronic spectrum. He was later supported by Pollitt and Saunders.<sup>67</sup> Foster and Fyfe<sup>49</sup> in a p.m.r. study confirmed (1.63) and could not detect any of the isomer (1.64). The presence of excess 1,3-dinitrobenzene<sup>113</sup> gives further reaction. Thus the final colour produced results from the anion<sup>114</sup> (1.65) formed from the oxidation of the initially formed Janovsky complex by the excess dinitrobenzene.

With an electron-withdrawing substituent, X, at the 5-position of 1,3-dinitrobenzene there is the possibility of the nucleophile attacking at either the 2- or the 4-position. Hence the two maxima observed<sup>61</sup> in the visible

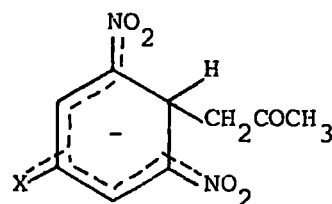
spectra of adducts from (1.66) in alkaline acetone have been attributed to



(1.66)



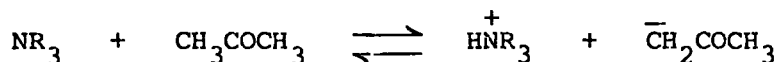
(1.67)



(1.68)

addition at the 2-position (1.67) (shorter wavelength band) and the 4-position (1.68) (longer wavelength band). A substituent at either the 2- or 4- and 6-positions resulted in only a single band.<sup>67</sup>

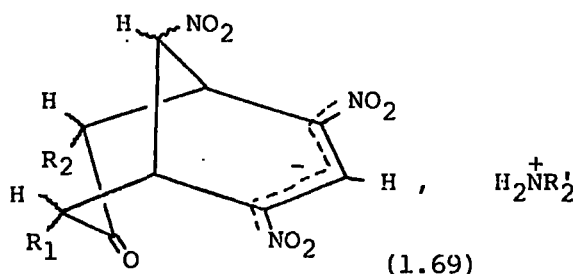
Conclusive spectroscopic evidence for the carbanion adduct from 1,3,5-trinitrobenzene was obtained by Foster and Fyfe.<sup>37</sup> They observed the p.m.r. spectrum of the 1,3,5-trinitrobenzene-methoxide adduct in acetone. The initial spectrum of the methoxide complex was slowly replaced by bands corresponding to (1.67; X = NO<sub>2</sub>). Generation of similar adducts has been achieved by the addition of a tertiary amine to solutions of 1,3,5-trinitrobenzene in a number of ketones<sup>115</sup> or aliphatic nitro-compounds,<sup>116</sup> the amine serving as a proton acceptor



Janovsky complexes derived from (1.66) and acetone in the presence of base have been investigated recently. Gitis and coworkers<sup>117</sup> found that the C<sub>2</sub>-adduct (1.67) alone was formed when X = Me or OMe but both (1.67) and (1.68) were formed if X was electron-withdrawing. The isomeric adducts have also been observed<sup>118</sup> from a series of derivatives of 3,5-dinitrobenzoic acid.

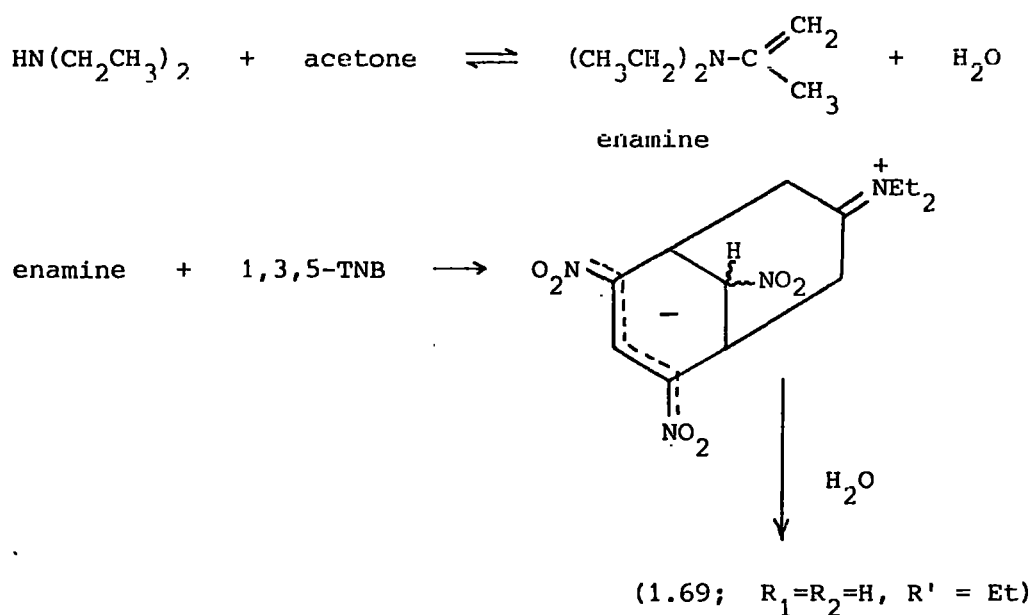
The interaction of 1,3,5-trinitrobenzene and ketones in the presence of secondary or primary amines has been the subject of some speculation. Foster and Fyfe<sup>119</sup> identified N,N-diethyl-p-nitroaniline and 2-acetyl-1,3-dinitropropane among the products. They also isolated a red compound from the reaction mixture as did Osugi and Muneo.<sup>120</sup> It showed an intense absorption

at 510 nm and was similar to a red product isolated by Abe<sup>121</sup> some years earlier. No consistent analyses for this compound were reported. However Strauss and Schran<sup>122</sup> later isolated a crystalline red solid and they interpreted their p.m.r. data in terms of a cyclic adduct (1.69;  $R_1=R_2=H$ ,  $R'=Et$ ).

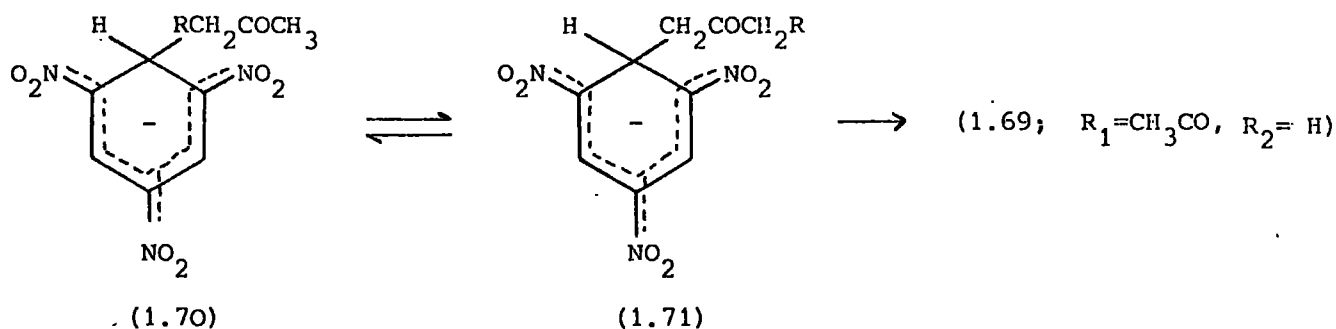


The cyclic adduct was obtained with primary and secondary amines but only the Janovsky complex (1.67;  $X = NO_2$ ) resulted with triethylamine as base.<sup>115</sup> However Foster and coworkers<sup>123</sup> found that cyclic adducts could be formed from more acidic ketones such as acetylacetone or dibenzyl ketone in the presence of triethylamine.

As a result of this, Strauss<sup>124</sup> postulated two distinct mechanistic pathways for the production of bicyclic adducts. In the case of acetone, diethylamine but not triethylamine would result in cyclisation, and since the basicities of the two amines do not differ appreciably an enamine intermediate was suggested.



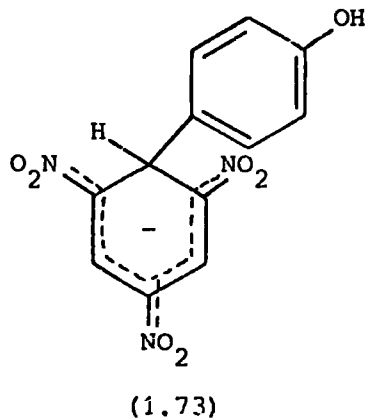
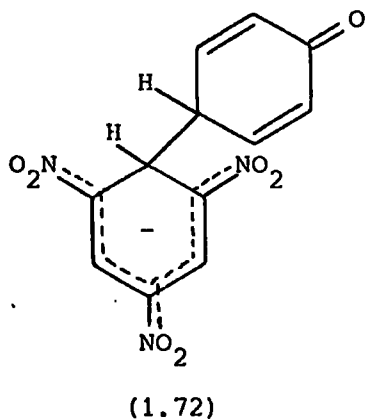
With more acidic ketones such as acetylacetone, rapid equilibration between (1.70 and 1.71;  $R = CH_3CO$ ) via a delocalized carbanion intermediate was thought to be involved.



Foster et al<sup>125</sup> showed the possibility of stereoisomerism at the carbon atoms  $\alpha$  to the ketonic function. Thus two products were isolated using dibenzyl ketone with small differences in their spectral properties which they attributed to the cis- and trans-isomers of (1.69; R<sub>1</sub>=R<sub>2</sub>=Ph). The field of carbanion additions and resulting cyclizations has been well reviewed recently by Strauss.<sup>126</sup>

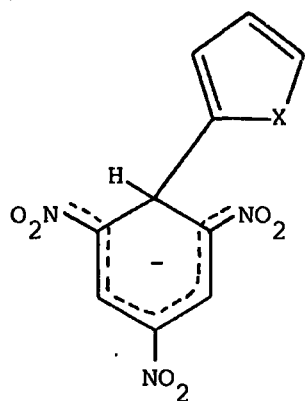
There have been a number of reports of a variety of Janovsky-type complexes involving the production of carbon-carbon bonds. Bernasconi<sup>127</sup> has shown that under conditions of excess substrate, 2,4,6-trinitrotoluene gave a  $\sigma$ -complex by attack of the benzyl anion on the substrate. It was not possible to obtain a p.m.r. spectrum to elucidate the site of attack since the production of a small concentration of radical anions wiped out the spectrum.

The ambident nature of the phenoxide ion has been demonstrated<sup>128</sup> with 1,3,5-trinitrobenzene and potassium phenoxide in methanolic DMSO. The initial p.m.r. spectrum, corresponding to the methoxide adduct, slowly changed and was assigned to the carbon-carbon bonded  $\sigma$ -complex (1.73) formed by rearomatisation



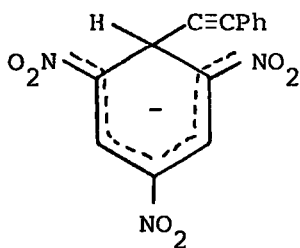
of the initially formed complex (1.72).

Nilsson and Wennerstrom have reported  $\sigma$ -complexes (1.74) - (1.76) derived from organometallics and 1,3,5-trinitrobenzene in pyridine. The species were well characterised by p.m.r. and visible spectroscopy showing

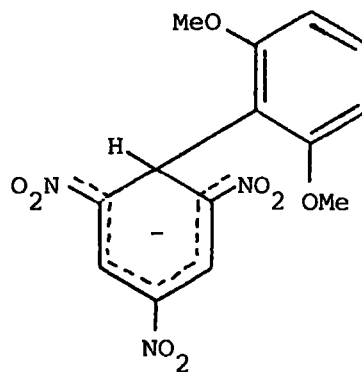


(1.74) <sup>129,130</sup>

(X = O, S, CH<sub>2</sub>)

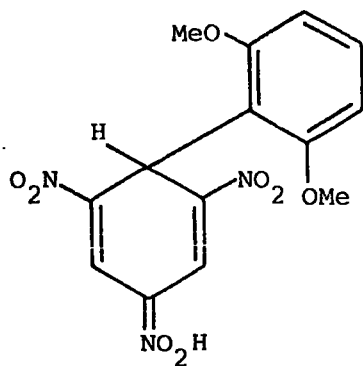


(1.75) <sup>131</sup>



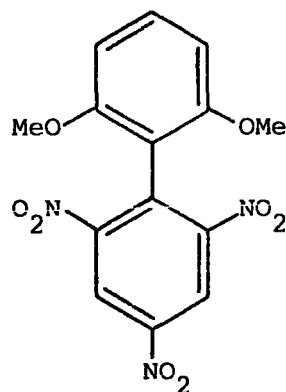
(1.76) <sup>132</sup>

features typical of anionic  $\sigma$ -complexes. Unlike complexes derived from oxygen bases, adducts such as (1.76) do not decompose to nitro-compound and protonated nucleophile (compare ref. 128). Instead compounds believed to be nitronic acids (1.77) can be isolated and characterised. <sup>132</sup> Under mild



(1.77)

oxidise  $\rightarrow$

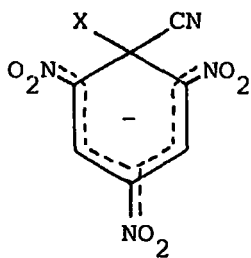


(1.78)

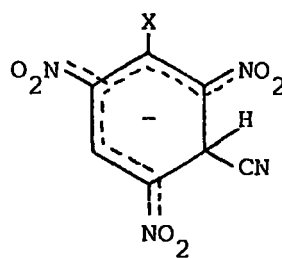
conditions (1.77) can be oxidised to the corresponding substituted biphenyl.

Recently Beletskaya <sup>133</sup> has produced p.m.r. evidence for anionic  $\sigma$ -complexes derived from 1,3,5-trinitrobenzene and organotin compounds in DMSO. Thus organometallics used in this way have considerable potential in organic synthesis.

There have been a number of studies <sup>134-141</sup> on complexes derived from nitroaromatics and cyanide ion, and the results were ascribed to (1.79; X = H).



(1.79)

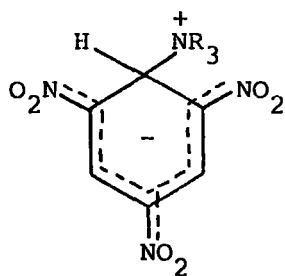


(1.80)

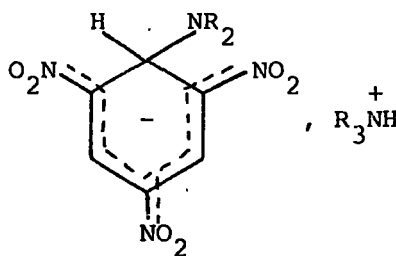
Buncel *et al*<sup>138</sup> found conclusive evidence for this in the p.m.r. spectrum of the complex generated *in situ* in chloroform. 2,4,6-Trinitrotoluene formed the C<sub>3</sub>-adduct (1.80; X = CH<sub>3</sub>) whereas addition at C<sub>1</sub> occurred for the benzaldehyde (1.79; X = CHO). Both (1.79 and 1.80; X = OCH<sub>3</sub>) were formed from 2,4,6-trinitroanisole with the C<sub>3</sub>-adduct predominating.

Complexes derived from nitrogen bases

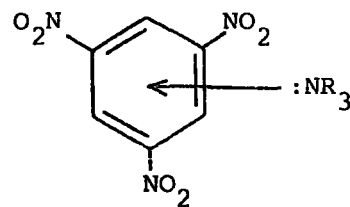
The interaction of 1,3,5-trinitrobenzene and aliphatic amines in a variety of solvents has been studied by a number of workers. Various modes of interaction are possible and the solvent used may be important. Zwitterionic adducts<sup>142-144</sup> such as (1.81) have been postulated. The ion-pair (1.82) was



(1.81)



(1.82)



(1.83)

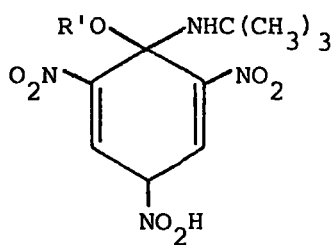
also considered for polynitroaromatic compounds in liquid ammonia and for the colour produced by piperidine and 1,3,5-trinitrobenzene in acetonitrile.<sup>145</sup>

In the latter system a donor complex (1.83) may also be produced.

Crampton and Gold<sup>146</sup> in a comprehensive study of 1,3,5-trinitrobenzene and aliphatic amines in DMSO solution by p.m.r., u.v./visible and conductivity measurements showed that the interaction produced a pair of ions. No interaction with tertiary amines was detected. The most likely pathway for  $\sigma$ -complex formation involves initial attack by amine to give the zwitterion followed by deprotonation by another molecule of amine to give the negatively

charged adduct.

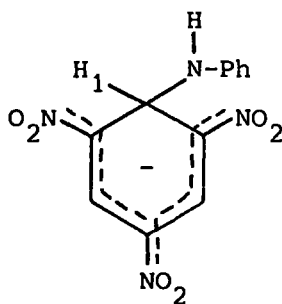
Picryl ethers appear not to have appreciable interaction with amines. Originally a zwitterionic intermediate was suggested<sup>42</sup> but was later proved to be a dealkylation product.<sup>147,148</sup> However using hindered picryl ethers and hindered amines, Clapp et al<sup>149</sup> managed to form neutral complexes in solution at low temperatures. Thus with mesityl picryl ether and t-butylamine in tetrahydrofuran at -57° a deep red solution resulted, the p.m.r. spectrum of which was consistent with (1.84; R' = mesityl). On warming the solution



(1.84)

to room temperature, the colour changed to the bright yellow of the resulting substituted picramide.

Aromatic amines have been thought to be involved in charge transfer complexes,<sup>150,151</sup> however there have been several interesting reports by Buncl and coworkers of aromatic amines displacing methoxide ions from the 1,3,5-trinitrobenzene-methoxide adduct giving the amine  $\sigma$ -complex. Thus addition of aniline to the potassium salt of (1.29) in DMSO caused the bands in the p.m.r. spectrum of the methoxy complex to slowly disappear while bands at 8.45, 6.30 and 5.88 p.p.m. ( $J_{\text{NH-H}_1} = 8.8 \text{ Hz}$ ) attributed to (1.85)<sup>152</sup> increased in intensity. The transformation was also followed by observing the changes

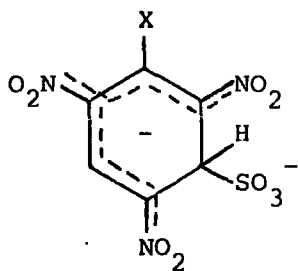


(1.85)

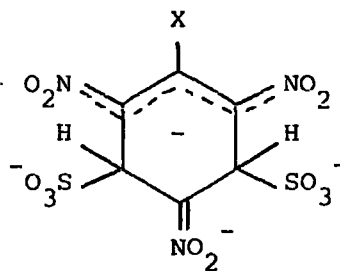
in the visible spectrum of diluted samples of solutions used for the p.m.r. measurements. The assignment was substantiated<sup>153</sup> by use of N-methyl-2,4,6-trideuterioaniline which served to removed the NH-H<sub>1</sub> coupling and reduce the complexity of the spectrum resulting from the aromatic protons of the amine which masked the signal for the H<sub>1</sub> absorption. A complex having similar spectral characteristics was obtained from 1,3,5-trinitrobenzene and potassium anilide.<sup>154</sup> A more recent report by Buncel<sup>155</sup> has revealed that the trinitrobenzene-anilide  $\sigma$ -complex can be readily formed from trinitrobenzene and aniline in the presence of DABCO or triethylamine in DMSO.

Complexes derived from sulphur bases

1,3,5-Trinitrobenzene dissolves in aqueous sodium sulphite giving a dark red solution<sup>156</sup> and it was from such a solution that Henry<sup>157</sup> isolated a dark red crystalline solid which was very stable when dry. The analysis yielded a stoichiometry of 1 TNB:2 sulphite. Norris originally suggested a charge-transfer complex<sup>158</sup> but visible<sup>135</sup> and p.m.r.<sup>159</sup> spectral measurements indicated a 1:1- $\sigma$ -complex (1.86; X = H) at low sulphite concentrations and a 1:2-complex (1.87; X = H) at higher sulphite concentrations. The



(1.86)

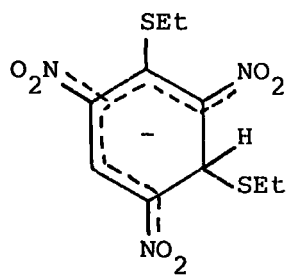


(1.87)

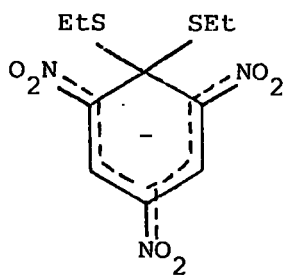
interaction of 1-X-2,4,6-trinitrobenzenes with sodium sulphite is the subject of further study in the present work.

Adducts from trinitrobenzene and picramides with thiolates and thiophenoxides have been observed.<sup>160</sup> With picramides complex formation predominates over proton abstraction.

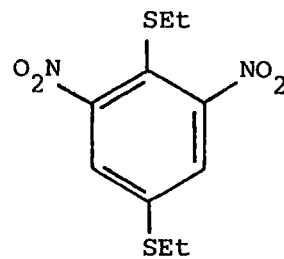
Sodium thioethoxide and ethylthiopicrate gives complex (1.88)<sup>161</sup> with



(1.88)



(1.89)



(1.90)

some of the 1,1-adduct (1.89); (1.88) quickly decomposes, the final product of the reaction being (1.90). Similar effects were observed with 2-ethylthio-tropone.<sup>162</sup>

THE STABILITY OF MEISENHEIMER COMPLEXES

Since the structures of anionic  $\sigma$ -complexes are now well characterised, recent studies have tended to concentrate on factors affecting complex stability. Kinetic and equilibrium measurements have shown that four of the main factors are:

- (i) nature of the parent compound,
- (ii) the attacking nucleophile,
- (iii) the solvent,
- (iv) micellar and cation effects.

Before discussing these a brief mention will be made of the methods which are often used to determine the equilibrium constants.

For reactive substrates, complexation occurs at low base concentrations and thus equilibrium constants can be determined directly by measurement of the optical density at an appropriate wavelength provided the extinction coefficient of the complex is known, or indirectly via Benesi-Hildebrand plots.<sup>163</sup>

Less reactive substrates, on the other hand, are only significantly converted to complex at very high base concentrations. Hence equilibrium constants calculated in terms of stoichiometric base concentrations are not true thermodynamic values. However the extension of acidity function concept,<sup>164</sup> originally proposed by Hammett and Deyrup,<sup>165</sup> to basic media has helped to overcome this problem.

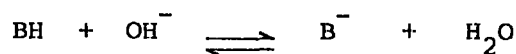
The acidity function of a medium,  $H_o$ , is defined as

$$H_o = pK_{BH^+} - \log_{10} \frac{[BH^+]}{[B]} \quad 1.1$$

and is the measure of the ability of the medium to transfer a proton to a neutral indicator molecule.

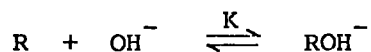


In aqueous alkaline media, the ionisation of an indicator by proton loss may be used to define an  $H_-$  acidity function.



$$\text{H}_- = \text{p}K_{\text{BH}} - \log_{10} \frac{[\text{BH}]}{[\text{B}^-]} \quad 1.2$$

In the case of base addition to the indicator:-



the appropriate function is  $J_-$  which is defined as

$$J_- = \text{p}(K K_w) + \log_{10} \frac{[\text{ROH}^-]}{[\text{R}]} \quad 1.3$$

When the solvent is methanol rather than water then a scale defined relative to a standard state in pure methanol is preferred. The  $J_M$  scale, defined according to Rochester<sup>164b</sup> as in equation 1.4, has been widely used.

$$J_M = \text{p}(K.K_{\text{MeOH}}) + \log_{10} \frac{[\text{ROME}^-]}{[\text{R}]} \quad 1.4$$

$K$  is the thermodynamic equilibrium constant for methoxide ion addition to a neutral substrate and  $K_{\text{MeOH}}$  is the autoprotolysis constant of methanol.

Thus if the acidity function ( $J_M$ ) of the medium is known and the ratio of complex to substrate is determined, then the thermodynamic equilibrium constant is easily calculated. Though the values of the equilibrium constants so obtained are probably not as accurate as those determined directly, they nevertheless give a value of the appropriate order of magnitude.

Having considered methods for determining equilibrium constants for adduct formation, factors affecting their magnitudes will now be discussed.

(i) Nature of the parent compound

Equilibrium constants and rate coefficients for Meisenheimer complex formation from a number of substrates and methoxide ions in methanol at 25°C are collected in Table 1.1. The main points which emerge from the data are:

(a) greater thermodynamic stability of adducts formed by alkoxide addition to the alkoxy-substituted carbon in polynitroanisoles compared to the adducts derived from the analogous polynitrobenzenes;

TABLE 1.1

<u>Substrate</u>	<u>Addition at Ring Carbon Carrying</u>				<u>Reference</u>
	<u>OMe</u>		<u>H</u>		
	<u>K</u> (l.mole <sup>-1</sup> )	<u>k<sub>1</sub></u> (l.mol <sup>-1</sup> sec <sup>-1</sup> )	<u>K</u> (l.mol <sup>-1</sup> )	<u>k<sub>1</sub></u> (l.mol <sup>-1</sup> sec <sup>-1</sup> )	
1,3-Dinitrobenzene			1 x 10 <sup>-6</sup>		72
2,4-Dinitroanisole	4.6 x 10 <sup>-5</sup>	2 x 10 <sup>-3</sup>			166,167
2,6-Dinitroanisole	9 x 10 <sup>-5</sup>				166
1,3,5-Trinitrobenzene			23.1	7,050	167
2,4,6-Trinitroanisole	17,000	17.3	2.71	950	40,64
2-Cyano-4,6-dinitroanisole	2,600	18.8			64
4-Cyano-2,6-dinitroanisole	280	6.1			64
2,4-Dicyano-6-nitroanisole	10	2			65
2,6-Dicyano-4-nitroanisole	34	<u>ca.</u> 12			65
2,4,6-Tricyanoanisole	0.4				66

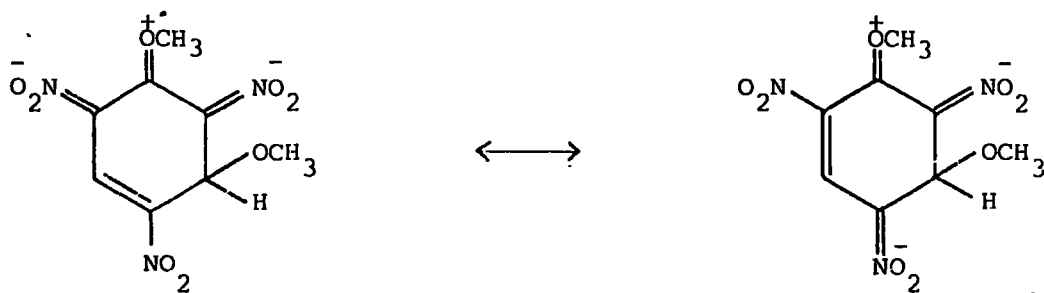
- (b) kinetic preference for addition at an unsubstituted ring carbon atom;
- (c) the importance of a nitro group para to the site of attack.

The stability of the 2,4,6-trinitroanisole-methoxide adduct over the 1,3,5-trinitrobenzene-methoxide complex has been interpreted in terms of electronic and steric effects.<sup>13</sup> The inductive effect of the methoxy group would favour base addition at C<sub>1</sub> through withdrawal of negative charge from this position. However, removal of the steric strain experienced by the methoxyl group and the ortho nitro groups of the parent ether on complexation was considered to be more important. The bending of the methoxyl group out of the plane of the ring and consequent reduction in the steric interaction provides a driving force for complexation. Crystallographic studies provide ample support for this.<sup>30-32</sup>

Bernasconi<sup>168</sup> has suggested that a further reason why addition is favoured at a position already carrying a methoxyl group may be the stabilising influence of multiple alkoxy substitution on an sp<sup>3</sup> carbon atom. There is evidence<sup>169,170</sup> that sp<sup>3</sup> carbon atoms carrying two or more alkoxy groups are stabilised relative to those carrying one or no alkoxy groups.

The faster rate of attack at an unsubstituted ring carbon atom was explained by Crampton and Gold<sup>39</sup> in terms of steric effects. They suggested that the steric strain passed through a maximum between the parent and the 1,1-dimethoxy-complex whereas steric effects would be expected to have a smaller effect in the transition state leading to the 1,3-complex. This argument was criticised by Fendler et al<sup>64</sup> on the grounds that 1,3-complexes were not observed with 1-methoxy-2,4-dinitronaphthalene and 1-methoxy-2,6-dinitrobenzene.

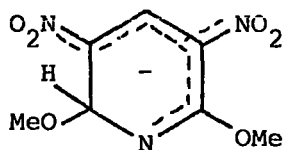
The faster formation of the 1,3-complex has been explained<sup>168</sup> in terms of resonance stabilisation of the form



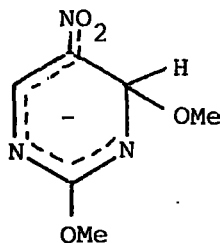
Such stabilisation is largely removed on going from the parent to the 1,1-complex, and thus its rate of formation will be reduced compared to that for the 1,3-complex. The factors governing 1,1- and 1,3-complex formation and stability appear to be more involved than Miller<sup>171</sup> allowed for in his calculations which predicted that the 1,3-adduct should be the thermodynamically stable species while the 1,1-complex should be formed more rapidly.

The effects of dimethoxy substitution and of a para nitro group with respect to the site of attack can be seen by comparing the complexes derived from 2,6-dinitroanisole and 1,3-dinitrobenzene. In the former relief of steric strain is the dominant factor whereas addition occurs para to a nitro group in 1,3-dinitrobenzene.

There appears to be a balance between steric factors and addition at an unsubstituted ring carbon. Thus 2-methoxy-3,5-dinitropyridine and 2-methoxy-



(1.91)



(1.92)

5-nitropyrimidine result in complexes (1.91)<sup>94,96</sup> and (1.92)<sup>97</sup> respectively on methoxide addition. The steric requirement of the aza group is less than that of a nitro group and if a methoxyl group is not flanked by two nitro groups then there is no driving force for 1,1-complex formation.

Zollinger et al<sup>34</sup> calculated that most of the negative charge of a  $\sigma$ -complex resides on the ring substituents especially the para nitro group. However a more refined method<sup>35</sup> indicated that a considerable proportion of the charge is present in the  $\pi$ -electron system, though of the ring substituents the para nitro group still carries most of the electron density. Thus the ability of the ring substituents to delocalise the negative charge is reflected in the complex stability. Comparing the equilibrium constants for

2,4-dinitroanisole and 2,4,6-trinitroanisole gives a value of ca. 38 kJ for the stabilising effect of an ortho nitro group. A similar value is obtained on comparing the equilibrium constants for 1,3-dinitrobenzene and 1,3,5-trinitrobenzene.

Replacing the nitro groups of 2,4,6-trinitroanisole successively by a less electronegative substituent such as a cyano group has a marked effect on complex stability.<sup>64-66</sup> A comparison of the data for the isomeric cyano-dinitroanisoles and 2,4,6-trinitroanisole reveals that replacing a para nitro group has a much greater effect than replacing an ortho group. Replacing all the nitro groups by cyano groups results in a 42,500-fold decrease in complex stability.

The para nitro group also appears to be important as regards 1,3-complex stability. Thus the 1,3-dimethoxy-2,4-dicyano-6-nitrocyclohexadienate complex (1.28) was not detected.<sup>65</sup> Likewise a transient species from 2,4,6-tricyanoanisole was not observed by either n.m.r. or calorimetric studies.<sup>66</sup>

(ii) Variation of reactivity with attacking nucleophile

For a meaningful comparison of nucleophilic reactivity, a study should be made of complexes derived from a single substrate and a variety of bases in a given solvent system. However many studies have involved a number of different solvents (see Table 1.2) though the equilibrium constants for formation of 1:1-complexes of 1,3,5-trinitrobenzene with a number of sulphur and oxygen bases have been measured in methanol.<sup>160</sup> The values reveal that the order of complex stability in  $\text{EtS}^- > \text{MeO}^- > \text{PhS}^- > \text{PhO}^-$ . (See footnote to Table 1.2 regarding  $\text{PhO}^-$ ).<sup>173</sup> In water the carbon basicity of sulphur and oxygen follows the same trend as above, sulphite ions resulting in a much more stable complex than hydroxide ions.

The greater affinity of carbon for a carbon rather than an oxygen nucleophile has been demonstrated by the observation that the stable adduct produced from addition of either methoxide ions or diethylamine to 1,3,5-

TABLE 1.2

Equilibrium Constants for Formation of Adducts from  
1,3,5-Trinitrobenzene with Various Nucleophiles

<u>Nucleophile</u>	<u>Solvent</u>	<u>K</u> ( $l.mol^{-1}$ )	<u>Reference</u>
MeO <sup>-</sup>	Methanol	23.1	168
	DMSO	ca. $10^9$	160
EtS <sup>-</sup>	Methanol	$3.5 \times 10^3$	160
PhS <sup>-</sup>	Methanol	1.95	160
	DMSO	$8 \times 10^4$	160
PhO <sup>-</sup>	Methanol	$<2 \times 10^{-3}$ *	160
HO <sup>-</sup>	Water	2.7	104
SO <sub>3</sub> <sup>2-</sup>	Water	$2.5 \times 10^2$	159
CN <sup>-</sup>	Methanol	39	172
	Ethanol	$1.27 \times 10^3$	172
	<u>n</u> -Propanol	$1.47 \times 10^3$	172
	<u>i</u> -Propanol	$1 \times 10^4$	172
	<u>n</u> -Butanol	$2 \times 10^3$	172
	<u>t</u> -Butanol	$5 \times 10^5$	172

\* It was assumed that addition occurred via oxygen, however recent results by Buncel have shown that phenoxide ions can form complexes through carbon addition. (Ref. 128).

trinitrobenzene<sup>37,119</sup> in acetone is in fact the acetone complex. A similar situation is observed between the ambident phenoxide ion and 1,3,5-trinitrobenzene mentioned earlier.

The interaction of 2,4,6-trinitroaniline with oxygen and sulphur bases parallels the carbon and Brønsted basicity series above. Thus sulphur bases (PhS<sup>-</sup>, EtS<sup>-</sup>) preferentially form complexes through attack at the C<sub>3</sub> position

whereas oxygen bases abstract amino protons besides forming the C<sub>3</sub>-adducts.<sup>160</sup>

For substrates such as 2,4,6-trinitroanisole, where isomeric addition is possible, the mode of interaction depends greatly upon the nucleophile.

Methoxide ions give the C<sub>1</sub>-adduct while sulphite ions result in addition at C<sub>3</sub>. It seems that bulky nucleophiles like sulphite have a greater steric requirement at C<sub>1</sub> and therefore form stable 1,3-complexes.

(iii) Solvent effects

A change of solvent has quite an important effect on Meisenheimer complex stability (see Table 1.2). The solvent systems used in the main have ranged from the protic solvents water and methanol, to the dipolar aprotic DMSO. The main difference between the two solvent types<sup>174</sup> is their ability to solvate anions.

Protic solvents have a greater hydrogen bonding interaction with small anions such as OH<sup>-</sup>, Cl<sup>-</sup>, OMe<sup>-</sup> and are therefore better at solvating these species than larger anions like SCN<sup>-</sup>, I<sub>3</sub><sup>-</sup>, picrate where the negative charge is more dispersed. However dipolar aprotic solvents have a greater polarizability interaction with large, easily polarizable, anions and are therefore better at solvating these than smaller weakly polarizable species.

Crampton and Gold<sup>33</sup> concluded from n.m.r. measurements that only the efficiency and not the mode of interaction changed in transferring from say methanol to DMSO. However for highly activated substrates such as picryl chloride<sup>175</sup> there is a slow reaction with DMSO leading to picric acid.

Methoxide ions, not being easily polarized are therefore desolvated in DMSO compared with methanol and consequently become more effective as nucleophiles.

This is manifest in the increase, by several orders of magnitude, of the equilibrium constant from ca. 15 in methanol to ca. 10<sup>9</sup> l.mol<sup>-1</sup> in DMSO for the 1,3,5-trinitrobenzene-methoxide adduct. This increase of ca. 10<sup>8</sup> gives, to a rough approximation, the change in activity coefficient,  $\gamma_{\text{OMe}^-}^{\text{MeOH}} / \gamma_{\text{OMe}^-}^{\text{DMSO}}$ , in going from methanol to pure DMSO. Thus using Parker's nomenclature<sup>174</sup> the equilibrium constants in both solvents can be related by the following expression

$$K_{\text{MeOH}} = K_{\text{DMSO}} \frac{\gamma_{\text{Complex}}^{\text{MeOH DMSO}}}{\gamma_{\text{TNB}}^{\text{MeOH DMSO}} \gamma_{\text{OMe}^-}^{\text{MeOH DMSO}}}$$

The activity coefficients of the complex and the parent nitro-compounds should change in the same way and therefore cancel; being large polarizable species they should be better solvated by DMSO. As would be expected there is a large increase in the equilibrium constant for methoxide than for thiophenoxide (ca.  $10^4$ ) since the former is destabilised to a greater extent.

It was shown<sup>65</sup> that the increase in equilibrium constant on changing to DMSO (for the isomeric dicyanonitroanisoles) resulted from an increase in  $k_1$ , the rate constant for complex formation, and a decrease in  $k_{-1}$ , the rate constant for decomposition. The increase in  $k_1$  can be explained in terms of the desolvation of the methoxide ion making it a more effective nucleophile - a 'naked' species being able to attack a given site faster than one surrounded by a solvent cage. The smaller rates of reversal to parent in the aprotic medium are attributed to the stabilising effect of the solvent on the highly polarizable  $\sigma$ -complex.

The arguments on solvent effects presented above, though giving an adequate qualitative description, are really a gross over-simplification of the problem. A better understanding is obtained with a knowledge of the enthalpy and entropy changes involved. In fact calorimetric data<sup>176</sup> have been obtained for the 2,4,6-trinitroanisole-sodium methoxide reaction. The  $\Delta H_{\text{reaction}}$  is ca.  $63 \text{ kJ mol}^{-1}$  more exothermic in 95% DMSO than in methanol, the main contribution to this being the desolvation of the methoxide ions for which the heat of transfer from methanol to DMSO is endothermic by ca.  $42 \text{ kJ mol}^{-1}$ . For the 1,3,5-trinitrobenzene-thiophenoxide<sup>177</sup> system the driving force here is stabilisation of the complex, the heat of transfer being ca.  $42 \text{ kJ mol}^{-1}$ , similar to that of the 2,4,6-trinitroanisole-methoxide adduct.

Using 4-cyano-2,6-dinitroanisole and 4-nitro-2,6-dicyanoanisole Terrier et al<sup>56</sup> have shown that the stabilising effect of DMSO on the 1,1- and 1,3-

complexes is approximately the same, the ratio of the equilibrium constants being independent of the solvent composition. The ratio of the rate constants for complex formation is also not solvent dependent indicating that transition state stabilisation is the same.

Buncel<sup>172</sup> has measured the equilibrium constants (see Table 1.2) and enthalpy changes for the 1,3,5-trinitrobenzene-cyanide complex in alcoholic solvents ranging from methanol to t-butanol. The enthalpy change in methanol was approximately zero, the entropy change being small and positive. In t-butanol, however, the enthalpy change was ca. 63 kJ mol<sup>-1</sup> and the entropy change -26 e.u.. This shows that the main effect is desolvation of the cyanide ion.

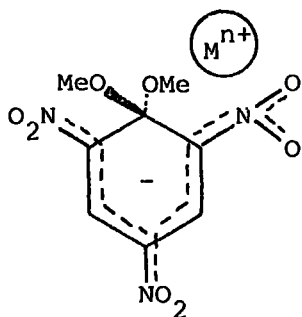
#### (iv) Micellar and cation effects

Since the similarity between protein and micelle structures and enzymic and micellar catalysis was recognized, there has been considerable interest in the effect of micelles on the rates of reactions.<sup>179</sup>

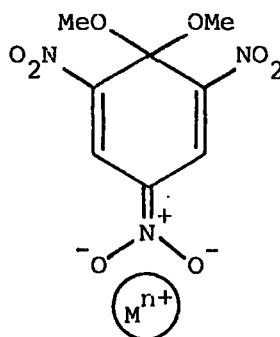
Fendler and coworkers<sup>180,181</sup> have investigated the effect of micellar surfactants on Meisenheimer complex equilibria. Cationic micelles such as hexadecyltrimethylammonium bromide increase the rate of formation and decrease the rate of decomposition of  $\sigma$ -complexes; anionic micelles have a retarding effect on complex formation and little effect on complex decomposition. Neutral micelles do not appear to effect complex formation or decomposition. The rate effects can be interpreted in terms of incorporation of the aromatic substrate into the micelle which, depending on its charge type, attracts or repels the anionic nucleophile.

It has been shown<sup>182-184</sup> that the increases in equilibrium constants for Meisenheimer complex formation which cannot be accounted for in terms of an acidity function or a salt effect, result from ion-pairing of cations with the  $\sigma$ -complex. The results show that the main effect on the equilibrium constant was a decrease in the rate of complex decomposition and that the order of ion-pairing effectiveness was  $\text{Ba}^{2+} > \text{Ca}^{2+} \gg \text{Na}^+ \sim \text{K}^+ > \text{Li}^+$ .

It was suggested that the ion-associate is of the form (1.93) with the cation held by a cage effect between the two oxygen atoms of the methoxy groups



(1.93)



(1.94)

and the electronegative substituent in the ortho position. This was favoured over the specific association of the cation with the para nitro group (1.94) since the 1,3,5-trinitrobenzene-methoxide equilibrium is only slightly affected by the presence of added cations.

Evidence for ion-pairing and the formation of (1.93) in particular has recently been shown from work with spiro-complexes<sup>185</sup> and 1,1-dimethoxy-complexes in the presence of crown ethers.<sup>186</sup> Values for the equilibrium constants for spiro-complex formation do not vary with base concentration and added salts unlike the analogous 1,1-dimethoxy-complexes. Formation of (1.93) is presumably not favoured sterically in the case of spiro-complex. In the presence of 18-crown-6-ether, equilibrium and rate constants for complex formation from a number of substituted dinitroanisoles were virtually independent of sodium methoxide concentration. The association constant for sodium ions with 18-crown-6-ether is  $2 \times 10^4 \text{ l.mole}^{-1}$ ,<sup>187</sup> some two orders of magnitude greater than values calculated for association with Meisenheimer complexes, and hence the concentration of free sodium ions available for association with the  $\sigma$ -adducts will be small in the presence of a slight excess of crown ether.

CHAPTER 2

EXPERIMENTAL

SOLUTIONS AND PREPARATION OF SUBSTRATES

A. Solvents

Water - Distilled water was boiled to remove carbon dioxide and subsequently protected from the atmosphere, by passing through a stream of nitrogen.

Methanol - AnalaR (A.R.) grade material was used without purification.

Ethanol - Commercial material used without purification.

Dimethyl sulphoxide - The commercial material was allowed to stand over calcium hydride for two or three days to remove water and then fractionated under reduced pressure, the middle fraction being collected.

Deuterated solvents - Deuterium oxide, tetradeuteriomethanol, deuteriochloroform and hexadeuteriodimethylsulphoxide, all of which were of isotopic purity >99%, were commercial samples used without purification.

B. Base and nucleophile solutions

Sodium hydroxide - A.R. sodium hydroxide pellets were washed several times with boiled-out distilled water and the washing discarded. The remaining solid was dissolved in more distilled water. The solution was standardised with 0.1M hydrochloric acid using phenol red indicator.

Aqueous buffer solutions<sup>187</sup> - Depending on the pH range required, aqueous buffer solutions were prepared by taking 50 ml. of 0.025M borax (pH range 8.00-10.80), 0.05M potassium dihydrogen phosphate (5.80-8.00) or 0.05M potassium hydrogen phthalate (2.20-5.90) and making up to 100 ml. with the appropriate volume of 0.1M hydrochloric acid or sodium hydroxide and water. More acidic buffers were prepared by adding a known volume of standard sodium hydroxide solution to the appropriate carboxylic acid to give the required  $[\text{RCOOH}]/[\text{RCOO}^-]$  ratio. The pH of the solutions was checked with an E.I.L. Model 23A direct reading pH-meter immediately before use. Acetic,

monochloroacetic and formic acids (98-100%), commercial samples, were used without purification. The acetic and formic acids were standardised against 0.1M sodium solution using phenolphthalein as indicator. Hydrochloric acid solutions were prepared by diluting A.R. concentrated acid ( $d = 1.18$ ) and standardising against 0.1M sodium hydroxide.

Sodium methoxide - Freshly cut pieces of sodium were washed with methanol and then immediately dissolved in A.R. methanol, which was purged with dry nitrogen prior to and during the addition of the sodium. The methoxide solution was centrifuged and the resulting clear solution titrated against standard hydrochloric acid.

Potassium and lithium methoxides - These solutions were prepared in an analogous manner to that for sodium methoxide.

Substituted sodium thiophenoxides - A weighed amount of the appropriate thiophenol was dissolved in a known volume of absolute alcohol and the required quantity of standardised sodium hydroxide solution in water added, the solution being made up with the necessary volume of solvent to give the composition 95/5 (v/v) ethanol-water, the solvent system used. A sufficient excess of the thiophenol was used to ensure a negligible equilibrium concentration of hydroxide and ethoxide ions.

Aqueous sodium sulphite - A.R.  $\text{Na}_2\text{SO}_3 \cdot 7\text{H}_2\text{O}$  was dried in an oven at  $140^\circ\text{C}$ . Solutions of known concentration were made up from the anhydrous solid and boiled-out distilled water.

#### C. Added salts

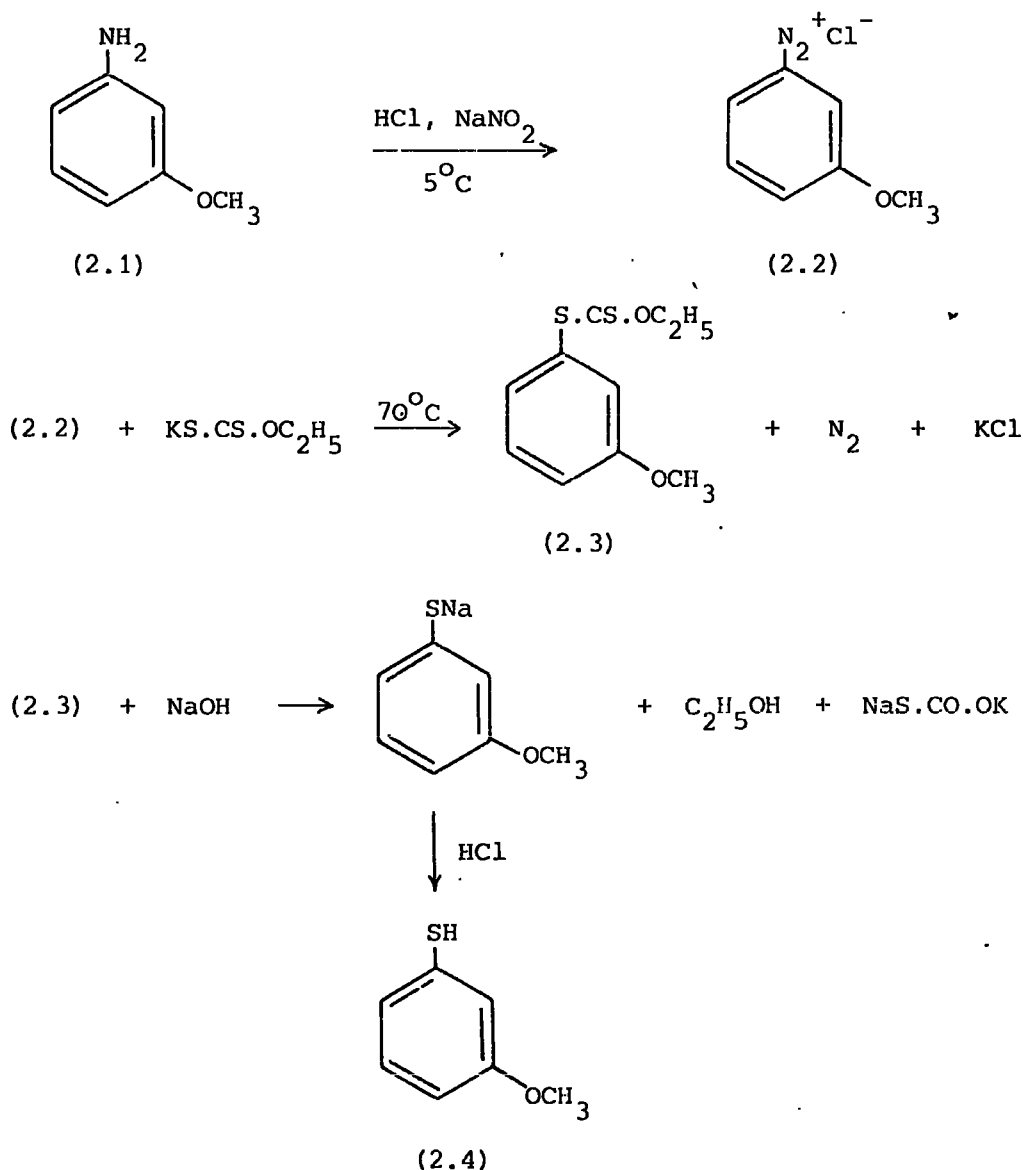
Sodium chloride, barium chloride and sodium sulphate, used to maintain constant ionic strength, were dried A.R. grade reagents.

#### D. Substituted thiophenols, $\text{RC}_6\text{H}_4\text{SH}$

The following were commercial specimens: R = H, 4-fluoro, 4-chloro, 4-bromo, 4-methyl, 3-methyl, 2-methyl, 4-t-butyl, 4-amino, 2-amino and 4-nitro.

Thiols with R = 3-chloro, 3-bromo, 3-methoxy, 4-methoxy, 3-acetyl and 4-acetyl were prepared from the corresponding anilines via the xanthate esters.<sup>188,189</sup>

The preparation of 3-methoxythiophenol was typical.



Concentrated hydrochloric acid (77 ml.) was added with stirring to m-anisidine (2.1) (50 gm., 0.4 mole). The precipitated amine hydrochloride was dissolved by adding water (ca. 80 ml.) and warming. The solution was cooled to 4-5°C before being diazotised with a pre-cooled solution of sodium nitrite (28 gm.) in water (ca. 140 ml.). The temperature was maintained at 5°C throughout the diazotisation (ca. 2 hours).

The resulting red oily solution was added, with stirring, over 1½ hours to a solution of potassium ethyl xanthate (65 gm.) and sodium carbonate (55 gm.)

in water (400 ml.) at 70°C. To prevent decomposition of the diazonium salt (2.2), only a portion of the solution was in the dropping funnel at any one time, the remainder being kept in an ice bath. After the addition, the temperature was maintained at 70°C for a further 35 minutes. The dark red-brown solution was cooled in an ice bath before the xanthate ester (2.3) was decanted from the aqueous layer.

A solution of sodium hydroxide (55 gm.) in water (120ml.) was added to the xanthate ester in methanol (500 ml.) and the mixture heated under reflux in a nitrogen atmosphere for 3 hours. After the hydrolysis, an equal volume of water was added and the solution acidified with concentrated hydrochloric acid. Most of the resulting red-brown oil was decanted off and the aqueous layer extracted several times with ether. The combined oil and ether extracts were dried with CaCl<sub>2</sub> overnight. After removing the ether, the product (2.4) was fractionally distilled under reduced pressure (ca. 5-10 mm Hg), the middle fraction being collected (ca. 90-100°C) (lit. 96-100°C/9-10 mm Hg).<sup>190</sup>

All thiophenols thus prepared and liquid commercial specimens were purified immediately prior to use by g.l.c. on a column packed with 17% 2-cyanoethylmethylsilicone on Chromosorb P.

The p.m.r. spectra of the thiols diluted with carbon tetrachloride indicated the expected structures and showed the absence of major impurities.

#### E. Aromatic nitro-compounds

1,3,5-Trinitrobenzene and 2,4-dinitrochlorobenzene were recrystallised commercial specimens, m.p.'s 121°C and 51°C respectively (lit. 122.5°C and 51°C).<sup>190</sup>

Picric Acid - Commercial picric acid was recrystallised from methanol to constant m.p. 122°C (lit. 122.5°C).<sup>190</sup>

Picramide, m.p. 191°C (lit. 192°C)<sup>190</sup> and N,N-dimethylpicramide, m.p. 141°C (lit. 138°C)<sup>190</sup> were recrystallised samples prepared in earlier work.<sup>159</sup>



and 8.8 p.p.m., of relative intensity 1:2, ascribed to the aldehydic and ring protons respectively of 4-bromo-3,5-dinitrobenzaldehyde (2.7). The washed product was recrystallised from methanol. Yield 10gms. m.p. 124-29°C (lit. 126°C).<sup>192</sup>

4-Methoxy-3,5-dinitrobenzaldehyde - The bromo-compound (7.4 gm.) was dissolved in the minimum volume (ca. 60 ml.) of warm methanol (50°C). 1.1 Equivalents of sodium methoxide (11.8 ml., 2.54M in methanol) were added slowly with stirring. An immediate orange-red colouration was produced which faded slightly after the methoxide addition. After about 3 hours, a yellow solid separated and most of the methanol was removed. Water was added, the solid dissolved and a dark brown oil separated. The aqueous layer was decanted off and the oil washed with more water. Recrystallisation from petroleum ether (40/60°) produced pale yellow needles, m.p. 87°C (lit. 86°C).<sup>192</sup>

1-(2-Hydroxyethoxy)-2,4-dinitronaphthalene, 1-(2-hydroxyethoxy)-2,4-dinitrobenzene and 1-(2-hydroxyethoxy)-2,6-dinitrobenzene were samples prepared in earlier work.<sup>184</sup>

1-(2-Hydroxyethoxy)-2,4,6-trinitrobenzene was prepared using the method of Blanksma and Fohr.<sup>193</sup> Sodium hydroxide (5.4 gm.) in water (5 ml.) and ethylene glycol (42 ml.) were added to a solution of picryl chloride (11 gm.) in ethylene glycol (20 ml.) and dioxan (4 ml.). The stirred mixture was heated at 60-70°C for 12 hours. The deep red solution was neutralised with dilute sulphuric acid. A yellow oil was deposited which slowly solidified. Recrystallisation from water gave pale yellow crystals, m.p. 62°C (lit. 61°C).<sup>193</sup>

1-(3-Hydroxypropoxy)-2,4-dinitronaphthalene - Sodium (0.57 gm.) was dissolved in propane-1,3-diol (35 ml.). A slurry of 1-chloro-2,4-dinitronaphthalene (6.3 gm.) in the diol (ca. 50 ml.) was slowly added to the stirred solution of the sodium salt, the mixture being warmed on a water bath. After approximately an hour, the red solution was poured into water (ca. 750 ml.). After a short time, solid precipitated from the red solution. Adding a

drop of concentrated sulphuric acid resulted in discharge of the red colour giving a pale yellow solid in a yellow solution. The product was filtered off at the pump and washed several times with water. After drying over  $P_2O_5$  under vacuum, the crude solid was dissolved in warm benzene and pale orange-brown needles appeared on standing. Further crystallisation resulted on the addition of petroleum ether (80/100<sup>o</sup>), m.p. 93-5<sup>o</sup>C. (Found: C, 52.9; H, 4.1; N, 10.0%. Required: C, 53.4; H, 4.1; N, 9.6%).

1-(4-Hydroxybutoxy)-2,4-dinitronaphthalene was prepared in a similar way, using the same quantities of reagents. The butane-1,4-diol was warmed to assist reaction with sodium. The product was worked up as described above. Precipitation from benzene with petroleum ether (80/100<sup>o</sup>) produced a pale yellow solid, m.p. 71-2<sup>o</sup>C. (Found: C, 55.8; H, 5.5; N, 8.6%. Required: C, 54.9; H, 4.6; N, 9.2%).

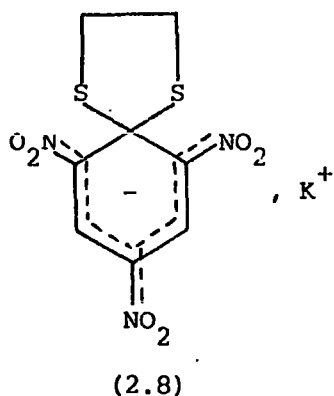
1-(2-Methoxy)-2,4-dinitronaphthalene - The sodium salt of 2-methoxyethanol, prepared by dissolving sodium (1 gm.) in the alcohol (50 ml.), was slowly added (over ca. 1 hour) to 1-chloro-2,4-dinitronaphthalene (10.5 gm.) slurried in 100 ml. of the alcohol. The temperature was gradually raised to 50<sup>o</sup>C during the addition and maintained there for a further hour. After cooling to room temperature, the orange-red solution was poured into a large volume of water (ca. 800 ml.) acidified by the addition of a drop of concentrated sulphuric acid. The precipitated yellow solid was collected, dried and recrystallised from a benzene-80/100<sup>o</sup> petroleum ether mixture giving pale yellow crystals. Yield 8 gms., m.p. 76-8<sup>o</sup>C. (Found: C, 53.1; H, 3.3; N, 9.2%. Required: C, 53.4; H, 4.1; N, 9.6%).

1-(2-Hydroxythioethoxy)-2,4-dinitrobenzene - The method used by Culvenor et al<sup>194</sup> for the picryl derivative was followed. 2,4-Dinitrochlorobenzene (8.1 gm.) was dissolved in absolute alcohol (150 ml.) and 2-mercaptoethanol (3.1 ml.) added. A slurry of anhydrous sodium acetate (4 gm.) in

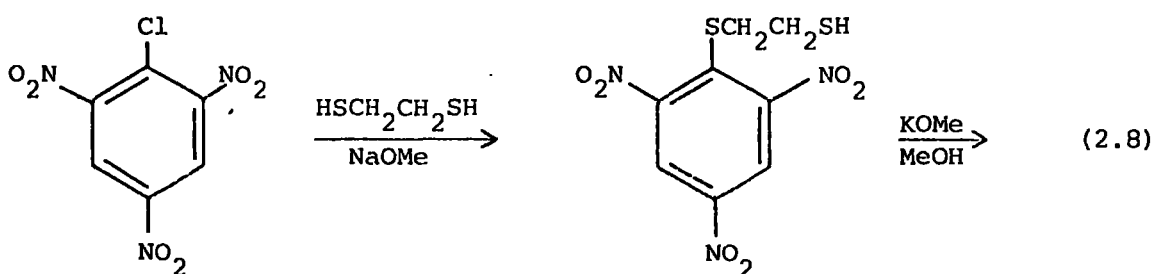
absolute alcohol (100 ml.) was slowly added to the stirred solution. The mixture was then heated to 70° for two hours on a water bath. After cooling, the product was precipitated when the solution was poured into a large volume of water. The fine, pale yellow solid was filtered off, dried and recrystallised from benzene giving bright yellow needles, m.p. 101-3°C (lit. 100°C).<sup>194</sup>

1-(2-Hydroxythioethoxy)-2,4,6-trinitrobenzene was prepared in a similar way. To picryl chloride (10 gm.) in absolute alcohol (125 ml.) 2-mercaptoethanol (3.1 ml.) was added. Sodium acetate (4 gm.) was slurried in absolute alcohol (100 ml.) and slowly added with stirring to the solution which turned from yellow to orange-red. After stirring for 1½ hours the solution was warmed to 50°C on a water bath for ca. 30 minutes. After cooling, the mixture was poured into water and the precipitated product collected. Recrystallisation from benzene of the dry solid yielded the required material, m.p. 72-3°C (lit. 72°C).<sup>194</sup>

Spiro-complex derived from 1-(2-mercaptothioethoxy)-2,4,6-trinitrobenzene - Pietra<sup>195</sup> has recently prepared the spiro-complex (2.8) from picryl chloride



and ethane-1,2-dithiol. Picryl chloride (5 gm.) was dissolved in methanol



(ca. 60 ml.) and ethane-1,2-dithiol (1.7 ml.) was added. One equivalent of sodium methoxide in methanol was slowly added to the stirred solution at room temperature. There was an immediate red colouration which faded after the addition of each of the first few drops. Addition of further drops of sodium methoxide resulted in a persistent red colour. One equivalent of potassium methoxide in methanol was added. After about half an hour some toluene was added and the mixture cooled to ca.  $-20^{\circ}\text{C}$ . The dark red powder was collected. (Found: C, 18.3; H, 1.5; N, 8.1%. Required: C, 28.0; H, 1.7; N, 12.2%). Analysis for potassium chloride revealed a content of ca. 18%. The p.m.r. spectrum of the product in  $\text{DMSO-d}_6$  showed the absence of any major organic impurities and was therefore used without any further purification.

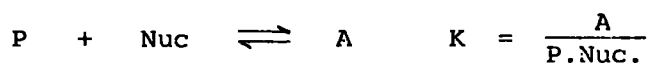
#### SPECTROSCOPIC TECHNIQUES

##### A. Visible spectroscopy

Since the complexes produced from the interaction of aromatic nitro-compounds with nucleophiles have large extinction coefficients<sup>6,8</sup> in the visible region, ( $\epsilon_{\text{max}}$  ca.  $2 \times 10^4 \text{ l.mol}^{-1} \text{ cm}^{-1}$ , 400-700 nm), visible spectroscopy has been the major tool used in studying both the kinetics and equilibria of the interactions.

The general spectral shapes were recorded on a Unicam SP800 or SP8000 instrument at room temperature ( $20 \pm 2^{\circ}\text{C}$ ). For quantitative work, accurate optical density measurements at suitable wavelengths were determined on a Unicam SP500 spectrophotometer, fitted with a thermostatted cell compartment ( $25^{\circ}\text{C}$ ). Solutions, on which measurements were to be performed, were made up immediately before use by appropriate dilution of freshly prepared stock solutions.

For reactive substrates (P) with large equilibrium constants (K) complete



conversion to complex (A) was achieved in dilute base solution where any further interactions (e.g. higher complex formation) are negligible. In such cases the extinction coefficient,  $\epsilon_A$ , of the complex (A) at the appropriate wavelength was found directly using the Beer-Lambert law:

$$\text{optical density (O.D.)} = \log_{10} \frac{I_0}{I} = \epsilon_A C_A l$$

where  $C_A$  is the concentration of complex (equal to the stoichiometric substrate concentration for complete conversion) and  $l$  is the pathlength of the cell (1 cm., unless otherwise stated). Knowing  $\epsilon_A$ , the concentration of the complex in less basic solutions could then be determined.

For less reactive substrates, with small equilibrium constants, where side reactions involving uncomplexed substrate took place, the extinction coefficient of the complex in water was determined by an extrapolation procedure<sup>166</sup> as follows. On going from water to 100% DMSO the equilibrium constants for complex formation increase by several orders of magnitude.<sup>6,8</sup> Thus for a given base concentration it was possible to achieve complete conversion to complex at some H<sub>2</sub>O-DMSO composition, above which increasing the DMSO content resulted in a linear increase in the optical density. Extrapolation of the linear portion to 0% DMSO gave a value for the optical density for complete conversion to complex in pure water.

#### B. Proton magnetic resonance spectroscopy

Two instruments were used: a 60 MHz Varian HA56/60 and a 90 MHz Bruker HX90E. Measurements were usually made at ambient probe temperature ( $40 \pm 2^\circ\text{C}$  for the Varian and  $22 \pm 2^\circ\text{C}$  for the Bruker) unless otherwise stated. Freshly prepared solutions of substrate (ca. 0.2M) in the appropriate solvent were used. Tetramethylsilane (TMS) was used as internal reference. However for aqueous solutions the sodium salt of 4,4-dimethyl-4-silapentane sulphonic acid was used.

### C. Stopped-flow spectrophotometry

This has been the main technique employed for the kinetic measurements in the present work. However, because of its versatility the stopped-flow apparatus has also been used for equilibrium and spectral shape measurements as described later.

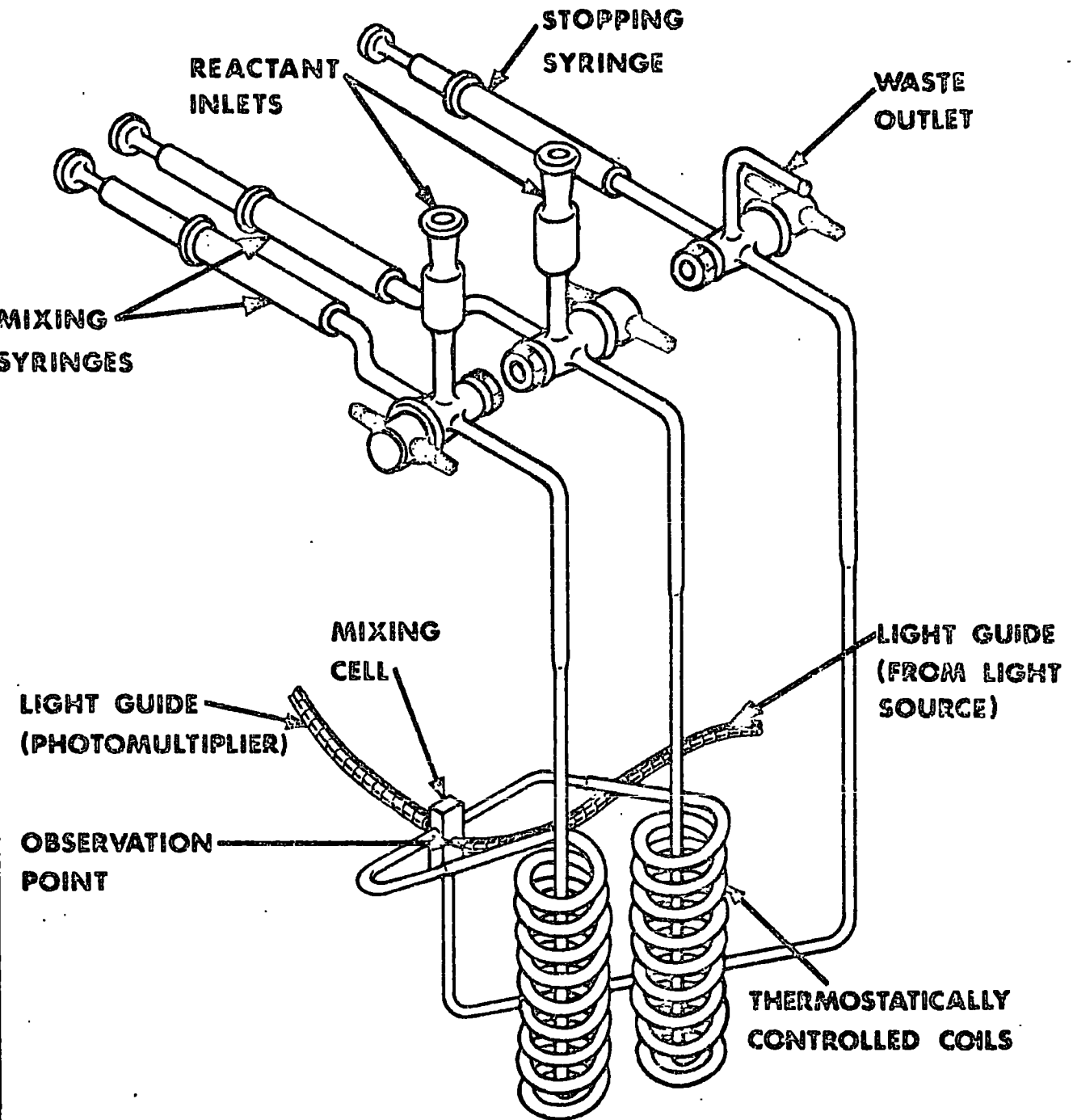
The instrument used here was a 'Canterbury' SF-3A apparatus (Nortech Laboratories Ltd., formerly NP Consulting) recently developed by Caldin and coworkers.<sup>196</sup> As it is somewhat different to other stopped-flow instruments at present available (e.g. the Durrum D-100 Series), some comment is perhaps appropriate.

Monochromatic light from a Bausch and Lomb high intensity grating monochromator (1350 grooves/nm., 500 nm blaze 33-86-76) was directed into a silica measuring cell (2 mm. path length) by means of a flexible silica light guide and from there by another light guide to a photomultiplier. The signal from the photomultiplier was fed to a Tektronix 5103N D11 single-beam storage oscilloscope. (Time-base calibrated within 5% and volts/division calibrated to better than 2%).

One advantage of the present system is that optical alignment is eliminated by use of the flexible light guides and consequently the mixing chamber and observation tube can be immersed in a large thermostat tank together with glass coils containing the reactant solution (see Figure 2.1). Thus the solution reaching the mixing chamber and the mixed solutions are at thermostat temperature.

The two reactant solutions are taken from reservoirs into 2 ml. driving syringes which are connected to the thermostatted coils by glass tubing. Activation of the syringes either pneumatically or manually causes reactant solutions at bath temperature to mix in the chamber and pass into the light path. Spent reactant solution is forced out into a stopping syringe the plunger of which comes up abruptly against a block, thus stopping the flow. At the same time the oscilloscope time-base is triggered by a microswitch and

FIGURE 2.1



the reaction in the stationary solution is followed spectrophotometrically.

Only reproducible traces were measured for both kinetic and equilibrium measurements.

As stated earlier, besides kinetic measurements, equilibrium and spectral shape measurements were made. They were performed on substrates where the life-time of the complex was too short to observe by conventional means. Optical density measurements were determined as follows. The base solution was placed in the light path and the voltage to the photomultiplier adjusted (between 0.5 and 1 kV., depending on wavelength) to give, typically, 5 volts for full scale deflection - 0 volts corresponding to 0% transmission and 5 volts corresponding to 100% transmission.

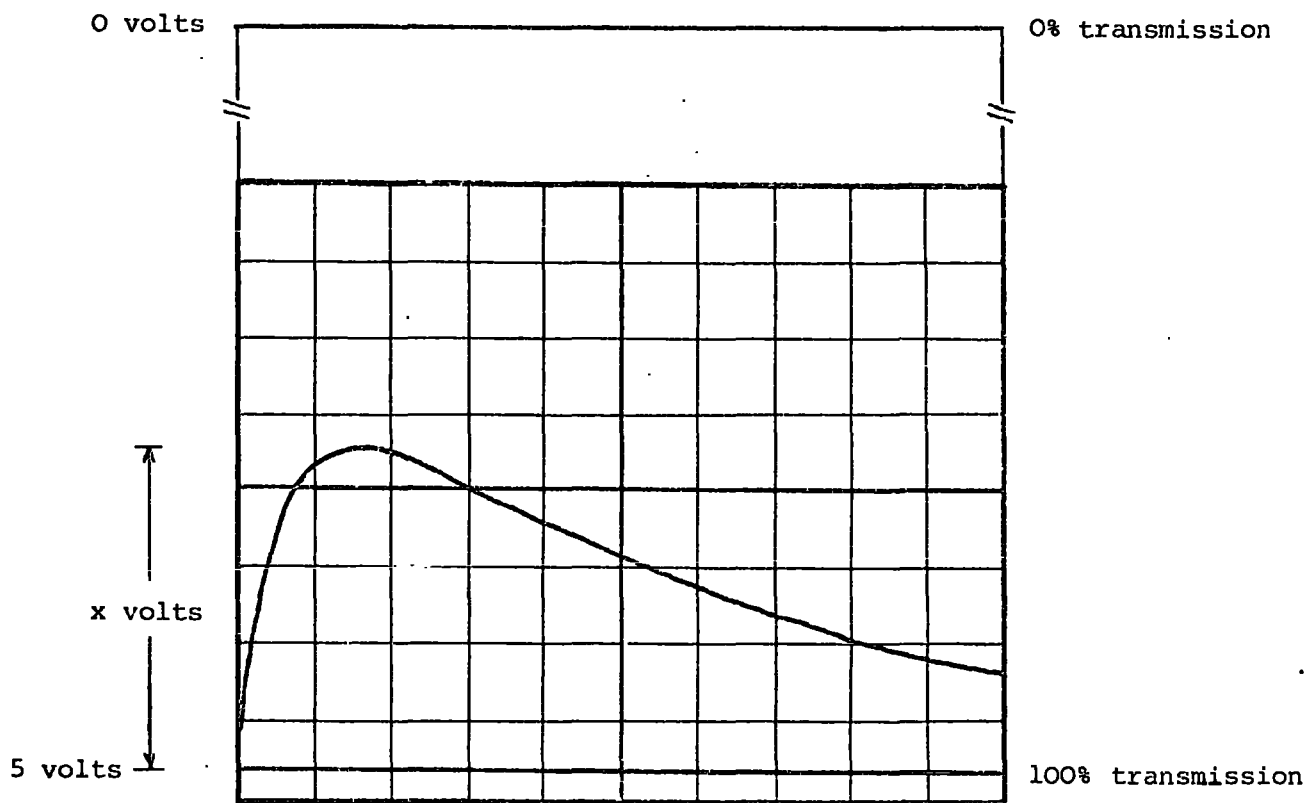


FIGURE 2.2

With base alone in the light path the photomultiplier signal was displayed and stored on the oscilloscope screen. This was taken as 100% transmission (5 volts) i.e. it was assumed the base solution had zero absorption. Without allowing the signal to be displayed, both reactants were flushed through the cell a number of times to remove any effects of back diffusion into the coils.

Runs were performed until voltage changes were reproducible. A typical trace is shown in Figure 2.2.

Knowing the mV/division setting on the oscilloscope, the voltage change,  $x$ , was determined. The optical density was calculated as follows:

light intensity,  $I$ , reaching photomultiplier  $\alpha$  voltage,  $V$ , displayed.

Thus,

$$\frac{V_o}{V} = \frac{I_o}{I}$$

$$\text{Hence O.D.} = \log_{10} \frac{I_o}{I} = \log_{10} \frac{V_o}{V} = \log_{10} \frac{5}{5-x}$$

Such optical density measurements were repeated at different wavelengths so obtaining a spectrum.

For kinetic measurements scale readings were not converted to optical densities but were used as a direct measure of concentration. This is valid if the optical density changes involved are  $<0.02$ . This can be demonstrated in Table 2.1.

TABLE 2.1

Vertical Scale Reading ( $y$ )	Volts (V)*	$\log \left( \frac{V_o}{V} \right) = \text{O.D.}$	$y \times \left[ \log \frac{V_o}{V} \text{ for } y=1 \right]$
0	5.00	0.0000	-
1	4.98	0.0017	0.0017
2	4.96	0.0035	0.0035
3	4.94	0.0052	0.0052
4	4.92	0.0070	0.0070
5	4.90	0.0088	0.0087
6	4.88	0.0106	0.0104
7	4.86	0.0123	0.0122
8	4.84	0.0141	0.0139

\* For 20 mV/division and 5 volts for 100% transmission

As can be seen the scale is approximately linear in optical density.

For a kinetic run a suitable time-base was chosen so that ca. 90% of the reaction could be followed on the first trace. The oscilloscope was then triggered by depressing the 'automatic trigger' button to obtain an 'infinity' scale reading. Where a reliable 'infinity' reading could not be obtained owing to secondary reactions, rate constants were calculated by Guggenheim's method.<sup>197</sup> Rate constants quoted, the average of 5-6 kinetic runs, were reproducible within 5%.

CHAPTER 3

A STOPPED-FLOW KINETIC STUDY OF THE REACTION OF SUBSTITUTED  
THIOPHENOXIDE IONS WITH 1-CHLORO-2,4-DINITROBENZENE - CORRELATION  
OF THE RATES WITH PROTON AND CARBON BASICITIES

INTRODUCTION

Thiophenoxide ions and thiolate ions in general, having been recognised to be strong nucleophiles, have been widely used in studies of nucleophilic substitutions.<sup>14,17</sup> Also it has been noted<sup>198</sup> that sulphur nucleophiles often have greater reactivities than would be expected from their Brønsted basicities. The latter give a measure of their thermodynamic affinity for protons represented in equation 3.1



Thus for the reaction of a series of oxygen nucleophiles with chloroacetate ions a good correlation was observed between the rates and the basicities of the nucleophile. However sulphite and thiosulphate ions had enhanced reactivity compared to their Brønsted basicities.<sup>198</sup>

This variance between reactivity and basicity has been explained in terms of the ease of polarisation. An atom whose outer electron shell is easily distorted (polarised) will readily adjust to the requirements of the transition state.<sup>199</sup> Thus for a series of atoms, those which have outer occupied electronic shells further away from the nucleus are necessarily more readily polarisable and therefore should be better nucleophiles.

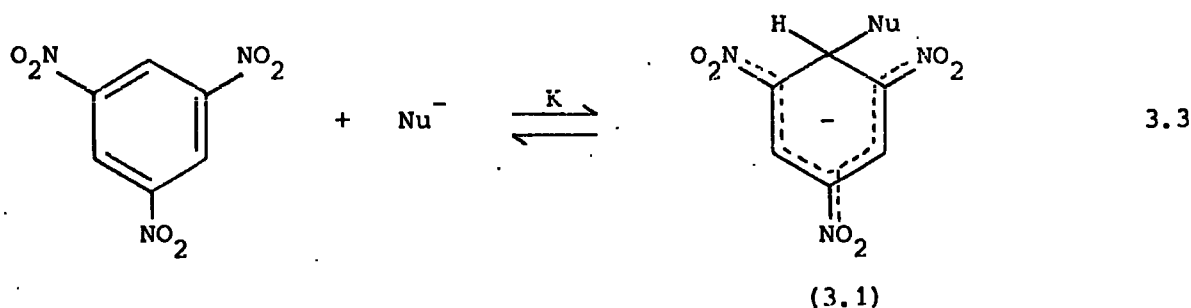
Basic and nucleophilic species clearly can be defined in a similar manner in that both possess a pair of electrons capable of being donated to an electrophilic substrate. However it has been suggested<sup>17</sup> that nucleophilicity should refer to rate phenomena and basicity to equilibria. Swain and Scott<sup>200</sup> have quantified the relative reactivity of various nucleophiles in terms of the linear free energy relationship (3.2) where  $k$  is the second-order rate

$$\log \frac{k}{k_0} = S_n \quad 3.2$$

coefficient for nucleophilic attack by a species whose nucleophilicity is  $n$  on a substrate whose sensitivity to a change in nucleophile is  $S$ ;  $k_0$  is the rate coefficient for attack by water, the solvent to which the above equation applies. The limitations of an equation such as (3.2) were realised and a number of modifications have been made to take into account such factors as polarisability and basicity.<sup>17</sup>

It has also been suggested that it is not reasonable to compare nucleophilic reactivity with basicity in the Brønsted sense. Rather the displacing tendencies (nucleophilicities) of various reagents at a given atom should be compared with their thermodynamic affinities for that atom. Therefore nucleophilic displacements at carbon, for example, should be referred to the 'carbon basicity',<sup>173</sup> or the thermodynamic affinity of the nucleophile for carbon.

The formation of stable Meisenheimer-type complexes from 1,3,5-trinitrobenzene and a variety of nucleophiles has provided a convenient and relatively easy method for determining carbon basicities. Equilibrium constants,  $K$ ,



which can readily be determined, were obtained for a series of oxygen and sulphur nucleophiles with 1,3,5-trinitrobenzene, and the values obtained used as a measure of carbon basicity. For the sulphur bases  $\text{EtS}^-$  and  $\text{PhS}^-$ ,<sup>160</sup> carbon basicities are considerably enhanced compared to the values expected from their proton basicities. This can be explained in terms of the 'hard'

and 'soft' acid and base concept,<sup>201</sup> sulphur being a 'soft' polarisable base has a greater affinity for the 'soft' carbon atom than the 'hard' proton.

In the present work the nucleophilicities of a series of substituted thiophenoxide ions have been determined by measuring the rates of displacement of chloride ion from 1-chloro-2,4-dinitrobenzene in 95/5 (v/v) ethanol-water. The rates are compared with the 'carbon basicities' of the thiophenoxides as measured by their thermodynamic affinities for 1,3,5-trinitrobenzene in the same solvent system.

#### EXPERIMENTAL

The preparation and purification of the solvents of the substituted thiophenols is described in Chapter 2. Kinetic measurements were made using a 'Canterbury' stopped-flow spectrophotometer. The increase with time of the concentrations of the reaction products, substituted phenyl 2,4-dinitrophenyl-sulphides, was measured. These have absorption maxima in the 350 nm region. However owing to the absorption of the substituted thiophenoxides at this wavelength measurements were made in the 400-410 nm range where the products still show significant absorption and where there is little interference from absorption by the substrate or the nucleophiles.

Nevertheless some difficulty was encountered with thiophenoxide ions containing 3-acetyl-, 4-acetyl- and 4-nitro-substituents. These thiophenoxides show considerable absorption in the visible region and therefore to obtain a suitable change in optical density, measurements were made at longer wavelengths (410-500 nm) using a substrate concentration of  $5 \times 10^{-4}$  M. For the 3- and 4-acetyl-substituents an increase in absorption with time was observed at the wavelength of observation. However 2,4-dinitrophenyl 4-nitrophenyl sulphide has a smaller absorption than the 4-nitrothiophenoxide ion at 503 nm and thus a decrease in optical density with time was observed. The slowness of the reaction in this case also gave rise to some difficulty. A stable baseline and hence a reliable 'infinity' value could not be obtained. Rate constants were therefore evaluated using Guggenheim's method.<sup>197</sup>

The concentration of 1-chloro-2,4-dinitrobenzene used for the other substituted thiophenoxides was  $5 \times 10^{-5} \text{ M}$  and two base concentrations ( $1 \times 10^{-2}$  and  $5 \times 10^{-3} \text{ M}$ ) were used in the presence of different excesses of the substituted thiophenol.

A well-known problem encountered when working with thiols is their aerial oxidation<sup>202</sup> to the corresponding disulphides especially in the presence of base. Since the rate of oxidation was expected to be several orders of magnitude slower than the substitution reaction under investigation no special precautions were taken. However measurements were made as soon as possible after preparation of the solutions.

RESULTS AND DISCUSSION

In all cases the concentration of the substituted thiophenoxide ions was in large excess (>10) over that of the substrate and the measured changes in absorbance followed first-order kinetics. A set of data from a typical run is given in Table 3.1. The calculated second-order rate coefficients  $k (= k_{\text{obs}}/$

TABLE 3.1

Rate Data for the Reaction of 1-Chloro-2,4-dinitrobenzene ( $5 \times 10^{-5} \text{ M}$ ) with Sodium 3-Methylthiophenoxide ( $1.03 \times 10^{-2} \text{ M}$ ) in 95% (v/v) Ethanol-Water at 25°

<u>Time</u> (sec)	<u>Scale Reading</u> (arbitrary units)	$k_{\text{obs}}$ ( $\text{sec}^{-1}$ )
0	1.95	-
0.05	2.80	3.32
0.10	3.57	3.46
0.15	4.21	3.48
0.20	4.75	3.50
0.25	5.20	3.50
0.35	5.85	3.46
0.40	6.10	3.44
0.50	6.50	3.43
0.65	6.91	3.45
$\infty$	7.50	-

[NaSC<sub>6</sub>H<sub>4</sub>R]) were, within experimental error, independent of the excess concentration of thiol. This can be shown by reference to the data for 4-bromothiophenol given in Table 3.2. The thiolate anion is therefore the

TABLE 3.2

Invariance of Second-order Rate Coefficient, k, with Base and Thiol Concentrations for Reaction of 1-Chloro-2,4-dinitrobenzenes with Sodium 4-Bromothiophenoxide

<u>[4-Bromothiophenol]</u> <sub>stoich</sub> (M)	<u>[HO<sup>-</sup>]</u> <sub>stoich</sub> (M)	<u>k<sub>obs</sub></u> (sec <sup>-1</sup> )	<u>k</u> (l.mole <sup>-1</sup> sec <sup>-1</sup> )
0.02	0.005	0.44 ± .01	88 ± 2
0.03	0.005	0.43 ± .01	86 ± 2
0.02	0.010	0.85 ± .02	85 ± 2
0.04	0.010	0.86 ± .02	86 ± 2

sole nucleophilic species and unionised thiol does not participate in the reaction.

The second-order rate coefficients for the reaction of the substituted thiophenoxides with 1-chloro-2,4-dinitrobenzene are given in Table 3.3. It is well established that the products of the reaction are the substituted phenyl 2,4-dinitrophenyl sulphides.<sup>203,204</sup> The nucleophilic displacement of chloride ion by thiophenoxide will occur by the accepted two-step intermediate complex mechanism.<sup>17</sup> Bunnett et al<sup>204,205</sup> have shown that the rate-determining step is the formation of the intermediate complex (3.2).

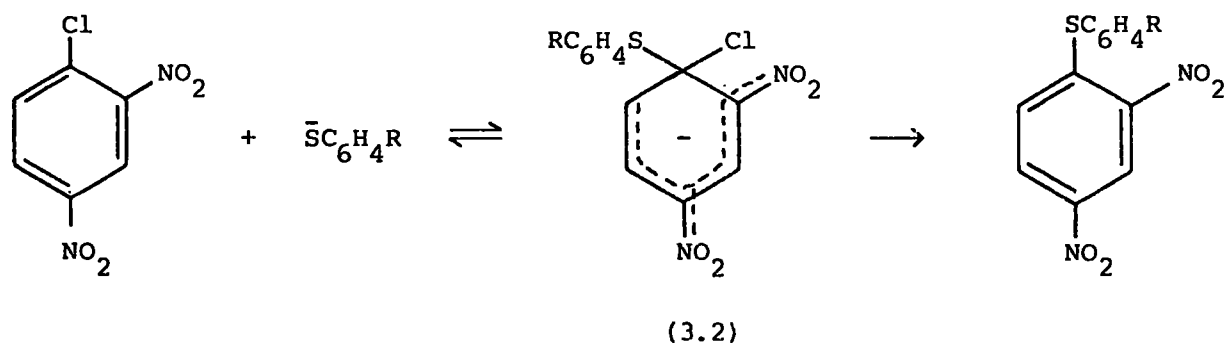


TABLE 3.3

Rate Coefficients for the Reaction of Substituted Thiophenoxides with  
1-Chloro-2,4-dinitrobenzene in 95% (v/v) Ethanol-Water at 25°

<u>Substituent</u>	$\frac{10^{-2}k}{(1.\text{mol}^{-1}\text{sec}^{-1})}$	$\frac{K^a}{(1.\text{mol}^{-1})}$	$\frac{pK_a^b}{}$
1. 4-NH <sub>2</sub>	21.0 ± 0.6	2.65 x 10 <sup>-3</sup>	10.45
2. 4-OMe	9.6 ± 0.2	450	9.71
3. 4-Me	6.4 ± 0.1	143	9.60
4. 3-Me	3.4 ± 0.1	69	9.52
5. H	1.90 ± 0.05	43.2	9.28
6. 4-F	1.82 ± 0.04	34	8.88
7. 3-OMe	1.96 ± 0.04	29.5	9.14
8. 4-Cl	0.98 ± 0.02	6.0	8.41
9. 3-COCH <sub>3</sub>	1.20 ± 0.02	4.9	8.27
10. 4-Br	0.86 ± 0.02	4.8	8.33
11. 3-Cl	0.56 ± 0.01	2.2	8.09
12. 3-Br	0.61 ± 0.01	2.0	8.20
13. 4-COCH <sub>3</sub>	0.32 ± 0.02	0.5	7.47
14. 2-Me	2.15 ± 0.03	70	9.87
15. 2-NH <sub>2</sub>	3.4 ± 0.1	59	9.02
16. 4-NO <sub>2</sub>	0.03 ± 0.01		

<sup>a</sup> Equilibrium constants referring to equation 3.3 ( $\text{Nu}^- = \text{RC}_6\text{H}_4\text{S}^-$ )  
from reference 189.

<sup>b</sup> The apparent acid dissociation constants ( $K_a$ ) for the thiophenols from  
reference 189.

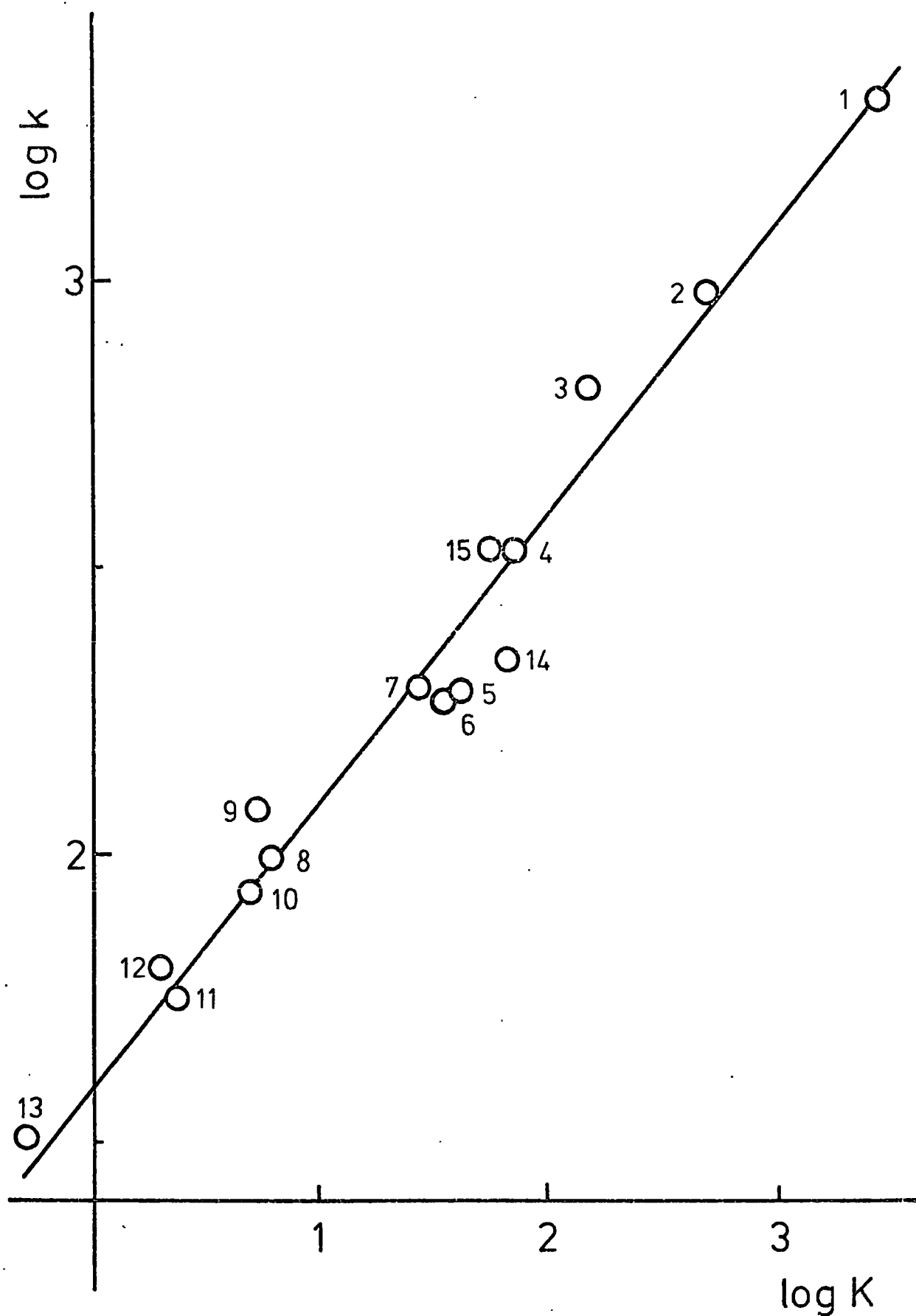
It does not seem unreasonable to assume that the intermediate complex (3.2) might bear some resemblance to the 1,3,5-trinitrobenzene adduct (3.1;  $\text{Nu} = \text{RC}_6\text{H}_4\text{S}$ ). In fact a plot (Figure 3.1) of  $\log k$  versus  $\log K$  gives an excellent straight line (slope =  $0.51 \pm 0.2$ , correlation coefficient  $r = 0.99$ ). However a similar plot (Figure 3.2) of  $\log k$  versus  $\text{pK}_a$  values for the corresponding thiols shows more scatter (slope =  $0.65 \pm 0.05$ ,  $r = 0.97$ ). There is thus definitely better correlation of the nucleophilic reactivities of the substituted thiophenoxide ions with their carbon basicities than with their proton basicities.

Correlation even holds good for the ortho substituted thiophenoxides where steric effects are most likely to be dominant. This is exemplified in the case of the 2-methylthiophenoxide ion. Figure 3.2 indicates that the reactivity of 2-methylthiophenoxide is considerably reduced compared with that expected from its proton basicity. This is likely to result from steric interaction in the transition state leading to the intermediate (3.2). However the point for 2-methylthiophenoxide falls virtually on the line in Figure 3.1 showing that the steric effects almost cancel. This is not surprising since it would be expected that the transition state for the substitution reaction might be similar to the  $\sigma$ -complex (3.1;  $\text{Nu} = \text{RC}_6\text{H}_4\text{S}$ ).

Furthermore, it has been argued<sup>206</sup> that the decrease in acid strength of 2-methylthiophenols and 2-alkylthiophenols in general compared with their 3- and 4-isomers results from steric inhibition of solvation of the anion. This factor will tend to increase its reactivity as a nucleophile while steric crowding in the transition state has an opposite effect.

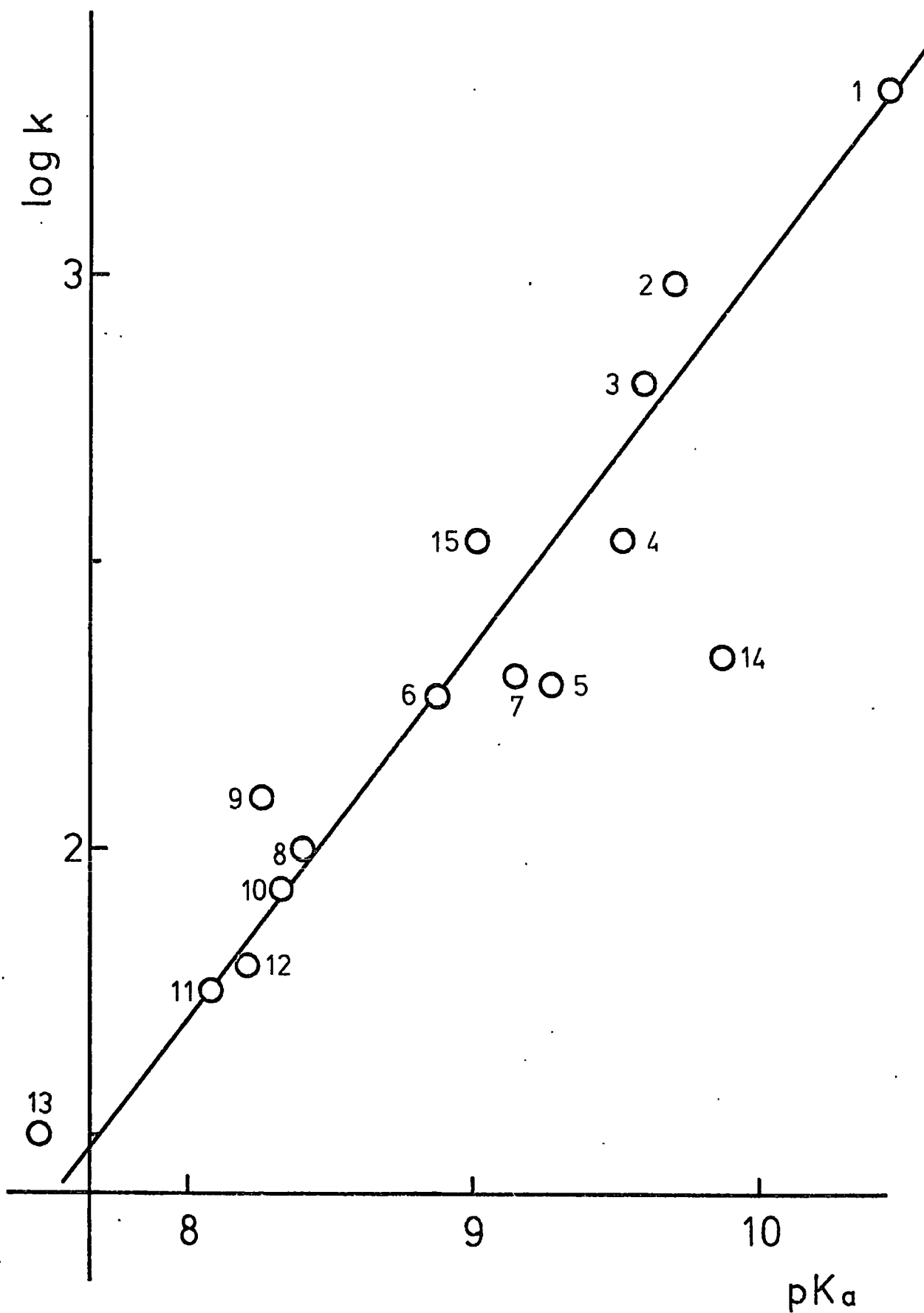
However when the ortho substituent is an amino group there is a very slight enhancement in the rate compared with that expected from the proton basicity. This can probably be explained in terms of a stabilising effect resulting from hydrogen bonding of the amino group with the ortho nitro group in the transition state.

FIGURE 3.1



Correlation of nucleophilic reactivities and carbon basicities for substituted thiophenoxides. The numbering of substituents corresponds with Table 3.3.

FIGURE 3.2



Correlation of nucleophilic reactivities and proton basicities for substituted thiophenoxides. The number of substituents corresponds with Table 3.3.

It is interesting to note that excellent agreement is observed (see Table 3.4) between the nucleophilic reactivities of substituted thiophenoxide ions and their carbon basicities for a number of systems quoted in the literature. In fact two groups of workers<sup>208-210</sup> have reported good carbon basicity-rate correlations for reaction of thiophenoxides with three different types of substrate since the equilibrium constants for 1,3,5-trinitrobenzene-thiophenoxide complexes were published.<sup>189</sup> In all cases quoted in Table 3.4, correlation coefficients for the carbon basicity-rate plots are significantly closer to unity than for the proton basicity plots.

Rate data are often correlated by means of these Brønsted-type plots or the Hammett  $\sigma$  relationship. The magnitude of the Brønsted  $\beta$  values and the value of  $\rho$  are often assumed to measure the extent of charge development in the transition state. Thus for the present work a  $\beta$  value of ca. 0.5 could be interpreted in terms of roughly half the negative charge being transferred from the nucleophile to the substrate in the transition state. However the use of the Hammett relation and Brønsted  $\alpha$  and  $\beta$  values has recently been criticised,<sup>213</sup> in that such interpretations of linear free energy relations are not consistent with structure-reactivity correlations invoking variable transition states. This is well exemplified in the similarity of the  $\beta$  values for the reaction of substituted thiophenoxide ions with p-nitrophenyl acetate (0.54)<sup>208</sup> and p-chloronitrobenzene (0.47)<sup>207</sup> and for the present work (0.51), the rate constants encompassing six orders of magnitude.

It is obvious that rate-equilibrium correlations will improve as the differences in structure and environment of the compounds being compared are decreased and it was suggested<sup>209</sup> that carbon basicities derived from Meisenheimer complexes were particularly suitable for correlation with the rates of nucleophilic addition at activated olefins since both involve attack at an  $sp^2$  carbon. This is borne out by the better correlation for substrates whose site of attack is an  $sp^2$  carbon over those where attack is either at an  $sp^3$  (4-substituted benzylbromides<sup>211</sup>) or an  $sp$  hybridised carbon (ethyl-

TABLE 3.4

Brønsted  $\beta$  Values and Correlation Coefficients (r) for Rate Correlations  
of a Number of Substrates and Substituted Thiophenoxides with Carbon  
(log K) and Proton ( $pK_a$ ) Basicities

	<u>Substrate</u> <sup>a</sup>	<u><math>pK_a</math></u> <sup>b</sup>		<u>log K</u>		<u>Reference</u>
		$\beta$	r	$\beta$	r	
1.	1-Chloro-2,4-dinitrobenzene	0.65	0.97	0.51	0.99	
2.	4-X-Nitrobenzenes X = F	0.49	0.950	0.39	0.992	207
	Cl	0.59	0.961	0.47	0.990	
	Br	0.58	0.947	0.46	0.983	
	I	0.57	0.938	0.45	0.978	
3.	4-Nitrophenyl acetate	0.72	0.961	0.54	0.998	208
4.	Phenylvinylsulphone	0.37	0.901	0.30	0.995	209
5.	2-X-3-Y-thiophenes					210
	X = NO <sub>2</sub> , Y = Br	0.43	0.91	0.36	0.969	
	X = Br, Y = NO <sub>2</sub>	0.42	0.832	0.34	0.937	
6.	4-X-Benzyl bromides					211
	X = OMe	0.14	0.889	0.12	0.954	
	Me	0.20	0.925	0.13	0.947	
	H	0.20	0.939	0.15	0.964	
	Br	0.26	0.950	0.19	0.981	
	NO <sub>2</sub>	0.37	0.932	0.28	0.983	
7.	Ethyl phenylpropiolate	0.24	0.879	0.23	0.916	212
8.	Ethyl 4-methoxyphenylpropiolate	0.24	0.90	0.24	0.958	212

<sup>a</sup> Solvent: 1            95/5 (v/v) ethanol-water  
                   2,5,6        Methanol  
                   4            50/50 (v/v) ethanol-water  
                   3,7,8        Ethanol

<sup>b</sup>  $pK_a$  values were those for the appropriate solvent system. The values in methanol not quoted in the literature were taken to be those in 95/5 (v/v) ethanol-water less 0.6.

phenylpropiolate<sup>212</sup>). This may be fortuitous since different sets of thiol substituents were used in each case and therefore such a comparison is not strictly justified. However the undoubtedly better rate correlation generally observed with carbon basicities results from the fact that in each reaction a carbon-sulphur bond is formed.

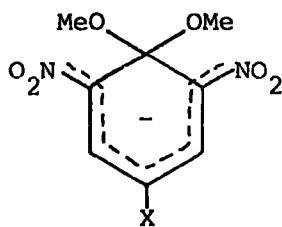
CHAPTER 4

AN EQUILIBRIUM AND KINETIC STUDY OF METHOXIDE ADDITION TO

AN ACTIVATED ANISOLE CONTAINING AN ALDEHYDE GROUP

INTRODUCTION

Meisenheimer complexes resulting from methoxide addition to highly activated anisoles have been extensively investigated.<sup>6,8</sup> Results indicate that at least two electron-withdrawing substituents are required for complexes to be observed. Equilibrium and kinetic measurements have been made for complexes of the type (4.1) derived from 4-X-2,6-dinitroanisoles and methoxide ions in



(4.1)

methanol and data for a number of such complexes are collected in Table 4.1.

TABLE 4.1

<u>X</u>	<u>K<sub>1</sub></u> (l.mol <sup>-1</sup> )	<u>k<sub>1</sub></u> (l.mol <sup>-1</sup> sec <sup>-1</sup> )	<u>k<sub>-1</sub></u> (sec <sup>-1</sup> )	<u>Reference</u>
SO <sub>2</sub> CF <sub>3</sub>	1.5 x 10 <sup>6</sup>	141	2.6 x 10 <sup>-4</sup>	59
NO <sub>2</sub>	17,000	17.3	1.04 x 10 <sup>-3</sup>	64
CN	280	6.1	22.0 x 10 <sup>-3</sup>	64
CO <sub>2</sub> Me	6 (5*)	0.36	6 x 10 <sup>-2</sup>	181
CF <sub>3</sub>	2 (1.2*)	-	-	181
Cl	4.3 x 10 <sup>-3</sup>	-	-	166
H	9 x 10 <sup>-5</sup>	-	-	166

\* Revised values based on measurements made in the presence of 18-crown-6-ether - reference 185

A number of electron-withdrawing groups, X, have thus been used, but there is no report of Meisenheimer complex formation from an anisole containing an aldehyde group which appears to have considerable electron-withdrawing ability reflected in its  $\sigma$  or  $\sigma^-$  values.<sup>214</sup>

With aldehydes it is well known that competing reactions occur involving solvent or nucleophilic addition to the carbonyl group forming the hemiacetal or hemiacetal ion.<sup>215</sup> Considerable work has been done on the hydration of aliphatic aldehydes and ketones, notably by Bell and coworkers.<sup>216</sup> Studies on substituted benzaldehydes in basic solution have indicated the formation of hemiacetals,<sup>217</sup> and recently equilibrium constants have been determined for the reversible addition of hydroxide ion to the carbonyl group of a series of substituted benzaldehydes in water.<sup>218</sup> The abnormal activation parameters observed for the nucleophilic substitution reaction of chloronitrobenzenes containing aldehyde or cyano groups with methoxide ion in methanol were attributed to the reversible formation of hemiacetal or imido ester respectively.<sup>219</sup>

The results which follow indicate that for 4-methoxy-3,5-dinitrobenzaldehyde in methanol competition exists between Meisenheimer complex and hemiacetal formation.

## EXPERIMENTAL

### P.m.r. measurements

Spectra were recorded at 60 MHz and at 90 MHz. Substrate solutions (ca. 0.2M) were made up in the appropriate solvent just before they were required. The Meisenheimer complex was generated in situ on adding, by syringe, methanolic sodium methoxide (2M) or lithium methoxide (1M).

### Visible spectral measurements

Spectral shapes were recorded on Unicam SP800 and SP8000 instruments. Optical density measurements for equilibrium and kinetic data were made at 25°C using a Unicam SP500 spectrophotometer. It was found convenient to make kinetic

measurements by addition from a syringe of a small volume of a concentrated solution of the parent aldehyde in methanol to a solution of methanolic methoxide which had previously been thermostatted in the measuring cell. Measurements were begun ca. 10 seconds after mixing and continued at suitable time intervals over 3-4 half-lives. Infinity readings were taken after 10 half-lives. The data for a typical run are given in Table 4.2. Rate and

TABLE 4.2

Rate Data for the Reaction of 4-Methoxy-3,5-dinitrobenzaldehyde  
( $3.9 \times 10^{-5}$  M) with Sodium Methoxide ( $2.02 \times 10^{-2}$  M) in Methanol at 25°C

<u>Time</u> (sec.)	<u>Optical Density*</u>	$10^3 k_{obs}$ (sec <sup>-1</sup> )
0	0.020	-
25	0.041	4.50
50	0.061	4.67
75	0.079	4.75
100	0.095	4.79
130	0.112	4.84
160	0.126	4.83
195	0.140	4.82
240	0.156	4.89
300	0.172	4.92
360	0.183	4.88
∞	0.217	-

\* Measured at 500 nm

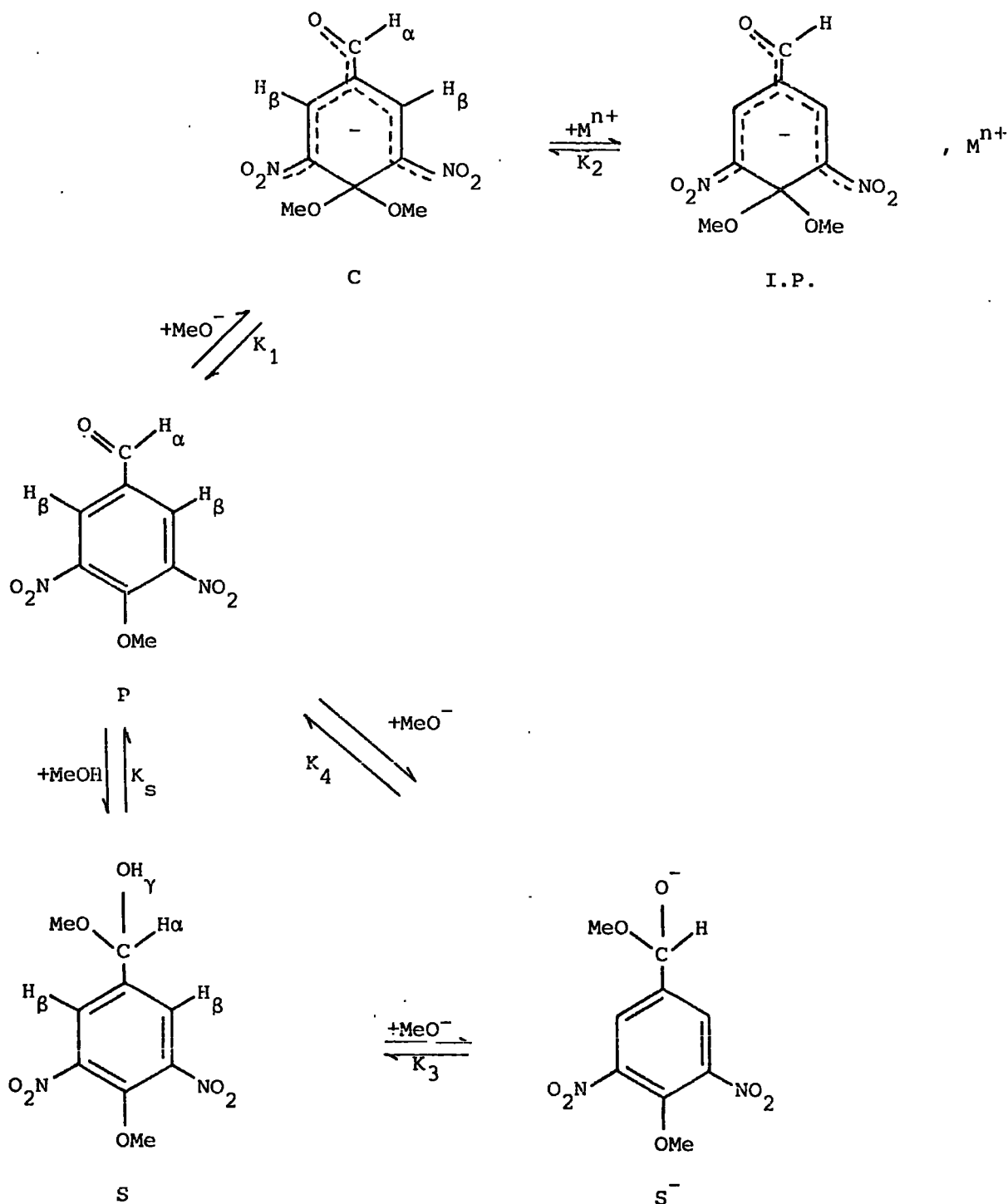
equilibrium measurements made by M.A. El Ghariani have been included for the sake of completeness.

## RESULTS AND DISCUSSION

### P.m.r. spectra

The spectrum of 4-methoxy-3,5-dinitrobenzaldehyde dissolved in deuteriochloroform shows three sharp singlets with shifts ( $\delta$ ) 10.1, 8.6 and 4.2 p.p.m. and relative intensities 1:2:3 which are attributed to the aldehydic, aromatic and methoxy protons respectively. In DMSO the spectrum is very similar, the shifts being  $\delta$ 10.1, 8.8 and 4.1 p.p.m.. Addition of a little concentrated sodium methoxide in methanol to the substrate in DMSO causes an immediate red colouration and new bands appear at  $\delta$ 9.13, 8.28 and 3.02 p.p.m. with relative intensities 1:2:6. On increasing the sodium methoxide concentration, these bands grow in intensity at the expense of those due to the parent. The new bands are consistent with the Meisenheimer complex (4.1; X = CHO) and the shifts to high field observed on complexation are similar to those found in analogous systems.<sup>6,8</sup>

However spectra obtained with methanol as solvent are more complicated. A solution of the parent in neutral methanol has a spectrum with three small bands at  $\delta$ 10.03, 8.67 and 4.1 p.p.m. attributed to the unchanged aldehyde. In addition more intense bands are observed which can be assigned to the hemiacetal (S in the scheme) formed by solvent addition to the carbonyl group. The ring protons ( $H_\beta$ ) give a singlet at  $\delta$ 8.22 p.p.m. while the CH ( $H_\alpha$ ) and OH ( $H_\gamma$ ) protons show spin-coupled bands at  $\delta$ 5.60 and 7.25 p.p.m. respectively. The low field portion of the spectrum is shown in Figure 4.1. The assignment given above is confirmed when tetradeuteriomethanol is used as solvent, the spectrum being similar to that in methanol except that the bands due to methanol addition at the carbonyl group are missing. Hemiacetal formation is fairly slow at 25°C and it is some minutes before equilibrium is established. Measurement of the relative intensities of the ring proton resonances at equilibrium gives a value for the equilibrium constant,  $K_s (= [S]/[P])$ , of  $8 \pm 1$ . Such quantitative equilibrium measurements for hemiacetal formation have recently been

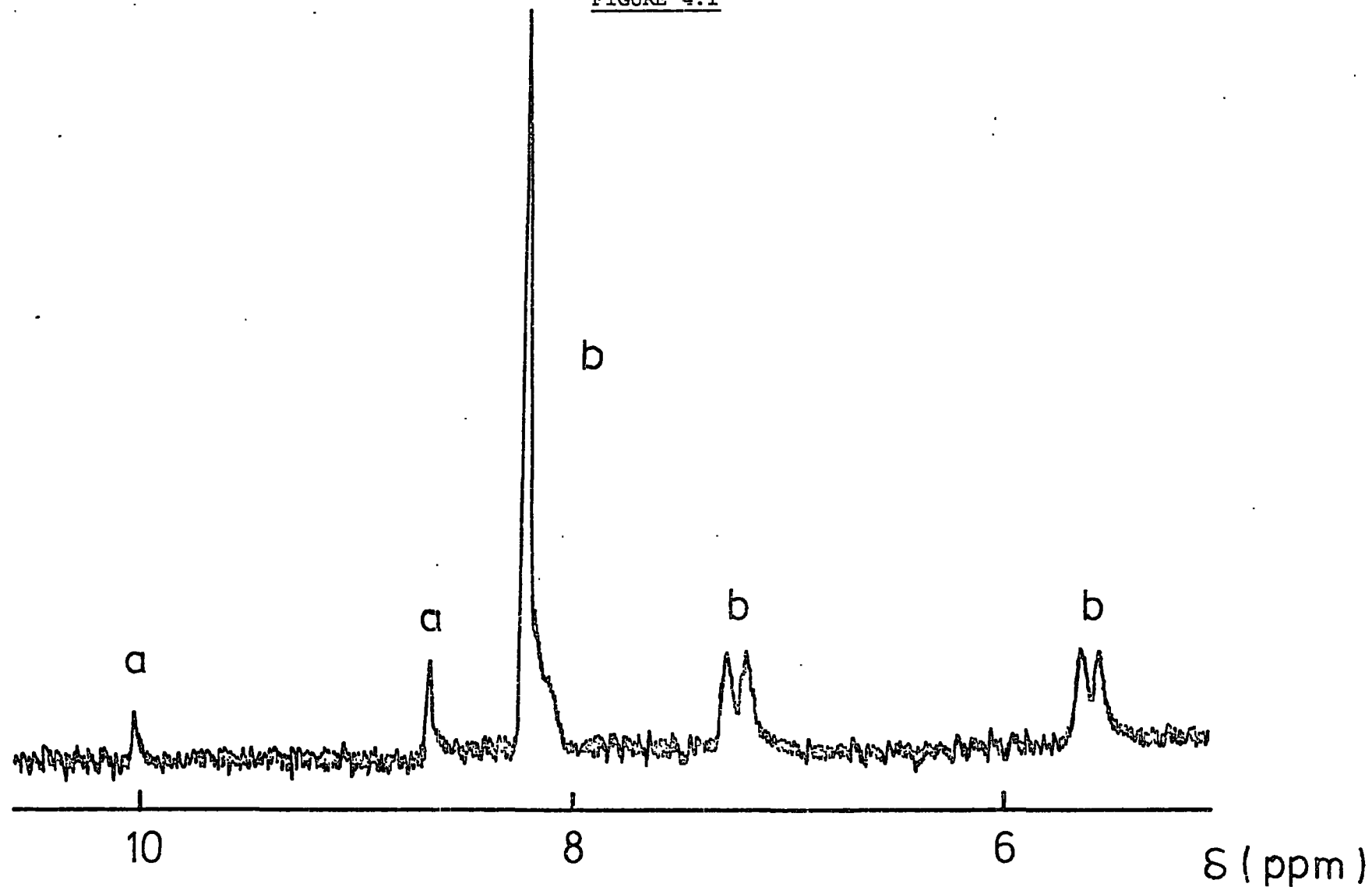


SCHEME

made for a series of substituted benzaldehydes in methanol. <sup>220</sup>

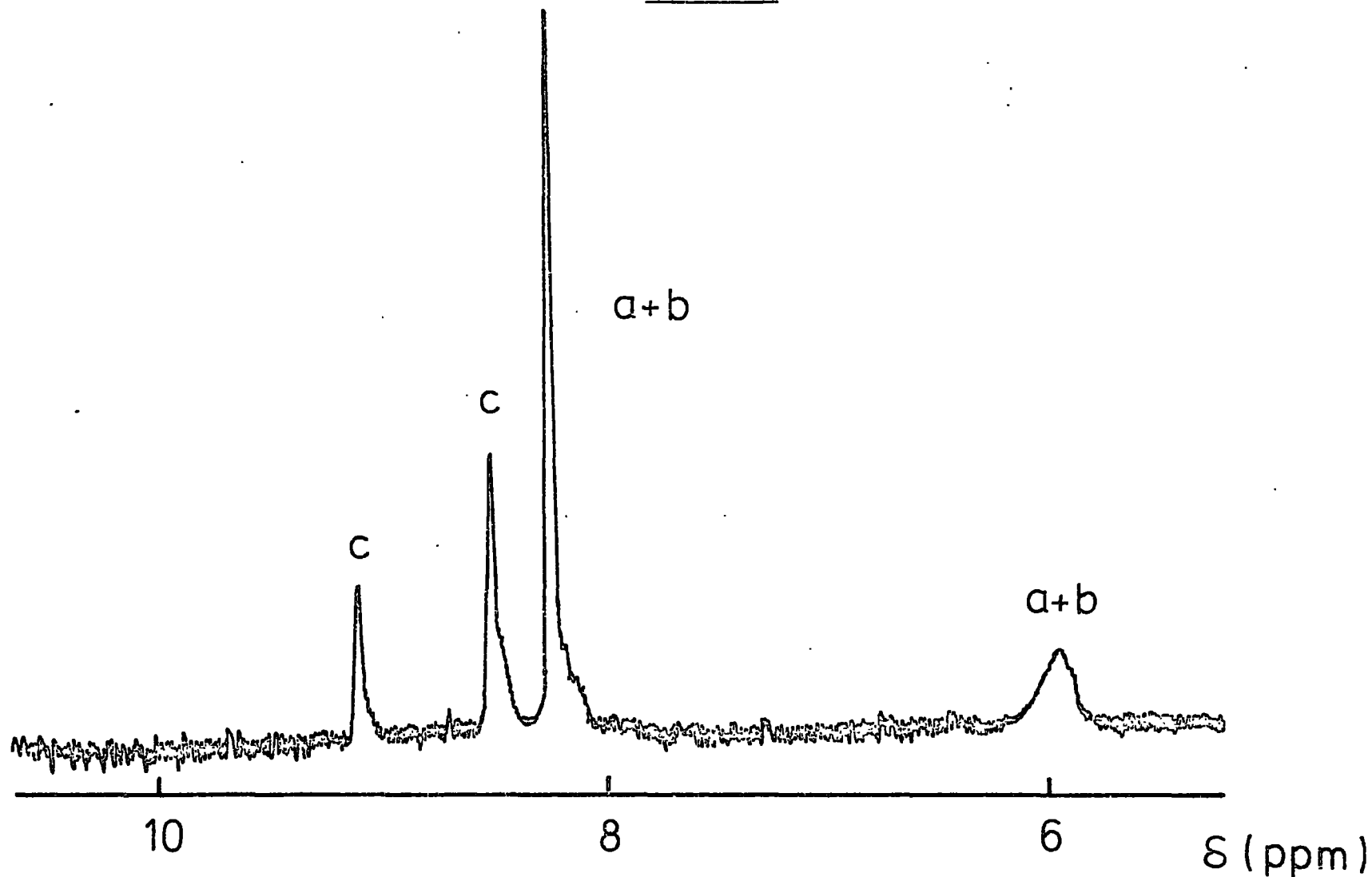
The addition of a little sodium methoxide to a solution of the parent in methanol results in the disappearance of the H<sub>γ</sub> resonance through proton exchange with the solvent (see Figure 4.2). Combined resonances are now

FIGURE 4.1



P.m.r. spectrum of 4-methoxy-3,5-dinitrobenzaldehyde (0.2M) in methanol. Bands labelled (a) are due to parent aldehyde and (b) to hemiacetal.

FIGURE 4.2



P.m.r. spectrum of 4-methoxy-3,5-dinitrobenzaldehyde (0.2M) in methanol containing sodium methoxide ( $[\text{NaOMe}]_{\text{stoich}} 0.08\text{M}$ ).

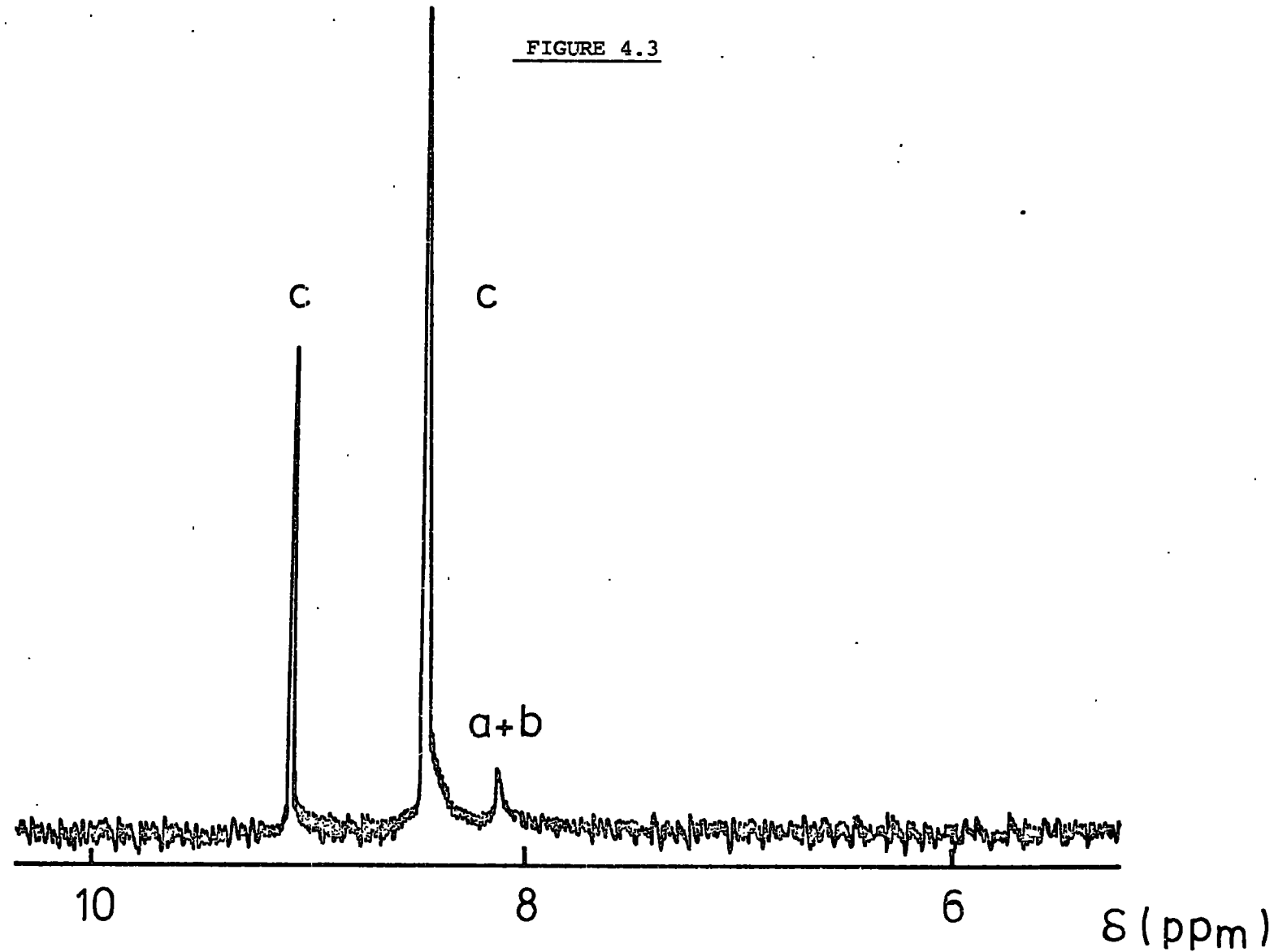
observed for the  $H_{\alpha}$  and  $H_{\beta}$  protons in the parent and hemiacetal. This indicates fairly fast exchange on the n.m.r. timescale. Addition of further methoxide causes the bands due to the Meisenheimer complex to increase at the expense of the combined parent and hemiacetal peaks (see Figure 4.3). Eventual complete conversion to complex is achieved with a sodium methoxide concentration of ca. 1M. However with lithium methoxide as added base, it is only possible to achieve ca. 50% conversion to complex even at high base concentrations. P.m.r. data for the parent aldehyde, Meisenheimer complex and hemiacetal are collected in Table 4.3.

#### Visible spectra

4-Methoxy-3,5-dinitrobenzaldehyde dissolved in methanol gives a colourless solution. In the presence of sodium methoxide a red colour develops and the spectrum shows maxima at 370 and 500 nm. This colour change is reversible on acidification. Since the charge on the hemiacetal ion,  $S^{-}$ , is isolated from the ring charge delocalisation is not possible and therefore the anion would not be expected to show any absorption in the visible region. Thus the observed spectrum is attributed to the Meisenheimer complex, C. The spectral shape is independent of base concentration but the optical density increased with increasing base concentration up to a concentration of ca. 1M when further increase caused no spectral change. Spectra of similar shape were obtained using lithium or tetra-n-butylammonium methoxides, however the limiting optical density achieved with lithium methoxide was only about half that obtained using the other two methoxides. This substantiates the p.m.r. data which indicates ca. 50% conversion to complex using lithium methoxide.

In methanol-DMSO mixtures spectra are similar to those in methanol but with the maxima shifted slightly to longer wavelengths. In media rich (>90%) in DMSO a transient yellow species was observed prior to the formation of the time stable complex (see Figure 4.4). By analogy with previous work,<sup>6,8,57</sup> this transient species is the isomeric Meisenheimer complex formed by methoxide addition to an unsubstituted ring carbon. As with other

FIGURE 4.3



P.m.r. spectrum of 4-methoxy-3,5-dinitrobenzaldehyde (0.2M) in methanol containing sodium methoxide ( $[\text{NaOMe}]_{\text{stoich}} 0.8\text{M}$ ).

TABLE 4.3

Chemical Shift Data [ $\delta$ (p.p.m.)]

<u>Solvent</u>	<u>Parent Aldehyde (P)</u>		
	<u>H<sub><math>\alpha</math></sub></u>	<u>H<sub><math>\beta</math></sub></u>	<u>OMe</u>
Deuteriochloroform <sup>a</sup>	10.1	8.6	4.2
Dimethyl sulphoxide <sup>a</sup>	10.1	8.8	4.1
Methanol	10.03	8.67	4.1
Tetradeteriomethanol	10.03	8.67	4.10

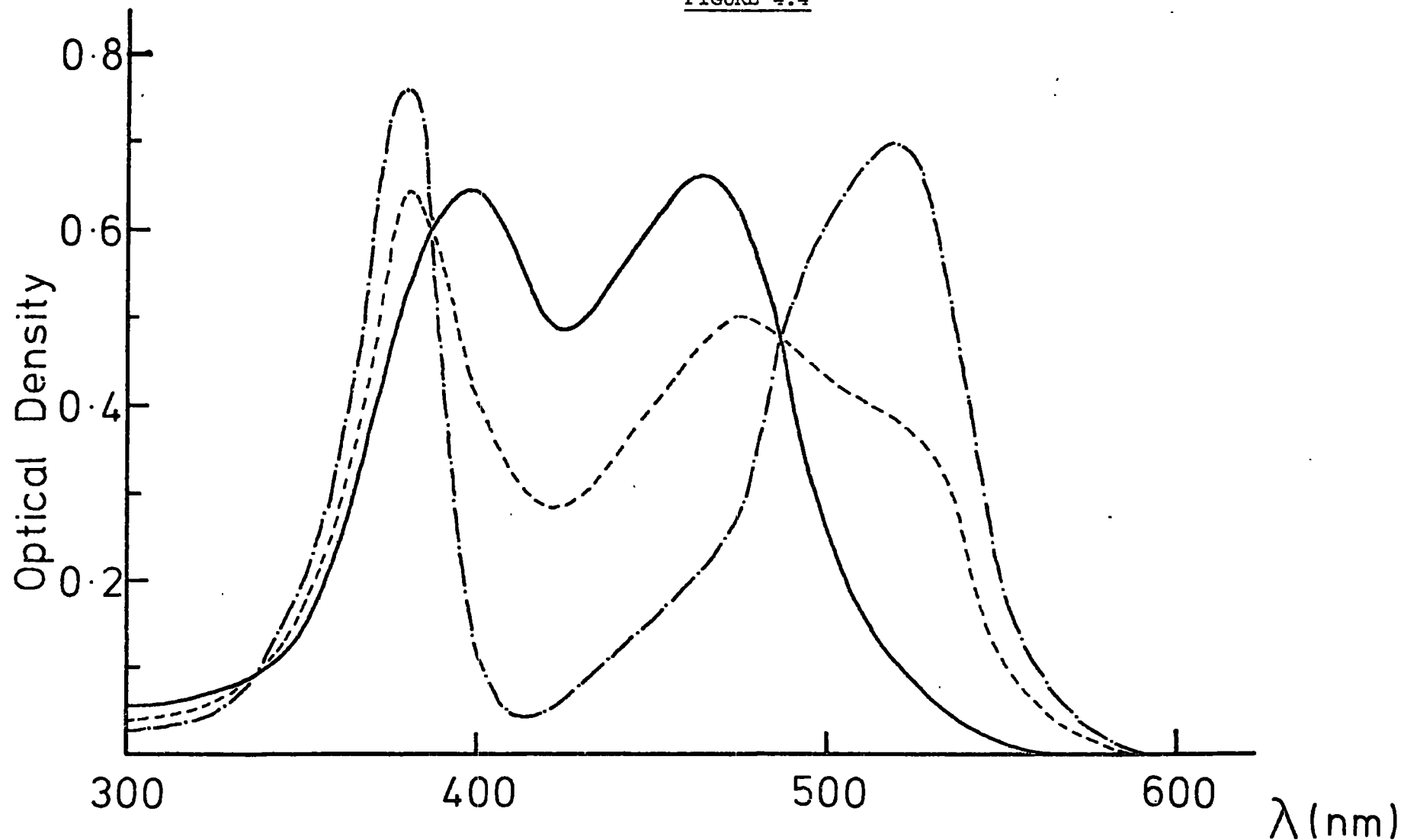
	<u>Meisenheimer Complex (C)</u>		
	<u>H<sub><math>\alpha</math></sub></u>	<u>H<sub><math>\beta</math></sub></u>	<u>OMe</u>
Dimethyl sulphoxide	9.13	8.28	3.02
Methanol	9.11	8.53	3.0

	<u>Hemiacetal (S)</u>				
	<u>H<sub><math>\alpha</math></sub></u>	<u>H<sub><math>\beta</math></sub></u>	<u>OMe (ring)</u>	<u>OMe</u>	<u>H<sub><math>\gamma</math></sub></u>
Methanol	5.60 <sup>b</sup>	8.22	4.02	3.5	7.25 <sup>b</sup>
Tetradeteriomethanol	5.60	8.23	4.02		

<sup>a</sup> Spectra recorded at 60 MHz

<sup>b</sup> These bands exhibit spin coupling with J ca. 7 Hz.

FIGURE 4.4



Visible spectrum of 4-methoxy-3,5-dinitrobenzaldehyde (ca.  $4 \times 10^{-5} \text{ M}$ ) in DMSO-methanol (96/4 v/v) containing sodium methoxide (ca.  $10^{-3} \text{ M}$ ). (—) Immediately after mixing reagents, (----) after ca. 5 minutes and (-·-·-) time stable spectrum.

1,3-complexes, its stability in methanol-rich media is too low for its observation. Visible spectral data for the 1,1- and 1,3-complexes is given in Table 4.4.

TABLE 4.4

Visible Spectral Data for the Isomeric Complexes of  
4-Methoxy-3,5-dinitrobenzaldehyde and Methoxide

	$\lambda_{\max}$	$10^{-4} \epsilon$	$\lambda_{\max}$	$10^{-4} \epsilon$
	(nm)	( $l.mol^{-1} cm^{-1}$ )	(nm)	( $l.mol^{-1} cm^{-1}$ )
1,1-complex <sup>a</sup>	370	1.9	500	1.5
1,3-complex <sup>b</sup>	398	1.7	465	1.7

<sup>a</sup> Methanol                      <sup>b</sup> 96/4 (v/v) DMSO-methanol

Equilibrium constants

Optical density measurements and equilibrium constants for lithium, tetra-n-butylammonium and sodium methoxides are given in Tables 4.5-4.8. The measurements can be interpreted in terms of the Scheme given earlier.

In neutral methanol the parent aldehyde, P, is in equilibrium with its hemiacetal, S, with an equilibrium constant,  $K_s (= [S]/[P])$  the value of which was directly determined from p.m.r. measurements. In basic solution, as with similar systems,<sup>215-219</sup> there will be an equilibrium between the hemiacetal and its conjugate base,  $S^-$ , denoted by  $K_3 (= [S^-]/[S][OMe^-])$ . There is also a direct path between P and  $S^-$  involving methoxide attack on the carbonyl group of the parent, the equilibrium constant for which,  $K_4 = [S^-]/[P][OMe^-] = K_s K_3$ . The equilibrium constant for Meisenheimer complex formation is  $K_1 (= [C]/[P][OMe^-])$ .

Evidence has been put forward<sup>182,183,185</sup> for the existence of ion-pairing of Meisenheimer complexes with cations in methanol. In the Scheme the association constant for ion-pairing is denoted by  $K_2 (= [I.P.]/[C][M^{n+}])$ . Such association constants generally decrease in the order barium > sodium >

TABLE 4.5

Equilibrium and Rate Constants<sup>a</sup> for the Reaction of 4-Methoxy-3,5-dinitrobenzaldehyde ( $3.9 \times 10^{-5}$  M) with Lithium Methoxide in Methanol at 25°C

<u>[LiOMe]</u> (M)	<u>O.D.</u> <sup>b</sup>	$\frac{K_C}{(l.mol^{-1})}$	$\frac{10^3 k_{obs}}{(sec^{-1})}$	$\frac{k_1^c}{(l.mol^{-1} sec^{-1})}$
0.0096	0.083	17.3	5.8	0.97
0.0192	0.13	15	5.9	0.94
0.038	0.17	11	7.8	1.1
0.058	0.195	8.7	7.9	1.05
0.096	0.22	6.4	7.9	1.21
0.193	0.24	3.7	10	1.5
0.92	0.29	(1.1)	-	-

<sup>a</sup> Data obtained by M.A. El Ghariani

<sup>b</sup> Measured at 500 nm

<sup>c</sup> Calculated from equation 4.10 using the values  $K_3 = 30 \text{ l.mol}^{-1}$ ,  $K_S = 8$

TABLE 4.6

Equilibrium and Rate Constants<sup>a</sup> for the Reaction of 4-Methoxy-  
3,5-dinitrobenzaldehyde ( $3.9 \times 10^{-5}$  M) with Tetra-n-butylammonium  
Methoxide in Methanol at 25°C

$[\text{Bu}_4^{\text{n}}\text{NOMe}]$	O.D. <sup>b</sup>	$K_C$ ( $\text{l.mol}^{-1}$ )	$K_C$ (calc) <sup>c</sup>	$10^3 k_{\text{obs}}$ ( $\text{sec}^{-1}$ )	$k_1$ <sup>d</sup> ( $\text{l.mol}^{-1} \text{sec}^{-1}$ )
0.0105	0.10	20	20	5.7	1.09
0.021	0.16	18	18	6.0	1.1
0.042	0.23	15.5	16	6.1	1.09
0.063	0.27	14	14	7.7	1.4
0.084	0.30	13	13	8.1	1.5
0.10	0.32	12	13	6.5	1.2
0.80	0.56	-	-	-	-

<sup>a</sup> Data obtained by M.A. El Ghariani

<sup>b</sup> Measured at 500 nm

<sup>c</sup> Calculated from equation 4.3 using the values,  $K_1 = 210$   
 $\text{l.mol}^{-1}$ ,  $K_2 = 10 \text{ l.mol}^{-1}$ ,  $K_3 = 30 \text{ l.mol}^{-1}$ ,  $K_s = 8$

<sup>d</sup> Calculated from equation 4.10 using the values  $K_3 = 30 \text{ l.mol}^{-1}$ ,  
 $K_s = 8$

TABLE 4.7

Equilibrium and Rate Constants<sup>a</sup> for the Reaction of 4-Methoxy-3,5-dinitrobenzaldehyde ( $3.9 \times 10^{-5}$  M) with Sodium Methoxide in

Methanol at 25°C

<u>[NaOMe]</u> (M)	<u>O.D.<sup>b</sup></u>	<u>K<sub>C</sub></u> (l.mol <sup>-1</sup> )	<u>K<sub>C</sub> (calc)<sup>c</sup></u>	<u>10<sup>3</sup>k<sub>obs</sub></u> (sec <sup>-1</sup> )	<u>k<sub>1</sub><sup>d</sup></u> (l.mol <sup>-1</sup> sec <sup>-1</sup> )
0.0096	0.115	26	24	4.55	1.07
0.0192	0.19	25	24	-	-
0.029	0.26	28	25	4.55	1.12
0.048	0.33	27	25	5.1	1.23
0.067	0.37	26	25	5.45	1.30
0.115	0.43	25	25	6.5	1.50
0.67	0.56	-	-	-	-
1.0	0.58	-	-	-	-
1.4	0.58	-	-	-	-
0.01 <sup>e</sup>	0.25	76	74	-	-
0.02 <sup>e</sup>	0.32	62	61	-	-
0.04 <sup>e</sup>	0.38	47	45	-	-

<sup>a</sup> Data obtained by M.A. El Ghariani

<sup>b</sup> Measured at 500 nm

<sup>c</sup> Calculated from equation 4.3 using the values,  $K_1 = 210 \text{ l.mol}^{-1}$ ,  $K_2 = 30 \text{ l.mol}^{-1}$ ,  $K_3 = 30 \text{ l.mol}^{-1}$ ,  $K_s = 8$

<sup>d</sup> Calculated from equation 4.10 using the values  $K_3 = 30 \text{ l.mol}^{-1}$ ,  $K_s = 8$

<sup>e</sup> Made up to constant ionic strength, 0.1M with sodium chloride

TABLE 4.8

Equilibrium and Rate Constants for the Reaction of 4-Methoxy-3,5-dinitrobenzaldehyde ( $3.95 \times 10^{-5} \text{ M}$ ) with Sodium Methoxide in Methanol at  $25^{\circ}\text{C}$

$\frac{[\text{NaOMe}]}{(\text{M})}$	O.D. <sup>a</sup>	$\frac{K_C}{(1.\text{mol}^{-1})}$	$\frac{K_C (\text{calc})^c}{(1.\text{mol}^{-1})}$	$\frac{10^3 k_{\text{obs}}}{(\text{sec}^{-1})}$	$\frac{k_1^d}{(1.\text{mol}^{-1} \text{sec}^{-1})}$
0.00398	0.06 <sup>b</sup>	29	27	5.32	1.4
0.00705	0.10 <sup>b</sup>	30	27	3.78	0.98
0.00976	0.135	31	27	4.47	1.14
0.0202	0.217	30	28	4.89	1.2
0.0404	0.320	30	28	5.00	1.3
0.0728	0.395	29	29	5.79	1.4
0.0976	0.43	29	29	6.01	1.5

<sup>a</sup> Measured at 500 nm

<sup>b</sup> Measurements were made with a substrate concentration of  $7.9 \times 10^{-5} \text{ M}$ .  
The values quoted are the actual values divided by 2.

<sup>c</sup> Calculated from equation 4.3 using the values  $K_1 = 240 \text{ l.mol}^{-1}$ ,  
 $K_2 = 30 \text{ l.mol}^{-1}$ ,  $K_3 = 30 \text{ l.mol}^{-1}$ ,  $K_s = 8$

<sup>d</sup> Calculated from equation 4.10 using the values  $K_3 = 30 \text{ l.mol}^{-1}$ ,  
 $K_s = 8$

tetra-n-butylammonium, and little association is observed with lithium ions.

The n.m.r. results show that in the presence of sodium methoxide complete conversion to complex is achieved at sufficiently high base concentration and therefore the limiting value of the optical density obtained with sodium methoxide corresponds to complete conversion to complex (plus ion-pair). As the visible spectral shape does not change over the whole range of base concentration, where the fraction of ion-pairs would be varying, it can be assumed that the extinction coefficients of the complex, C, and its ion-pair, I.P., are identical. Thus the stoichiometric equilibrium constant,  $K_C$ , can be defined as follows:

$$K_C = \frac{[C] + [I.P.]}{([P]_{\text{stoich}} - [C] - [I.P.])[OMe^-]_{\text{free}}} \quad 4.1$$

$$= \frac{\text{O.D. (500 nm)}}{(0.58 - \text{O.D. (500 nm)})[OMe^-]_{\text{free}}}$$

But  $[P]_{\text{stoich}} = [C] + [I.P.] + [P] + [S] + [S^-]$

Substitution for  $[P]_{\text{stoich}}$ ,  $[C]$  and  $[I.P.]$  in equation 4.1. in terms of  $K_1$ ,  $K_2$ ,  $K_3$ ,  $K_s$  and  $[M^{n+}]$  gives

$$K_C = \frac{K_1(1 + K_2[M^{n+}])}{1 + K_s + K_s K_3 [OMe^-]} \quad 4.2$$

In the present case  $K_s = 8$  and thus equation 4.2 reduces to

$$K_C = \frac{K_1(1 + K_2[M^{n+}])}{9 + 8K_3[OMe^-]} \quad 4.3$$

The implications of equation 4.3 with respect to  $M^{n+}$  will be considered for each methoxide in turn.

(i) Lithium methoxide

When using lithium methoxide as base it can be assumed that  $K_2 = 0$  in the light of previous results.<sup>182, 183</sup> Therefore equation 4.3 reduces to

$$K_C = \frac{K_1}{9 + 8K_3[\text{OMe}^-]}$$

which on rearranging gives

$$\frac{1}{K_C} = \frac{9}{K_1} + \frac{8K_3[\text{OMe}^-]}{K_1} \quad 4.4$$

In agreement with equation 4.4 a plot of  $\frac{1}{K_C}$  versus  $[\text{LiOMe}]$  is linear (Figure 4.5). The value of  $K_1$  ( $210 \pm 40 \text{ l.mol}^{-1}$ ) and  $K_3$  ( $30 \pm 6 \text{ l.mol}^{-1}$ ) are obtained from the intercept and slope respectively.

(ii) Tetra-n-butylammonium methoxide

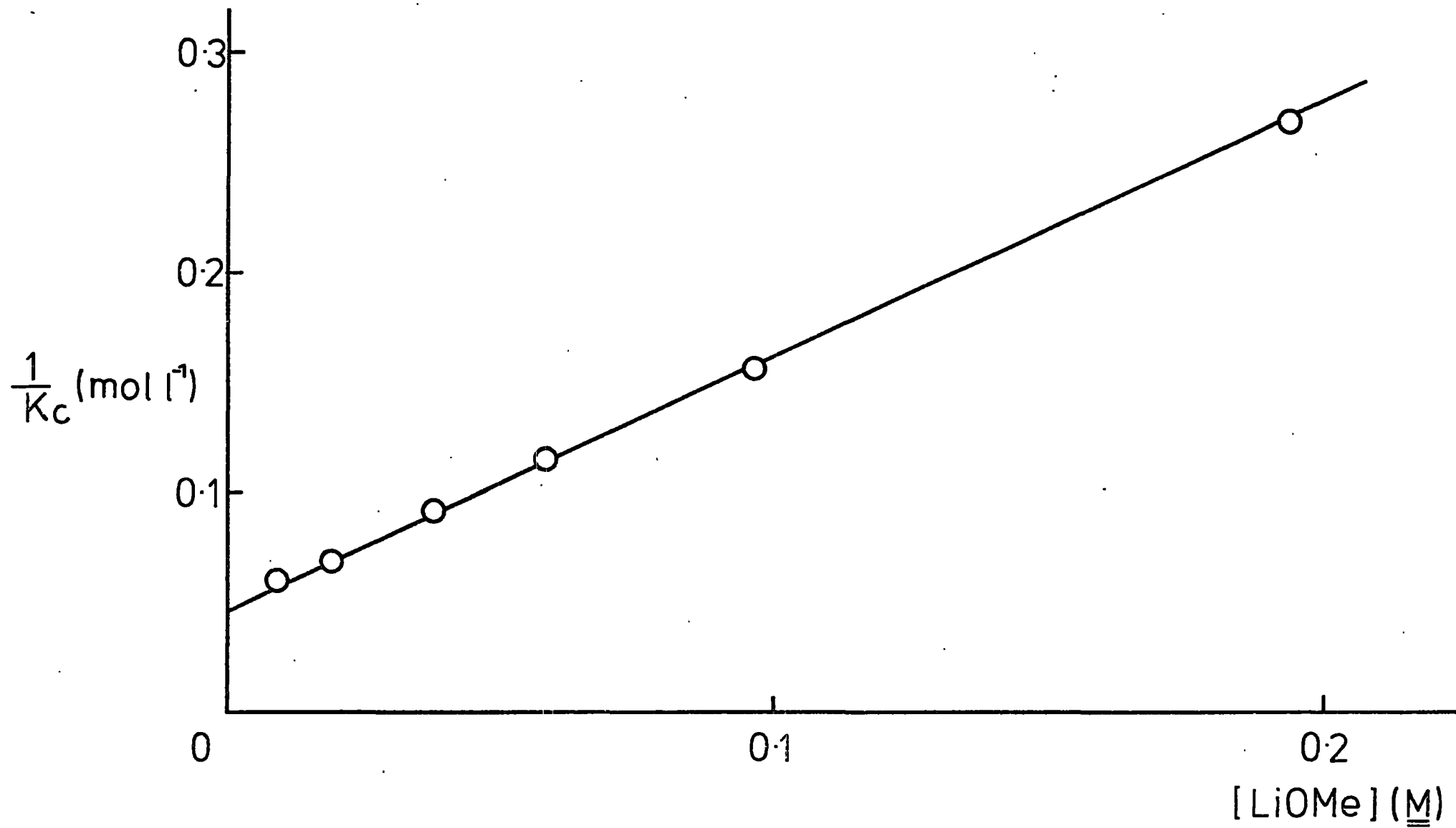
Tetra-n-butylammonium ions are known<sup>182,183</sup> to stabilise Meisenheimer complexes probably by dispersion interaction. Association constants appear to be independent of ring substituents in the complexes and have values of ca.  $10 \text{ l.mol}^{-1}$ . Using this value for  $K_2$  and the values of  $K_1$  and  $K_3$  calculated using lithium methoxide, excellent agreement is obtained between the observed values of  $K_C$  and those calculated using equation 4.3 (see Table 4.6).

(iii) Sodium methoxide

With sodium ions it is thought that in the ion associate the cation is held by a cage effect by the two methoxy groups at the position of addition and by the electronegative ortho-substituent. For sodium ions<sup>182,183</sup> association constants are in the range  $20\text{-}100 \text{ l.mol}^{-1}$  depending on the ring substituents. Taking a value of  $K_2 = 30 \text{ l.mol}^{-1}$ , experimental and calculated values of  $K_C$  are found to agree well for the data given in Table 4.7. The effect of sodium ions on the equilibria can be seen by comparing the values of  $K_C$  obtained at constant ionic strength with those obtained in the absence of added salt. The calculated values of  $K_C$  given in Table 4.8 correlate better with the experimental ones using  $240 \text{ l.mol}^{-1}$  as a value for  $K_1$ .

The addition of barium ions produces quite a marked increase in the stoichiometric equilibrium constant,  $K_C$ , (see Table 4.9) and this is in agreement with observations made with other 1,1-dimethoxy-complexes.<sup>183</sup>

FIGURE 4.5



Plot of equation 4.4. for reaction of 4-methoxy-3,5-dinitrobenzaldehyde with lithium methoxide in methanol.

TABLE 4.9

Equilibrium Constants for the Reaction of 4-Methoxy-3,5-  
dinitrobenzaldehyde ( $3.95 \times 10^{-5} \text{M}$ ) with Sodium Methoxide  
in Methanol in the Presence of Added Barium Chloride

$10^3 [\text{Ba}^{2+}]_{\text{stoich}}$ (M)	O.D. <sup>a</sup>	$K_C$ ( $\text{l.mol}^{-1}$ )	$K_2'$ <sup>b</sup> ( $\text{l.mol}^{-1}$ )	$10^{-3} K_2'$ <sup>c</sup> ( $\text{l.mol}^{-1}$ )
1	0.241	36.5	785	2.25
2	0.281	48.2	777	2.22
5	0.321	63.6	511	1.35
10	0.366	87.7	413	0.98
15	0.399	113	384	0.83

<sup>a</sup> Measured at 500 nm

<sup>b</sup> Calculated from equation 4.5 using the values  $K_1 = 210 \text{ l.mol}^{-1}$ ,  $K_2 = 30 \text{ l.mol}^{-1}$ ,  $K_3 = 30 \text{ l.mol}^{-1}$ ,  $K_s = 8$  and assuming no association of the barium ions with methoxide.

<sup>c</sup> Calculated from equation 4.5 using the above values and assuming a value of  $10^2$  for the association constant of barium and methoxide ions.

It is easily shown that equation 4.3 is modified to give

$$K_C = \frac{K_1(1 + K_2[Na^+] + K_2'[Ba^{2+}])}{9 + 8K_3[OMe^-]} \quad 4.5$$

to take into account ion-pairing between the complex and barium ions. Using the values of  $K_1$ ,  $K_2$ , and  $K_3$  as above and the observed values of  $K_C$ , values for  $K_2'$  can be calculated (Table 4.9). They are somewhat lower than those obtained for similar complexes. However the values of  $K_2'$  were calculated using the stoichiometric concentration of barium ions which will in fact be considerably reduced through ion-pairing with methoxide ions. Assuming a value of  $10^2$  for the association constant of barium and methoxide ions in methanol, the concentrations of free barium ions were determined and these were then used to re-estimate values of  $K_2'$  (Table 4.9). The decrease in the calculated values of  $K_2'$  may result from not taking into account the changes in spectral properties which were observed with the 2-methoxycarbonyl complex on complexation with barium ions.<sup>173</sup> A value of ca.  $2 \times 10^3 \text{ l.mol}^{-1}$  would therefore seem appropriate for  $K_2'$ . It should be noted that the values obtained are only very approximate and they should be regarded as giving an order of magnitude. However they do demonstrate the strong association of the complex with barium ions.

#### Kinetic measurements

Observed first-order rate constants for complex formation are given with the equilibrium data in Tables 4.5-4.8.

A rate equation can be derived in terms of the above Scheme, as follows, where  $k_1$  is the rate constant for Meisenheimer complex formation and  $k_{-1}$  the rate constant for reversal to reactants.

$$\frac{d}{dt}[C + I.P.] = k_1[P][OMe^-] - k_{-1}[C] \quad 4.6$$

$$\text{But } [C + I.P.] = [P]_{\text{stoich}} - [P] - [S] - [S^-] \quad 4.7$$

Assuming  $P \rightleftharpoons S$ ,  $S \rightleftharpoons S^-$  and  $C \rightleftharpoons I.P.$  are all fast equilibria, substituting for [I.P.], [S] and  $[S^-]$  in 4.7 and then for [C] in 4.6 gives

$$\frac{d}{dt}[C + I.P.] = k_1[P][OMe^-] - \frac{k_{-1}([P]_{\text{stoich}} - [P](1 + K_S(1 + K_3[OMe^-])))}{(1 + K_2[M^{n+}])} \quad 4.8$$

At equilibrium

$$\frac{d}{dt}[C + I.P.] = 0 = k_1[P]_{\infty}[OMe^-] - \frac{k_{-1}([P]_{\text{stoich}} - [P]_{\infty}(1 + K_S(1 + K_3[OMe^-])))}{(1 + K_2[M^{n+}])}$$

$$\therefore [P]_{\text{stoich}} = \frac{k_1[P]_{\infty}[OMe^-](1 + K_2[M^{n+}]) + k_{-1}[P]_{\infty}(1 + K_S(1 + K_3[OMe^-]))}{k_{-1}}$$

Substituting for  $[P]_{\text{stoich}}$  in equation 4.8 gives

$$\frac{d}{dt}[C + I.P.] = ([P] - [P]_{\infty}) \left( k_1[OMe^-] + \frac{k_{-1}(1 + K_S(1 + K_3[OMe^-]))}{(1 + K_2[M^{n+}])} \right) \quad 4.9$$

From equation 4.7  $[C + I.P.] = [P]_{\text{stoich}} - [P](1 + K_S(1 + K_3[OMe^-]))$

$$\therefore \frac{d}{dt}[C + I.P.] = - \frac{d[P]}{dt} (1 + K_S(1 + K_3[OMe^-]))$$

Hence equation 4.9 gives

$$\frac{-d[P]}{dt} = ([P] - [P]_{\infty}) \left( \frac{k_1[OMe^-]}{1 + K_S(1 + K_3[OMe^-])} + \frac{k_{-1}}{1 + K_2[M^{n+}]} \right)$$

$$\text{But } - \frac{d[P]}{dt} = k_{\text{obs}}([P] - [P]_{\infty})$$

$$\therefore k_{\text{obs}} = \frac{k_1[OMe^-]}{1 + K_S(1 + K_3[OMe^-])} + \frac{k_{-1}}{1 + K_2[M^{n+}]}$$

$$K_1 = \frac{k_1}{k_{-1}} \text{ and using equation 4.2}$$

$$k_{\text{obs}} = \frac{k_1}{1 + K_S(1 + K_3[OMe^-])} \left( [OMe^-] + \frac{1}{K_C} \right) \quad 4.10$$

Values of  $k_1$  calculated using equation 4.10 and given in Tables 4.5-4.8 agree well for the three methoxides.

Values of rate and equilibrium constants obtained from the present work are collected in Table 4.10.

TABLE 4.10

Equilibrium and Rate Constants for the Reaction of 4-Methoxy-3,5-dinitrobenzaldehyde with Methoxide in Methanol at 25°C

$K_s = 8 \pm 1 \text{ l.mol}^{-1}$	$k_1 = 1 \pm 0.2 \text{ l.mol}^{-1} \text{ sec}^{-1}$
$K_1 = 210 \pm 40 \text{ l.mol}^{-1}$	$k_{-1} = 5 \pm 1 \times 10^{-3} \text{ sec}^{-1}$
$K_2 = \text{ca. } 30 \text{ l.mol}^{-1}$	
$K_2' = \text{ca. } 2 \times 10^3 \text{ l.mol}^{-1}$	
$K_3 = 30 \pm 6 \text{ l.mol}^{-1}$	

Comparing these results with the data given in Table 4.1 shows that the aldehyde group has a similar stabilising effect to a cyano group. However in the light of the present work and Miller's earlier results with aldehyde and cyano substituents,<sup>219</sup> it may be that the Fendlers' results for 4-cyano-2,6-dinitroanisole<sup>64</sup> are anomalous. Their structural measurements were made in DMSO and consequently incursion of imido ester formation would not have been detected. It would therefore be of interest to obtain the p.m.r. spectrum of 4-cyano-2,6-dinitroanisole in methanol. In the present case if hemiacetal formation is neglected the value of the equilibrium constant for complex formation turns out to be an order of magnitude smaller than the true value of  $K_1$ .

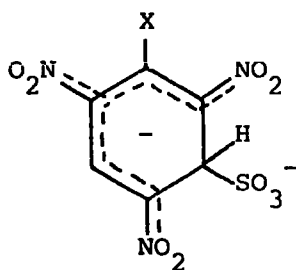
Thus it would seem preferable to make structural studies in the same solvent as that used for kinetic and equilibrium measurements. This argument has recently been substantiated in a study of the methoxide addition to a cyanothiophene derivative;<sup>102</sup> in DMSO base attack occurs at a ring carbon whereas in methanol attack is at the cyano group.

CHAPTER 5

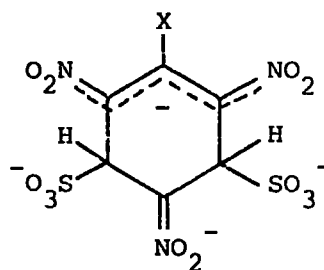
A KINETIC AND P.M.R. STUDY OF THE INTERACTION OF 1-X-2,4,6-  
TRINITROBENZENES WITH SODIUM SULPHITE IN WATER

INTRODUCTION

Complexes formed from activated aromatic compounds and sulphite ions in aqueous media have been observed and characterised for some time. Sodium sulphite solutions were known to dissolve 1,3,5-trinitrobenzene and 2,4,6-trinitrotoluene giving coloured solutions<sup>156</sup> from which the parent compounds could be re-isolated. Cuta and Beranck<sup>134</sup> investigated the visible spectrum of 1,3,5-trinitrobenzene (TNB) in dilute potassium sulphite solutions and showed that the observed spectrum resulted from a 1:1 interaction in which they postulated (5.1; X = H) as being the adduct.



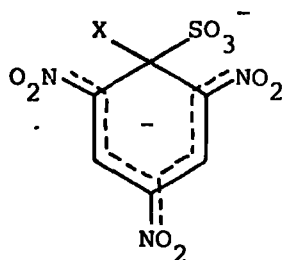
(5.1)



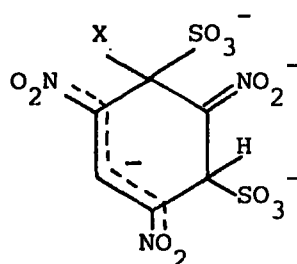
(5.2)

The changes in the visible spectrum observed on increasing the sulphite concentration were attributed to the formation of higher complexes resulting from the addition of two or three sulphite groups. The isolation of a red crystalline solid of stoichiometry 1 TNB:2 SO<sub>3</sub><sup>2-</sup> from aqueous solutions<sup>157</sup> was also an indication of higher complex formation.

P.m.r. studies of the reactions of sulphite ion with a number of 1-X-2,4,6-trinitrobenzenes (X = H, OH, OCH<sub>3</sub>, NH<sub>2</sub>, NHCH<sub>3</sub>, N(CH<sub>3</sub>)<sub>2</sub>, NPh and NCH<sub>3</sub>Ph) in water and aqueous DMSO have clearly established that the coloured species are  $\sigma$ -complexes having the basic structure (5.2).<sup>159</sup> Thus for X  $\neq$  H there was no evidence for sulphite attack at C<sub>1</sub> to give species such as (5.3) and (5.4).



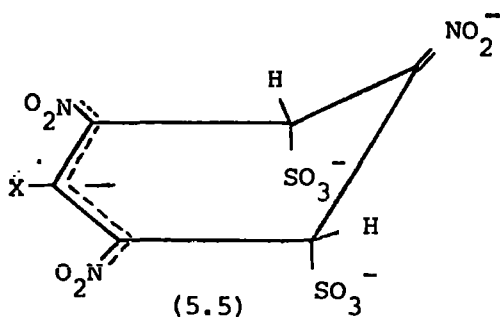
(5.3)



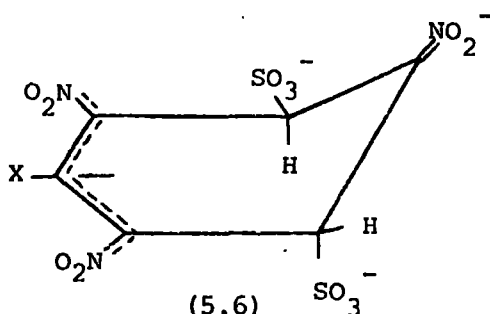
(5.4)

However 2,4,6-trinitrobenzaldehyde is unusual in that sulphite addition apparently occurs at unsubstituted ring positions and at C<sub>1</sub>.<sup>221</sup>

The possibility of cis-(5.5) and trans-(5.6) isomerism in the 1:2-adducts had been suggested<sup>6,8</sup> but until recently no spectroscopic evidence for such



(5.5)



(5.6)

isomerism had been observed. However in a kinetic study of the interaction of 1,3,5-trinitrobenzene and sodium sulphite in water, Bernasconi and Bergstrom<sup>222</sup> found evidence for the formation of two distinct species of similar stability having the stoichiometry 1 TNB:2 SO<sub>3</sub><sup>2-</sup> thought to be the cis- and trans-isomers (5.5 and 5.6; X = H). It has also been shown<sup>221</sup> that one of the 1:2-adducts from 2,4,6-trinitrobenzaldehyde exhibits cis-trans isomerism.

In the present work the formation of di-adducts from a series of 1-X-2,4,6-trinitrobenzenes (X = H, OMe, OH, NH<sub>2</sub>, NHMe and NMe<sub>2</sub>) has been investigated. For X ≠ H kinetic measurements on 1:2-complex formation were made to see if, introducing time as an additional parameter, it is possible to 'separate' the cis- and trans-isomers.

## EXPERIMENTAL

### P.m.r. measurements

Samples were prepared by dissolving the substrate in a solution of sodium

sulphite (1 or 2M) in water or deuterium oxide to give ca. 0.2M solutions. Spectra were recorded at different temperatures between ca. 6 and 80°C as soon as possible after making up the solutions. Spectra were recorded at 60 MHz (X = H) or 90 MHz (remainder) using sodium 4,4-dimethyl-4-silapentane-1-sulphonate as internal reference.

#### Kinetic measurements

Kinetic runs were performed by mixing aqueous solutions of the substrate with aqueous solutions of sodium sulphite in a 'Canterbury' stopped-flow spectrophotometer and monitoring changes in light absorption. Solutions for kinetic runs were prepared by the appropriate dilution with water of stock solutions of the substrate in methanol and sodium sulphite in water, constant ionic strength being maintained by the addition of sodium sulphate. Measurements were made at wavelengths in the range 400-550 nm.

#### RESULTS AND DISCUSSION

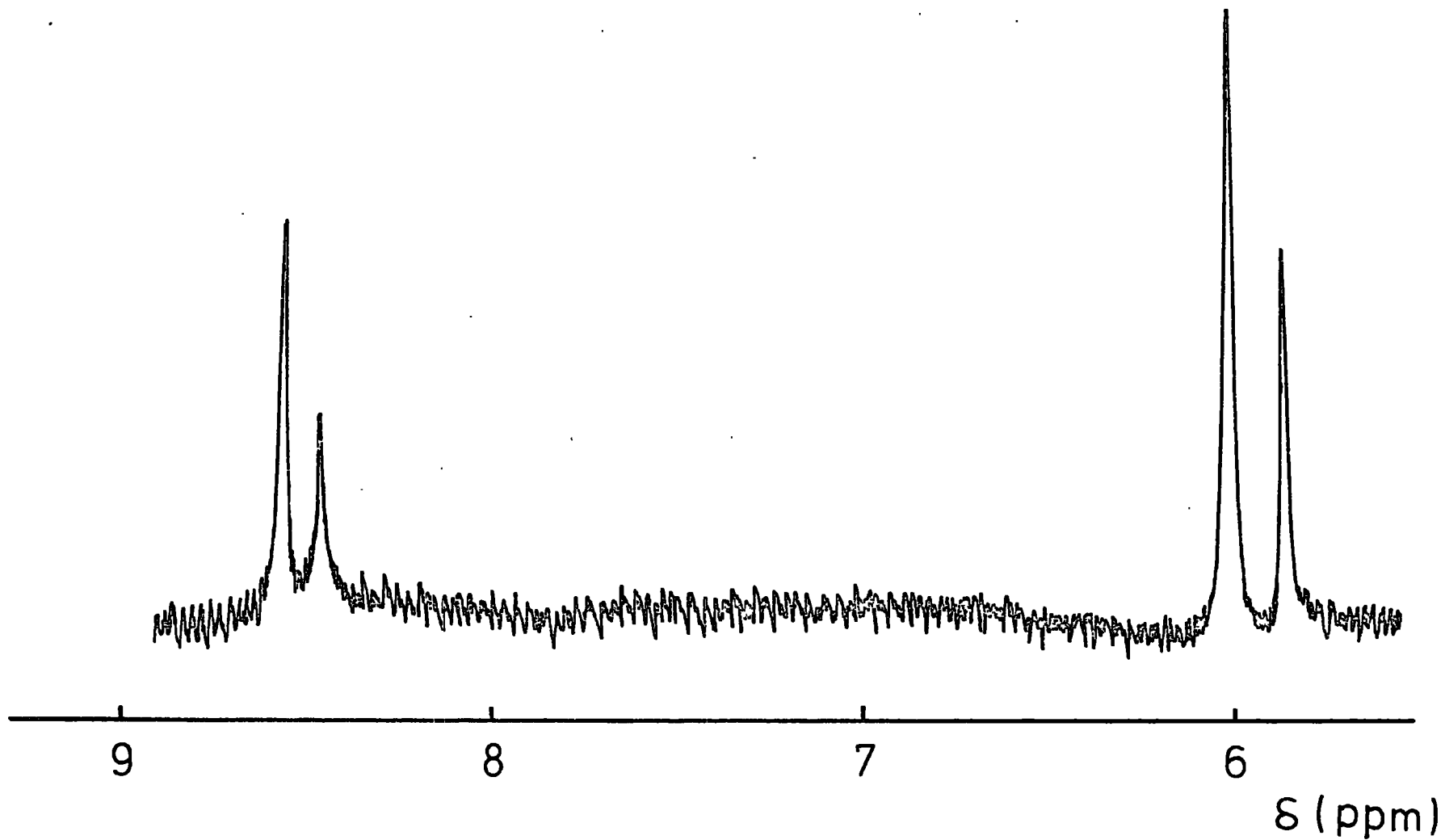
##### P.m.r. spectra

###### (i) 1,3,5-Trinitrobenzene

The spectrum of a solution of 1,3,5-trinitrobenzene (ca. 0.2M) in aqueous sodium sulphite (1M) shows bands which can be attributed to the two isomers (5.5 and 5.6; X = H). The solution cooled to 5° gives a spectrum with two sharp bands at  $\delta$ 8.6 and 8.5 p.p.m. attributed to the hydrogens at the  $sp^2$  hybridised carbon atoms in the di-adducts and two sharp bands at  $\delta$ 6.05 and 5.9 p.p.m. attributed to the hydrogens attached to the  $sp^3$  hybridised carbon atoms (see Figure 5.1). As required for complexes of 1:2 stoichiometry the bands at  $\delta$ 8.6 and 6.05 p.p.m. have relative intensities 1:2 as do the bands at  $\delta$ 8.5 and 5.90 p.p.m.. At this temperature the isomers are present in the ratio 6:4.

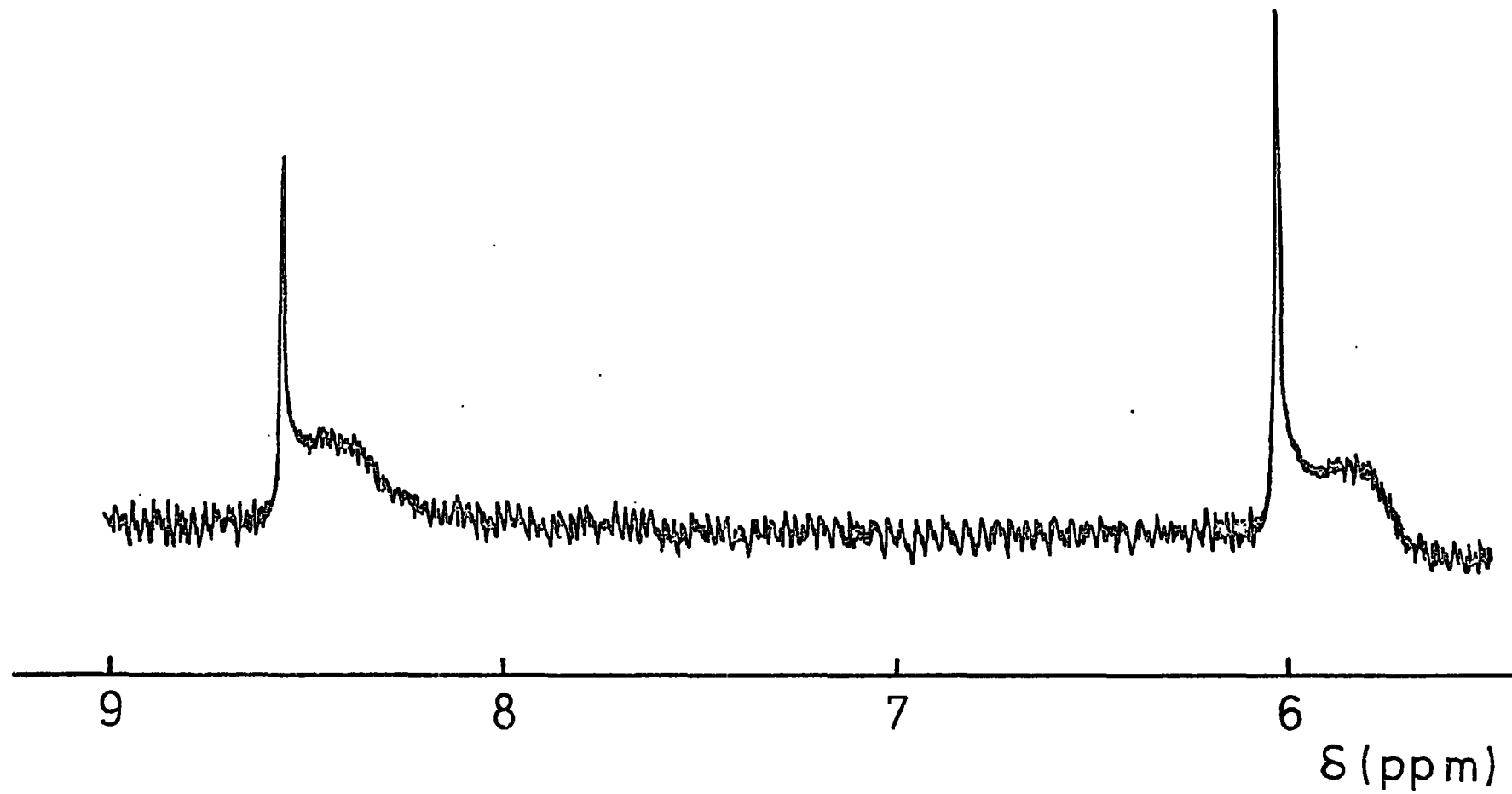
On warming the sample to 30°, the bands at  $\delta$ 8.6 and 6.05 p.p.m. remain sharp while the bands from the other isomer broaden considerably, (Figure 5.2).

FIGURE 5.1



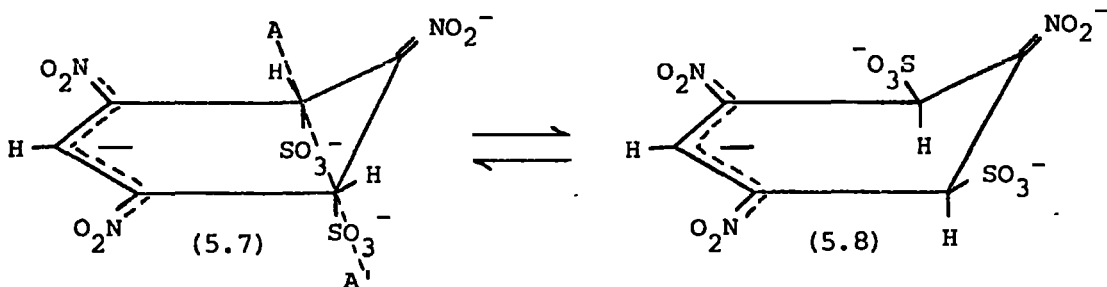
P.m.r. spectrum of 1,3,5-trinitrobenzene (0.2M) in aqueous sodium sulphite solution (1M) at 5°C.

FIGURE 5.2



P.m.r. spectrum of 1,3,5-trinitrobenzene (0.2M) in aqueous sodium sulphite solution (1M) at 30°C.

The broadness of these bands at probe temperature explains the failure to observe them in previous measurements.<sup>159</sup> This broadening, which is reversed on re-cooling, could be explained in terms of an increase in the rate, for one isomer, of sulphite exchange either between ring positions or with the solution. Alternatively an explanation for this effect may be found in considering the non-planarity of the 1:2 complexes. Thus in structures (5.5 and 5.6; X = H) the substituents H and  $\text{SO}_3^-$  may take up either pseudo-axial or -equatorial positions at the  $\text{sp}^3$  hybridised carbon atoms analogous to substituents in cyclohexane. However in the trans-complex (5.6; X = H) repulsion between  $\text{NO}_2^-$  and the bulky sulphite groups may result in a near planar molecule rendering the two hydrogens equivalent. On the other hand, in the cis-form (5.5; X = H) one of the two possible conformations (5.7) or (5.8) may be much preferred. It is therefore possible to envisage a



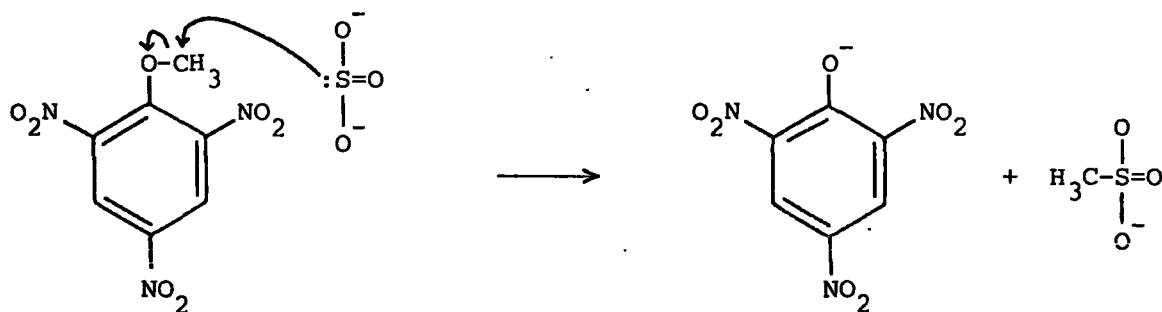
situation where change in the rate of 'flipping' of the molecule about AA', and hence interconversion of the conformers, (5.7) and (5.8), with temperature could result in the observed broadening. It would seem reasonable to suggest that (5.7) would be the conformation preferred since the electrostatic repulsion between the sulphite groups in axial positions and the nitro group carrying the localised negative charge would be considerably reduced compared to (5.8) where the sulphite groups are 'equatorial'.

These p.m.r. results are in accord with those found by Strauss<sup>223</sup> in deuterium oxide and are consistent with Bernasconi's<sup>222</sup> kinetic treatment in terms of cis-trans isomerism.

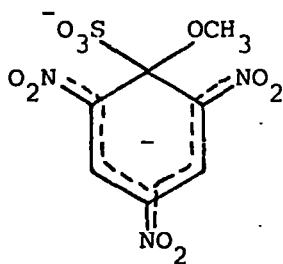
(ii) 2,4,6-Trinitroanisole

The spectrum of a freshly prepared solution of 2,4,6-trinitroanisole in 1M sodium sulphite solution in deuterium oxide at 25° shows, apart from the residual solvent peak, two sharp singlets at  $\delta 6.1$  and 4.18 p.p.m. of relative intensity 2:3 attributed to the ring protons and the methoxyl protons respectively in the 1:2-adduct (Figure 5.3). Cooling the solution to ca. 5° has no effect on the position or shape of the band at  $\delta 6.1$  p.p.m.; the absorption also remains unchanged at 50°. However singlets at  $\delta 6.27$  and 2.82 p.p.m. begin to increase in intensity at the expense of those at  $\delta 6.1$  and 4.18 p.p.m. (Figure 5.4). After some time at 50° and on returning to 25° the initial absorptions almost disappear leaving intense bands at  $\delta 6.27$  and 2.82 p.p.m. A small band at  $\delta 3.36$  p.p.m. is also present (Figure 5.5).

These changes in the spectrum can be accounted for in terms of demethylation of the uncomplexed anisole by sulphite ion to give picrate and methanesulphonate ions, as follows:-

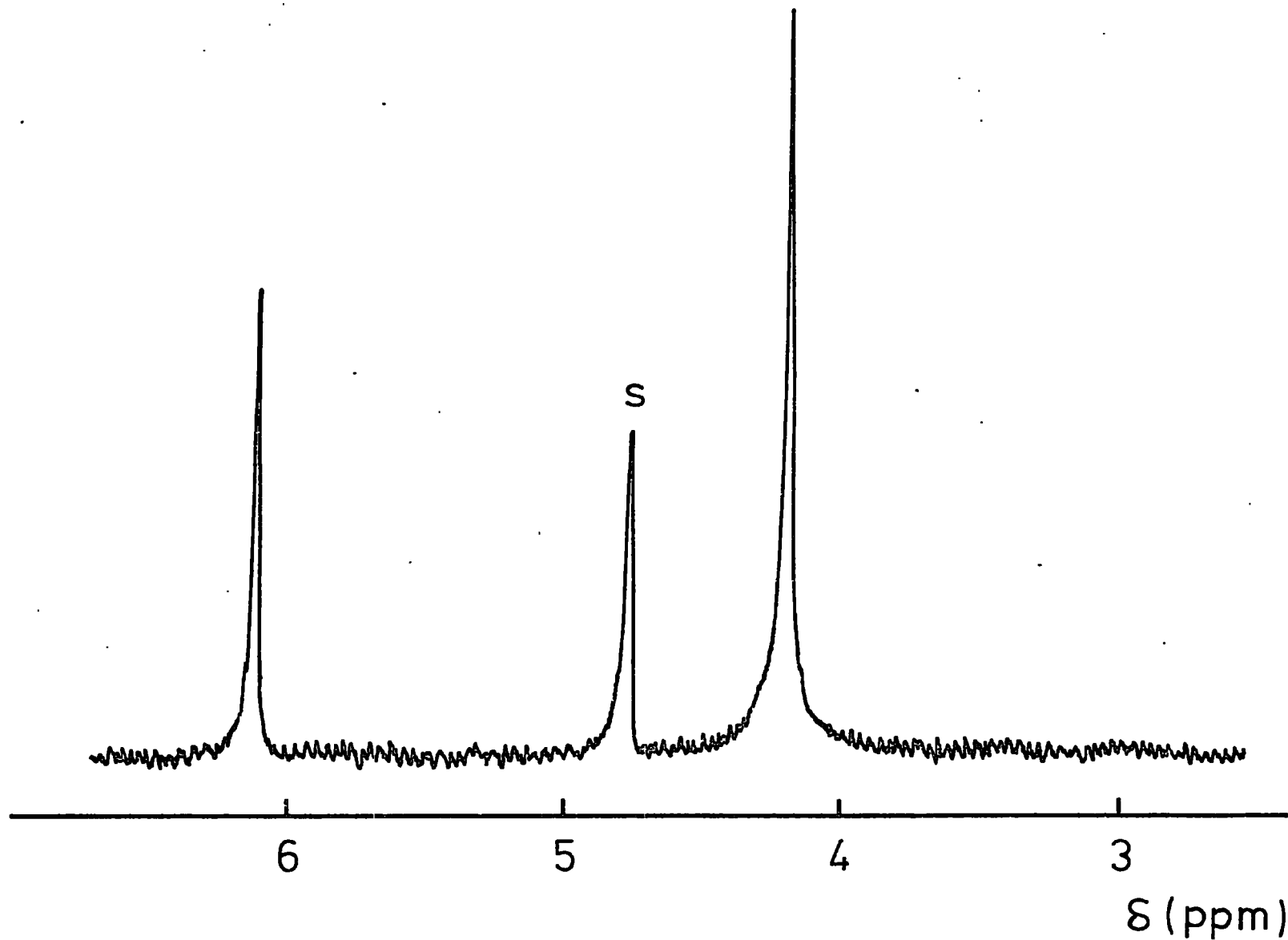


The picrate ion then forms the 1:2-adduct with sulphite resulting in the band at  $\delta 6.2$  p.p.m. (see picric acid). The small absorption at  $\delta 3.36$  p.p.m. almost certainly results from methanol produced by direct nucleophilic substitution of the methoxyl group by the solvent or even by sulphite, though the latter seems unlikely since steric effects around C<sub>1</sub> in the intermediate (5.9)



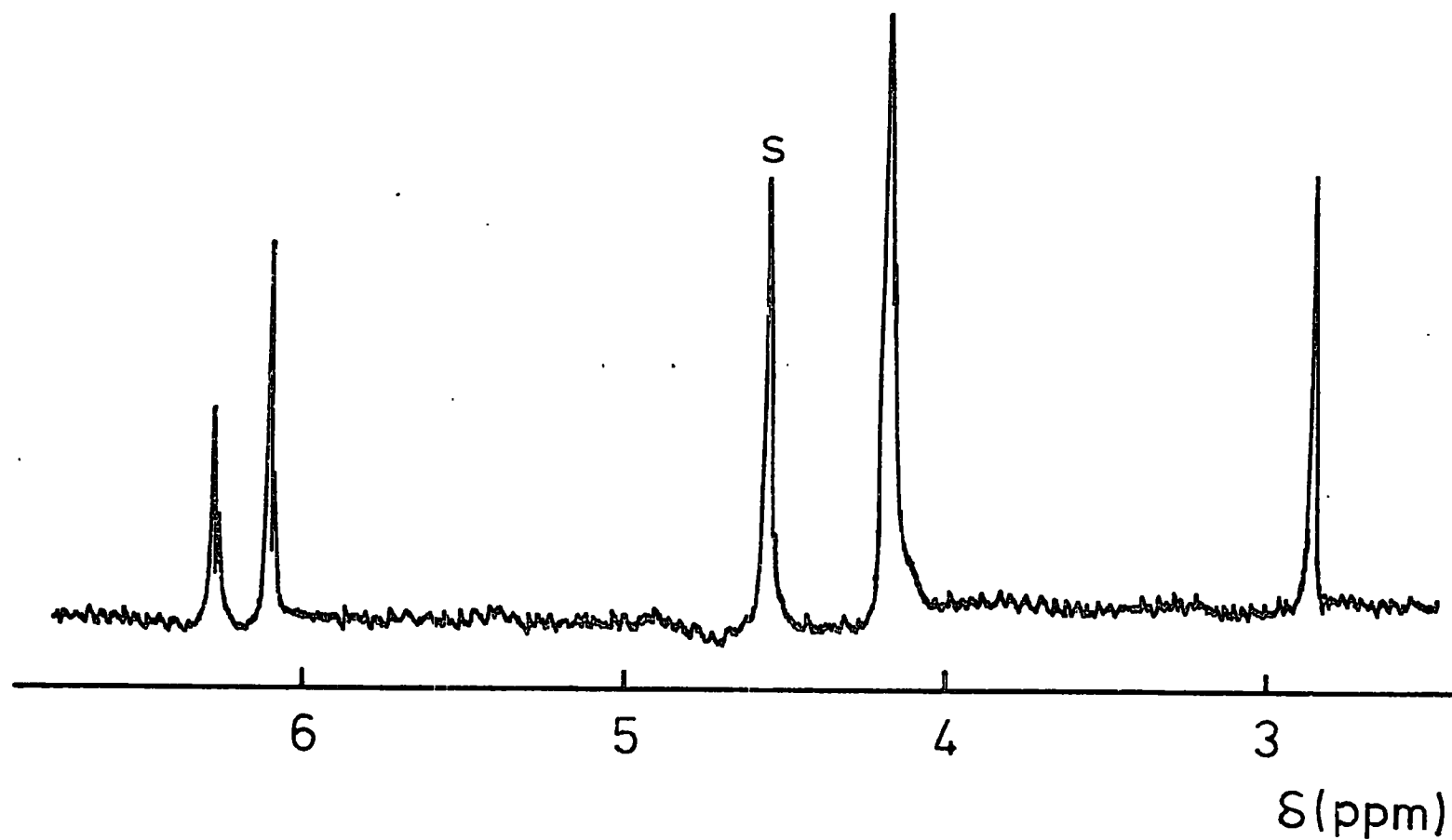
(5.9)

FIGURE 5.3



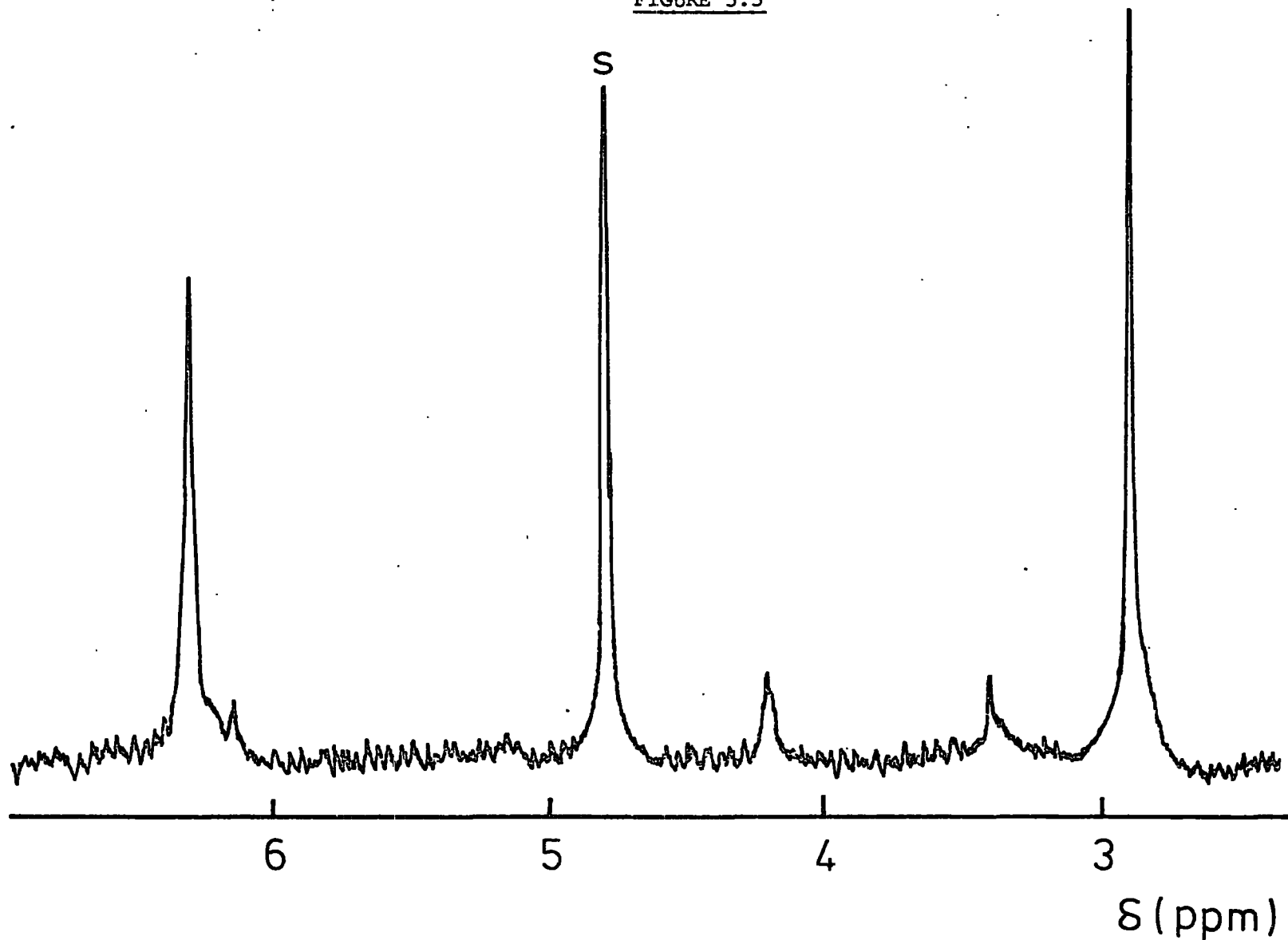
P.m.r. spectrum of 2,4,6-trinitroanisole (0.2M) in 2M sodium sulphite solution in  $D_2O$  at  $25^\circ C$  immediately after preparing the sample. Band marked 's' is solvent peak.

FIGURE 5.4



P.m.r. spectrum of 2,4,6-trinitroanisole (0.2M) in 2M sodium sulphite solution in  $D_2O$  at ca.  $50^\circ C$ .  
Recorded ca. 30 mins after preparing the sample. Band marked 's' is solvent peak.

FIGURE 5.5



P.m.r. spectrum of 2,4,6-trinitroanisole (0.2M) in 2M sodium sulphite solution in  $D_2O$ . Temperature returned to  $25^\circ C$  and recorded ca. 2 hours after preparing the sample. Band marked 's' is solvent peak.

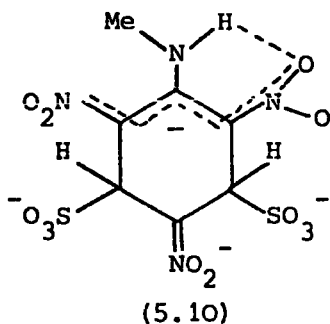
would be expected to be large. The peak at  $\delta 2.82$  p.p.m. can be attributed to the methyl resonance of methylsulphonate. Addition of a drop of methanol resulting in an intense absorption at  $\delta 3.36$  p.p.m. confirmed the above assignment.

(iii) N,N-Dimethylpicramide

The spectrum, recorded at  $25^\circ$ , of a  $0.2M$  solution of N,N-dimethylpicramide in  $2M$  sodium sulphite in deuterium oxide shows two sharp singlets at  $\delta 6.31$  and  $3.17$  p.p.m. of relative intensity 1:3 assigned to the ring and methyl protons respectively in the 1:2-adducts. No change in the shape or position of the ring proton resonance was observed over the temperature range  $7-87^\circ$  and no new peaks appeared at the higher temperatures.

(iv) N-Methylpicramide

The spectrum of the 1:2-adduct of N-methylpicramide at  $25^\circ$  shows three sharp singlets at  $\delta 6.29$ ,  $6.16$  and  $3.23$  p.p.m. of relative intensities 1:1:3. The presence of two singlets in the ring proton region has been accounted for<sup>159</sup> in terms of structure (5.10) in which the amino proton is hydrogen-bonded to an ortho-nitro group thus making the ring protons non-equivalent.



No changes in the ring proton resonances were observed over a temperature range of ca.  $40^\circ$  around room temperature.

(v) Picramide

The ring protons of the picramide-sulphite 1:2-complex absorb at  $\delta 6.21$  p.p.m.. Cooling the sample to  $10^\circ$  and warming to ca.  $80^\circ$  has no effect on the shape or position of the absorption. However a few minutes at the higher temperatures is sufficient to cause the disappearance of the ring proton

resonance as a result of some further interaction between uncomplexed substrate and either sulphite ion or the solvent.

(vi) Picric acid

The di-adduct of picric acid and sodium sulphite shows a single resonance at  $\delta 6.3$  p.p.m. for the ring protons. The spectrum remains unchanged on cooling to  $7^{\circ}$  and warming to  $40^{\circ}$ . However above this temperature the band broadens considerably and moves slightly to lower field. Sharp singlets of roughly equal intensity appear at  $\delta 6.48$  and  $5.75$  p.p.m.. The broadening effect is reversed on cooling back to  $25^{\circ}$ , although the two sharp singlets still remain.

The appearance of the two singlets at  $\delta 6.48$  and  $5.75$  p.p.m. almost certainly results from decomposition of the substrate. The broadening with temperature of the resonance at  $\delta 6.3$  p.p.m. might, as in the case of the 1,3,5-trinitrobenzene system, be due to sulphite exchange or to an increase in the rate of 'ring-flipping'.

The n.m.r. results indicate that decomposition of the substrate occurs most readily with picramides, 2,4,6-trinitroanisole and picric acid, while N-methyl- and N,N-dimethyl-picramides are more resistant. The equilibrium constants for 1:2-adduct formation from the latter two substrates are at least two orders of magnitude higher than those for the other compounds. This suggests that decomposition involves nucleophilic attack on the substrate, or possibly the 1:1-adduct. Thus as expected the 1:2-adducts which carry several negative charges are resistant to nucleophilic attack.

Chemical shift data for the 1:2-adducts are collected in Table 5.1.

Kinetic measurements

The concentrations of substrate were generally between  $10^{-5}$  and  $10^{-4}$  M whereas the concentration of sulphite ions was always at least an order of magnitude greater. Thus attainment of equilibrium followed first-order kinetics. A set of data for a typical run is given in Table 5.2.

TABLE 5.1

Chemical Shift Data<sup>a</sup> for the 1:2-Adducts from 1-X-  
2,4,6-Trinitrobenzenes and Sodium Sulphite

<u>X</u>	<u>Ring Protons</u>		<u>Methyl Protons</u>
H	8.6 (1)	6.05 (2)	-
	8.5 (1)	5.9 (2)	-
OMe	6.1		4.18
OH	6.3		-
NH <sub>2</sub>	6.21		-
NHMe	6.29 (1)	6.16 (1)	3.23
NHMe <sub>2</sub>	6.31		3.17

<sup>a</sup> Shifts measured in p.p.m. downfield from internal sodium 4,4-dimethyl-4-silapentane-1-sulphonate

TABLE 5.2

Rate Data for the 1:2-Complex Formation of N,N-Dimethyl-  
picramide ( $1 \times 10^{-5}$  M) and Sodium Sulphite ( $2 \times 10^{-2}$  M) at  
Ionic Strength 0.3M in Water at 25°C

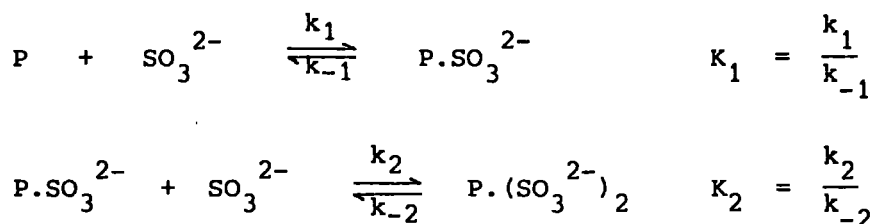
<u>Time</u> (m.sec)	<u>Scale Reading</u> (arbitrary units)	$\frac{k_{obs}}{1}$ (sec <sup>-1</sup> )
0	6.52	-
50	5.00	5.9
100	3.85	6.0
150	3.01	6.0
200	2.40	6.0
250	1.94	5.9
300	1.60	5.9
350	1.35	5.9
∞	0.60	-

Measurements were made in the wavelength range 400-550 nm and the observed rate constants were independent, within experimental error, of the wavelength of measurement. This can be demonstrated in the case of 2,4,6-trinitroanisole by reference to Table 5.3.

In all cases over the wavelength range studied, and regardless of sulphite concentration, only two relaxation times were observed. The first process (1:1-complex formation) was always accompanied by an increase in absorbance irrespective of wavelength and sulphite concentration. The second process manifested itself either by an increase or decrease in absorbance depending on the wavelength and sulphite concentration. Thus for 2,4,6-trinitroanisole at 550 nm a decrease in absorbance was observed at all sulphite concentrations. However at 430 nm, low sulphite concentrations ( $< 2.5 \times 10^{-3} \text{ M}$ ) resulted in an increase and high sulphite concentrations ( $\geq 2.5 \times 10^{-3} \text{ M}$ ) a decrease in absorbance.

The observed first-order rate constants are given in Tables 5.4-5.8. Though the present work is primarily concerned with 1:2-adduct formation, rate constants for 1:1-complex formation of 2,4,6-trinitroanisole and picric acid are given (Tables 5.9 and 5.10) to complement those reported recently by Norris et al.<sup>224</sup>

The plots of  $k_{\text{obs}}$  versus sulphite concentration are consistent with the following scheme:-



Since the relaxation times are well separated then according to standard procedures,<sup>225</sup> the observed rate constants for the attainment of each equilibrium are given by:-

$$k_{\text{obs}1} = k_1 [\text{SO}_3^{2-}] + k_{-1} \quad 5.1$$

TABLE 5.3

Invariance of Rate Constant for 1:2-Complex Formation with  
Wavelength for 2,4,6-Trinitroanisole and Sodium Sulphite <sup>a</sup>

in Water at 25°C

<u><math>10^3[\text{SO}_3^{2-}]</math></u>	<u><math>\lambda</math></u>	<u><math>k_{\text{obs}}</math></u>
(M)	(nm)	(sec <sup>-1</sup> )
12	400	0.42 ± .02
	430	0.39
	500	0.38
	550	0.43
25	400	1.78 ± .1
	430	1.66
	500	1.81
	550	1.61
50	400	5.10 ± .2
	430	4.66
	500	4.94
	550	4.87
75	400	9.53 ± .2
	430	9.72
	500	9.61
	550	9.95
100	430	17.08
	500	16.6

<sup>a</sup> These measurements were made without added salt

TABLE 5.4

(i) Rate Constants for 1:2-Complex Formation of 2,4,6-Trinitro-anisole<sup>a</sup> and Sodium Sulphite<sup>b</sup> in Water at 25°C

$10^3[\text{SO}_3^{2-}]$	$k_{\text{obs}}$
(M)	(sec <sup>-1</sup> )
1	0.14 <sup>c</sup>
2	0.18 ± .01 <sup>d</sup>
5	0.31 ± .01 <sup>d</sup>
7.5	0.49 ± .01 <sup>e</sup>
10	1.1 ± .1
25	3.5 ± .1
50	7.8 ± .1
75	11.6 ± .5

<sup>a</sup> Substrate  $1.5 \times 10^{-5}$  M unless otherwise stated.

<sup>b</sup> Made up to ionic strength 0.3M with sodium sulphate

<sup>c</sup> Determined via Guggenheim's method

<sup>d</sup> Substrate  $1 \times 10^{-4}$  M      <sup>e</sup> Substrate  $5 \times 10^{-5}$  M

(ii) Rate Constants for 1:2-Complex Formation of 2,4,6-Trinitro-anisole and Sodium Sulphite<sup>a</sup> in Water at 25°C

$10^5[\text{Substrate}]$	$10^3[\text{SO}_3^{2-}]$	$k_{\text{obs}}$
(M)	(M)	(sec <sup>-1</sup> )
2	10	3.8 ± .1
4	50	30.5 ± 1
1.5	100	62 ± 4
1.5	200	129 ± 10
4		124 ± 10
2	300	169 ± 10
4	400	275 ± 10

<sup>a</sup> Made up to ionic strength 2.1M with sodium sulphate

TABLE 5.5

Rate Constants for 1:2-Complex Formation of Picramide  
and Sodium Sulphite<sup>a</sup> in Water at 25°C

<u>10<sup>5</sup>[Substrate]</u>	<u>10<sup>3</sup>[SO<sub>3</sub><sup>2-</sup>]</u>	<u>k<sub>obs</sub></u>
(M)	(M)	(sec <sup>-1</sup> )
5	5	7.9 ± .3
	10	8.4 ± .3
2	20	9.5 ± .3
	25	10.3 ± .3
1.5	50	13.7 ± .3
	100	20.8 ± .3

<sup>a</sup> Made up to ionic strength 0.3M with sodium sulphate

TABLE 5.6

Rate Constants for 1:2-Complex Formation of N-Methylpicramide  
and Sodium Sulphite<sup>a</sup> in Water at 25°C

<u>10<sup>5</sup>[Substrate]</u>	<u>10<sup>3</sup>[SO<sub>3</sub><sup>2-</sup>]</u>	<u>k<sub>obs</sub></u>
(M)	(M)	(sec <sup>-1</sup> )
1.5	5	1.7 ± .04
	10	3.3 ± .1
	20	6.4 ± .2
	30	10.2 ± .3
	50	16.1 ± .3
	100	33.4 ± 1

<sup>a</sup> Made up to ionic strength 0.3M with sodium sulphate

TABLE 5.7

Rate Constants for 1:2-Complex Formation of N,N-Dimethyl-  
picramide and Sodium Sulphite<sup>a</sup> in Water at 25°C

<u>10<sup>5</sup>[Substrate]</u>	<u>10<sup>3</sup>[SO<sub>3</sub><sup>2-</sup>]</u>	<u>k<sub>obs</sub></u>
(M)	(M)	(sec <sup>-1</sup> )
1	1	0.19 ± .01
	2	0.45 ± .01
	5	1.4 ± .1
	10	3.2 ± .1
	20	5.9 ± .1
	50	15.4 ± .1
	100	32.3 ± .1

<sup>a</sup> Made up to ionic strength 0.3M with sodium sulphate

TABLE 5.8

Rate Constants for 1:2-Complex Formation of Picric Acid and  
Sodium Sulphite<sup>a</sup> in Water at 25°C

<u>10<sup>5</sup>[Substrate]</u>	<u>10<sup>3</sup>[SO<sub>3</sub><sup>2-</sup>]</u>	<u>k<sub>obs</sub></u>
(M)	(M)	(sec <sup>-1</sup> )
34	25	5.3 ± .3
8	50	6.7 ± .2
46	100	11.9 ± .2
8	200	27.2 ± .3
3.1	300	50.0 ± .3
2.6	400	77.7 ± 1

<sup>a</sup> Made up to ionic strength 2.1M with sodium sulphate

TABLE 5.9

Rate Constants for 1:1-Complex Formation of 2,4,6-Trinitroanisole  
and Sodium Sulphite in Water at 25°C

<u>10<sup>5</sup>[Substrate]</u>	<u>10<sup>3</sup>[SO<sub>3</sub><sup>2-</sup>]</u>	<u>k<sub>obs</sub></u>
(M)	(M)	(sec <sup>-1</sup> )
10	1	39.7 ± 1
5	2	45.0 ± 1
2	5	59.5 ± 1
1	7.5	70.5 ± 1
2	10	80.2 ± 2
2	12	86.1 ± 3

TABLE 5.10

Rate Constants for 1:1-Complex Formation of Picric Acid and  
Sodium Sulphite in Water at 25°C

<u>10<sup>5</sup>[Substrate]</u>	<u>10<sup>3</sup>[SO<sub>3</sub><sup>2-</sup>]</u>	<u>k<sub>obs</sub></u>
(M)	(M)	(sec <sup>-1</sup> )
35	20	116 ± 2 <sup>a</sup>
23		122 ± 2 <sup>b</sup>
	40	120 ± 2 <sup>a</sup>
12	50	142 ± 2 <sup>b</sup>
17	60	124 ± 3 <sup>a</sup>
	80	132 ± 3 <sup>a</sup>
12		156 ± 3 <sup>b</sup>

<sup>a</sup> Made up to ionic strength 0.3M with sodium sulphate

<sup>b</sup> Made up to ionic strength 2.1M with sodium sulphate

$$k_{\text{obs}_2} = \frac{k_2 K_1 [\text{SO}_3^{2-}]^2}{1 + K_1 [\text{SO}_3^{2-}]} + k_{-2} \quad 5.2$$

Equation 5.1 indicates that a plot of  $k_{\text{obs}_1}$  versus sulphite concentration should be linear. However equation 5.2 describes a more complex dependence on sulphite concentration, which is quadratic at low concentrations ( $K_1 [\text{SO}_3^{2-}] \ll 1$ ) and linear at high concentrations ( $K_1 [\text{SO}_3^{2-}] \gg 1$ ), equation 5.2 reducing to:-

$$k_{\text{obs}_2} = k_2 [\text{SO}_3^{2-}] + k_{-2} \quad 5.3$$

Formation of the 1:2-adducts involves the interaction of two negatively charged species and it would be expected that the activity coefficients ( $f_i$ ) of the species will vary with ionic strength (I) according to the Debye-Hückel limiting law

$$-\log f_i = A z^2 \sqrt{I} \quad 5.4$$

where A is a constant (= .509) and  $z$  is the charge on the ion.<sup>226</sup> From transition state theory the rate constant for a reaction in a given medium is related to the activity coefficients of the reacting species in that medium via the Brønsted-Bjerrum equation<sup>227</sup>

$$k = k^{\circ} \frac{f_A f_B}{f^{\ddagger}} \quad 5.5$$

where  $k^{\circ}$  is the limiting value of the rate constant at zero ionic strength, and  $f^{\ddagger}$  can be regarded as the activity coefficient of the transition state. Combination of equations 5.4 and 5.5 readily gives:-

$$\log k = \log k^{\circ} + 2A z_A z_B \sqrt{I} \quad 5.6$$

Thus equation 5.6 predicts a variation in rate with ionic strength. Although equation 5.4 refers to very dilute solutions compared to the ones used in the present work, it nevertheless gives an indication of the variations expected on changing the ionic strength. It would be anticipated that the change in  $k_{\text{obs}}$  with sulphite concentration will not follow equation 5.2 unless constant

ionic strength is maintained. This can be shown in the case of trinitroanisole by reference to Figure 5.6.

For picramide, N-methyl- and N,N-dimethyl-picramides, where  $K_1 > 10^4$  l.mol<sup>-1</sup>, equation 5.3 should hold for sulphite concentrations  $>10^{-3}$  M and this is in fact observed (see Figure 5.7). Thus plots of  $k_{obs}$  versus sulphite concentration were straight lines. The slope and intercept gave values for  $k_2$  and  $k_{-2}$  respectively. However in the case of N-methyl- and N,N-dimethyl-picramides, the intercepts are small and therefore cannot be determined with any accuracy. The values of  $k_{-2}$  for these substrates quoted in Table 5.11 were obtained from combination of the present  $k_2$  values and equilibrium constants determined by Crampton.<sup>159</sup>

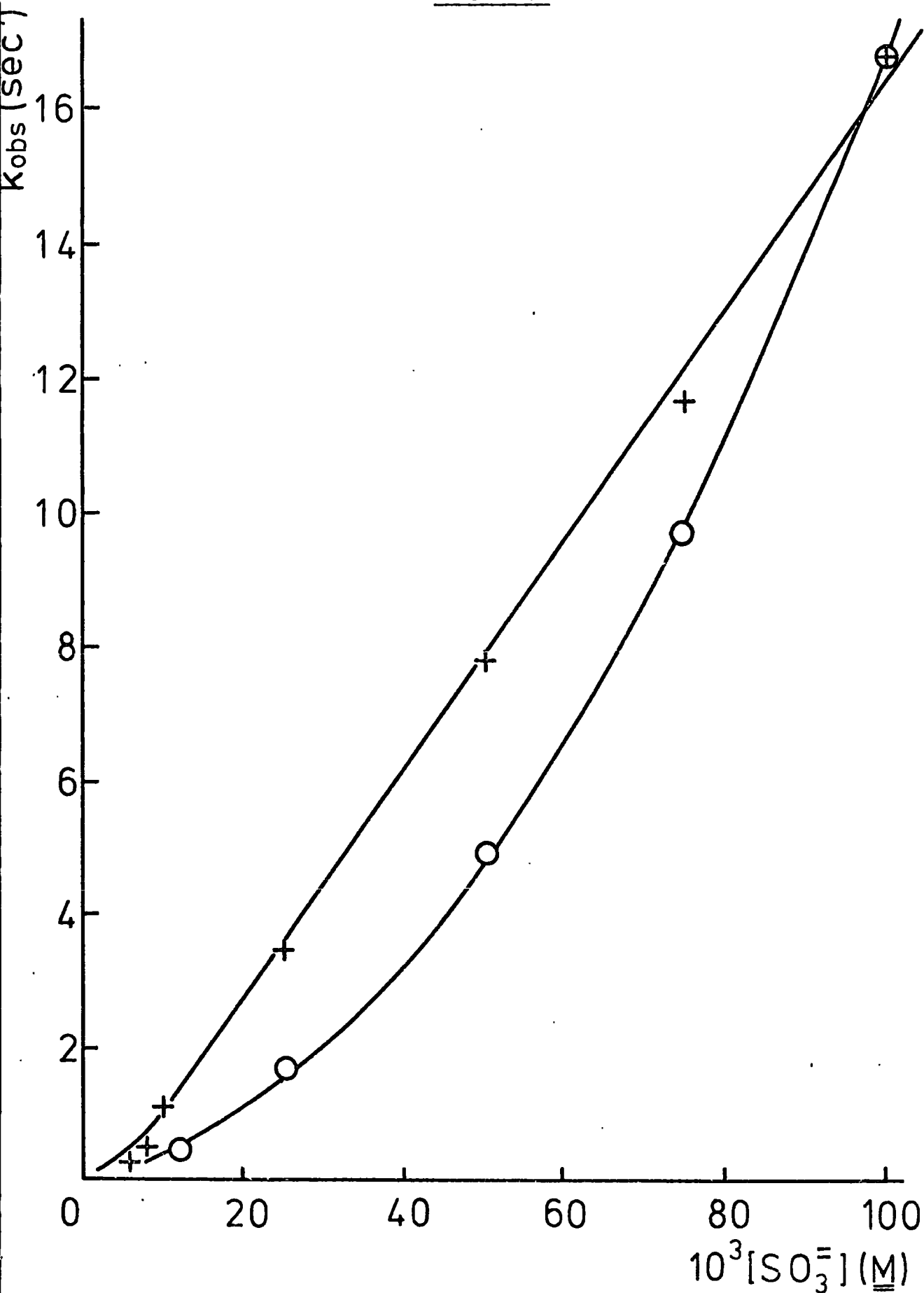
In the case of 2,4,6-trinitroanisole and picric acid, where the equilibrium constants ( $K_1$ ) are at least two orders of magnitude smaller, linearity between  $k_{obs}$  and  $[SO_3^{2-}]$  is not observed until  $[SO_3^{2-}] > 0.01M$  and  $[SO_3^{2-}] > 0.2M$  respectively. For these substrates  $k_2$  was determined from the linear portion of the  $k_{obs_2}$  versus  $[SO_3^{2-}]$  plot. Substitution of this value into equation 5.2 together with  $K_1$  obtained from the first relaxation time yielded a value for  $k_{-2}$ .

The rate and equilibrium data for 1:2-adduct formation are given in Table 5.11.

The low stability and smaller rate constants of formation of both 1:1- and 1:2-complexes of the picrate anion almost certainly reflect the initial negative charge on the substrate.

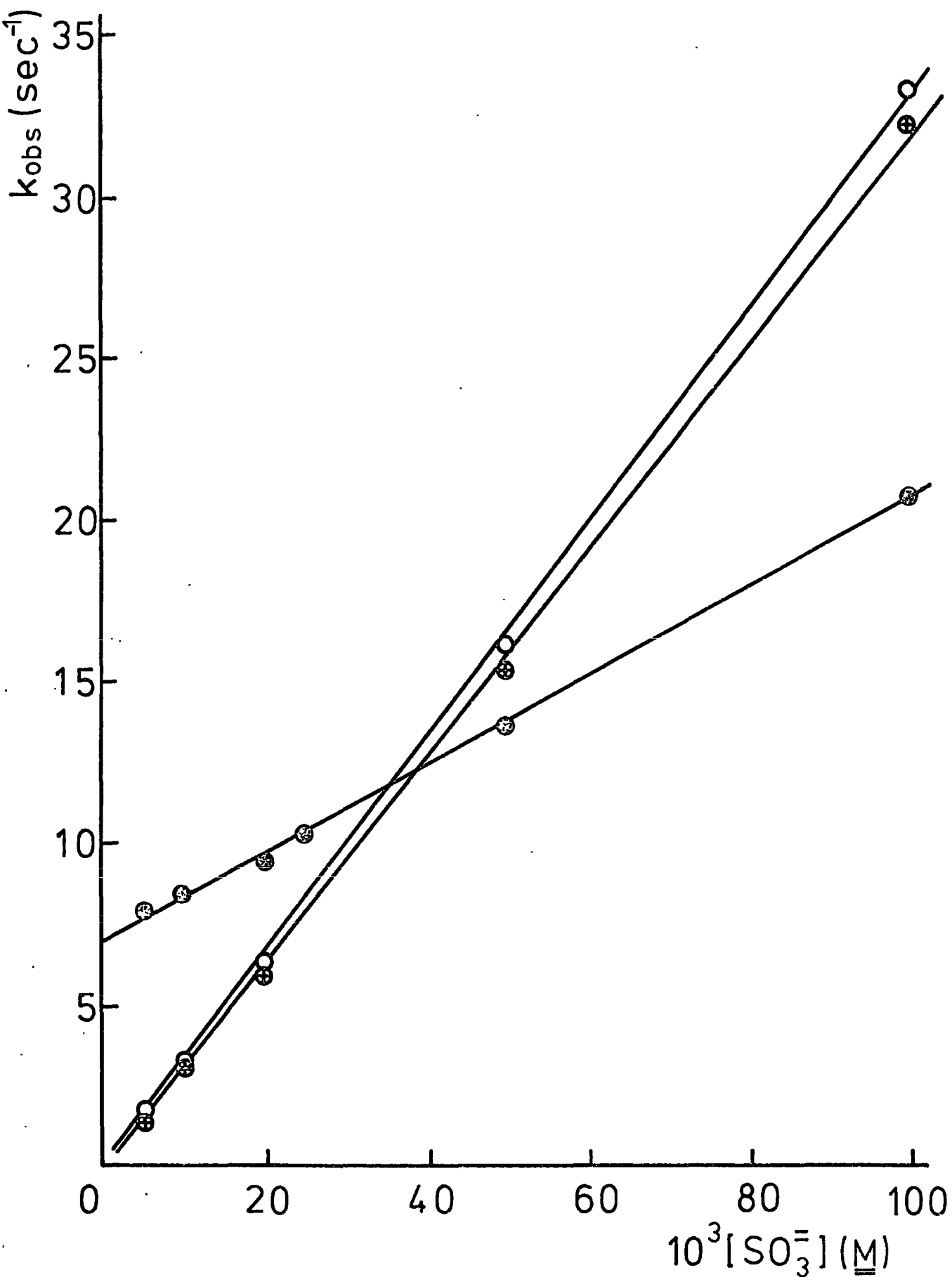
It is interesting to note that the equilibrium constant for the formation of the di-adduct of N,N-dimethylpicramide and methoxide ion in methanol at 25° is ca. 1 l.mol<sup>-1</sup>,<sup>76</sup> over three orders of magnitude smaller than that for complexation involving sulphite ion in water. Allowing for the fact that water is better than methanol at solvating the more localised negative charges of the 1:2-complex, it indicates the greater affinity of sulphur than oxygen for carbon especially since the steric requirement of the sulphite ion will be much greater than for methoxide.

FIGURE 5.6



Plots of  $k_{obs}$  versus sulphite concentration for 1:2-complex formation from 2,4,6-trinitroanisole (O) without added salt, (+) solution made up to ionic strength 0.3M with sodium sulphate.

FIGURE 5.7



Plots of  $k_{obs}$  versus sulphite concentration for 1:2-complex formation from (●) picramide, (⊕) N,N-dimethylpicramide and (○) N-methylpicramide. Ionic strength 0.3M maintained by addition of sodium sulphate.

TABLE 5.11

Rate and Equilibrium Data for 1:1- and 1:2-Complex Formation for  
1-X-2,4,6-Trinitrobenzenes and Sodium Sulphite in Water at 25°C

<u>X</u>	<u>k<sub>1</sub></u> (l.mol <sup>-1</sup> sec <sup>-1</sup> )	<u>k<sub>-1</sub></u> (sec <sup>-1</sup> )	<u>X<sub>1</sub><sup>a</sup></u> (l.mol <sup>-1</sup> )	<u>k<sub>2</sub></u> (l.mol <sup>-1</sup> sec <sup>-1</sup> )	<u>k<sub>-2</sub></u> (sec <sup>-1</sup> )	<u>K<sub>2</sub><sup>a</sup></u> (l.mol <sup>-1</sup> )
H <sup>b</sup>	3.54 x 10 <sup>4</sup>	125	286 (221)	195	21	9.3 (9.2 <sup>c</sup> )
OMe	(4.8 ± 0.4) x 10 <sup>3</sup>	35 ± 2	140 ± 20 (210) <sup>c</sup>	170 ± 10 <sup>d</sup> 650 ± 50 <sup>e</sup>	0.12 ± .02 <sup>d</sup>	(1.4 ± 0.3) x 10 <sup>3d</sup> (0.9 x 10 <sup>3</sup> ) <sup>c</sup>
OH	280 ± 23 <sup>d</sup> 567 ± 58 <sup>e</sup>	109 ± 1 <sup>d</sup> 112 ± 3 <sup>e</sup>		275 ± 5 <sup>e</sup>	4 ± 1 <sup>e</sup>	69 <sup>e</sup>
NH <sub>2</sub>	5.7 x 10 <sup>4f</sup>	7 <sup>f</sup>	8.1 x 10 <sup>3f</sup> (8.6 x 10 <sup>3</sup> )	137 ± 2 <sup>d</sup>	7 ± .1 <sup>d</sup>	19.6 <sup>d</sup> (18.5) <sup>c</sup>
NHMe	1.4 x 10 <sup>4f</sup>	0.2 <sup>f</sup>	7 x 10 <sup>4f</sup> (6.8 x 10 <sup>4</sup> )	333 ± 4 <sup>d</sup>	(0.19) <sup>g</sup>	(1.8 x 10 <sup>3</sup> ) <sup>c</sup>
NMe <sub>2</sub>	4.1 x 10 <sup>3f</sup>	0.14 <sup>f</sup>	2.9 x 10 <sup>4f</sup> (3 x 10 <sup>4</sup> )	323 ± 3 <sup>d</sup>	(.005) <sup>g</sup>	(6.2 x 10 <sup>4</sup> ) <sup>c</sup>

<sup>a</sup> Kinetic values ( $k_1/k_{-1}$  and  $k_2/k_{-2}$ ). Figures in parentheses are equilibrium values

<sup>b</sup> From reference 222.

<sup>c</sup> From reference 159.

<sup>d</sup> Ionic strength 0.3M.

<sup>e</sup> Ionic strength ~~0.3~~<sup>2.1</sup>M.

<sup>f</sup> Reference 224.

<sup>g</sup> Calculated from  $k_2/K_2$ .

As with the 1:1-complexes,<sup>224</sup> the increased stability of the 1:2-adducts of N-methyl- and N,N-dimethyl-picramides results mainly from smaller values of  $k_{-2}$  rather than steric factors favouring complex formation.

It seems from the present work that when  $X \neq H$  only one isomer of the 1:2-adduct is formed. It may be that the substituent at  $C_1$  (X) forces the ortho-nitro groups into such a conformation which allows for more effective solvation of the negative charges on the adjacent sulphite groups and on the nitro groups themselves. Assuming Bernasconi's assignments<sup>222</sup> for the cis- and trans-isomers of the 1,3,5-trinitrobenzene 1:2-complex it may be inferred that for  $X \neq H$  the trans-complex is formed since the values of  $k_2$  are very similar. This fits in with the supposition, presented earlier, that the observed broadening in the p.m.r. spectrum results from the cis-isomer.

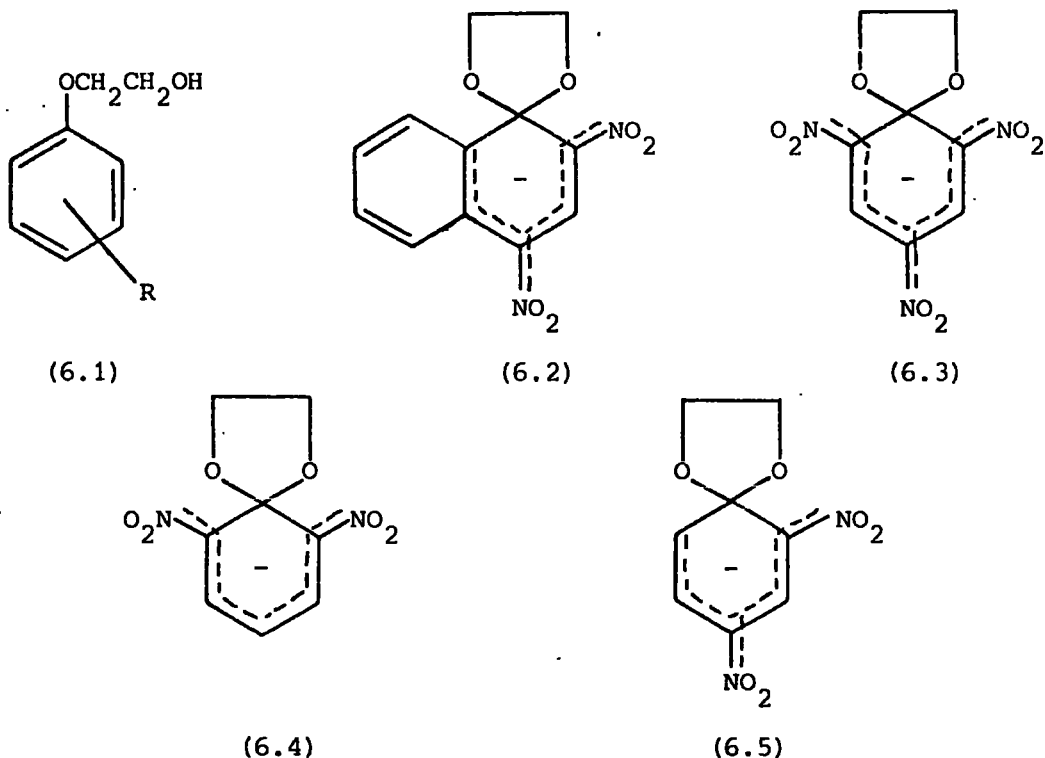
Alternatively, it has been pointed out<sup>228</sup> that failure to observe a third relaxation time in such systems may be due to an equality or similarity in the rates of dissociation for both cis- and trans-isomers. Nevertheless, it can be argued that since there appears to be no evidence, especially in the p.m.r. spectra, for the existence of two isomers at equilibrium, only one isomer is preferred, the concentration of the other, if formed at all, being too small for detection.

CHAPTER 6

EQUILIBRIUM AND KINETIC STUDIES ON SPIRO-COMPLEX FORMATION IN WATER

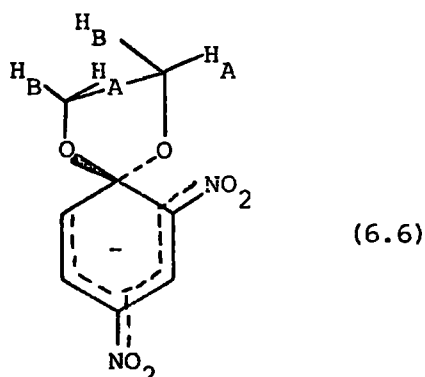
INTRODUCTION

There is convincing structural evidence for spiro-complex formation on treating suitably ring-activated 2-hydroxyethoxy aromatics (6.1) with base.<sup>49,52</sup> Solid complexes of structure (6.2)-(6.5) have been isolated from the respective

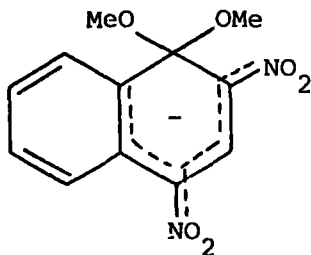


glycol ethers. Analysis of the p.m.r. spectra of solutions of these adducts has confirmed their spiro structure.

Such complexes have also provided convincing evidence for the  $sp^3$  hybridisation of the  $C_1$  carbon atom of the cyclohexadienyl systems in Meisenheimer complexes.<sup>52</sup> Thus the non-equivalence of the methylene protons in (6.5) results from two protons being cis ( $H_A$ ) and two protons being trans ( $H_B$ ) to the ortho-nitro group as shown in (6.6.):



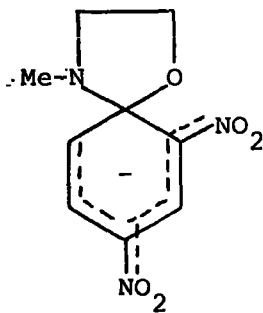
It has been inferred<sup>8,45</sup> that spiro-complexes have considerably greater stability than their corresponding non-cyclic analogues. However Fendler *et al*<sup>52</sup> reported similar equilibrium and rate constants for complexes (6.2) and (6.7). Nevertheless, in contrast with Fendler's report, results



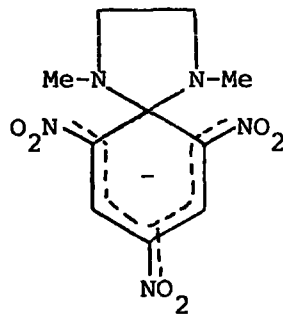
(6.7)

obtained by Crampton<sup>184</sup> indicate considerably greater stabilities for complexes (6.2), (6.4) and (6.5) than for their dimethoxy analogues.

Spiro-Meisenheimer complexes are also of current interest as models for the intermediates in nucleophilic aromatic substitution reactions. They have been used in this respect by Bernasconi and coworkers<sup>81,82,229,230</sup> who reported



(6.8)



(6.9)

data for (6.8)<sup>81</sup> and (6.9)<sup>229</sup> in water and water-DMSO mixtures.

In the present work equilibrium and kinetic measurements have been made in water for the four differently activated complexes (6.2)-(6.5). The results indicate, as found in methanol,<sup>184</sup> that the kinetic and equilibrium parameters are many orders of magnitude greater than those of their non-cyclic analogues.

#### EXPERIMENTAL

Solutions of suitable concentration were prepared immediately before use from freshly made stock solutions of reagents. U.v. and visible spectral

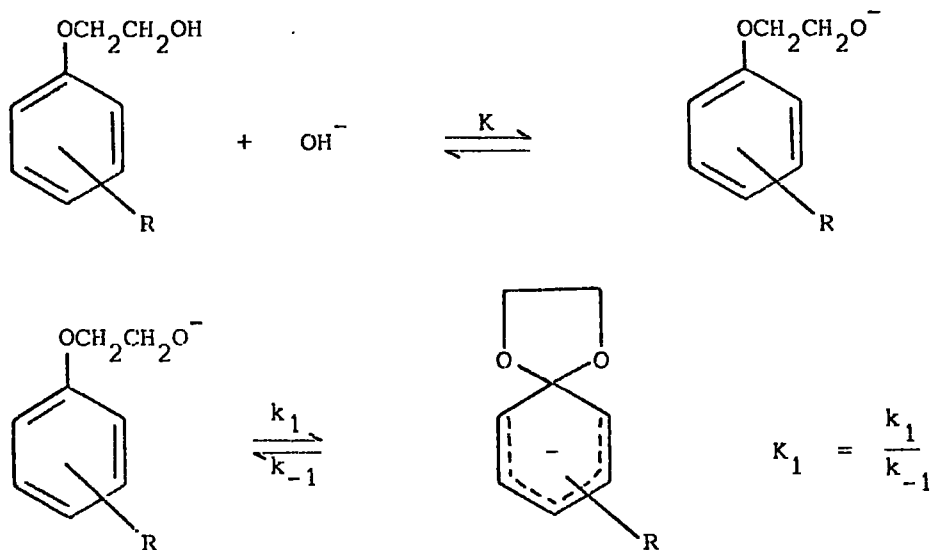
shape measurements were made with a Unicam SP8000 recording spectrophotometer. Accurate optical density values for equilibrium determinations were made using an SP500 instrument. Kinetic data were obtained using a 'Canterbury' stopped-flow spectrophotometer. Both kinetic and equilibrium measurements were made in the visible region of the spectrum at the absorption maxima of the spiro-complexes. P.m.r. spectra for the 2,4,6-trinitrobenzene derivative were recorded with a Varian HA56/60 instrument.

RESULTS

The results obtained for the four complexes will be treated individually. However the following general considerations are applicable in all cases.

Spiro-complex formation

In the present case the probable mechanism for spiro-complex formation in alkaline media is that suggested by Crampton<sup>184</sup> and Bernasconi<sup>81</sup> and represented in the following scheme.



The parent glycol ether is in fast equilibrium with the glycolate anion whose internal cyclisation to the spiro-complex is slow. At the wavelength of measurement the parent ethers show little or no absorption. Since there is no possibility of the negative charge on the glycolate anion being delocalised into the aromatic system, it is assumed that the anions will have zero or very

small extinction coefficients at these wavelengths.

The measured stoichiometric equilibrium constant,  $K_C$ , can then be defined by equation 6.1 from which equation 6.2 can be readily deduced.

$$K_C = \frac{[\text{spiro complex}]}{([\text{glycol ether}] + [\text{anion}])[\text{OH}^-]} \quad 6.1$$

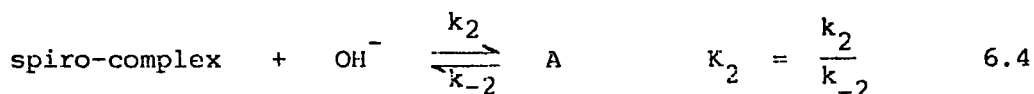
$$K_C = \frac{KK_1}{(1 + K[\text{OH}^-])} \quad 6.2$$

Kinetic measurements were made using concentrations of base in large excess of the substrate concentration or in buffer solutions where the pH was constant during any one kinetic run. In either case attainment of equilibrium followed first-order kinetics, the rate constant for which is given by equation 6.3.

$$k_{\text{obs}} = \frac{k_1 K [\text{OH}^-]}{(1 + K[\text{OH}^-])} + k_{-1} \quad 6.3$$

#### Formation of hydroxide adducts from spiro-complexes

In alkaline media containing  $>0.1M$  sodium hydroxide the fast formation of the intensely coloured spiro-complex was followed by a slower process resulting in a decrease in absorption in the visible and an increase in the u.v. region of the spectrum. These changes were reversible and did not result in destruction of the substrate. If it is assumed that an interaction occurs between spiro-complex and one hydroxide ion to form an adduct A then equation 6.4 results.



Measurement of the relaxation times by stopped-flow spectrophotometry revealed that in all cases the second process associated with the decrease in absorbance was at least an order of magnitude slower than that for spiro-complex formation. Equation 6.5 for the observed first-order rate constant for the slower process is obtained by standard methods. <sup>225</sup>

$$k_{\text{obs}}' = \frac{k_2 K K_1 [\text{OH}^-]}{1 + K[\text{OH}^-] + K K_1 [\text{OH}^-]} + k_{-2} \quad 6.5$$

Very much slower irreversible reactions resulting in the formation of the respective substituted phenols were also observed.

(i) 1-(2-Hydroxyethoxy)-2,4-dinitronaphthalene

The variation of spectral shape with base concentration is shown in Figure 6.1. Two reversible equilibria are present. The first interaction, dominant in dilute base solution, corresponds to spiro-complex formation (6.2) with  $\lambda_{\text{max}}$  495 ( $\epsilon$   $1.8 \times 10^4$ ) and 342 nm ( $\epsilon$   $1.3 \times 10^4$  l.mol<sup>-1</sup> cm<sup>-1</sup>). Data for a typical kinetic run are given in Table 6.1. As the base concentration is

TABLE 6.1

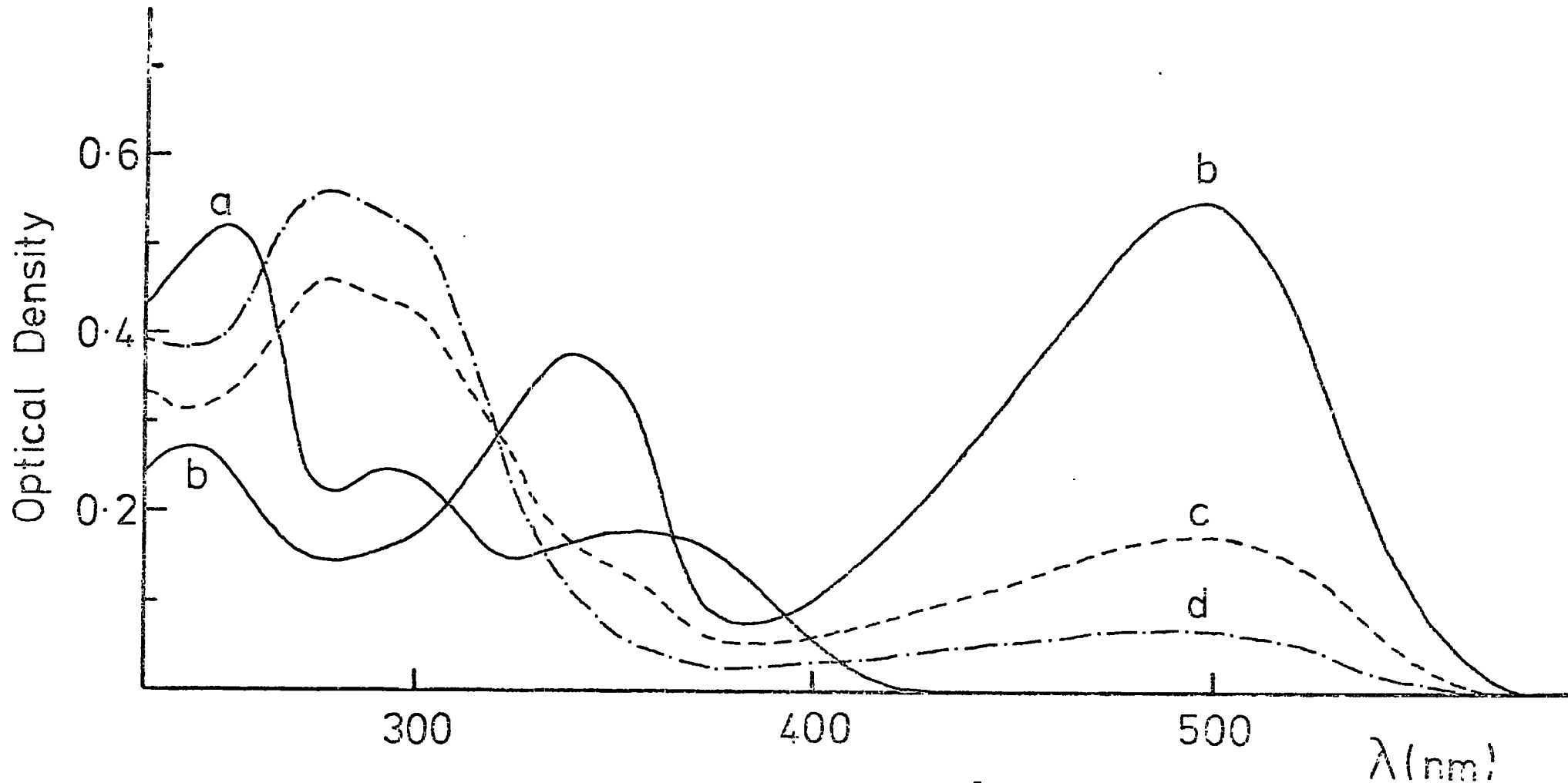
Rate Data for the Formation of Complex (6.2) from 1-(2-Hydroxyethoxy)-2,4-dinitronaphthalene ( $6 \times 10^{-6}$  M) at pH<sup>a</sup> 10.5 in Water at 25°C

<u>Time</u> (m.sec)	<u>Scale Reading</u> (arbitrary units)	$\frac{k_{\text{obs}}}{\text{(sec}^{-1}\text{)}}$
0	1.45	-
5	2.27	31
10	2.94	31
15	3.58	31
20	4.18	33
25	4.55	32
30	4.94	32
40	5.54	32
50	5.95	32
60	6.30	32
70	6.50	32
$\infty$	7.11	-

<sup>a</sup> Borax buffer,  $1.25 \times 10^{-2}$  M

increased the changes indicate conversion to a second species with  $\lambda_{\text{max}}$  275 ( $\epsilon$   $2 \times 10^4$ ) and 300 nm ( $\epsilon$   $1.8 \times 10^4$  l.mol<sup>-1</sup> cm<sup>-1</sup>). Eventually a very slow

FIGURE 6.1



Visible spectra of 1-(2-hydroxyethoxy)-2,4-dinitronaphthalene ( $3 \times 10^{-5} M$ ) in water containing (a) 0, (b) 0.01, (c) 1.0 and (d) 2.0M sodium hydroxide.

reaction gave a species with a spectrum ( $\lambda_{\max}$  390 and 430 nm) identical to that of 2,4-dinitronaphthol.

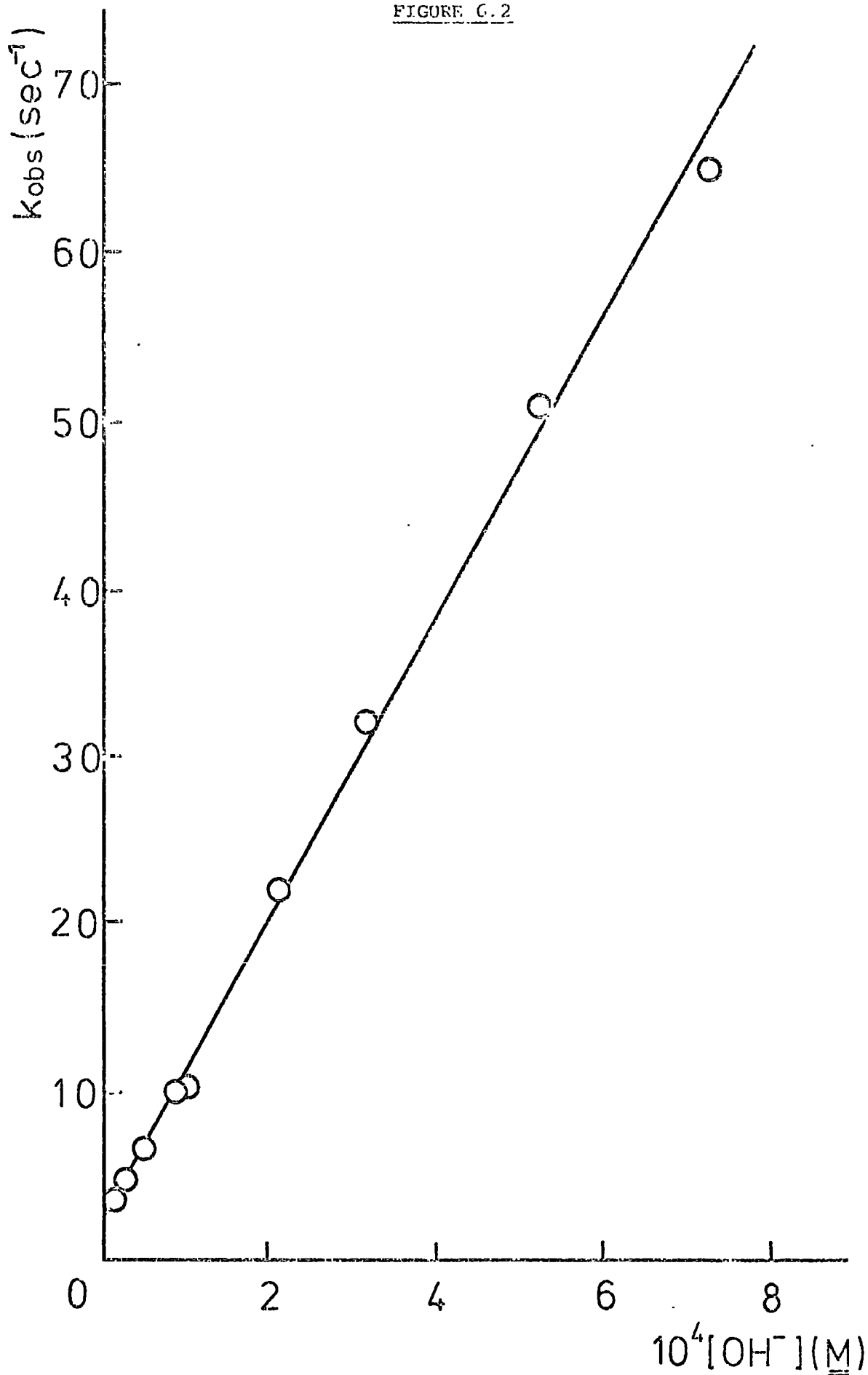
Equilibrium and kinetic data for spiro-complex formation are collected in Table 6.2. Conversion to complex is complete in ca.  $1 \times 10^{-2}$  M sodium hydroxide and therefore optical density measurements in aqueous buffer solutions allowed direct determination of  $K_C$ . The values obtained are independent of base concentration and this indicates that in equation 6.2  $K[OH^-] \ll 1$  and therefore  $K_C$  gives directly  $KK_1 [(3 \pm 0.3) \times 10^4 \text{ l.mol}^{-1}]$ . The value of the rate constant,  $k_{\text{obs}}$ , for spiro-complex formation decreases with decreasing pH to a minimum value of  $2.3 \pm .1 \text{ sec}^{-1}$  at pH 7 and this value then corresponds to  $k_{-1}$  in equation 6.3. A plot of  $k_{\text{obs}}$  versus  $[OH^-]$  is linear (Figure 6.2) with slope  $(= k_1K) (9 \pm 1) \times 10^4 \text{ l.mol}^{-1} \text{ sec}^{-1}$ . Linearity here again indicates that  $K[OH^-] \ll 1$  (see equation 6.3). The results in Table 6.2 show that variation of buffer concentration at constant pH does not affect the value of  $k_{\text{obs}}$ , within experimental error, indicating the absence of buffer catalysis.

Observation by stopped-flow spectrophotometry at 495 nm shows that in solutions containing  $>0.1$  M sodium hydroxide the initial fast build-up of colour is followed by a much slower fading reaction. Measurements of optical density after the attainment of the second equilibrium are given in Table 6.3 and were used to calculate values of  $K_2$ , the equilibrium constant for higher complex formation, using  $K_2 = (0.535 - \text{O.D.}_{495}) / \text{O.D.}_{495} \times [OH^-]$ . The values thus obtained increase with base concentration no doubt reflecting that the basicity of the medium should be represented by an acidity function, of the  $J_2$ -type<sup>164b</sup> which these figures could be used to define.

Rate constants for the second relaxation time at two base concentrations are in Table 6.3. In this case since  $K[OH^-] \ll 1 \ll K_1K[OH^-]$  equation 6.5 reduces to

$$k_{\text{obs}}' = k_2[OH^-] + k_{-2} \quad 6.6$$

FIGURE G.2



Plot of  $k_{\text{obs}}$  versus  $[\text{OH}^-]$  for spiro-complex formation from 1-(2-hydroxyethoxy)-2,4-dinitronaphthalene in water at  $25^\circ\text{C}$ .

TABLE 6.2

Equilibrium and Kinetic Data- for Formation of Complex (6.2) from  
1-(2-Hydroxyethoxy)-2,4-dinitronaphthalene in Aqueous Buffers at 25°C

<u>pH</u>	<u>Conditions</u>	<u>O.D.</u> <sup>a</sup>	$\frac{10^{-4} K_C}{(1.\text{mol}^{-1})}$	$\frac{k_{\text{obs}}}{(\text{sec}^{-1})}$
7.1	b			2.2 ± 0.1
7.4	c			2.4
7.6	c			2.3
8.0	d	0.003		2.5
8.97	d	0.123	3.2	3.2
9.0	e			3.2
9.23	d	0.180	3.0	
9.36	d	0.239	3.5	4.4
9.65	d	0.301	2.9	6.3
9.77	d	0.347	3.1	
9.9	f			9.9
10.0	g			10.1
10.04	d	0.393	2.5	
10.14	d	0.431	3.0	
10.32	d			22
10.5	d	0.480	2.8	32
10.72	d			51
10.86	d			65
12	h	0.535		

<sup>a</sup> Measured with Unicam SP500 for  $3 \times 10^{-5} \text{M}$  substrate at 495 nm

<sup>b</sup> Phosphate buffer,  $2.5 \times 10^{-2} \text{M}$       <sup>c</sup> Phosphate buffer,  $5 \times 10^{-2} \text{M}$

<sup>d</sup> Borax buffer,  $1.25 \times 10^{-2} \text{M}$       <sup>e</sup> Borax buffer,  $5 \times 10^{-2} \text{M}$

<sup>f</sup> Phenol-sodium phenoxide,  $2.5 \times 10^{-2} \text{M}$

<sup>g</sup> Phenol-sodium phenoxide,  $0.25 \text{M}$

<sup>h</sup> Sodium hydroxide,  $1 \times 10^{-2} \text{M}$

TABLE 6.3

Equilibrium and Kinetic Data for Hydroxide Addition to  
Spiro-complex (6.2) ( $\times \times 10^{-5} M$ ) in Water at 25°C

<u>[NaOH]</u>	<u>O.D.</u>	$K_2^b$ ( $l.mol^{-1}$ )	$k_{obs}^a$ ( $sec^{-1}$ )
0.01	0.535		
0.10	0.490	1.0	$0.04 \pm 0.01$
0.15	0.46	1.1	
0.20	0.43	1.2	
0.31	0.38	1.3	
0.51	0.29	1.6	$0.05 \pm 0.01$
0.71	0.22	2.0	
1.0	0.16	2.3	

<sup>a</sup> Measured at 495 nm

<sup>b</sup> Calculated using  $K_2 = (0.535 - O.D._{495}) / O.D._{495} \times [NaOH]$

Combination of  $k_{obs}^a$  with the known values of  $K_2$  enabled values of  $k_2$  and  $k_{-2}$  to be determined. These measurements were not made at constant ionic strength so that some variation of these parameters with base concentration would be expected; formation of these higher complexes involves reaction of two negatively charged species and a positive salt effect would, a priori, be expected.

(ii) 1-(2-Hydroxyethoxy)-2,4,6-trinitrobenzene

The p.m.r. spectrum of the glycol ether has bands at  $\delta 9.1$  (singlet; equivalent ring protons, 4.6 (singlet; OH) and 3.7 and 4.2 p.p.m. (two multiplets; methylene protons). In water in the presence of one equivalent of base, the spectrum showed peaks at  $\delta 8.55$  (singlet; ring protons) and 4.3 p.p.m. (singlet; methylene protons) attributable to the spiro-complex.

In aqueous solutions the parent ether is in equilibrium with the spiro-complex,  $\lambda_{\text{max}}$  417 ( $\epsilon$   $2.5 \times 10^4$ ) and 470 nm ( $\epsilon$   $1.8 \times 10^4$  l.mol<sup>-1</sup> cm<sup>-1</sup>). Even in neutral or slightly acidic media some complex is present indicating a very large value for  $KK_1$ . The value of  $1.8 \times 10^7$  l.mol<sup>-1</sup> obtained by Murto<sup>45</sup> is in accord with this.

Rates of colour formation, measured at 420 nm by mixing solutions of the parent in  $10^{-4}$  M hydrochloric acid with alkaline buffers were accurately first-order. The data for a typical run are given in Table 6.4. Variation of the

TABLE 6.4

Rate Data for the Formation of Complex (6.3) from 1-(2-Hydroxy-ethoxy)-2,4,6-trinitrobenzene ( $5 \times 10^{-6}$  M) at pH<sup>a</sup> 7.5 in Water at 25°C

<u>Time</u> (sec)	<u>Scale Reading</u> (arbitrary units)	$\frac{k_{\text{obs}}}{(\text{sec}^{-1})}$
0	1.63	-
0.5	3.08	0.54
1.0	4.22	0.55
1.5	5.18	0.57
2.0	5.80	0.57
2.5	6.27	0.56
3.0	6.63	0.56
3.5	6.90	0.56
4.0	7.15	0.57
4.5	7.30	0.57
$\infty$	7.78	-

<sup>a</sup> Phosphate buffer,  $5 \times 10^{-2}$  M

rate constant with pH is given in Table 6.5 and, within experimental error, the values of  $k_{\text{obs}}$  are independent of buffer concentration. From the plot of  $k_{\text{obs}}$  versus  $[\text{OH}^-]$  which was linear (Figure 6.3) a value of  $(1.6 \pm 0.3) \times 10^6$

TABLE 6.5

Kinetic Data for Formation of Complex (6.3) from 1-(2-Hydroxy-ethoxy)-2,4,6-trinitrobenzene<sup>a</sup> in Aqueous Buffers at 25°C

<u>pH</u>	<u>Conditions</u>	$\frac{k_{obs}}{(\text{sec}^{-1})}$
5.8	b	0.11 ± 0.01
6.0	b	0.11
6.0	c	0.11
6.0	d	0.11
6.2	b	0.12
6.6	b	0.15
7.0	b	0.25
7.5	b	0.56
8.0	b	1.4
8.5	e	5.3
8.7	e	8.4
9.0	e	15.6
9.0	f	14
9.25	e	30

<sup>a</sup> Substrate concentration is in the range  $5 \times 10^{-6} - 1 \times 10^{-4} \underline{\text{M}}$

<sup>b</sup> Phosphate buffer,  $5 \times 10^{-2} \underline{\text{M}}$

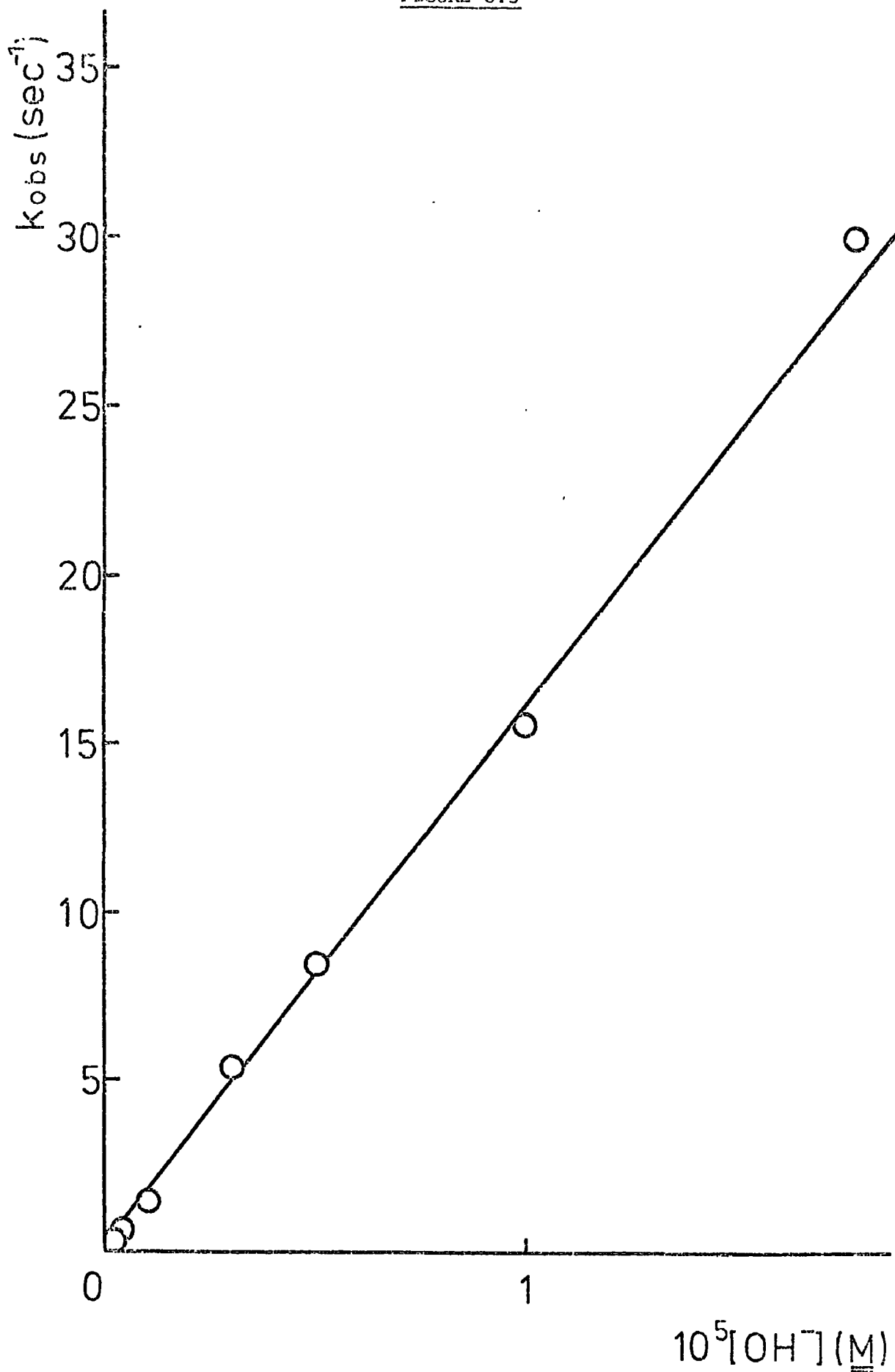
<sup>c</sup> Phosphate buffer,  $2.5 \times 10^{-2} \underline{\text{M}}$

<sup>d</sup> Phosphate buffer,  $0.1 \underline{\text{M}}$

<sup>e</sup> Borax buffer,  $1.25 \times 10^{-2} \underline{\text{M}}$

<sup>f</sup> Borax buffer,  $0.125 \underline{\text{M}}$

FIGURE 6.3



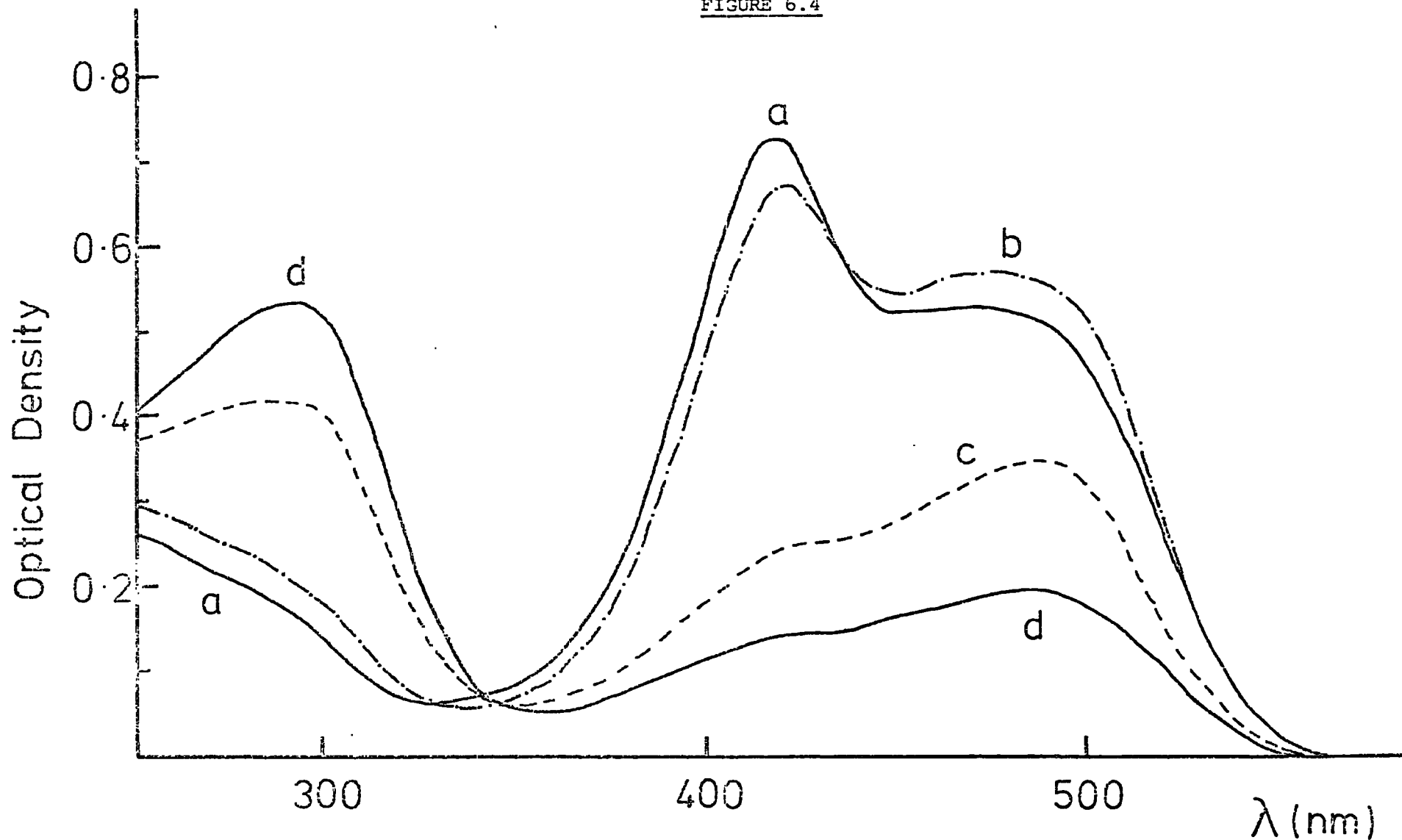
Plot of  $k_{\text{obs}}$  versus  $[\text{OH}^-]$  for spiro-complex formation from 1-(2-hydroxyethoxy)-2,4-dinitronaphthalene in water at  $25^\circ\text{C}$ .

$1. \text{mol}^{-1} \text{sec}^{-1}$  was obtained for  $k_1K$ . For this substrate also  $k[\text{OH}^-] \ll 1$ . The intercept was too small to determine a value of  $k_{-1}$  with any accuracy. However using equation 6.3 for every point in the range  $6 \leq \text{pH} \leq 7$  gave  $k_{-1} = 0.095 \pm .01 \text{ sec}^{-1}$ . Combination of this value with that for  $k_1K$  gives a value of  $1.7 \times 10^7 \text{ l.mol}^{-1}$  for  $KK_1$  which is in excellent agreement with that obtained independently by Murto.<sup>45</sup> In more acidic solutions the values of  $k_{\text{obs}}$  increased above the minimum value due to an acid catalysed pathway between parent and complex. This will be discussed in detail in Chapter 7. However these effects are unimportant above pH 6 and need not be considered in this instance.

In solutions containing  $>0.1\text{M}$  sodium hydroxide further reversible reactions occur which can be shown by reference to Figure 6.4. In the range  $0.1-1.0\text{M}$  base the absorption at 417 nm decreases in intensity and that at 480 nm increases. As the base concentration is increased further a band in the u.v. at  $\lambda_{\text{max}} 290 \text{ nm}$  increases at the expense of the visible absorption. These changes can be interpreted in terms of two successive equilibria involving the spiro-complex with one (A) and two (B) hydroxide ions respectively. From the changes in optical density with base concentration, it was possible to calculate approximate values for the equilibrium constants  $K_2$  and  $K_3$  (defined as  $[\text{B}]/[\text{A}][\text{OH}^-]$ ) assuming that, as with other di-adducts containing three nitro groups,<sup>6,8,44</sup> complex A will only have one absorption in the visible region. Thus  $K_2$  has a value of ca.  $0.1 \text{ l.mol}^{-1}$  at  $1\text{M}$  base increasing to  $0.2$  at  $2\text{M}$  and  $0.5$  at  $3\text{M}$  base. The value of  $K_3$  is ca.  $0.5 \text{ l.mol}^{-1}$  at  $2\text{M}$  base and increases with base concentration.

Kinetic measurements of the formation of adduct A from the spiro-complex were made at 420 nm in solutions containing  $0.3-0.5\text{M}$  base. The value obtained for the first-order rate constant,  $k_{\text{obs}}$ , is  $0.9 \pm 0.2 \text{ sec}^{-1}$ . In this instance equation 6.6. will apply but as  $K_2[\text{OH}^-] \ll 1$  and hence  $k_{-2} \gg k_2[\text{OH}^-]$  the value of  $k_{\text{obs}}$  will be close to that of  $k_{-2}$ .

FIGURE 6.4



Visible spectra of 1-(2-hydroxyethoxy)-2,4,6-trinitrobenzene ( $3 \times 10^{-5} \text{M}$ ) in water containing (a) 0.1, (b) 1.0, (c) 3.0 and (d) 4.0M sodium hydroxide.

(iii) 1-(2-Hydroxyethoxy)-2,6-dinitrobenzene

The visible spectrum of a solution of the substrate in dilute (<0.1M) sodium hydroxide solutions has a maximum at 575 nm attributed to the spiro-complex (6.4). In more concentrated solutions a second interaction is also present giving rise to species A with  $\lambda_{\max}$  297 nm ( $\epsilon$   $2.2 \times 10^4$  l.mol<sup>-1</sup>cm<sup>-1</sup>) (Figure 6.5). Since appreciable concentrations of A were formed before complete conversion to spiro-complex was achieved, it was not possible to determine directly the extinction coefficient of the latter. However using an extrapolation procedure<sup>166,184</sup> on data obtained in DMSO-water mixtures where conversion to complex was complete gave  $\epsilon = (1.85 \pm 0.2) \times 10^4$  l.mol<sup>-1</sup>cm<sup>-1</sup>. The measured values of  $K_C$  in Table 6.6 are constant in dilute base solutions but decrease in solutions containing >0.1M sodium hydroxide. One explanation could involve the  $K[OH^-]$  term in equation 6.2. However it seems unlikely that the values of K will differ greatly amongst the substrates studied and a more plausible explanation is the intervention of higher adduct formation. Examination of the system by stopped-flow spectrophotometry at 575 nm indicates that after the initial spiro-complex formation, typical data being given in Table 6.7, a slower reaction occurs accompanied by a decrease in absorption at this wavelength. The relaxation times of these processes are such that the optical density measured with a conventional spectrophotometer corresponds to the value after the attainment of the second equilibrium. Values of  $K_2$  may therefore be determined as follows.

At equilibrium

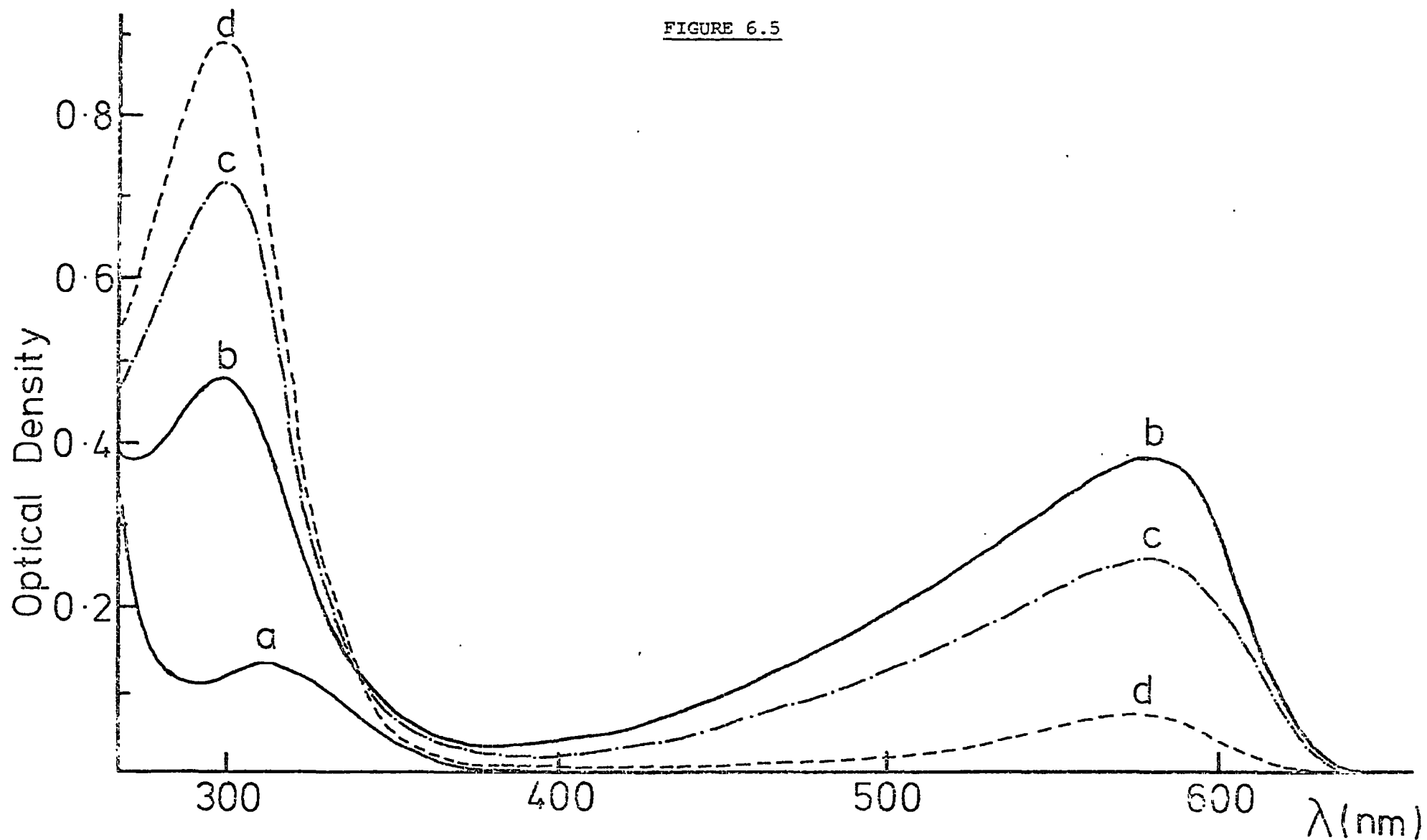
$$[\text{parent}]_{\text{stoich}} = [\text{parent}] + [\text{spiro}] + [\text{A}] \quad 6.7$$

$$K_C = \frac{[\text{spiro}]}{[\text{parent}][OH^-]} \quad 6.8$$

and

$$K_C' = \frac{[\text{spiro}]}{([\text{parent}] + [\text{A}])[OH^-]} \quad 6.9$$

FIGURE 6.5



Visible spectra recorded immediately after preparing the samples of 1-(2-hydroxyethoxy)-2,6-dinitrobenzene ( $4.7 \times 10^{-5} \text{ M}$ ) in water containing (a) 0, (b) 1.0, (c) 2.0 and (d) 4.0M sodium hydroxide.

TABLE 6.6

Equilibrium and Kinetic Data for Complex Formation from 1-(2-Hydroxyethoxy)-2,6-dinitrobenzene in Water at 25°C

$10^5 [\text{Parent}]_{\text{Stoich}}$	[NaOH]	Equilibrium O.D. <sup>a</sup>	$K_C^b$	$K_2^c$	$k_{\text{obs}}^d$	$k_{\text{obs}}^{\prime e}$
(M)	(M)		( $1.\text{mol}^{-1}$ )	( $1.\text{mol}^{-1}$ )	( $\text{sec}^{-1}$ )	( $\text{sec}^{-1}$ )
27	0.010	0.064 <sup>f</sup>	1.29		138 ± 3	
24	0.020	0.113 <sup>f</sup>	1.30			
21	0.030	0.147 <sup>f</sup>	1.31			
15	0.051	0.172 <sup>f</sup>	1.31		155 ± 8	
15	0.051 <sup>g</sup>	0.167 <sup>f</sup>	1.25		143 ± 4	
7.5	0.051	0.085 <sup>f</sup>	1.30			
9.0	0.071	0.141	1.31			
6.0	0.103	0.131	1.30		152 ± 5	
6.0	0.206	0.230	1.28	(0.3)	180 ± 8	0.105
6.0	0.31	0.30	1.21	0.59		
3.0	0.35				185 ± 8	0.110
6.0	0.41	0.36	1.16	0.55		
6.0	0.51	0.40	1.09	0.57	218 ± 8	0.115
6.0	0.72	0.44	0.91	0.64		

<sup>a</sup> Measured with a Unicam SP500 at 575 nm. <sup>b</sup> Calculated using  $K_C = \text{O.D. (575)} / ([\text{Parent}]_{\text{stoich}} \times 1.85 \times 10^4 - \text{O.D. (575)}) [\text{OH}^-]$

<sup>c</sup> Calculated using equation 6.11. <sup>d</sup> Rate of colour formation at 575 nm. <sup>e</sup> Rate of colour fading at 575 nm.

<sup>f</sup> Measurements were made with 4 cm cells. Values quoted for 1 cm path-length. <sup>g</sup> Made up to ionic strength 0.2M with NaCl

TABLE 6.7

Rate Data for the Formation of Complex (6.4) from 1-(2-Hydroxy-ethoxy)-2,6-dinitrobenzene ( $3 \times 10^{-5}M$ ) and Sodium Hydroxide (0.35M)  
in Water at 25°C

<u>Time</u> (m.sec)	<u>Scale Reading</u> (arbitrary units)	$\frac{k_{obs}}{(\text{sec}^{-1})}$
0	2.20	-
2	3.59	180
4	4.60	184
6	5.32	189
8	5.80	191
10	6.08	185
12.5	6.40	195
15	6.55	194
17.5	6.63	188
20	6.71	197
$\infty$	6.80	-

which corresponds to the measured value of the equilibrium constant at higher base concentrations

$$K_2 = \frac{[A]}{[\text{spiro}][\text{OH}^-]} \quad 6.10$$

Substituting in equation 6.10 for [spiro] from equation 6.9 and [A] from equation 6.7 and rearranging gives

$$K_2 = \frac{1}{K_C'[\text{OH}^-]^2} - \frac{[\text{parent}]}{K_C'([\text{parent}]_{\text{stoich}} - [\text{spiro}])[\text{OH}^-]^2}$$

$$= \frac{1}{K_C'[\text{OH}^-]^2} - \frac{[\text{parent}]}{[\text{spiro}][\text{OH}^-]}$$

$$= \left( \frac{1}{K_C'} - \frac{1}{K_C} \right) \cdot \frac{1}{[\text{OH}^-]^2} \quad 6.11$$

Treatment of the data in Table 6.6, according to equation 6.11 at the higher base concentrations gives a value for  $K_2$  of  $0.6 \pm 0.2 \text{ l.mol}^{-1}$ .

An alternative approach to the calculation of  $K_2$  values is afforded by stopped-flow spectrophotometric measurements. The two relaxation times corresponding to spiro-complex and di-adduct formation are sufficiently well separated to allow the determination of optical densities both before and after the attainment of the second equilibrium. This enabled the change in spiro-complex concentration  $\Delta[\text{spiro}]$  between the first and second equilibria to be calculated. The equilibrium concentration of the di-adduct A is related to  $\Delta[\text{spiro}]$  and  $K_C$  as follows:-

$$[A] = \Delta[\text{spiro}] + \Delta[\text{parent}]$$

where  $\Delta[\text{parent}]$  is the concentration of substrate converted to the spiro-complex to maintain the equilibrium.

$$\text{But } \Delta[\text{parent}] = \frac{\Delta[\text{spiro}]}{K_C[\text{OH}^-]}$$

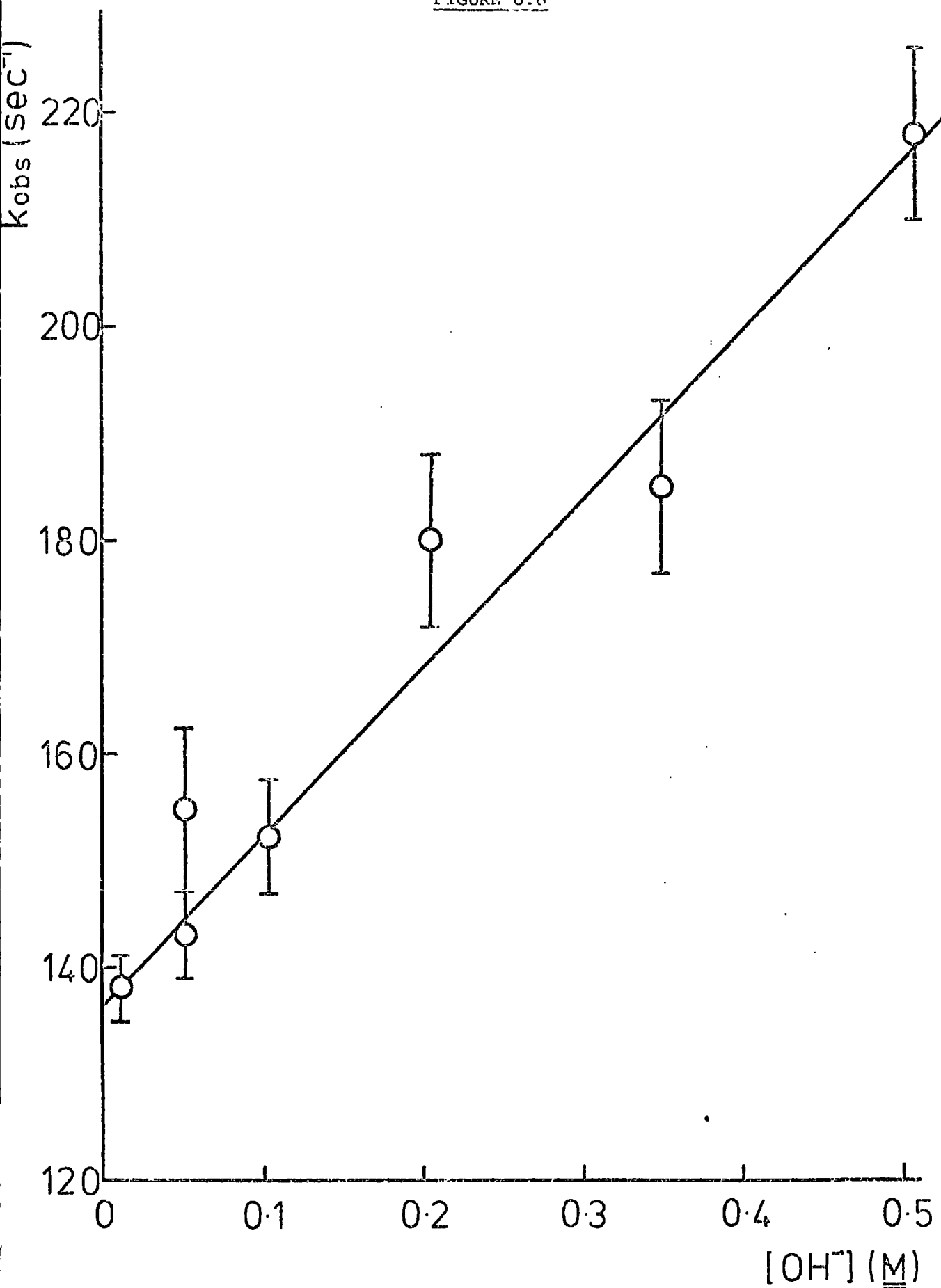
$$\therefore A = \Delta[\text{spiro}] \left( 1 + \frac{1}{K_C[\text{OH}^-]} \right) \quad 6.12$$

Using equations 6.12 and 6.10, measurements with a series of different base and substrate concentrations gave  $K_2 = 0.6 \pm 0.2 \text{ l.mol}^{-1}$ , in good agreement with the value above determined independently.

A plot of  $k_{\text{obs}}$  for spiro-complex formation versus base concentration is linear (Figure 6.6) and absence of curvature indicates that  $K[\text{OH}^-] \ll 1$  (equation 6.3). The slope therefore gives a value of  $160 \pm 20 \text{ l.mol}^{-1} \text{ sec}^{-1}$  for  $k_1 K$  and the intercept  $137 \pm 5 \text{ sec}^{-1}$  for  $k_{-1}$ .

Substituting the values of  $KK_1$  and  $K_2$  together with  $k_{\text{obs}}$  and the base concentration in equation 6.5 gave values for  $k_2 (= 6 \times 10^{-2} \text{ l.mol}^{-1} \text{ sec}^{-1})$  and

FIGURE 6.6



Plot of  $k_{obs}$  versus  $[\text{OH}^-]$  for spiro-complex formation from 1-(2-hydroxyethoxy)-2,6-dinitrobenzene in water at 25°C.

$k_{-2}$  ( $= 0.1 \text{ sec}^{-1}$ ).

A much slower irreversible reaction was observed producing 2,6-dinitrophenol,  $\lambda_{\text{max}}$  430 nm.

(iv) 1-(2-Hydroxyethoxy)-2,4-dinitrobenzene

The results in this case can be treated in a similar manner to those of the 2,6-dinitrobenzene isomer. The spiro-complex shows absorption in the visible region with  $\lambda_{\text{max}}$  487 nm [ $\epsilon$  ( $1.5 \pm 0.3$ )  $\times 10^4 \text{ l.mol}^{-1} \text{ cm}^{-1}$  determined by the extrapolation procedure<sup>166,184</sup> mentioned earlier]. Optical density ( $< 0.1M$ ) (Table 6.8) gave a value for  $K_C$  of  $0.05 \text{ l.mol}^{-1}$  which was independent of the base concentration. Examination at 487 nm by stopped-flow spectrophotometry of solutions containing higher base concentrations revealed that the very rapid colour formation was followed by a slower reaction in which the absorption decreased to a smaller value and remained constant for some time. This is interpreted as indicating the formation of a second adduct, A having a smaller visible absorption than the spiro-complex. Again stopped-flow spectrophotometric measurements allowed optical density changes to be measured between the first and second equilibria. By means of equations 6.12 and 6.10 a value of  $K_2 = 0.8 \pm 0.2 \text{ l.mol}^{-1}$  was then calculated.

The rate of colour formation at 487 nm was very fast. Measurement by the stopped-flow technique at  $0.5M$  and  $0.8M$  base gave a minimum value for  $k_{\text{obs}}$  of ca.  $620 \text{ sec}^{-1}$  and this will therefore represent a minimum value for  $k_{-1}$ . Since rate measurements of this order of magnitude are reaching the limit of the stopped-flow technique, Bernasconi's<sup>230</sup> value of ca.  $1450 \text{ sec}^{-1}$  for  $k_{-1}$  obtained using a temperature-jump method may be more appropriate. The rate constant,  $k_{\text{obs}}$ , for the fading reaction had a value of  $0.7 \text{ sec}^{-1}$  in  $0.5M$  sodium hydroxide giving an approximate value for  $k_{-2}$ .

A much slower irreversible reaction gave 2,4-dinitrophenol,  $\lambda_{\text{max}}$  360 and 400 nm (shoulder).

TABLE 6.8

Equilibrium Data for Complex Formation from 1-(2-Hydroxy-ethoxy)-2,4-dinitrobenzene in Water at 25°C

$10^5 [\text{Parent}]_{\text{Stoich}}$ (M)	[NaOH] (M)	Equilibrium O.D. <sup>a</sup>	$K_C$ ( $l \cdot \text{mol}^{-1}$ )
135	.010	.050	.061
120	.020	.078	.053
105	.031	.098	.051
75	.051	.111	.049
75	.051 <sup>b</sup>	.117	.051
37	.051	.053	.046
45	.071	.093	.049
30	.082	.081	.056
30	.10	.085	.046
30	.21	.163	.044
30	.31	.244	.045
30	.41	.318	.044
30	.52	.376	.042
30	.62	.466	.043
30	.72	.523	.041
30	.83	.584	.041

<sup>a</sup> Measured with a Unicam SP500 at 487 nm. Values quoted are for 4 cm path-length.

<sup>b</sup> Made up to ionic strength 0.2M with NaCl

## DISCUSSION

The spectroscopic evidence for the formation in methanolic sodium methoxide of spiro-complexes rather than, for example, alkoxide adducts has been well established.<sup>184</sup> Visible spectra in water containing dilute base correspond closely to those in methanol and the similarities of the equilibrium and kinetic parameters indicate that in this solvent too spiro-complex formation is being observed. Bernasconi<sup>230</sup> has also provided arguments in favour of spiro-complex formation in the case of complex (6.5) in aqueous DMSO solutions. Furthermore p.m.r. spectra indicate the formation of (6.3) from the parent glycol ether in aqueous base.

Equilibrium and rate constants for the formation in water of spiro-complexes from the parent glycol ethers are collected in Table 6.9. The corresponding values in methanol are also quoted, as are the value for the corresponding 1,1-dimethoxy complexes. The increase in values of  $KK_1$  with the increase in activation in the aromatic system results both from increases in the values of  $k_1K$  and decreases in  $k_{-1}$ . The measurements do not allow determination of the values of  $K$ , the equilibrium constant governing proton loss from the glycol side chain. However for comparison, the corresponding values for reaction of hydroxide ions with 2-methoxyethanol and 2-chloroethanol are 0.16 and 0.5  $\text{l.mol}^{-1}$  respectively.<sup>231</sup> It seems probable in view of the isolation of the hydroxy-proton from the aromatic system that the values of  $K$  for the four glycol ethers studied will not vary greatly so that the values of  $KK_1$  will largely reflect differences in values of  $K_1$ .

Perhaps the most significant fact deriving from these results is the high value of  $k_{-1}$  compared to the value for the corresponding process for the analogous 1,1-dimethoxy-Meisenheimer complexes. For example the value for  $k_{-1}$  of  $0.095 \text{ sec}^{-1}$  for complex (6.3) can be compared with values  $5.5 \times 10^{-4}$  and  $6 \times 10^{-4} \text{ sec}^{-1}$  reported<sup>232,233</sup> for the cleavage of methoxide ion from complex (6.10) in water. Similarly the value of  $k_{-1}$  for complex (6.2) is

TABLE 6.9

Equilibrium and Kinetic Data for Spiro-complex and 1,1-Dimethoxy-complex Formation in Methanol<sup>a</sup> at 25°C

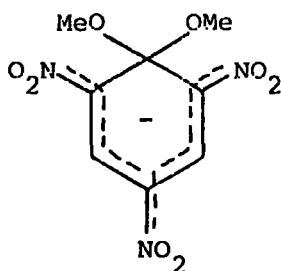
<u>Complex</u>	<u>Spiro-complex</u>				<u>1,1-Dimethoxy-complex</u>		
	$\frac{KK_1}{1}$ <sup>b</sup> (1.mol <sup>-1</sup> )	$\frac{KK_1}{1}$ <sup>c</sup> (1.mol <sup>-1</sup> )	$\frac{k_1 K}{1}$ (1.mol <sup>-1</sup> sec <sup>-1</sup> )	$\frac{k_{-1}}{1}$ (sec <sup>-1</sup> )	$\frac{K_1}{1}$ (1.mol <sup>-1</sup> )	$\frac{k_1}{1}$ (1.mol <sup>-1</sup> sec <sup>-1</sup> )	$\frac{k_{-1}}{1}$ (sec <sup>-1</sup> )
(6.2)	$3 \times 10^4$ ( $3.5 \times 10^3$ )	$3.9 \times 10^4$ ( $3.8 \times 10^3$ )	$9 \times 10^4$ ( $2.5 \times 10^4$ )	2.3 (6.5)	(205) <sup>d</sup>	(0.93) <sup>d</sup>	$1.8 \times 10^{-3}$ <sup>e</sup> ( $4.6 \times 10^{-3}$ ) <sup>d</sup>
(6.3)	$1.8 \times 10^{7f}$	$1.7 \times 10^7$	$1.6 \times 10^6$	0.095	(17,000) <sup>g</sup>	(17.3) <sup>g</sup>	$6 \times 10^{-4}$ <sup>h</sup> ( $1.04 \times 10^{-3}$ ) <sup>g</sup>
(6.4)	1.3 (0.22)	1.2 (0.22)	$1.6 \times 10^2$ (80)	137 (360)	$(9 \times 10^{-5})^i$	(-)	(-)
(6.5)	0.05 ( $1.1 \times 10^{-2}$ )		>30 (>5.5)	>620 (>500)	$(4.6 \times 10^{-5})^i$	$(2.1 \times 10^{-3})^i$	(42) <sup>i</sup>

<sup>a</sup> Values in parenthesis refer to methanol as solvent - from reference 184 unless otherwise state.

<sup>b</sup> Equilibrium values      <sup>c</sup> Kinetic values      <sup>d</sup> Reference 182      <sup>e</sup> Reference 234

<sup>f</sup> Reference 45      <sup>g</sup> Reference 64      <sup>h</sup> References 232, 233      <sup>i</sup> Reference 166

<sup>j</sup> Reference 167



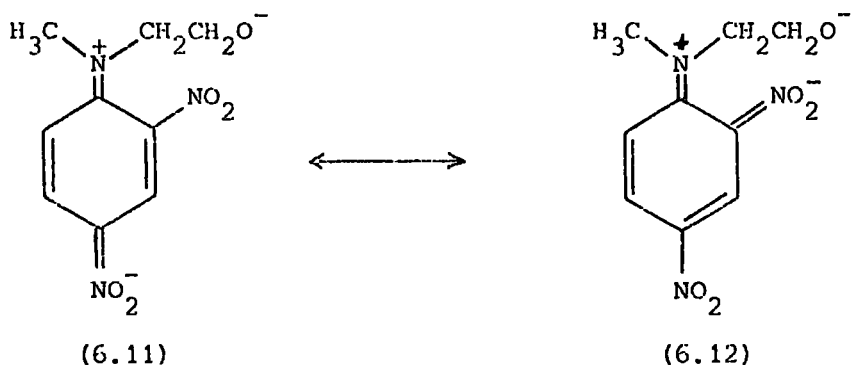
(6.10)

three orders of magnitude larger than that ( $1.8 \times 10^{-3} \text{ sec}^{-1}$ ) for methoxide loss from the 1,1-dimethoxy-2,4-dinitronaphthalene adduct in water.<sup>234</sup> These results thus confirm those obtained in methanol<sup>184</sup> which indicated that the rate constants for ring-opening of spiro-complexes are much higher than for base expulsion from non-cyclic analogues. This has particular significance in view of the fact that spiro-complexes have been used as models for the intermediates in nucleophilic aromatic substitution reactions.<sup>81,82,229,230</sup> One possible explanation for the difference in complex decomposition is the release of steric strain in the opening of the dioxolan ring of the spiro-adducts, although, as will be discussed in Chapter 8, relief of ring-strain may not be a dominant factor affecting the magnitude of the  $k_{-1}$  values. A further effect indicating the ease of ring-opening of spiro-complexes is the observation of general acid catalysis in their catalysed decomposition; this will be discussed in detail later.

The values of  $KK_1$  in water for complexes (6.2), (6.4) and (6.5) are between five and ten times larger than the corresponding values in methanol (Table 6.9), this increase resulting from larger values of  $k_1K$  and smaller values of  $k_{-1}$ . Some of this increase may result from the larger values of  $K$  expected in water than in methanol.<sup>235</sup> The increase in complex stability in aqueous media may also be due to the better solvating capabilities of water. In both methanol and water the relative stabilities of the four complexes (6.2)-(6.5) parallel those of the corresponding non-cyclic systems.

It is also of interest to compare data for complex (6.5) with those for the similarly activated complex (6.8). The equilibrium constant for the formation

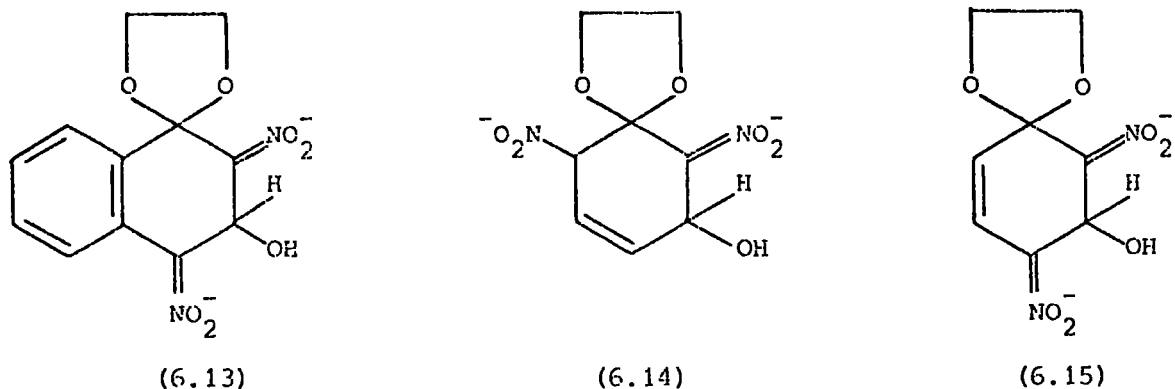
of (6.8) is  $5 \times 10^{-3} \text{ l.mol}^{-1}$ , a factor of ten smaller than the value for (6.5) while the value of  $k_{-1}$  ( $930 \text{ sec}^{-1}$ ) for (6.8) is similar to that for (6.5). Bernasconi et al<sup>81,230</sup> have argued that one of the main reasons resulting in the lower stability of (6.8) is ground state resonance stabilisation (6.11)  $\leftrightarrow$  (6.12) resulting in a smaller value of the rate of formation, since the rates of



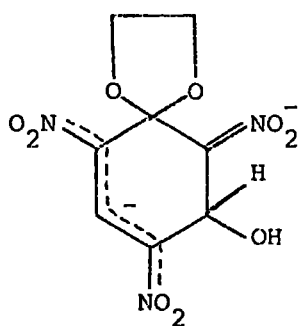
of reversion to reactants are virtually identical for (6.5) and (6.8).

Formation of higher complexes

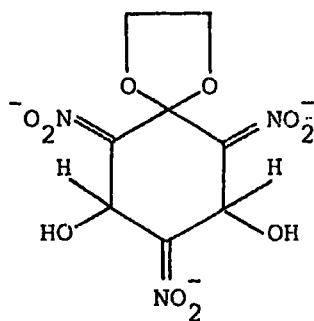
There is evidence from visible spectral shape and stopped-flow spectrophotometric measurements for further reversible interactions in more concentrated ( $>0.1M$ ) sodium hydroxide solutions. In the light of the many known examples<sup>6,8</sup> of the formation of higher hydroxide and alkoxide adducts from activated aromatic compounds in concentrated base solutions, it seems likely that the observed interactions are of this type. In the case of the spiro-complexes (6.2), (6.4) and (6.5) the results indicate only one further interaction with hydroxide ions so that the most probable structure for the hydroxide adducts are respectively (6.13), (6.14) and (6.15). For complex



(6.5) there are two possible sites of attack, however addition at the 5-position is precluded since the two negative charges cannot be localised in an analogous manner to (6.15). Two interactions are observed for complex (6.3) and likely structures for the adducts with one and two hydroxide ions are (6.16) and (6.17) respectively. Unfortunately p.m.r. measurements which would



(6.16)



(6.17)

unambiguously prove these structures were not successful due to solubility problems. Nevertheless, as would be expected for structures having no delocalised negative charge (6.13)-(6.15) and (6.17) show absorption in the u.v. region of the spectrum at about 300 nm, and not in the visible region. The absence of visible absorption in the spectrum of these complexes rules out the possibility that they might arise from hydroxide addition to the parent glycol ethers rather than to the spiro-complexes themselves. Complex (6.17) appears to be one of the first examples of an adduct formed by addition of three basic groups to a benzenoid ring, although multi-charged adducts have previously been postulated.<sup>236</sup>

No formation of higher complexes was observed<sup>184</sup> in solutions of methanolic sodium methoxide of similar concentration, although corresponding interactions would presumably also be observed in methanol at sufficiently high methoxide concentrations. Thus there appears to be a special propensity for the formation of di-adducts in water.<sup>237</sup> For example N,N-dimethylpicramide gives the di-adduct in water even in dilute sodium hydroxide solution<sup>76</sup> and sodium sulphite readily gives di-adducts in dilute solution as mentioned in the previous chapter. The ready formation of these complexes in water may result

from the ability of this polar solvent to stabilise multi-charged species especially when the charges are localised on the nitro groups.

The equilibrium and rate constants associated with the formation of the hydroxide adducts are summarised in Table 6.10. These values were obtained

TABLE 6.10

Collected Data for Formation of Hydroxide Adducts from Spiro-complexes

<u>Adduct</u>	$\lambda_{\text{max}}$ (nm)	$K_2^a$ ( $\text{l.mol}^{-1}$ )	$k_2$ ( $\text{l.mol}^{-1}\text{sec}^{-1}$ )	$k_{-2}$ ( $\text{sec}^{-1}$ )
(6.13)	275,300	1.0	0.04	0.04
(6.14)	297	0.6	0.06	0.1
(6.15)		0.8	0.5	0.7
(6.16)	<u>ca.</u> 500	0.1	0.09	0.9
(6.17)	290			

<sup>a</sup> Equilibrium constant defined as  $[\text{hydroxide adduct}]/[\text{spiro}][\text{OH}^-]$

in solutions containing 0.1-1.0M sodium hydroxide and are therefore not thermodynamic values, but should be regarded as giving the orders of magnitude of the parameters quoted rather than precise values. However it is of interest to note that the equilibrium constant  $K_2$  for formation of the hydroxide adduct from the trinitro-substituted compound is smaller than the corresponding values for hydroxide addition to the dinitro-compounds. This may be associated with the very high stability of the spiro-complex (6.3).

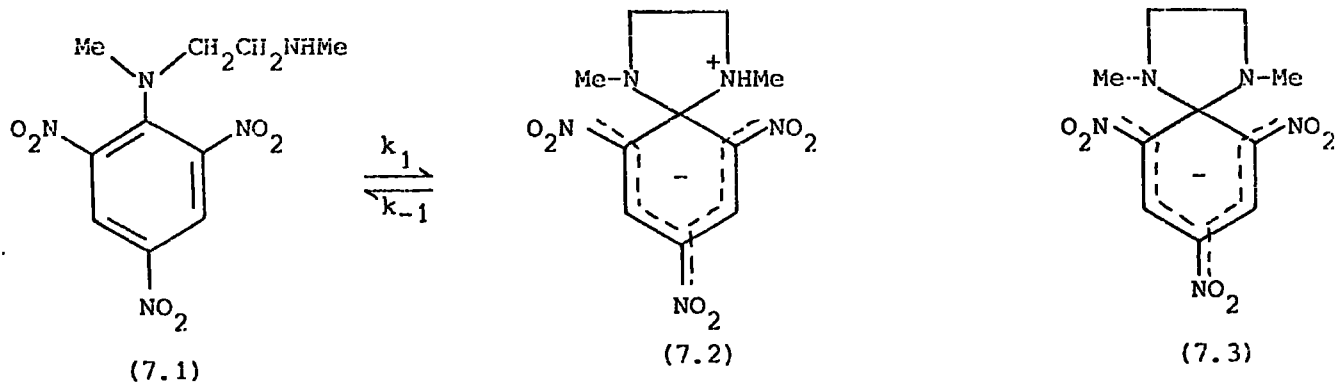
CHAPTER 7

THE GENERAL ACID CATALYSED RING OPENING OF SPIRO-COMPLEXES

INTRODUCTION

The results presented in the previous chapter indicate important differences between spiro-complexes and similarly activated 1,1-dimethoxy-complexes. In particular the values for the rate constants for ring opening of the spiro-complexes are orders of magnitude greater than rates of decomposition of non-cyclic analogues. A probable consequence of this ease of ring opening is the observation discussed in the present work of general acid catalysis in their reversal to the parent glycol ethers.

This behaviour of spiro-complexes is interesting in view of their use as models for intermediates in nucleophilic aromatic substitution reactions<sup>81,81,229,230</sup> Bernasconi and Gehriger<sup>229</sup> in a recent kinetic study of the formation of



complex (7.3) found the reaction to be subject to general acid catalysis.

This probably results from the unexpectedly high value of the rate constant  $k_{-1}$  for reversion of the zwitterionic intermediate to the parent (7.1) so that in the overall reaction to give (7.3) deprotonation of (7.2) may be the rate limiting.

It was then suggested<sup>229</sup> that in some cases general base catalysis in nucleophilic aromatic substitution reactions may result from slow proton transfer rather than slow leaving group departure. Although not disputing this argument, it may be that spiro-complexes are subject to special factors not present in non-cyclic analogues and their use as intermediates in nucleophilic aromatic substitution reactions may not be meaningful.

EXPERIMENTAL

Kinetic measurements were made at 25°C with a 'Canterbury' stopped-flow spectrophotometer in the visible region of the spectrum at the maximum absorption of the complexes. The rates of ring opening of the spiro-complexes (6.2) and (6.3) to give the parent glycol ethers were measured in acidic buffers and in dilute hydrochloric acid solutions. Experimental data were obtained by mixing solutions of the spiro-complex (ca.  $10^{-5}$  M - generated in situ by making up solutions of the parent ether in very dilute sodium hydroxide ca.  $10^{-4}$  M) with appropriate buffers, and monitoring the decrease in light absorption with time. The acidities of the solutions were measured by mixing equal volumes of the substrate and buffer solution and recording the pH at 25°.

RESULTS

The proposed mechanism for the formation of complexes (6.2) and (6.3) in aqueous alkaline buffers was given in the previous chapter and for that scheme the first-order rate constant governing complex formation is given by equation 6.3. No buffer catalysis could be detected in phosphate, borax or phenol buffers. In the present work the observed rate constant,  $k_{obs}$ , for the ring opening of complexes (6.2) and (6.3) in acidic solutions can be expressed by equation 7.1 as a pH independent term  $k_{-1}$  together with terms due to catalysis by protons and undissociated acids.

$$k_{obs} = k_{-1} + k_{H^+} + \sum k_{HA} [HA] \quad 7.1$$

The decomposition of the complex was in all cases an accurately first-order process and typical data are given in Tables 7.1 and 7.2.

The results presented in Table 7.3 for complex (6.2) show that in acetic acid-sodium acetate buffers the observed rate constant depends linearly on the concentration of undissociated acid but is unaffected by acetate ions. Catalytic coefficients for the acidic species were calculated and are given in the footnotes to Table 7.3. The value of  $2.3 \text{ sec}^{-1}$  required for the uncatalysed ring opening of (6.2) is in precise agreement with that obtained

TABLE 7.1

Rate Data for the Decomposition of Complex (6.2) ( $1 \times 10^{-5} \text{M}$ ) in Formic Acid (0.26M)-Sodium Formate (0.26M) Buffer at 25°C

<u>Time</u> (m.sec)	<u>Scale Reading</u> (arbitrary units)	<u>k<sub>obs</sub></u> (sec <sup>-1</sup> )
0	6.22	-
10	5.03	23.8
20	4.10	23.7
30	3.42	23.0
40	2.83	23.1
50	2.38	23.0
60	2.00	23.2
70	1.62	24.4
80	1.41	24.2
∞	0.60	-

TABLE 7.2

Rate Data for the Decomposition of Complex (6.3) ( $3.3 \times 10^{-6} \text{M}$ ) in Chloroacetic Acid (0.10M)-Sodium Chloroacetate (0.10M) Buffer at 25°C

<u>Time</u> (m.sec)	<u>Scale Reading</u> (arbitrary units)	<u>k<sub>obs</sub></u> (sec <sup>-1</sup> )
0	5.75	-
50	4.78	4.6
100	3.98	4.7
150	3.37	4.6
200	2.85	4.7
250	2.45	4.7
300	2.17	4.7
350	1.92	4.7
400	1.73	4.7
∞	1.00	-

TABLE 7.3

Kinetic Data for the Ring Opening of Complex (6.2) in Acidic

Buffers and in Hydrochloric Acid in Water at 25°C

<u>Acid</u>	$\frac{[\text{HA}]_{\text{Stoich}}}{(\text{M})}$	$\frac{[\text{Na}^+\text{A}^-]_{\text{Stoich}}}{(\text{M})}$	<u>pH</u>	$\frac{k_{\text{obs}}}{(\text{sec}^{-1})}$	$\frac{k_{\text{calc}}^{\text{a}}}{(\text{sec}^{-1})}$
Acetic	0.026	0.026	4.65	3.4	3.4
	0.105	0.105	4.7	5.3	5.3
	0.26	0.26	4.7	8.8	9.2
	0.026 <sup>b</sup>	0.026 <sup>b</sup>	4.4	3.2	3.6
	0.105 <sup>b</sup>	0.105 <sup>b</sup>	4.45	5.1	5.5
	0.26 <sup>b</sup>	0.26 <sup>b</sup>	4.65	8.8	9.2
	0.026	0.013	4.3	3.8	3.8
	0.105	0.052	4.45	5.6	5.5
	0.26	0.13	4.45	9.6	9.4
	0.052	0.105	4.9	3.7	3.8
Formic	0.026	0.026	3.6	7.6	8.3
	0.104	0.104	3.6	12.9	13.0
	0.26	0.26	3.55	23.1	22.8
Chloroacetic	0.025	0.025	2.9	38	34
	0.10	0.10	2.9	54	56
	0.25	0.25	2.9	100	100
Hydrochloric	0.01			187	182
	0.018			300	320

<sup>a</sup> Calculated from equation 7.1 with  $k_{-1}$   $2.3 \text{ sec}^{-1}$ , and with the following values for the catalytic coefficients for acidic species: proton  $(1.8 \pm 0.3) \times 10^4 \text{ l.mol}^{-1}\text{sec}^{-1}$ ; acetic,  $25 \text{ l.mol}^{-1}\text{sec}^{-1}$ ; formic,  $60 \text{ l.mol}^{-1}\text{sec}^{-1}$ ; chloroacetic,  $300 \text{ l.mol}^{-1}\text{sec}^{-1}$ .

<sup>b</sup> Ionic strength,  $I = 0.3\text{M}$ , with sodium chloride

for  $k_{-1}$  from the measurements in alkaline media. The value for  $k_{-1}$  was also determined in deuterium oxide. Measurements in solutions where  $6 < \text{pH} < 8$  give the value of  $k_{-1}$  directly since terms due to catalysis by hydroxide ions, protons or buffer are negligible (Figure 7.1). The data in Table 7.4 give a value

TABLE 7.4

Solvent Isotope Effect on the Uncatalysed Ring-Opening of Complex (6.2)

<u>Solvent</u>	<u>pH</u>	<u>Conditions</u>	$\frac{k_{\text{obs}}}{(\text{sec}^{-1})}$
H <sub>2</sub> O	6.2	a	2.4 ± 0.1
	7.1	a	2.3
	7.1	b	2.2
	8.0	a	2.4
	<u>pD</u> <sup>c</sup>		
D <sub>2</sub> O	7.5	a	1.7 ± 0.1
	7.6	a	1.75

a Phosphate buffer, 0.05M

b Phosphate buffer, 0.025M

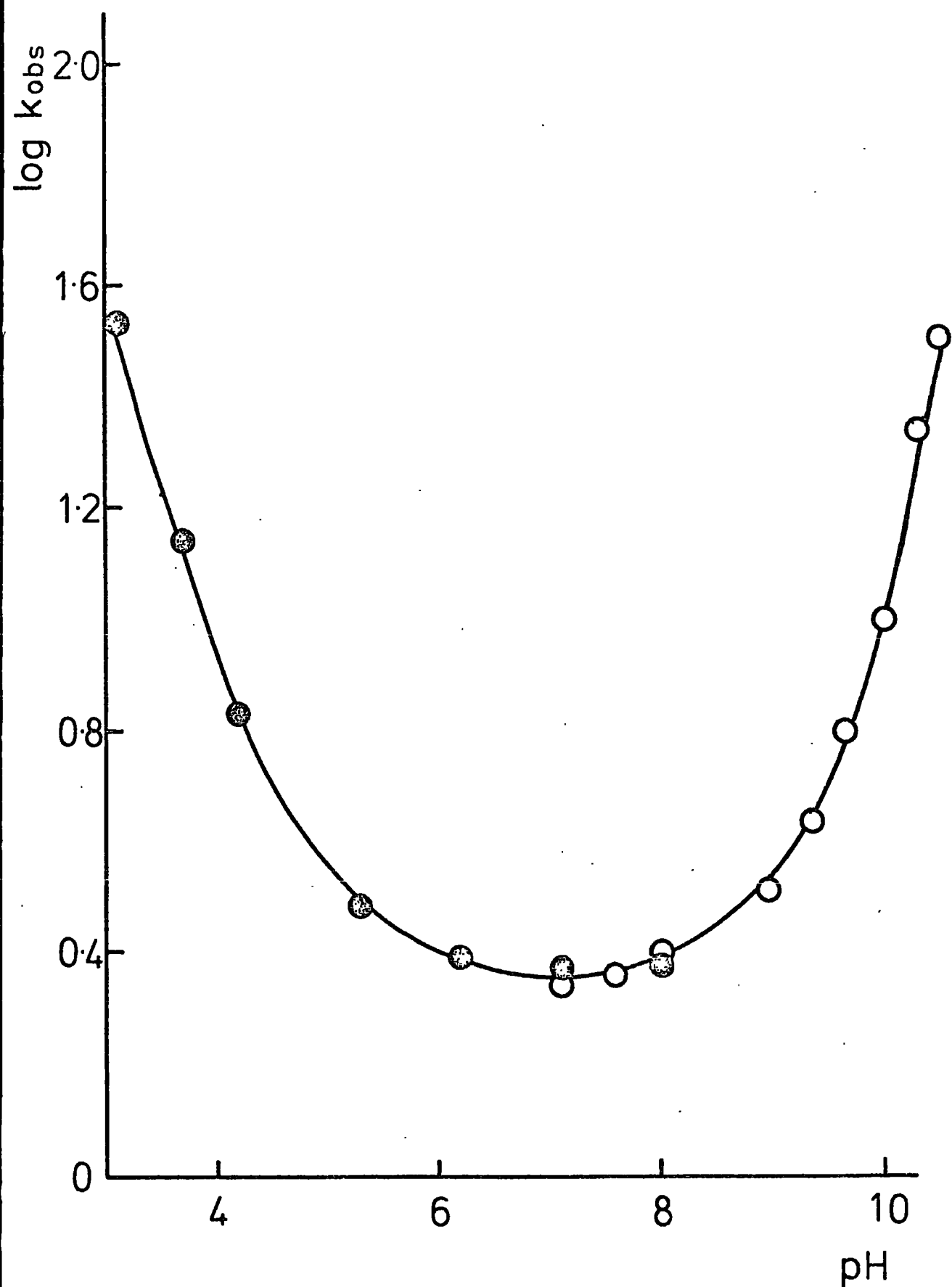
c pD = pH + 0.4 - Reference 238

for the solvent isotope effect  $k_{-1}(\text{H}_2\text{O})/k_{-1}(\text{D}_2\text{O})$  of 1.3. The rates in hydrochloric acid are too large to allow determination of  $k_{\text{D}_3\text{O}^+}/k_{\text{H}_3\text{O}^+}$  with any certainty.

The results for the acid catalysed ring opening of (6.3) are given in Table 7.5. Again catalysis by protons and undissociated acid in addition to a spontaneous process is evident. The calculated values of the respective catalytic rate coefficients are collected at the foot of Table 7.5. Since in this case the catalytic coefficient for protons is an order of magnitude smaller than for complex (6.2), the  $k_{\text{D}_3\text{O}^+}/k_{\text{H}_3\text{O}^+}$  isotope effect can be determined with a little more certainty. The data give a value of 1.5.

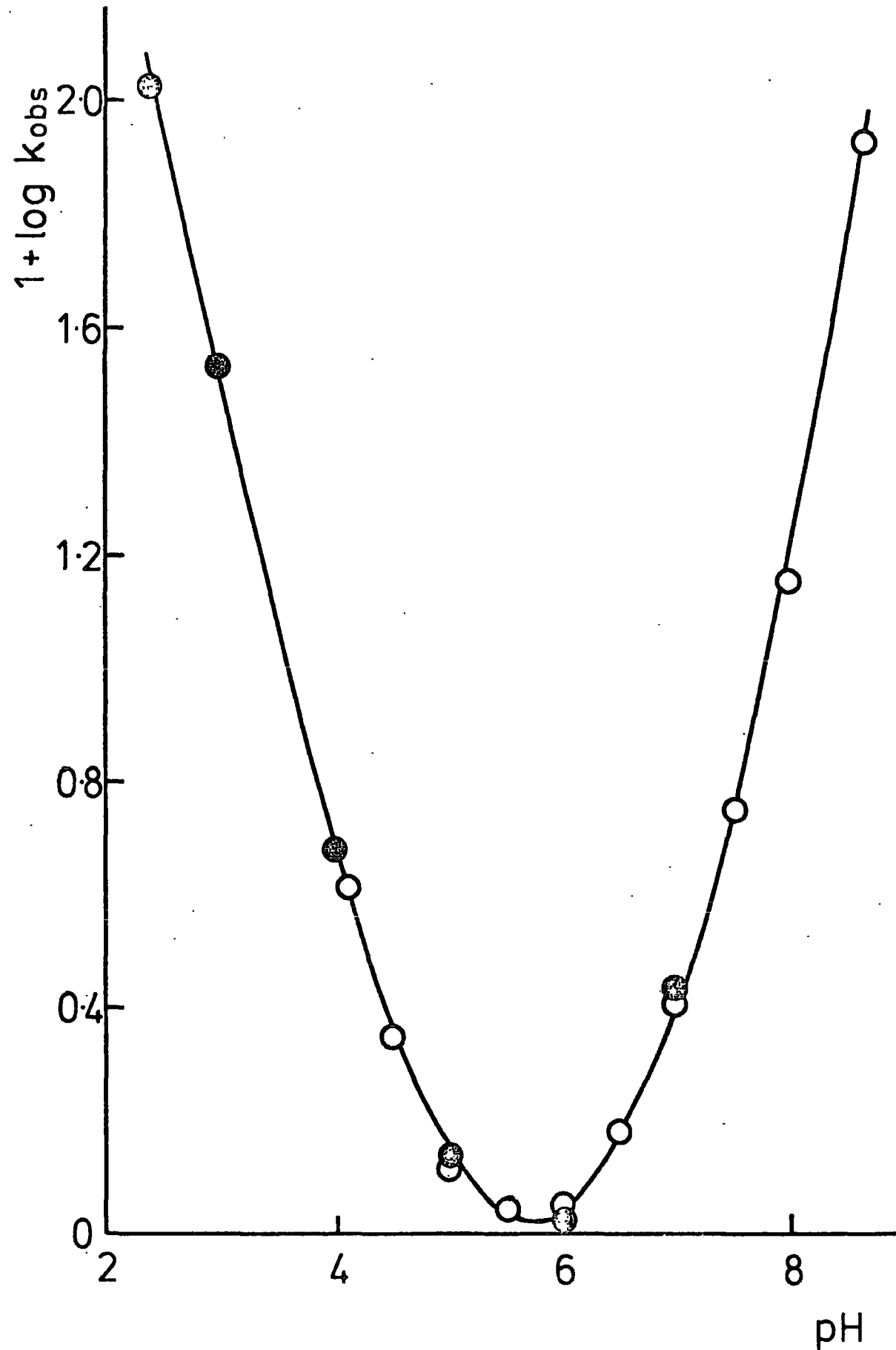
The catalytic rate coefficients for the various acids can be correlated in terms of the Brønsted relation first proposed by Brønsted and Pedersen.<sup>239</sup>

FIGURE 7.1



pH-Rate profile for the formation (O) and decomposition (●) of the spiro-complex from 1-(2-hydroxyethoxy)-2,4-dinitronaphthalene in alkaline and acidic buffers.

FIGURE 7.2



pH-Rate profile for the formation (O) and decomposition (●) of the spiro-complex from 1-(2-hydroxyethoxy)-2,4,6-trinitrobenzene in alkaline and acidic buffers.

TABLE 7.5

Kinetic Data for the Acid Catalysed Ring-Opening of Complex (6.3)  
in Buffers and in Hydrochloric Acid in Water at 25°C

<u>Acid</u>	<u>[HA]<sub>Stoich</sub></u> (M)	<u>[Na<sup>+</sup>A<sup>-</sup>]<sub>Stoich</sub></u> (M)	<u>pH</u>	<u>k<sub>obs</sub></u> (sec <sup>-1</sup> )	<u>k<sub>calc</sub><sup>a</sup></u> (sec <sup>-1</sup> )
Acetic	0.025	0.025	4.65	0.16	0.16
	0.10	0.10	4.7	0.22	0.23
	0.25	0.25	4.7	0.35	0.36
	0.25	0.125	4.4	0.41	0.41
	0.125	0.25	5.0	0.21	0.22
Formic	0.026	0.026	3.65	0.61	0.63
	0.104	0.104	3.6	0.85	0.87
	0.26	0.26	3.6	1.25	1.25
Chloroacetic	0.025	0.025	2.9	3.6	3.3
	0.10	0.10	2.85	4.7	4.4
	0.25	0.25	2.9	5.9	6.0
Hydrochloric	0.0093			20.8	20.5
	0.0186			39.3	40
	0.030			60	60
DCl in D <sub>2</sub> O	0.0093			31.7	31
	0.0186			60.5	61

<sup>a</sup> Calculated using equation 7.1 with  $k_{-1}$  0.095 sec<sup>-1</sup> and with the following values for the catalytic coefficients for acidic species: proton,  $2.2 \times 10^3$  l.mol<sup>-1</sup>sec<sup>-1</sup>; acetic 0.9 l.mol<sup>-1</sup>sec<sup>-1</sup>; formic, 2.3 l.mol<sup>-1</sup>sec<sup>-1</sup>; chloroacetic, 12 l.mol<sup>-1</sup>sec<sup>-1</sup>.

It relates the effectiveness of a catalyst to its acid-base strength and can be represented, for acid catalysis, in the form of equation 7.2

$$k_{HA} = G_{HA} K_a^\alpha \quad 7.2$$

$k_{HA}$  is the catalytic rate constant,  $K_a$  the acid dissociation constant and  $G_{HA}$  and  $\alpha$  are constants for a given series of catalysts in a given solvent.

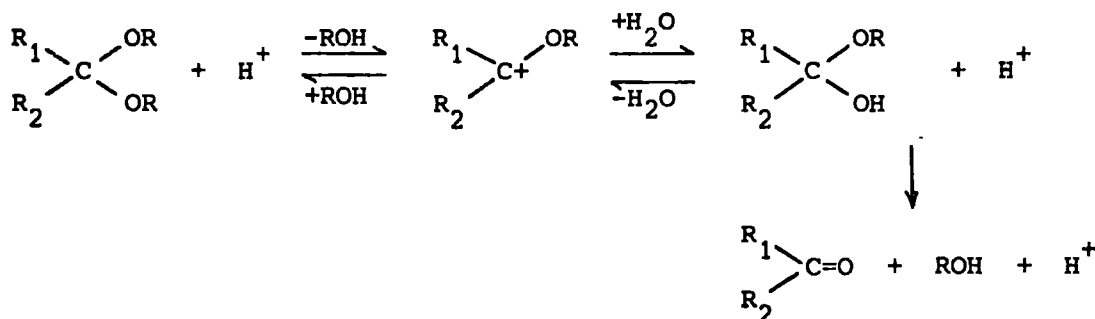
Hence

$$\begin{aligned} \log k_{HA} &= \log G_{HA} + \alpha \log K_a \\ &= \log G_{HA} - \alpha pK_a \end{aligned} \quad 7.3$$

Thus plots of  $\log k_{HA}$  versus  $pK_a$ , shown in Figure 7.3, are linear and give values of the Brønsted coefficient,  $\alpha$ , of  $0.5 \pm 0.1$ . From these graphs catalytic effects of weaker acids such as dihydrogen phosphate ion can be estimated. Such estimates confirm that under the experimental conditions used in the present work and in the previous chapter, no catalytic effects would be observable due to phthalate, phosphate or borax buffers.

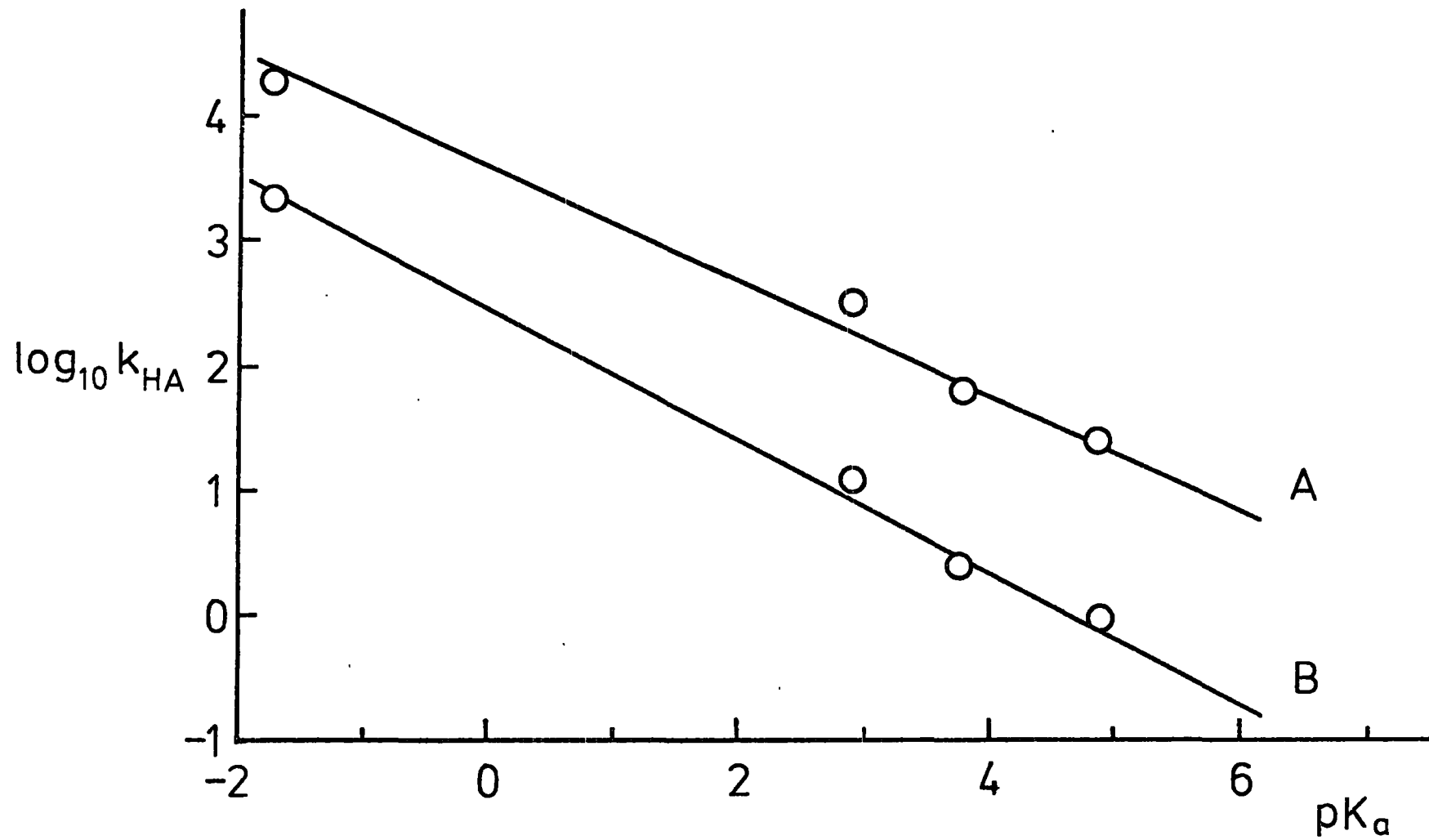
### DISCUSSION

The spiro-complexes (6.2) and (6.3) and Meisenheimer complexes in general are structurally related to acetals and ketals. These are normally hydrolysed in acidic media by an A1 mechanism involving pre-equilibrium protonation followed by rate-limiting breakdown of the protonated substrate according to the following scheme.<sup>240</sup>

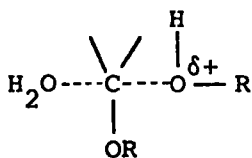


Participation of the solvent as nucleophilic reagent in attacking the protonated substrate giving an A2 mechanism appears not to take place. Such a mechanism would involve transition-states such as (7.4) or (7.5).

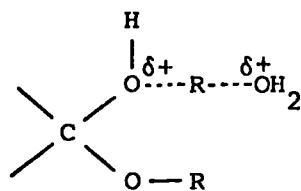
FIGURE 7.3



Brønsted plots for the acid catalysed ring opening in water; A, complex (6.2) and B, complex (6.3).

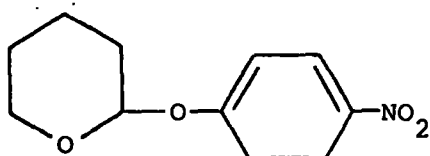


(7.4)

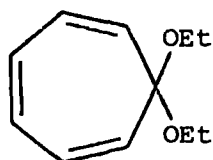


(7.5)

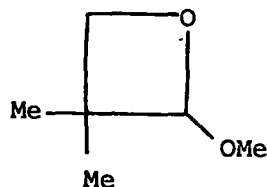
General acid catalysis involving proton transfer as part of the rate-determining step has only been observed<sup>241</sup> when C-O bond breaking is facilitated by a good leaving group, for example (7.6), or by formation of an especially



(7.6)



(7.7)

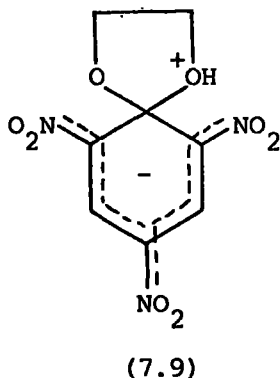


(7.8)

stable oxocarbenium ion as in (7.7), or by ring strain as in (7.8). Having a good electron-withdrawing phenyl substituent in (7.6) also has the simultaneous effect of reducing the basicity of the substrate thus increasing the possibility of rate-determining protonation. It should be noted however that spiro-complexes (6.2) and (6.3) differ from normal acetals in that they are negatively charged so that reaction with acid involves charge neutralisation rather than charge formation. Moreover the reactions of Meisenheimer complexes and spiro-complexes in particular are very much faster; the uncatalysed decomposition of acetals is extremely slow.<sup>240,241a</sup> This difference probably results from the fact that the incipient cation intermediate is energetically unfavourable, whereas the corresponding species for Meisenheimer complexes resembles the uncharged final product.

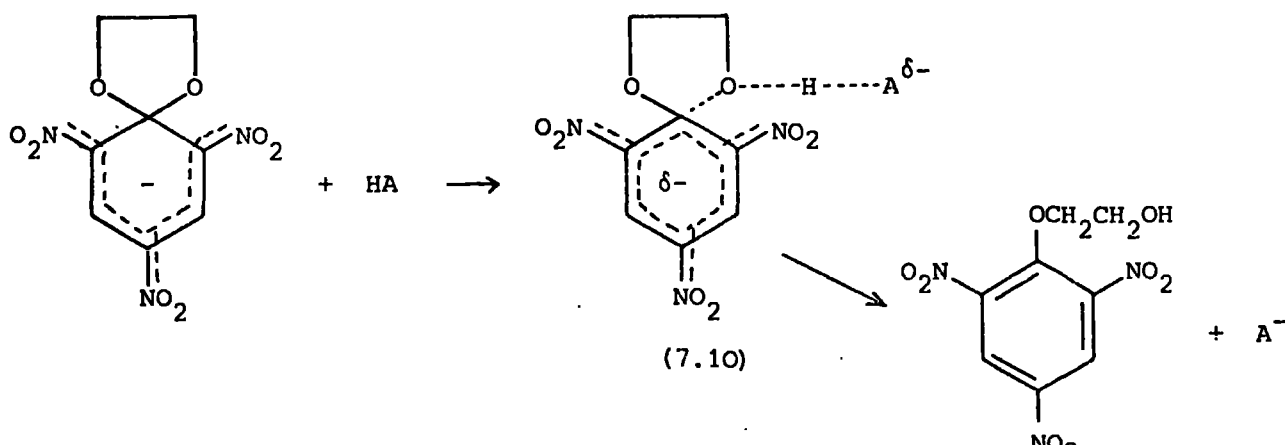
The present results show that the ring opening of the complexes (6.2) and (6.3) to give the parent glycol ethers is subject to general acid catalysis which indicates that proton transfer is involved in the rate-determining step. This in itself therefore excludes an A1 mechanism. Furthermore the value of

1.5 observed for the isotope effect  $k_{D_3O^+}/k_{H_3O^+}$  for complex (6.3) is too low for reaction by the A1 mechanism where values are usually  $>2.7$ .<sup>241a</sup> One possible mechanism is slow proton transfer to give (7.9) followed by fast C-O



bond-breaking. This is the mechanism shown to be operating in the case of complex (7.3). However the acidity of (7.9) is likely to be many orders of magnitude higher than that of the corresponding acid (7.2) ( $pK_a$  6.64),<sup>229</sup> since protonated ethers and alcohols typically<sup>242</sup> have  $pK_a$  values of -3 to -4. It could be argued that the acidity of (7.9) will be decreased relative to a normal protonated ether because of its zwitterionic nature. Nevertheless evidence<sup>154,189</sup> suggests that the  $C_6H_2(NO_2)_3^-$  entity is electron demanding relative to hydrogen. Thus it can be concluded that (7.9) would be very much more acidic than the catalysing acids. However the results indicating values of 0.5 for the Brønsted coefficient,  $\alpha$ , imply that the proton is about half way between catalyst and substrate in the transition state. This renders the above mechanism very unlikely.

A much more probable mechanism is one postulated<sup>241a,b</sup> for the general acid catalysed hydrolysis of acetals in which proton transfer and C-O bond cleavage are concerted (A-S<sub>E</sub>2). This is shown in the following scheme.

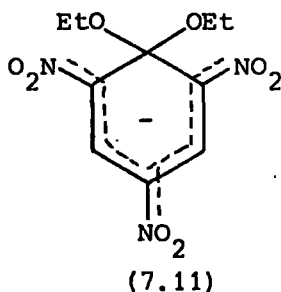


The effect of partial C-O bond-breaking in the transition state will be to increase greatly the basicity of the oxygen in the dioxolan ring, making the value of  $\alpha = 0.5$  reasonable. Additional evidence in favour of a concerted process comes from comparison of the complexes (6.2) and (6.3) themselves. Previous results indicate a faster rate of spontaneous ring opening of (6.2) than (6.3), and therefore the greater susceptibility to acid catalysis of (6.2) suggests that C-O bond-breaking is involved in the rate-determining step.

The principle of microscopic reversibility<sup>243</sup> dictates that a pathway exists via the above scheme for the formation of the spiro-complex from the parent glycol ether. This has been observed for both complexes in acidic buffers (see Figures 7.1 and 7.2). The possibility must also be considered that this rather than the alternative path described in Chapter 6 is the major pathway for spiro-complex formation in alkaline solutions. This would then imply that hydroxide ion catalysis of ring-closure involves a transition state (7.10; A = OH) while the ring opening involves a bimolecular reaction of the spiro-complex with water. There are two pieces of evidence that this is not the case. Firstly data in Table 7.3 indicate that the uncatalysed ring-opening of (6.2) proceeds at rather similar rates in H<sub>2</sub>O and D<sub>2</sub>O with  $k_{-1}(\text{H}_2\text{O})/k_{-1}(\text{D}_2\text{O})$  1.3; if water were acting as a general acid the reaction should be much slower in D<sub>2</sub>O.<sup>244</sup> Secondly, the Brønsted plots can be used to calculate the values expected for catalysis by water assuming that water fits these plots. The value predicted for reaction of (6.3) is  $1 \times 10^{-4} \text{ sec}^{-1}$  compared with the experimental value of  $0.095 \text{ sec}^{-1}$  while the predicted value for (6.2) is  $1.7 \times 10^{-2} \text{ sec}^{-1}$  compared with the observed  $2.3 \text{ sec}^{-1}$ . These results suggest that the uncatalysed ring-opening is a unimolecular reaction and that the major pathway in alkaline media is as shown in Chapter 6.

#### Comparison with dialkoxy-Meisenheimer complexes

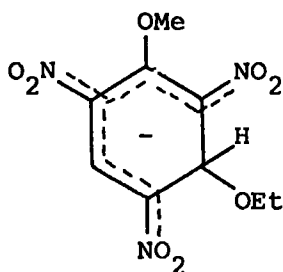
There have been several reports<sup>38,64,232,234,245,247</sup> of the acid catalysed decomposition of 1,1-dialkoxy-complexes such as (7.11). General acid catalysis



was not observed<sup>38</sup> and an A1 mechanism has been postulated.<sup>245</sup> The failure to observe general acid catalysis in this instance might result from the less ready C-O bond breaking and/or easier protonation of the ether oxygen. Evidence that C-O bond breaking is facilitated in spiro-complexes relative to the non-cyclic systems has been presented earlier and it has been suggested that this may be due to the relief of steric interactions in the ground state of the spiro-complex.<sup>246</sup> Nevertheless comparison of the hydronium ion catalysed decomposition of (7.11) ( $k_{H_3O^+} 1.2 \times 10^4 \text{ l.mol}^{-1} \text{ sec}^{-1}$ )<sup>232,245</sup> with that of (6.3) ( $k_{H_3O^+} 2.2 \times 10^3 \text{ l.mol}^{-1} \text{ sec}^{-1}$ ) indicates that the dialkoxy-complex is more readily protonated than the spiro-complex. This implies that the basicity of the ether oxygen in (7.11) is greater than in (6.3) and it is of interest to speculate on the reasons for this increased basicity. It has been shown<sup>182,183</sup> that in methanol 1,1-dimethoxy-complexes interact with alkali-metal cations by ion-pair association. It was suggested that a favourable site existed between the oxygen atoms of the methoxy groups where a cation might be held by a cage effect. No such interaction with cations was observed for spiro-complexes either in methanol<sup>184</sup> or water. A stabilising effect in the case of the proton similar to that observed with other cations would account for the increased basicity of (7.11).

The question, of course, arises whether general catalysis would be expected to be the exception or the rule in the acid catalysed decomposition of  $\sigma$ -complexes, in the light of the difference between cyclic and non-cyclic adducts mentioned earlier. It must be mentioned however that the decomposition

of the sodium ethoxide adduct of 1,3,5-trinitrobenzene is subject to general catalysis.<sup>248</sup> Ainscough and Caldin<sup>38</sup> also observed catalysis by acids other than  $\text{H}_3\text{O}^+$  for the decomposition of the product of the 'fast' reaction between 2,4,6-trinitroanisole and sodium ethoxide. Originally thought to be a charge-transfer complex, it seems almost certain to be the 1,3-adduct (7.12) in the light of later p.m.r.<sup>36</sup> and kinetic<sup>40</sup> studies. Buffer catalysis has

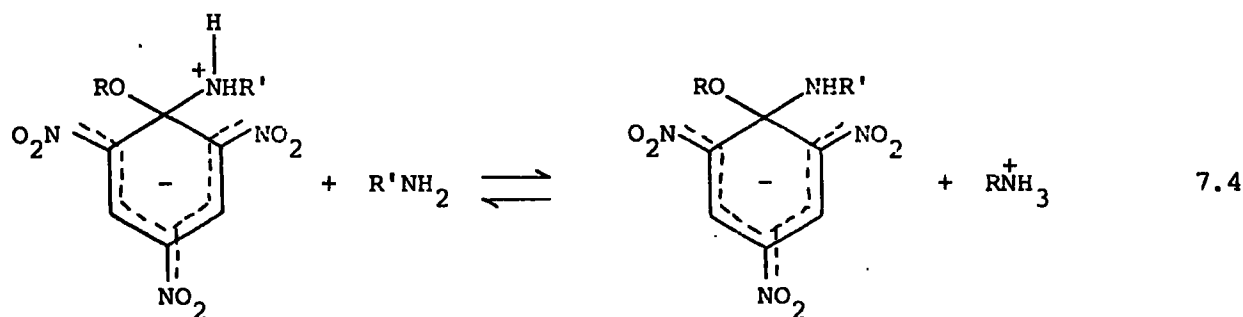


(7.12)

also been observed in the reactions of several hydroxide ion adducts.<sup>249</sup>

It is worth noting that in the cases where general acid catalysis is observed (spiro-complexes and adducts formed from attack at a ring carbon carrying hydrogen), the  $k_{-1}$  values for the uncatalysed decomposition are several orders of magnitude larger than for those complexes where only specific hydronium ion catalysis is observed (1,1-dialkoxy-complexes). Therefore it seems probable that the observations of general acid catalysis with spiro-complexes which is not peculiar to these adducts results from the easier C-O bond-breaking rather than an increase in basicity of the system.

The specific base-general acid mechanism of base catalysis in nucleophilic aromatic substitution reactions, a mechanism which has been favoured by the majority of recent discussions,<sup>19</sup> requires that the decomposition of the  $\sigma$ -complex (7.13) be subject to general acid catalysis and that the equilibrium 7.4



(7.13)

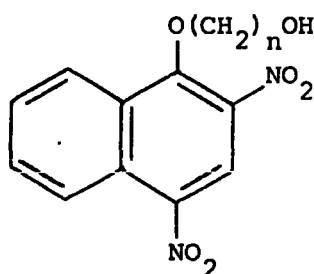
is established rapidly. This has been demonstrated in the reaction of 2,4-dinitronaphthyl ethyl ether with n-butyl- and t-butyl-amine in DMSO. However Bernasconi has shown<sup>229</sup> in the light of his results with complex (7.3) that under certain circumstances proton transfer from nitrogen may be the rate-determining step.

## CHAPTER 8

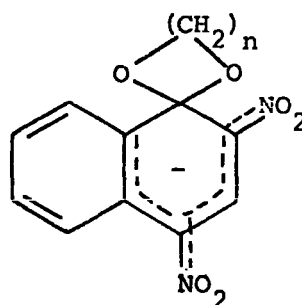
THE EFFECT OF RING-SIZE ON SPIRO-COMPLEX FORMATIONINTRODUCTION

The work presented in Chapter 6 involved comparison of the values of rate and equilibrium constants for formation of spiro-complexes with those for similarly activated 1,1-dimethoxy-complexes. The results show that rate constants for both complex formation and decomposition are orders of magnitude greater than those for the non-cyclic analogues. It has been suggested<sup>246</sup> that the main reason for the higher value of  $k_{-1}$  in the case of the spiro-complexes involves relief of steric strain on ring-opening.

Measurements made so far, however, have involved spiro-complexes with five-membered dioxolan rings. Therefore to obtain more information regarding kinetic and equilibrium parameters for spiro-complex formation, the present work has involved investigation of the cyclisation of the parent ethers (8.1;  $n = 3,4$ ) to the complexes (8.2;  $n = 3,4$ ) containing six- or seven-membered rings.



(8.1)



(8.2)

EXPERIMENTAL

P.m.r. measurements were recorded in DMSO- $d_6$  at 20° with a Bruker HX90E instrument. U.v.-visible spectral measurements were made with Unicam SP500 or SP8000 instruments or with a 'Canterbury' stopped-flow spectrophotometer. Rate constants associated with spiro-complex formation were determined using the stopped-flow method. Measurements were made in the region of the

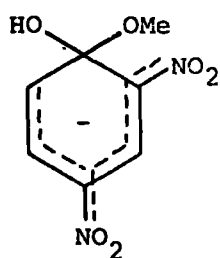
absorption maximum of the coloured species at which wavelength the reactants were transparent. Although a slower reaction yielding 2,4-dinitronaphthol was also observed, the base line after completion of the initial colour forming reaction was sufficiently stable to allow an 'infinity' value to be obtained. Rate constants for the slower process were determined, using the SP500 spectrophotometer, by measuring the increase with time of optical density at 430 nm.

Besides its use for kinetic measurements the stopped-flow spectrophotometer was used to determine equilibrium optical densities and general spectral shapes.

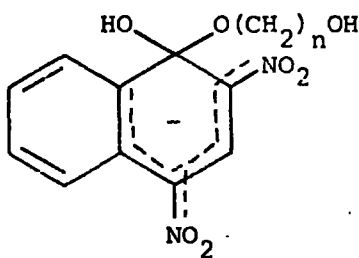
### RESULTS AND DISCUSSION

In the presence of dilute (<0.1M) aqueous sodium hydroxide both the parent ethers (8.1; n = 3,4) immediately gave a red colour with  $\lambda_{\text{max}} = 495 \pm 2$  nm. This was followed by the fairly fast formation of the yellow 2,4-dinitronaphthol identified by the u.v.-visible spectrum which showed maxima at 390 and 430 nm. The rate constants for 2,4-dinitronaphthol formation were measured at several base concentrations. The values of the second-order constant were found to be  $(6 \pm 1) \times 10^{-2} \text{ l.mol}^{-1} \text{ sec}^{-1}$  for the two parent compounds. In media containing DMSO the initial red colour was more intense and faded less rapidly.

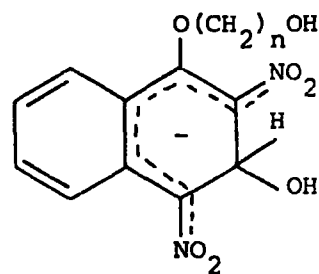
In view of the fact that Hasegawa and Abe,<sup>109,110</sup> in a related system, have obtained visible spectral evidence for the formation of adduct (8.3) as an observable intermediate from 2,4-dinitroanisole and hydroxide ions in aqueous DMSO, the possibility must be considered that the observed red colour results not from spiro-complex formation but rather from hydroxide addition. The most likely adducts are (8.4) or (8.5). Though visible spectral measurements



(8.3)



(8.4)



(8.5)

are not structurally meaningful, p.m.r. measurements are more conclusive in this respect.<sup>6,8</sup> Measurements in water were precluded by low solubility and the fast decomposition of the substrate. Measurements in DMSO were more successful.

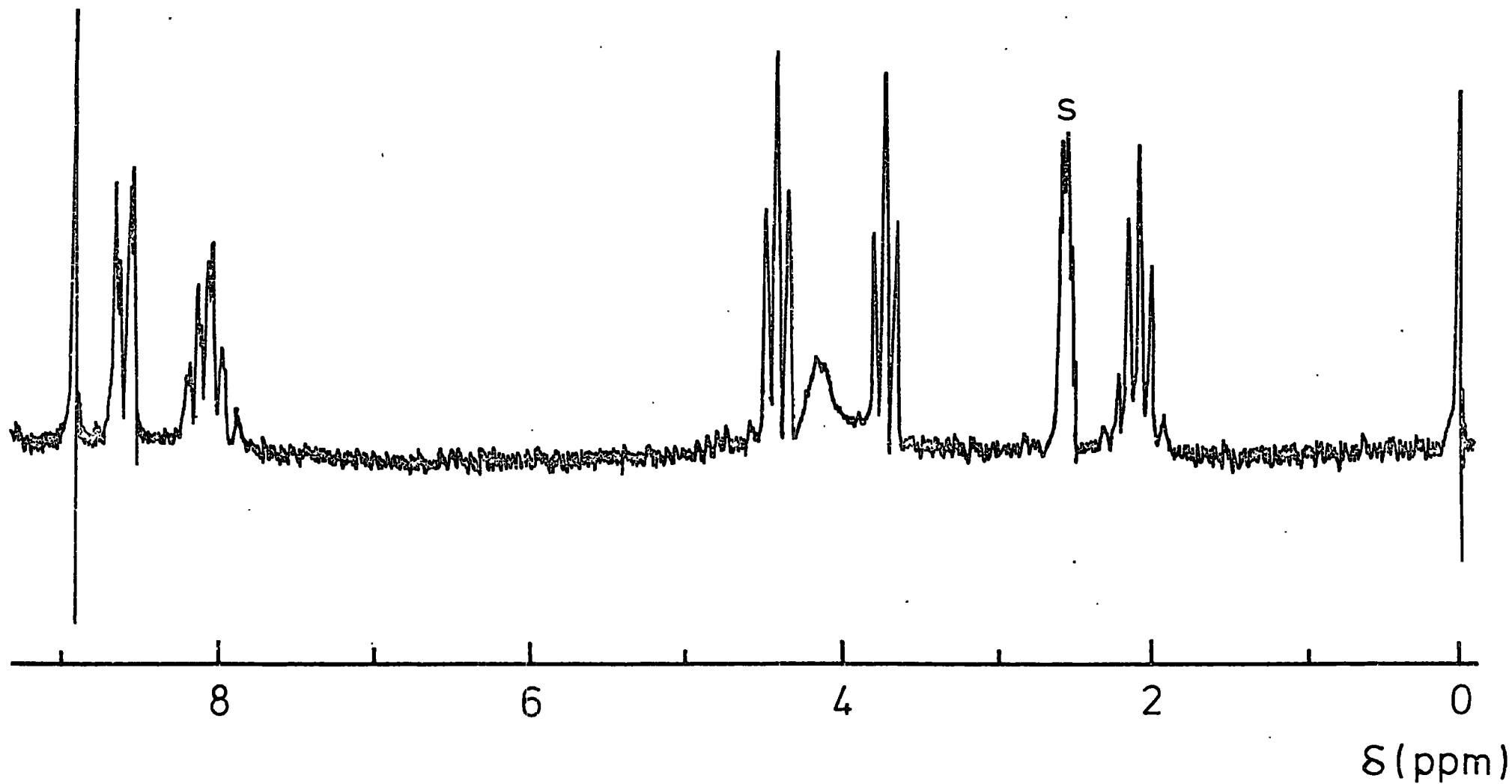
#### P.m.r. spectra

The spectrum (Figure 8.1) of 1-(3-hydroxypropoxy)-2,4-dinitronaphthalene 0.2M in DMSO-d<sub>6</sub> shows three sets of bands due to ring protons at δ8.90 (singlet; H<sub>3</sub>), 8.60 (overlapping doublet of doublets; H<sub>5</sub> and H<sub>8</sub>) and 8.03 p.p.m. (multiplet; H<sub>6</sub> and H<sub>7</sub>). These positions are close to those observed for other 2,4-dinitronaphthyl ethers.<sup>52,184,234</sup> The α-CH<sub>2</sub> group absorbs at δ4.40 (triplet; J = 6.5 Hz), the β-CH<sub>2</sub> group at 2.08 (pentet; J = 6.5 Hz) and the γ-CH<sub>2</sub> group at 3.70 p.p.m. (triplet; J = 6 Hz), while the hydroxy proton gives a broad band at δ4.20 p.p.m..

On the addition of sodium deuterioxide in deuterium oxide the spectrum which results is that shown in Figure 8.2. The aromatic protons now absorb at δ8.92 (singlet; H<sub>3</sub>), 8.77 (doublet of doublets; H<sub>8</sub>), 8.05 (doublet of doublets; H<sub>5</sub>) and 7.40 p.p.m. (multiplet; H<sub>6</sub> and H<sub>7</sub>). Generally the aromatic protons show shifts to high field expected on formation of an anionic complex. The small shifts to low field on complex function of the H<sub>3</sub> and H<sub>8</sub> resonances are analogous to those observed previously in similar systems.<sup>52,184,234</sup> The reasons advanced by Fendler et al<sup>52,234</sup> for the direction and magnitude of the shifts of the aromatic protons on complexation may be applicable here.

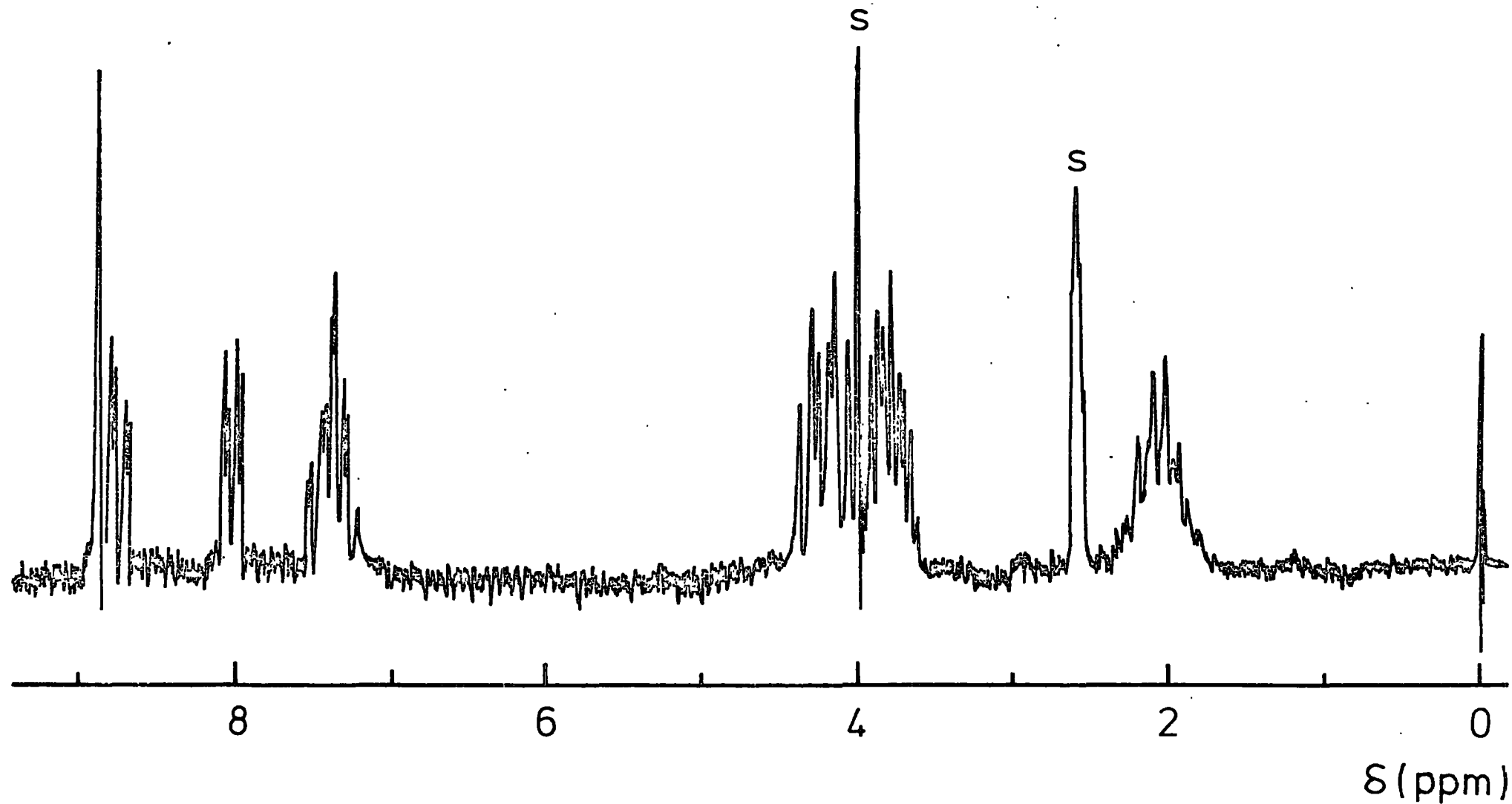
Of particular interest is the appearance of bands due to the methylene protons in the complex. These give two overlapping triplets at δ4.26, two quartets at δ3.81 and a multiplet at δ2.08 p.p.m. (Figure 8.3). The sharp band at δ4.0 p.p.m. marked 'S' in Figure 8.2 is due to the rapidly exchanging hydroxylic protons in the solvent. Addition of different base concentrations resulted in the shift of this solvent absorption and indicated that no bands are obscured by this peak.

FIGURE 8.1



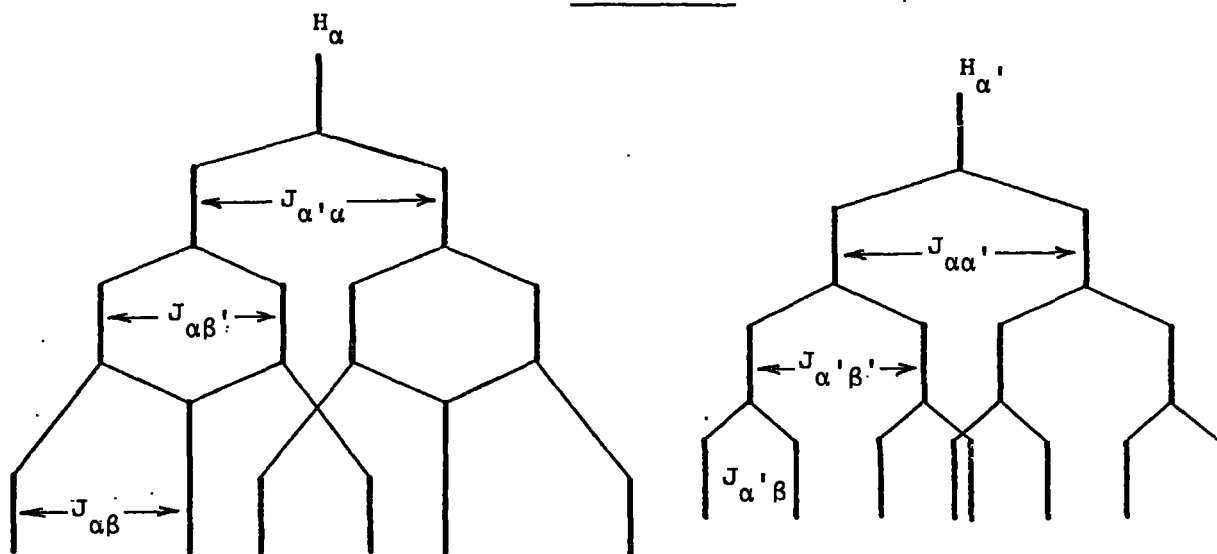
P.m.r. spectrum of 1-(3-hydroxypropoxy)-2,4-dinitronaphthalene (0.2M) in DMSO- $d_6$ . Bands marked 's' are due to solvent.

FIGURE 8.2



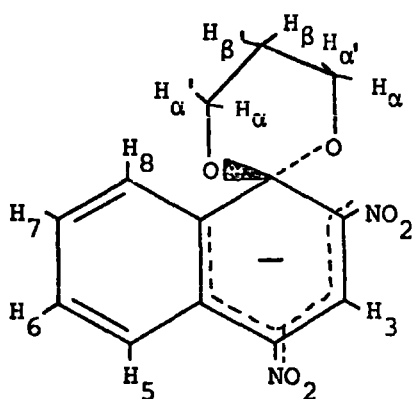
P.m.r. spectrum of 1-(3-hydroxypropoxy)-2,4-dinitronaphthalene in DMSO- $d_6$  after the addition of sodium deuterioxide in  $D_2O$ , Bands marked 's' are due to solvent.

FIGURE 8.3

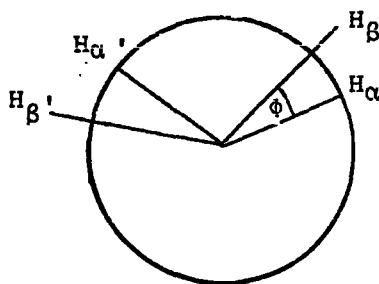


Splitting patterns for the  $H_{\alpha}$  and  $H_{\alpha'}$  protons in complex (8.6)

The observed spectrum is in agreement with structure (8.6) in which the molecule is symmetrical about the plane of the naphthalene ring. The two equivalent protons labelled  $H_{\alpha}$  are cis and the two equivalent protons labelled



(8.6)



$\phi$  ca. 20-30°

(8.7)

$H_{\alpha'}$  are trans to the 2-nitro group. From the spectrum a value for  $J_{\alpha\alpha'}$  of 11 Hz is obtained which is in the range expected for geminal coupling constants for methylene groups attached to oxygen in six-membered rings.<sup>250</sup> The values of the vicinal coupling constants are  $J_{\alpha\beta}$  8 Hz,  $J_{\alpha\beta'}$  8 Hz,  $J_{\alpha'\beta}$  4 Hz and  $J_{\alpha'\beta'}$

7.5 Hz. Since vicinal coupling constants are related to the dihedral angle,  $\phi$ , via the Karplus equation<sup>250,251</sup> (equation 8.1, where A, B and C are constants dependent on the system), these values provide information as to the

$$J_{vic} = A + B \cos \phi + C \cos 2\phi \quad 8.1$$

conformation in the dioxolan ring. Equation 8.1 indicates that the coupling constants are large when  $\phi$  is close to  $0^\circ$  and  $180^\circ$  and small when  $\phi$  is close to  $90^\circ$  (Figure 8.4) Hence the observed values are best described by a situation

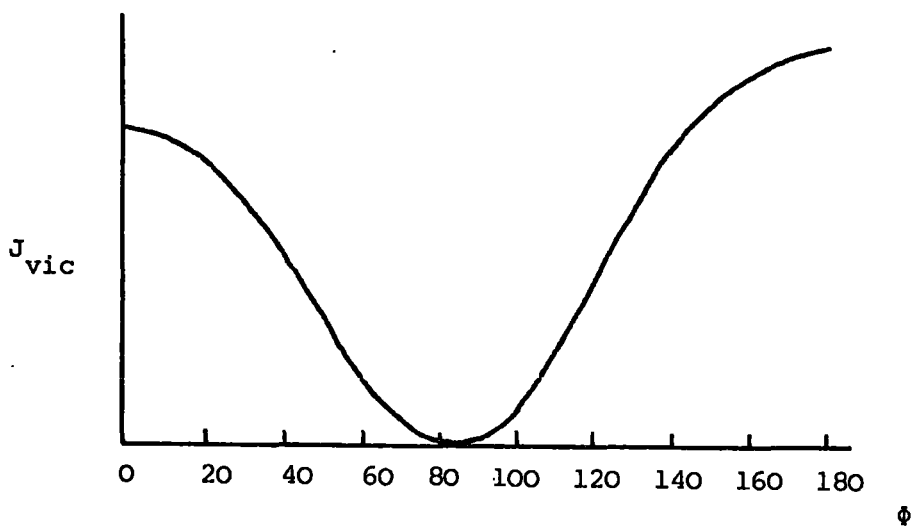


FIGURE 8.4

represented diagrammatically in (8.7) where the dihedral angle between  $H_\alpha$  and  $H_\beta$  is ca.  $20-30^\circ$ . However it should be noted that the possibility of the observed spectrum representing the time-average of two or more conformations in rapid equilibrium cannot be discounted. If this is the situation then the measured coupling constants are weighted averages. Confirmation of the assignment of the n.m.r. parameters was provided by irradiation of the  $\beta$  and  $\beta'$  methylene protons at  $\delta 2.08$  p.p.m., when the expected pair of doublets,  $J = 11$  Jz, was observed for the  $\alpha$  and  $\alpha'$  protons. The  $\alpha$ -hydrogens would be expected to be the downfield doublet since they are closer to the ortho-nitro group. Thus the observed spectrum is not consistent with the alternative structures (8.4) and (8.5).

The spectrum of the parent (8.1;  $n = 4$ ) shows bands due to the aromatic ring-protons very similar ( $\pm 0.04$  p.p.m.) to those observed for (8.1;  $n = 3$ ).

The  $\alpha$ -CH<sub>2</sub> group absorbs at  $\delta$ 4.32 (triplet;  $J = 6$  Hz), the  $\beta$ -CH<sub>2</sub> group at 1.98 (pentet;  $J = 6$  Hz), the  $\gamma$ -CH<sub>2</sub> group at 1.70 (pentet;  $J = 6$  Hz) and the  $\delta$ -CH<sub>2</sub> group at 3.53 p.p.m. (triplet;  $J = 6$  Hz), while the hydroxyl proton gives a singlet at  $\delta$ 4.35 p.p.m.. The spectrum in the presence of base indicates cyclisation to give the spiro-complex (8.2;  $n = 4$ ) but provides less precise structural information than the spectrum of (8.2;  $n = 3$ ). Bands are observed due to the aromatic protons at 8.90 (singlet; H<sub>3</sub>), 8.73 (doublet of doublets; H<sub>8</sub>), 7.93 (doublet of doublets; H<sub>5</sub>) and 7.40 p.p.m. (multiplet; H<sub>6</sub> and H<sub>7</sub>). The methylene protons  $\alpha$  to the ring now give a multiplet at  $\delta$ 3.85 and those  $\beta$  to the ring a band at  $\delta$ 1.71 p.p.m.. Collected data for both complexes are given in Table 8.1.

#### Kinetic and equilibrium data

Kinetic measurements were made with base concentrations in large excess of the substrate concentration so that first-order kinetics were observed. Typical data are given in Table 8.2. Collected data for measurements made in water and in water-DMSO mixtures are given in Tables 8.3 and 8.4. It will be assumed, and justified later, that in these media as in DMSO the initial colour-forming reaction is spiro-complex formation. The mechanism of complex formation in alkaline media will be assumed to be the same as that suggested earlier for the  $n = 2$  complexes. The measured equilibrium and rate constants,  $K_C$  and  $k_{obs}$ , will therefore be given by equations 6.2. and 6.3.

The parent molecules (8.1;  $n = 3,4$ ) are unlikely<sup>235</sup> to have  $pK_a$  values much lower than 15 so that values of  $K$  will probably be less than  $0.1 \text{ l.mol}^{-1}$ . Hence at the sodium hydroxide concentrations used in the present work, the values of the term  $(1 + K[OH^-])$  in equations 6.2 and 6.3 will be close to unity. Accordingly plots of  $k_{obs}$  versus base concentration were linear and yielded values of  $k_{-1}$  (intercept) and  $k_1K$  (slope). Combination of these data gave values of  $KK_1$  (kinetic). In water the values of  $k_{-1}$  can be obtained reasonably accurately although, because of the smallness of the slopes, particularly for

TABLE 8.1

Collected PMR Data<sup>a</sup> for the Parent Ethers (8.1; n = 3,4) and Spiro-complexes (8.2; n = 3,4)

	<u>H<sub>3</sub></u>	<u>H<sub>5</sub></u>	<u>H<sub>8</sub></u>	<u>H<sub>6</sub></u>	<u>H<sub>7</sub></u>	<u>α-CH<sub>2</sub></u>	<u>β-CH<sub>2</sub></u>	<u>γ-CH<sub>2</sub></u>	<u>δ-CH<sub>2</sub></u>	<u>OH</u>
(8.1; n = 3)	8.90(s)	8.60(dd)		8.03(m)		4.40(t) <sup>b</sup>	2.08(p) <sup>b</sup>	3.70(t) <sup>c</sup>		4.20(s)
(8.2; n = 3)	8.92(s)	8.05(dd)	8.77(dd)	7.40(m)		4.26, 3.8 <sup>d</sup>	2.08(m)			
(8.1; n = 4)	8.89(s)	8.56(dd)		8.03(m)		4.32(t) <sup>c</sup>	1.98(p) <sup>c</sup>	1.70(p) <sup>c</sup>	3.53(t) <sup>c</sup>	4.35(s)
(8.2; n = 4)	8.91(s)	7.97(dd)	8.74(dd)	7.41(m)		3.84(m)	1.72(br,s)			

<sup>a</sup> All shifts are on the  $\delta$  scale and quoted in p.p.m. relative to internal tetramethylsilane

<sup>b</sup> J = 6.5 Hz.

<sup>c</sup> J = 6 Hz.

<sup>d</sup> J<sub>αα'</sub> = 11 Hz, J<sub>αβ</sub> = 8 Hz, J<sub>αβ'</sub> = 8 Hz, J<sub>α'β</sub> = 4 Hz, J<sub>α'β'</sub> = 7.5 Hz.

s = singlet, m = multiplet, t = triplet, p = pentet, dd = doublet of doublets, br = broad

TABLE 8.2

Kinetic Data for the Reaction of 1-(3-Hydroxypropoxy)-2,4-dinitro-  
naphthalene ( $2.34 \times 10^{-5}$  M) with Sodium Hydroxide (0.10M) in Water

<u>Time</u> (sec)	<u>Scale Reading</u> <sup>a</sup> (arbitrary units)	<u>k<sub>obs</sub></u> (sec <sup>-1</sup> )
0.20	2.77	1.04
0.40	3.35	1.05
0.60	3.78	1.02
0.80	4.17	1.03
1.00	4.46	1.02
1.20	4.73	1.04
1.40	4.93	1.04
1.60	5.10	1.04
1.80	5.20	1.02
∞	5.80	-

<sup>a</sup> Measurements at 500 nm

TABLE 8.3

Kinetic and Equilibrium Data for Spiro-complex Formation  
from 1-(3-Hydroxypropoxy)-2,4-dinitronaphthalene at 25°C

<u>Medium</u>	<u>[NaOH]</u>	<u>10<sup>5</sup>[Substrate]</u>	<u>k<sub>obs</sub></u>	<u>O.D.<sup>a,b</sup></u>	<u>k<sub>C</sub></u>
	(M)	(M)	(sec <sup>-1</sup> )		(l.mol <sup>-1</sup> )
Water <sup>c</sup>	0.025	4.67	0.89 ± .02	0.020	1.3 <sup>e</sup>
	0.025 <sup>d</sup>	4.67	0.88		
	0.050	4.67	0.93	0.039	1.3
	0.075	4.67	0.99	0.056	1.3
	0.10	2.34	1.04	0.040	1.4
	0.15	2.34	1.12	0.056	1.4
80/20 (v/v) Water-DMSO	0.012	4.4	0.32	0.060	8 <sup>f</sup>
	0.023	2.2	0.34	0.055	8
	0.047	2.2	0.41	0.100	8
	0.081	1.5	0.53	0.096	8
	0.110	1.2	0.60	0.087	8
60/40 (v/v) Water-DMSO	0.012	1.0	0.185		
	0.024	1.0	0.30		
	0.050	1.0	0.56		
40/60 (v/v) Water-DMSO	0.012	0.5	1.13		
	0.024	0.5	2.08		
	0.050	0.5	4.42		

<sup>a</sup> Values are quoted for 1 cm pathlength.

<sup>b</sup> Measurements at 500 nm      <sup>c</sup> Contains 0.5% DMSO from stock solution of substrate

<sup>d</sup> Containing 0.10M sodium chloride.

<sup>e</sup> Calculated with a value of  $\epsilon = (1.4 \pm 0.4) \times 10^4 \text{ l.mol}^{-1} \text{ cm}^{-1}$

<sup>f</sup> Calculated with a value of  $\epsilon = (1.6 \pm 0.4) \times 10^4 \text{ l.mol}^{-1} \text{ cm}^{-1}$

TABLE 8.4

Kinetic and Equilibrium Data for Spiro-complex Formation  
from 1-(4-Hydroxybutoxy)-2,4-dinitronaphthalene at 25°C

<u>Medium</u>	<u>[NaOH]</u>	<u>10<sup>5</sup>[Substrate]</u>	<u>k<sub>obs</sub></u>	<u>O.D.<sup>a,b</sup></u>	<u>K<sub>C</sub></u>
	(M)	(M)	(sec <sup>-1</sup> )		(l.mol <sup>-1</sup> )
Water <sup>c</sup>	0.075	4.4	0.68 ± .02	0.019	0.5 <sup>d</sup>
	0.10	4.4	0.70	0.026	0.5
	0.125	4.4	0.72	0.032	0.5
	0.15	4.4	0.73	0.037	0.5
	0.20	4.4	0.76	0.048	0.5
80/20 (v/v) Water-DMSO	0.037	3.3	0.34	0.040	2.5 <sup>e</sup>
	0.055	6.5	0.37	0.125	2.5
	0.073	3.3	0.38	0.079	2.5
	0.092	3.3	0.41	0.095	2.5
	0.110	3.3	0.43	0.108	2.5
60/40 (v/v) Water-DMSO	0.015	1.63	0.14	0.086	30 <sup>f</sup>
	0.037	1.63	0.22	0.145	30
	0.055	0.82	0.28	0.090	30
	0.092	0.82	0.42		

<sup>a</sup> Values are quoted for 1 cm pathlength

<sup>b</sup> Measurements at 500 nm

<sup>c</sup> Contains 0.5% DMSO from stock solution of substrate

<sup>d</sup> Calculated with a value of  $\epsilon = (1.3 \pm 0.3) \times 10^4 \text{ l.mol}^{-1} \text{ cm}^{-1}$

<sup>e</sup>  $\epsilon = (1.5 \pm 0.3) \times 10^4 \text{ l.mol}^{-1} \text{ cm}^{-1}$

<sup>f</sup>  $\epsilon = (1.8 \pm 0.3) \times 10^4 \text{ l.mol}^{-1} \text{ cm}^{-1}$

(8.2;  $n = 4$ ), values of  $k_1K$  are less reliable. As the proportion of DMSO is increased the accuracy of  $k_1K$  increases while that of  $k_{-1}$ , whose values approach zero, decreases.

An alternative approach to the calculation of  $K_C$  values, and hence  $KK_1$ , is afforded by the use of stopped-flow spectrophotometry to measure values of optical density after completion of the initial colour-forming reaction but before appreciable decomposition to 2,4-dinitronaphthol has occurred. Such values are given in Tables 8.3 and 8.4. Unfortunately the measurements do not yield values for the extinction coefficients of the complexes in water since Benesi-Hildebrand plots<sup>163</sup> have intercepts close to zero. However in media rich in DMSO conversion into complex was complete so that extinction coefficients could be obtained directly. For example for (8.2;  $n = 3$ ) in 80% DMSO  $\lambda_{\max}$  508 nm  $\epsilon = 2.7 \times 10^4 \text{ l.mol}^{-1} \text{ cm}^{-1}$ . By analogy with previous results, values of  $\epsilon$  will decrease with increasing proportion of water in the solvent. Thus extrapolation of data obtained in water-DMSO mixtures gave the values of  $\epsilon$  quoted in Tables 8.3 and 8.4. The necessarily high uncertainty associated with these values leads to the high error limits given for the calculated values of  $KK_1$  (equil.). The data collected in Table 8.5 show that the agreement between  $KK_1$  values determined kinetically and spectrophotometrically is not particularly good. This may indicate that the values used for  $\epsilon$  are too high or that measured values of  $k_1K$  are too high.

As expected<sup>6,8</sup> values of the equilibrium constants  $KK_1$  increase as the proportion of DMSO in the solvent is increased. These changes reflect the increase in values of the rate constants for complex formation and the decrease in the rate constant for ring-opening resulting from the stabilising effect of DMSO on the complex. The steady change in the values of the parameters with solvent composition, also observed by Bernasconi<sup>81,230</sup> for spiro-complexes, is a strong argument that the mode of interaction does not change with solvent.

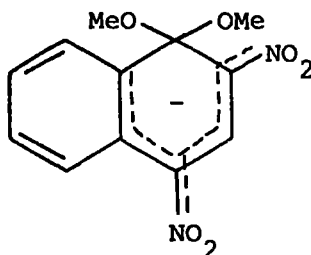
TABLE 8.5

Variation of Rate and Equilibrium Parameters with Solvent Composition

	<u>Water</u>	<u>80/20 (v/v) Water-DMSO</u>	<u>60/40 (v/v)</u>	<u>40/60 (v/v)</u>
$k_{-1}$ ( $\text{sec}^{-1}$ )	0.85±0.2	0.28±0.02	0.07±0.01	
$k_1K$ ( $1.\text{mol}^{-1}\text{sec}^{-1}$ )	1.7±0.3	2.9±0.3	10±1	90±5
(8.2; n=3)				
$K_1K$ (kinetic) ( $1.\text{mol}^{-1}$ )	2.0±0.5	10±2	140±30	
$K_1K$ (equil.) ( $1.\text{mol}^{-1}$ )	1.3±0.4	8±2		
$k_{-1}$ ( $\text{sec}^{-1}$ )	0.64±0.04	0.30±0.02	0.09±0.01	
$k_1K$ ( $1.\text{mol}^{-1}\text{sec}^{-1}$ )	0.6±0.3	1.2±0.1	3.5±0.3	
(8.2; n=4)				
$K_1K$ (kinetic) ( $1.\text{mol}^{-1}$ )	0.9±0.5	4±0.5	40±5	
$K_1K$ (equil.) ( $1.\text{mol}^{-1}$ )	0.5±0.2	2.5±1	30±5	

Evidence for spiro-complex formation in water

Using stopped-flow spectrophotometry it was possible to determine the visible spectra of the initial complexes in water. The position of the absorption maximum at 495 nm is exactly the same as that for the spiro-complex (8.2;  $n = 2$ ). Addition at the  $C_3$  position, ortho to the two nitro groups, would be expected<sup>6,8</sup> to give rise to absorption at longer wavelengths. Thus complex (8.5) or a complex produced by internal attack of the side chain at  $C_3$  are rendered unlikely. However by analogy with the dimethoxy-complex<sup>182</sup> (8.8) where  $\lambda_{max}$  is 498 nm, the adduct (8.4) might be expected to show absorption



(8.8)

in this region. Furthermore this structure, (8.4), is almost certain to be an intermediate in the substitution reaction leading to the reaction product 2,4-dinitronaphthol. If it is assumed that the data in Table 8.6 refer to formation of adducts (8.4;  $n = 3,4$ ) then the knowledge that the second-order

TABLE 8.6

Equilibrium and Rate Data for Spiro-complex Formation in Water at 25°C

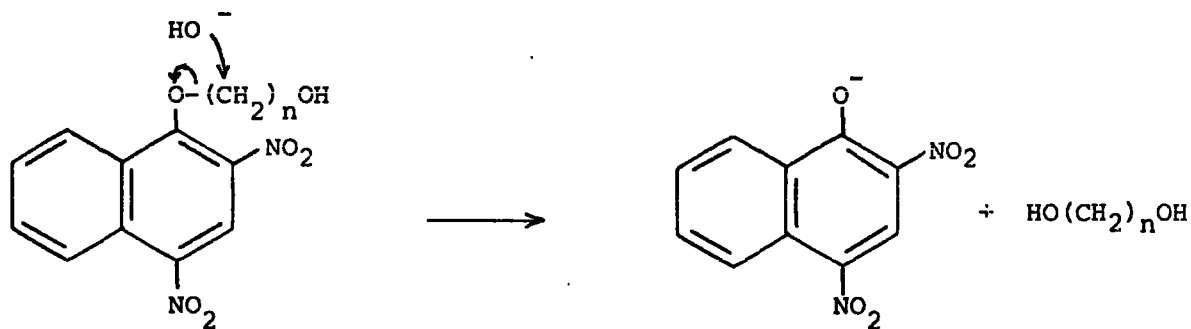
<u>Complex</u>	$\frac{K_1 K}{(l.mol^{-1})}$	$\frac{k_1 K}{(l.mol^{-1} sec^{-1})}$	$\frac{k_{-1}}{(sec^{-1})}$
(8.2; $n = 2$ )	$3 \times 10^4$	$9 \times 10^4$	2.3
(8.2; $n = 3$ )	1.7 <sup>a</sup>	1.7	0.85
(8.2; $n = 4$ )	0.7 <sup>a</sup>	0.6	0.64

<sup>a</sup> Average from kinetic and spectrophotometric measurements

rate constants for nucleophilic displacement in water have values of  $(6 \pm 1) \times 10^{-2} \text{ l.mol}^{-1} \text{ sec}^{-1}$  leads to the conclusion that expulsion of hydroxide from (8.4) is faster than expulsion of alkoxide by at least an order of magnitude. Such a marked reversal of normal leaving group tendencies<sup>252</sup> does not favour this hypothesis.

Further evidence that the observed colour is unlikely to result from (8.4) comes from measurements with 1-(2-methoxyethoxy)-2,4-dinitronaphthalene, a compound structurally similar to the substrates under investigation but where spiro-complex formation is not possible. In solutions containing  $10^{-5} \text{ M}$  substrate and  $0.5 \text{ M}$  sodium hydroxide the change in optical density at 500 nm was  $<0.001$  (quoted for 1 cm cell). Assuming a value for the extinction coefficient at this wavelength of  $1.5 \times 10^4 \text{ l.mol}^{-1} \text{ cm}^{-1}$  allows an upper limit of  $2 \times 10^{-2} \text{ l.mol}^{-1}$  to be set for the equilibrium constant for complex formation. However in media rich in DMSO the substrate gives an orange colour with base which may signify hydroxide ion addition.

Though hydrolysis of these compounds probably proceeds via intermediates such as (8.4) nevertheless there is the possibility of a dealkylation mechanism taking place, as follows



Measurements in DMSO-rich media with the 2-methoxyethyl derivative seem to indicate that this is not the case and the fact that DMSO appears not to change the mode of interaction would suggest that such a mechanism does not occur in water. However use of  $^{18}\text{OH}^-$  would prove conclusively which is the major pathway since the dealkylation mechanism would result in no  $^{18}\text{O}$

incorporation in the naphthol unlike the intermediate complex mechanism.

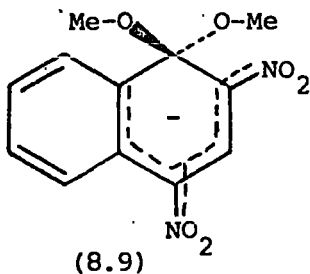
#### Effect of ring-size on spiro-complex formation

The results in Table 8.6 show that there is a very large decrease in stability on increasing the ring-size from five to six or seven members. This decrease reflects large changes in values of the rate constant for spiro-complex formation while values of the rate constant for ring-opening are little affected by ring-size. Some decrease in the values of the equilibrium constant,  $K$ , governing proton loss from the side-chain might be expected as the number of methylene groups increases due to attenuation of inductive effects. A further possible reason for variations in the values of  $K$  might be differential stabilisation of the parent alcohols by intramolecular hydrogen-bonding to the 2-nitro group. There seems to be no compelling reason why such stabilisation should increase with increasing chain length. However the  $pK_a$  values for 1,2-ethanediol, 1,3-propanediol and 1,4-butanediol are reported to be equal.<sup>235</sup>

The main differences are then likely to be connected with the internal cyclisation step. The present observation that the rate of cyclisation falls dramatically on going from (8.2;  $n = 2$ ) to (8.2;  $n = 3$ ) has a parallel with kinetic studies involving neighbouring-group participation.<sup>253</sup> For example measurements with halohydrin anions,  $Cl(CH_2)_m O^-$ , indicate that the rate of cyclisation decreases by  $10^3$  on going from  $m = 4$  (five-membered ring) to  $m = 5$  (six-membered ring). One important factor is likely to be the loss of rotational freedom of the side-chain. This will lead to an increasingly unfavourable entropy loss as the chain length increases. The effects of ring-size on ring-strain are less easy to predict. Formation of the dioxolan ring in the spiro-complex (8.2;  $n = 2$ ) involves eclipsing interactions between adjacent methylene hydrogens. However a model indicates that little deformation of bond angles is required so that this may not be a particularly strained structure. The proposed structure (8.6) for the six-membered ring

involves some expansion of bond angles, and unfavourable interactions between adjacent hydrogen atoms is still present as the conformation adopted is only partially 'staggered'. It may be that in the seven-membered ring (8.2;  $n = 4$ ) ring strain is less than in the six-membered case. Therefore a decrease in ring strain working in opposition to the expected increase in entropy loss would provide an explanation for the similar stabilities of (8.2;  $n = 3$ ) and (8.2;  $n = 4$ ). Other factors such as solvation may also be important.

The similarity of  $k_{-1}$  values in Table 8.6 probably indicates that most of the entropy loss and ring-strain connected with cyclisation are already present in the transition state for ring formation. The slightly larger value of  $k_{-1}$  for (8.2;  $n = 2$ ) may be as a result of steric interactions caused by the completely eclipsed conformation of the methylene hydrogens in the dioxolan ring. However as a whole the argument of ring-strain being the cause of the high rate of complex decomposition for spiro-complexes relative to their non-cyclic analogues is probably not justified. An alternative explanation may be found in terms of the conformational differences about the C-O bonds in the two types of complex. The preferred conformation of the 1,1-dimethoxy-complex will be as shown in (8.9) in which there is considerably



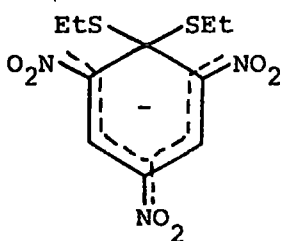
more freedom about the C-O bonds than in the spiro-complexes. Much of this freedom may well be lost on passage to the transition state for C-O bond breaking and hence the smaller values of complex decomposition for the non-cyclic adducts.

CHAPTER 9

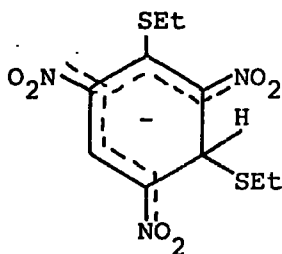
THIO-ANALOGUES OF SPIRO-COMPLEXES

INTRODUCTION

There have been several previous studies of the formation of  $\sigma$ -complexes from trinitro-activated substrates and thiolate ions. Spectral data and equilibrium constants have been reported for the addition of sodium thioethoxide and thiophenoxide to 1,3,5-trinitrobenzene<sup>160,177</sup> and some nitro-anilines.<sup>160</sup> In these cases addition occurs at unsubstituted ring positions. Pietra and Biggi<sup>161</sup> studied the reaction of sodium thioethoxide and ethyl thiopicrate and found n.m.r. evidence for the formation of two products (9.1) and (9.2).



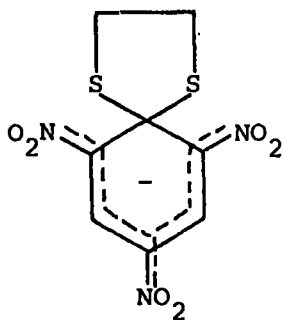
(9.1)



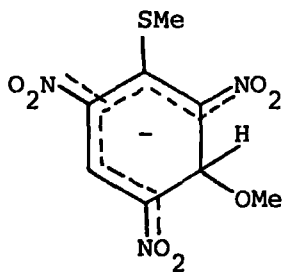
(9.2)

Both isomers were present at equilibrium with the 1,3-adduct (9.2) predominating. This is in marked contrast to the analogous reactions of oxygen bases with alkyl picrates where addition at the 3-position is kinetically preferred but addition at the 1-position gives the thermodynamically more stable product. Pietra and Biggi's result suggests that the stabilising effects of two thioalkoxy groups attached to the same carbon atom are diminished relative to the effects of two alkoxy groups.<sup>40,168</sup> By removing the possibility of attack at an unsubstituted ring position, Pietra et al<sup>195</sup> isolated and characterised a stable gem-adduct, the spiro-complex (9.3), for which kinetic and equilibrium data have been obtained in the present work.

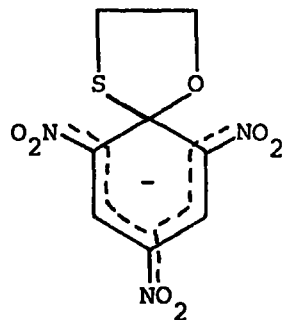
The preference for 1,3-adducts also appears to be the case when only one oxygen atom is replaced by sulphur. Thus Gitis et al<sup>254</sup> observed that complex (9.4) predominates in the reaction of methyl thiopicrate with methoxide ions.



(9.3)



(9.4)



(9.5)

However evidence will be presented later for the formation of the spiro-complex (9.5).

A. 1-(2-MERCAPTHIOETHOXY)-2,4,6-TRINITROBENZENE

EXPERIMENTAL

Freshly prepared stock solutions of buffers and substrate were diluted with water to give test solutions of the appropriate concentration immediately before measurements were made. U.v.-visible spectral shapes were recorded using a Unicam SP8000 spectrophotometer and equilibrium optical density measurements were obtained using an SP500 instrument. Kinetic measurements of complex decomposition in acidic buffers and dilute hydrochloric acid were made using the stopped-flow method by means of a 'Canterbury' spectrophotometer. P.m.r. spectra were recorded using a Bruker HX 90E instrument.

RESULTS AND DISCUSSION

The complex (9.3) dissolved in water gives a dark red solution which shows absorption in the visible region at  $\lambda_{\max}$  458 ( $\epsilon$   $1.8 \times 10^4$ ) and 550 nm (shoulder;  $\epsilon$   $7.7 \times 10^3$  l.mol<sup>-1</sup>cm<sup>-1</sup>). The spectrum of the complex dissolved in DMSO has  $\lambda_{\max}$  454 ( $\epsilon$   $2 \times 10^4$ ), 540 (shoulder;  $\epsilon$   $8 \times 10^3$ ) and 565 nm ( $\epsilon$   $8.6 \times 10^3$  l.mol<sup>-1</sup>cm<sup>-1</sup>). The complex in water undergoes slow irreversible decomposition. In DMSO the rate of decomposition is much slower, in accord with previous observations that DMSO has a stabilising effect on anionic  $\sigma$ -complexes.<sup>6</sup>

The p.m.r. spectrum of the complex dissolved in DMSO-d<sub>6</sub> shows two singlets at  $\delta$ 8.33 and 3.86 p.p.m. attributed to the ring and methylene protons respectively. Thus the spectral data are in agreement with Pietra's observations.<sup>195</sup>

Equilibrium optical density measurements and calculated equilibrium constants,  $K_C$ , are given in Table 9.1. The values of  $K_C$  were evaluated using

TABLE 9.1

Equilibrium Measurements for Complex (9.3) in Aqueous Buffers at 25°C

<u>pH</u>	<u>O.D.</u> <sup>a</sup>	$\frac{10^{-8} K_C}{(1.\text{mol}^{-1})}$
4.22	.098	9.5
4.65	.225	10
5.15	.426	10
5.65	.583	9.5
6.10	.653	8
6.63	.710	
7.2	.715	
7.6	.720	

<sup>a</sup> Measurements made at 458 nm

equation 6.2 assuming an analogous mechanism for complex formation.

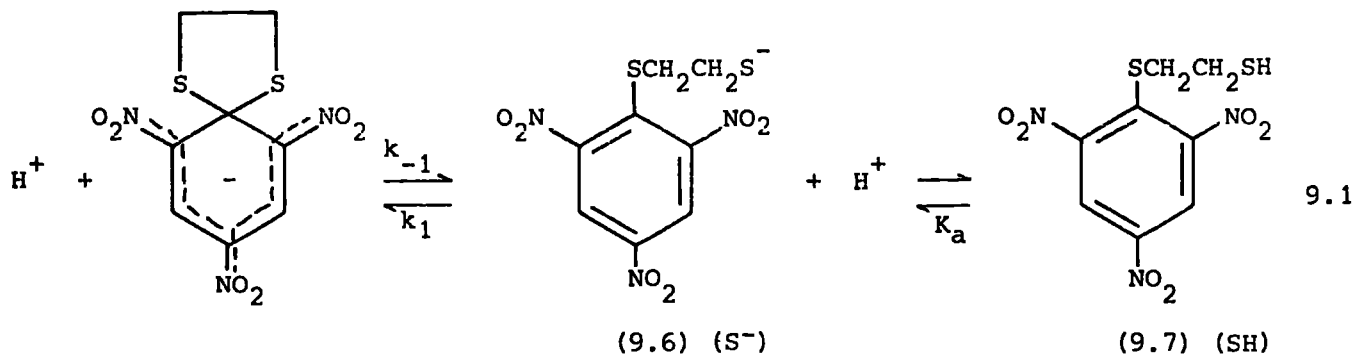
Rate measurements for complex decomposition were carried out under conditions where the pH of the solution did not vary or the concentration of acid was in large excess of the substrate concentration. Hence first-order kinetics were observed; a typical data set is given in Table 9.2.

TABLE 9.2

Rate Data for Decomposition of Complex (9.3) ( $3.1 \times 10^{-5} M$ )  
in Dilute Hydrochloric Acid ( $5 \times 10^{-3} M$ ) at  $25^{\circ}C$

<u>Time</u>	<u>Scale Reading</u>	<u><math>k_{obs}</math></u>
(m.sec)	(arbitrary units)	( $sec^{-1}$ )
0	7.21	-
10	5.00	37
20	3.40	38
30	2.35	38
40	1.58	38
50	1.09	38
60	0.75	39
70	0.54	38
$\infty$	0.04	-

The results in Table 9.3. for complex decomposition in various acidic buffers and dilute hydrochloric acid indicate the absence of general catalysis and only a feeble catalytic effect due to hydronium ions. This would suggest a mechanism for ring-opening according to equation 9.1. in which proton



transfer reactions between (9.6) and (9.7) involving buffer and solvent species are fast compared to  $k_1$  and  $k_{-1}$  and are probably diffusion controlled. <sup>255</sup>

TABLE 9.3

Kinetic Data for Decomposition of Complex (9.3) in Acidic  
Buffers and Dilute Hydrochloric Acid in Water at 25°C

<u>Acid</u>	<u>[HA]</u>	<u>[Na<sup>+</sup>A<sup>-</sup>]</u>	<u>10<sup>5</sup>[Substrate]</u>	<u>pH</u>	<u>k<sub>obs</sub></u>	<u>10<sup>-10</sup>k<sub>1</sub>K<sup>a</sup></u>
	(M)	(M)	(M)		(sec <sup>-1</sup> )	(1.mol <sup>-1</sup> sec <sup>-1</sup> )
Acetic	.026	.026	1.4	4.71	60.6 ± 1	4.2
	.065	.065	1.4	4.70	60.3	4.3
	.13	.13	1.4	4.72	60.2	4.0
	.26	.26	1.4	4.78	60	3.5
	.039	.013	2	4.2	46	4.4
	.39	.13	2	4.2	39.5	
Formic	.026	.026	1.4	3.65	40 ± 1	
	.065	.065	1.4	3.62	40	
	.13	.13	1.4	3.60	39	
	.26	.26	1.4	3.60	37	
	.039	.013	1.5	3.22	40	
	.195	.065	1.5	3.17	37	
Chloroacetic	.39	.13	1.5	3.10	36	
	.025	.025	1.5	2.92	38	
	.063	.063	1.5	2.9	37	
	.125	.125	1.5	2.92	34	
	.25	.25	1.5	2.80	31	
	.02	.005	1.5		40	
	.1	.025	1.5	2.5	37	
	.062	.062	1.5	2.93	37.5	
.062 <sup>b</sup>	.062 <sup>b</sup>	1.5	2.58	37.6		
HCl			4.5	5.05 <sup>c</sup>	86 ± 2	4.3
			3.0	5.20 <sup>c</sup>	120 ± 3	5
	.0025		3.1		39 ± 1	
	.0025 <sup>b</sup>		3.1		38	
	.005		3.1		38	
	.005 <sup>b</sup>		3.1		37	
	.0075		3.1		39	
	.0075 <sup>b</sup>		3.1		37	
	.01		1.5		39	
	.05		1.5		40	
.1		1.5		41		
.25		1.5		42		
DCl	.005		1.8		33	

<sup>a</sup> Calculated using equation 9.5 with k<sub>-1</sub> = 39 sec<sup>-1</sup>.

<sup>b</sup> Made up to ionic strength 0.25M with sodium chloride.

<sup>c</sup> Phthalate buffer, 0.025M

Moreover the absence of general acid catalysis and the very small catalytic coefficient of hydronium ions seems to suggest that the major pathway between the complex and (9.7) involves a spontaneous ring-opening of (9.3), which is supported by  $k_{-1}(\text{H}_2\text{O})/k_{-1}(\text{D}_2\text{O}) = 1.2 \pm 0.1$  indicating no involvement by the solvent. In contrast the decomposition of the oxygen analogue, complex (6.3), in acidic media involved a concerted proton transfer - ring-opening mechanism.

The observed rate constant for decomposition of the spiro-complex according to equation 9.1 can be derived as follows:

$$-\frac{d[\text{Spiro}]}{dt} = k_{-1}[\text{Spiro}] - k_1[\text{S}^-]$$

Assuming equilibration of  $\text{S}^-$  and SH is fast compared to  $k_1$  and  $k_{-1}$

$$\text{then } -\frac{d[\text{Spiro}]}{dt} = k_{-1}[\text{Spiro}] - k_1 K_a \frac{[\text{SH}]}{[\text{H}^+]} \quad 9.2$$

where  $K_a = \frac{[\text{S}^-][\text{H}^+]}{[\text{SH}]}$  is the acid dissociation constant of the thiol.

From the stoichiometry

$$[\text{Spiro}]_{\text{stoich}} = [\text{Spiro}] + [\text{S}^-] + [\text{SH}]$$

$$\therefore [\text{SH}] = [\text{Spiro}]_{\text{stoich}} - [\text{Spiro}] - [\text{S}^-]$$

Since  $K_a$  is of the order of  $10^{-10} \text{ mol.l}^{-1}$  (see later) and  $[\text{H}^+] > 10^{-6} \text{ M}$  then  $\frac{[\text{SH}]}{[\text{S}^-]} > 10^4$  and thus  $[\text{S}^-]$  can be neglected.

Substituting in equation 9.2. gives:

$$-\frac{d[\text{Spiro}]}{dt} = k_{-1}[\text{Spiro}] - \frac{k_1 K_a}{[\text{H}^+]} (\text{constant} - [\text{Spiro}]) \quad 9.3$$

At equilibrium

$$0 = k_{-1}[\text{Spiro}]_{\text{eq}} - \frac{k_1 K_a}{[\text{H}^+]} (\text{constant} - [\text{Spiro}]_{\text{eq}}) \quad 9.4$$

Combining equations 9.3 and 9.4 gives:

$$-\frac{d[\text{Spiro}]}{dt} = k_{-1}([\text{Spiro}] - [\text{Spiro}]_{\text{eq}}) + \frac{k_1 K_a}{[\text{H}^+]} ([\text{Spiro}] - [\text{Spiro}]_{\text{eq}})$$

$$\therefore k_{\text{obs}} = k_{-1} + \frac{k_1 K_a}{[\text{H}^+]}$$

Since  $\frac{K_a}{[H^+]} = \frac{[S^-]}{[SH]} = k[OH^-]$

$$k_{obs} = k_{-1} + k_1 K [OH^-] \quad 9.5$$

This is formally equivalent to the observed rate constant for complex formation in basic media.

Inspection of the data obtained in dilute hydrochloric acid reveals that the observed rate constants passes through a minimum ( $39 \pm 1 \text{ sec}^{-1}$ ) which corresponds to the pH independent term  $k_{-1}$  in equation 9.5. Data in Table 9.3 indicate a value of  $(4 \pm 1) \times 10^{10} \text{ l.mol}^{-1} \text{ sec}^{-1}$  for  $k_1 K$ . Combination of this result with  $k_{-1}$  leads to a value of  $(10 \pm 2) \times 10^8 \text{ l.mol}^{-1}$  for  $K_1 K$ , in good agreement with that obtained from equilibrium measurements (Table 9.1).

The decrease in the observed rate constants with buffer concentration noticed with formic and chloroacetic acid buffers may result from some kind of medium effect rather than a direct salt effect as added sodium chloride causes little change in  $k_{obs}$ .

Comparison with the dioxygen analogue

The kinetic and equilibrium parameters for complexes (6.3) and (9.3) are listed in Table 9.4. The larger values of  $K_1 K$  for complex (9.3) compared to

TABLE 9.4

Equilibrium and Kinetic Parameters for Complexes (6.3) and (9.3) in Water at 25°C

<u>Complex</u>	$\frac{K_1 K}{(\text{l.mol}^{-1})}$	$\frac{k_1 K}{(\text{l.mol}^{-1} \text{sec}^{-1})}$	$\frac{k_1^a}{(\text{sec}^{-1})}$	$\frac{k_{-1}}{(\text{sec}^{-1})}$
(6.3)	$1.8 \times 10^7$	$1.6 \times 10^6$	$1.6 \times 10^7$	.095
(9.3)	$(10 \pm 2) \times 10^8$	$(4 \pm 1) \times 10^{10}$	$(4 \pm 1) \times 10^6$	39

that for the oxygen analogue (6.3) reflects a larger value of  $k_1 K$ , however the  $k_{-1}$  value is also larger. Nevertheless it must be remembered that thiols are

stronger acids than alcohols by 5 or 6  $pK_a$  units.<sup>256</sup> Assuming a  $pK_a$  of 10 for (9.7) gives a value for  $K$  of ca.  $10^4 \text{ l.mol}^{-1}$  whereas a value for  $K$  of ca.  $10^{-1} \text{ l.mol}^{-1}$  is likely for the oxygen analogue. Thus the rate constants for spiro-complex formation of both sulphur and oxygen complexes are approximately the same. This leads to the result that the equilibrium constant,  $K_1$ , for spiro-complex formation is about three or four orders of magnitude greater for the dioxolan complex than for its thio-analogue. This contrasts with the result for 1,3,5-trinitrobenzene,<sup>160</sup> where addition occurs at an unsubstituted ring position and values for the equilibrium constants for addition of methoxide and thioethoxide are  $23^{167}$  and  $3.5 \times 10^3^{160} \text{ l.mol}^{-1}$  respectively. This reversal in stability parallels that observed by Pietra for the ethyl thiopicrate-thioethoxide system.<sup>161</sup>

One possible reason for the instability of 1,1-dithioalkoxy-complexes relative to the 1,3-adducts is steric crowding around the  $C_1$  position, sulphur being more sterically demanding than oxygen. This is supported by the large value of  $k_{-1}$  for (9.3) when compared to the oxygen analogue (6.3). Bernasconi<sup>40,168</sup> suggested that the stability of 1,1-dialkoxy-complexes owed itself in part to the particular stabilising effect of electronegative substituents attached to the saturated carbon atom. It could be argued therefore that the much reduced electronegativity of sulphur compared to oxygen contributes to the relative instability of thio-analogues of 1,1-dialkoxy-complexes.

The absence of any significant effect on the rate of complex decomposition by acidic species is indicative of the weak proton basicity of sulphur.<sup>256</sup> Indeed the use of thioacetals as protective groups for carbonyl functions in synthetic reactions, in spite of their ready formation,<sup>257</sup> is not very attractive because of their resistance to acid hydrolysis.<sup>258</sup> In terms of Pearson's<sup>201</sup> concept of hard and soft acids and bases it might be expected that a more likely way of effecting decomposition would be the use of a 'softer' acidic species (sulphur being considered as a soft base). In this respect the

dramatic catalytic effect of added mercuric ions (see Table 9.5) on the decomposition of complex (9.3) is not unexpected. In fact mercury (II) has been used to effect cleavage of thioacetals.<sup>259</sup>

TABLE 9.5

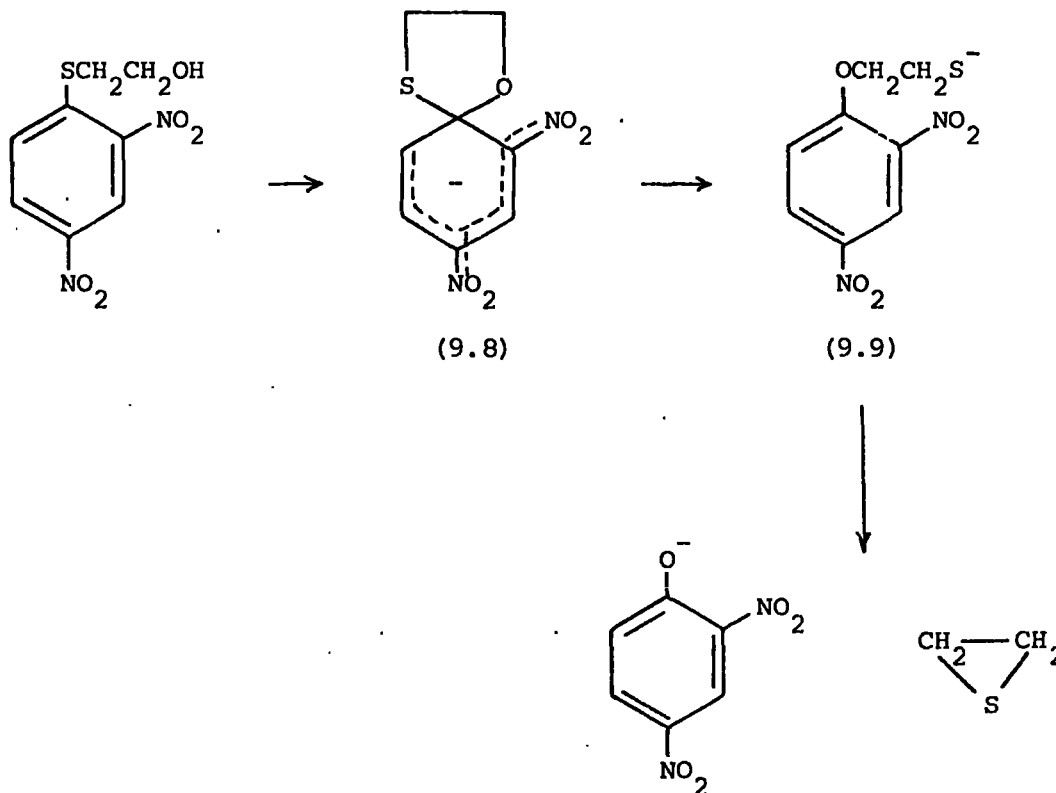
Kinetic Data for the Decomposition<sup>a</sup> of Complex (9.3) in  
the Presence of Added Mercuric Chloride

<u>10<sup>6</sup>[HgCl<sub>2</sub>]</u> (M)	<u>10<sup>5</sup>[Substrate]</u> (M)	<u>k<sub>obs</sub></u> (sec <sup>-1</sup> )
2.6	1.8	43
5.2	5.4	51
7.7	5.4	68
10.3	5.4	100

<sup>a</sup> Chloroacetic acid buffer (0.025M) at pH 2.90

B. 1-(2-HYDROXYTHIOETHOXY)-2,4,6-TRINITROBENZENE

It has been shown<sup>194</sup> that 1-(2-hydroxythioethoxy)-2,4-dinitrobenzene and the analogous picryl derivative undergo a reversed Smiles-type rearrangement in alkaline media to give the substituted phenol and ethylene sulphide according to the following scheme.



The results obtained in the present work for the picryl system support the above scheme and the kinetic and thermodynamic parameters obtained are compared with complexes (6.3) and (9.3).

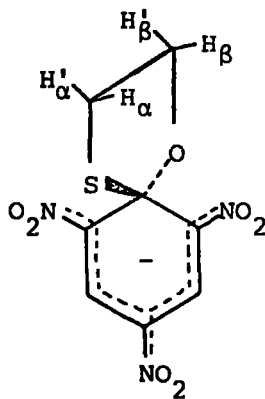
EXPERIMENTAL

P.m.r. spectra of the substrate in DMSO-d<sub>6</sub> in the absence and presence of base were recorded using a Bruker HX90E instrument. Spectral shape measurements in the u.v.-visible region of the spectrum were made by means of a Unicam SP800 spectrophotometer and a 'Canterbury' stopped-flow spectrophotometer. Kinetic measurements were made using the stopped-flow method for the picryl derivative and a Unicam SP500 for the 2,4-dinitrophenyl derivative.

RESULTS AND DISCUSSION

The p.m.r. spectrum of a 0.2M solution of the substrate in DMSO-d<sub>6</sub> shows three sets of bands at δ9.14 (singlet), 3.59 (triplet; J = 6 Hz) and 3.04 p.p.m. (triplet; J = 6 Hz) ascribable to the ring, β-CH<sub>2</sub> and α-CH<sub>2</sub> protons respectively. The hydroxyl proton gives a broad band centred at ca. δ3.60 p.p.m. Support for this assignment comes from the spectrum of the 2,4-dinitrophenyl derivative. In this case the hydroxyl resonance (δ5.21 p.p.m.) is split into a triplet (J ca. 6 Hz). The methylene proton absorptions occur at δ3.32 and 3.79 p.p.m., the latter being a quartet through coupling with the α methylene protons (J ca. 6 Hz) and the hydroxyl proton (J ca. 6 Hz). Thus the resonance at δ3.59 p.p.m. in the spectrum of the picryl derivative can be assigned to the methylene protons β to the ring and the 3.04 p.p.m. resonance to the α methylene protons.

Addition of less than one equivalent of sodium deuterioxide in D<sub>2</sub>O produced a bright red solution and resulted in the appearance of new absorptions at δ8.71 (singlet), 8.47 (singlet), 4.62 (multiplet), 3.58 (multiplet) and 2.47 p.p.m. (singlet). With time the bands at δ8.71 and 2.47 p.p.m. increased in intensity at the expense of those at δ8.47, 4.62 and 3.58 p.p.m. The latter set of bands are consistent with the spiro-complex (9.10), the non-equivalence of the



(9.10)

two methylene groups being caused by the two different heteroatoms in the five-membered ring. By comparison with the methylene proton resonances for

complexes (6.3) and (9.3) at  $\delta$ 4.3 and 3.86 p.p.m. respectively, the multiplet at  $\delta$ 4.62 p.p.m. can be assigned to the  $H_{\beta\beta}$  ' protons and the multiplet at  $\delta$ 3.58 p.p.m. to the  $H_{\alpha\alpha}$  ' protons. Vicinal coupling of the methylene protons results in multiplet splitting of the resonances; equation 8.1 indicates that  $J_{\alpha\beta} > J_{\alpha\beta}$  ' since the dihedral angles are 0 and  $120^\circ$  respectively. Addition of further base causes the parent peaks to disappear and the signals due to the complex to increase in intensity. Eventually only peaks at  $\delta$ 8.71 and 2.47 p.p.m. remain and these can be ascribed to the picrate anion and ethylene sulphide respectively.

Addition of dilute sodium hydroxide solution ( $<0.1M$ ) or aqueous alkaline buffers to an aqueous solution of 1-(2-hydroxythioethoxy)-2,4,6-trinitrobenzene (ca.  $4 \times 10^{-5}M$ ) results in the rapid formation of a red colour which slowly fades leaving a yellow solution. The u.v.-visible spectrum of this final solution has  $\lambda_{max}$  at 355 and 410 nm (shoulder), characteristic of the picrate anion.<sup>236</sup> Investigation of the system by stopped-flow spectrophotometry confirmed that there are two relaxation times. For the fast process an increase in optical density was always observed between 380 and 560 nm. The spectral shape in this region had  $\lambda_{max}$  at 435 and ca. 500 nm (shoulder), similar to that observed for other picrylic Meisenheimer complexes.<sup>6,8</sup> The second relaxation time was accompanied by a decrease in optical density at wavelengths  $>450$  nm and an increase at wavelengths  $<450$  nm. This isosbestic point shifted to lower wavelength as the pH and hence the proportion of the initial species increased.

Optical density measurements made at 435 nm after the first relaxation time are given in Table 9.6 together with calculated equilibrium constants.

Both relaxation times followed first-order kinetics and typical data are given in Tables 9.7 and 9.8. The same rate was obtained for the second process irrespective of the wavelength of observation. Rate constants for the formation and decomposition of the complex at different base concentrations are given in Tables 9.9 and 9.10.

TABLE 9.6

Equilibrium Measurements for Complex (9.5) in Aqueous Buffers at 25°C

<u>pH<sup>a</sup></u>	<u>10<sup>5</sup> [Substrate]</u> ( <u>M</u> )	<u>O.D.<sup>b</sup></u>	<u>10<sup>-3</sup> K<sub>C</sub></u> ( <u>l.mol<sup>-1</sup></u> )
8.4	4.02	.021	9.9
8.9	4.02	.055	9.8
9.15	6.1	.133	8.0
9.45	4.02	.142	7.0
9.50	4.27	.168	7.0
9.75	4.27	.240	6.3
9.88	4.02	.325	7.9
10.40	4.02	.492	5.2
	4.02	.87 <sup>c</sup>	

<sup>a</sup> Borax buffers 0.0125M

<sup>b</sup> Measured at 435 nm and quoted for 1 cm path-length

<sup>c</sup> Optical density for complete conversion in 10<sup>-2</sup>M sodium hydroxide

TABLE 9.7

Rate Data for the First Relaxation Time for the Decomposition at 25°C  
of 1-(2-Hydroxythioethoxy)-2,4,6-trinitrobenzene (4.02 x 10<sup>-5</sup>M) at pH 9.88

<u>Time</u> ( <u>sec</u> )	<u>Scale Reading</u> ( <u>arbitrary units</u> )	<u>k<sub>obs</sub></u> ( <u>sec<sup>-1</sup></u> )
0	0.70	-
0.1	2.55	3.58
0.2	3.82	3.54
0.3	4.75	3.58
0.4	5.38	3.58
0.5	5.80	3.54
0.6	6.10	3.51
0.7	6.33	3.53
∞	6.85	-

TABLE 9.8

Rate Data for the Second Relaxation Time for the Decomposition at 25°C of 1-(2-Hydroxythioethoxy)-2,4,6-trinitrobenzene ( $4.02 \times 10^{-5}$  M) at pH 9.88

<u>Time</u> (sec)	<u>Scale Reading</u> (arbitrary units)	$\frac{k_{obs}}{(\text{sec}^{-1})}$
0	0.80	-
2	1.85	0.087
4	2.75	0.088
6	3.52	0.089
8	4.13	0.089
10	4.65	0.088
12	5.13	0.090
14	5.45	0.088
16	5.78	0.089
18	6.02	0.088
$\infty$	7.36	-

TABLE 9.9

Variation of the First Relaxation Time with pH for the Decomposition of 1-(2-Hydroxythioethoxy)-2,4,6-trinitrobenzene in Aqueous Alkaline Buffers at 25°C

$10^5$ [Substrate] (M)	pH <sup>a</sup>	$\frac{k_{obs}}{(\text{sec}^{-1})}$
6.1	9.15	2.46 ± .05
4.27	9.50	2.65
4.27	9.75	2.95
4.02	9.88	3.55
3.65	10.2	4.3 ± .1
3.65	10.4	5.3
4.02	10.4	6.0
3.65	10.6	6.6

<sup>a</sup> Borax buffers - 0.0125M

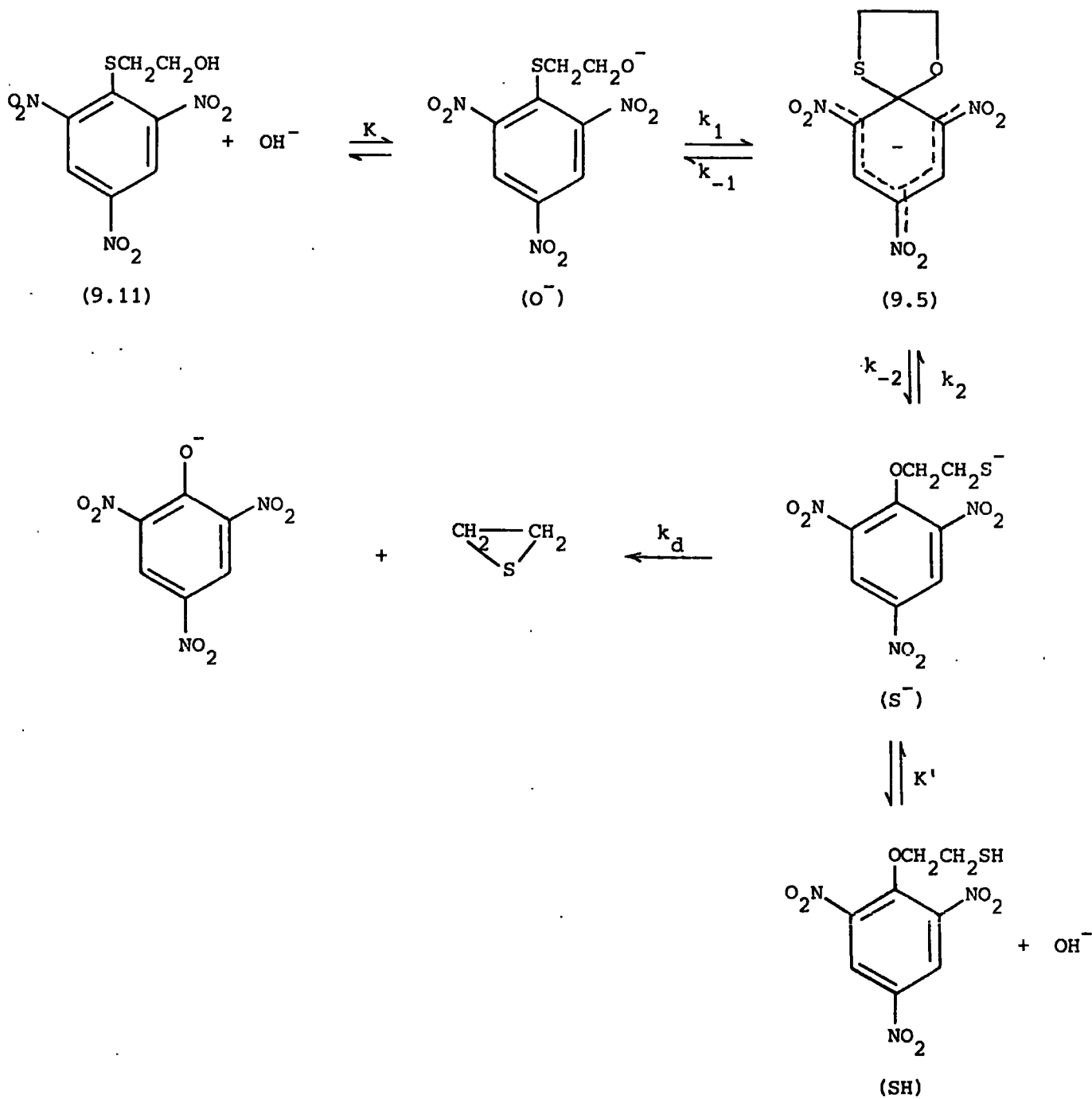
TABLE 9.10

Variation of the Second Relaxation Time with pH for the Decomposition of  
1-(2-Hydroxythioethoxy)-2,4,6-trinitrobenzene in Aqueous Alkaline Buffers at 25°C

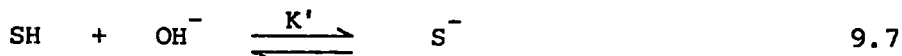
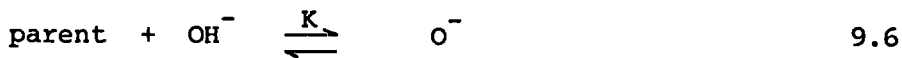
<u>10<sup>5</sup>[Substrate]</u> (M)	<u>pH</u> <sup>a</sup>	<u>λ</u> <sup>λ</sup> (nm)	<u>k<sub>obs</sub></u> (sec <sup>-1</sup> )
6.1	9.15	500	.025
4.27	9.50	500	.043
		415	.043
4.27	9.75	500	.061
		410	.060
4.02	9.88	500	.089
		408	.089
3.65	10.2	500	.117
3.65	10.4	500	.134
4.02	10.4	500	.140
		400	.139
3.65	10.6	500	.151

<sup>a</sup> Borax buffers - 0.0125M

The results can be accommodated in terms of the following scheme:



It is assumed that the proton transfer equilibria 9.6 and 9.7 are fast and K and K' have values of ca. 10<sup>-1</sup> and ca. 10<sup>4</sup> l.mol<sup>-1</sup> respectively. Then the



equilibrium concentration of  $O^-$ , which is given by  $K[\text{parent}][\text{OH}^-]$ , will be always small at the base concentrations used in the present work. Each process will be considered in turn.

First relaxation time

The rate constant for the colour-forming reaction is defined by:

$$k_{\text{obs}} = - \frac{d(\text{O.D.}_{\text{eq}} - \text{O.D.})}{dt(\text{O.D.}_{\text{eq}} - \text{O.D.})} \quad \text{where O.D. = optical density}$$

From the stoichiometry

$$[\text{Spiro}] = [\text{parent}]_{\text{stoich}} - [\text{parent}] - [\text{S}^-] - [\text{SH}] \quad 9.8$$

If equilibrium 9.7 is fast then  $[\text{SH}] = \frac{[\text{S}^-]}{K'[\text{OH}^-]}$

Substituting in equation 9.8 gives

$$[\text{Spiro}] = [\text{parent}]_{\text{stoich}} - [\text{parent}] - [\text{S}^-] \left( 1 + \frac{1}{K'[\text{OH}^-]} \right)$$

Similarly if  $\text{spiro} \rightleftharpoons \text{S}^-$  is fast then  $[\text{S}^-] = \frac{[\text{spiro}]}{K_2}$  9.9

and  $[\text{spiro}] \times \text{constant} = [\text{parent}]_{\text{stoich}} - [\text{parent}]$  9.10

where constant =  $1 + \frac{1}{K_2} \left( 1 + \frac{1}{K'[\text{OH}^-]} \right)$

But  $\text{O.D.} \propto [\text{spiro}]$

$\therefore \text{O.D.} \propto ([\text{parent}]_{\text{stoich}} - [\text{parent}]) \times \frac{1}{\text{constant}}$

Similarly  $\text{O.D.}_{\text{eq}} \propto ([\text{parent}]_{\text{stoich}} - [\text{parent}]_{\text{eq}}) \times \frac{1}{\text{constant}}$

$\therefore \text{O.D.}_{\text{eq}} - \text{O.D.} \propto ([\text{parent}] - [\text{parent}]_{\text{eq}}) \times \frac{1}{\text{constant}}$

$\therefore k_{\text{obs}} = - \frac{d([\text{parent}] - [\text{parent}]_{\text{eq}})}{dt([\text{parent}] - [\text{parent}]_{\text{eq}})}$

$\therefore - \frac{d[\text{parent}]}{dt} = k_{\text{obs}} ([\text{parent}] - [\text{parent}]_{\text{eq}})$

Thus spiro-complex formation should show first-order kinetics and this is observed experimentally (see Table 9.7).

(i) Derivation of  $k_{obs}$

$$\frac{d[\text{spiro}]}{dt} = k_1[\text{O}^-] - (k_{-1} + k_{-2})[\text{spiro}] + k_2[\text{S}^-]$$

Since equilibrium 9.6 and 9.9 are fast then

$$\begin{aligned} \frac{d[\text{spiro}]}{dt} &= k_1K[\text{parent}][\text{OH}^-] - (k_{-1} + k_{-2})[\text{spiro}] + k_{-2}[\text{spiro}] \\ &= k_1K[\text{parent}][\text{OH}^-] - k_{-1}[\text{spiro}] \end{aligned}$$

Substituting for spiro from equation 9.10 gives

$$\frac{d[\text{spiro}]}{dt} = k_1K[\text{parent}][\text{OH}^-] - k_{-1} \left( \frac{[\text{parent}]_{\text{stoich}} - [\text{parent}]}{\text{constant}} \right) \quad 9.11$$

At equilibrium  $\frac{d[\text{spiro}]}{dt} = 0$

$$\therefore 0 = k_1K[\text{parent}]_{\text{eq}}[\text{OH}^-] - k_{-1} \left( \frac{[\text{parent}]_{\text{stoich}} - [\text{parent}]_{\text{eq}}}{\text{constant}} \right) \quad 9.12$$

9.11 - 9.12 gives

$$\frac{d[\text{spiro}]}{dt} = k_1K[\text{OH}^-]([\text{parent}] - [\text{parent}]_{\text{eq}}) + k_{-1} \left( \frac{[\text{parent}] - [\text{parent}]_{\text{eq}}}{\text{constant}} \right)$$

But from equation 9.10  $\frac{d[\text{spiro}]}{dt} = - \frac{d[\text{parent}]}{dt} \times \frac{1}{\text{constant}}$

$$\begin{aligned} \therefore - \frac{d[\text{parent}]}{dt} \times \frac{1}{\text{constant}} &= k_1K[\text{OH}^-]([\text{parent}] - [\text{parent}]_{\text{eq}}) \\ &+ \frac{k_{-1}([\text{parent}] - [\text{parent}]_{\text{eq}})}{\text{constant}} \end{aligned}$$

$$\therefore k_{obs} = k_1K[\text{OH}^-] \times \text{constant} + k_{-1}$$

It seems probable that the value of the constant  $(1 + \frac{1}{K_2} (1 + \frac{1}{K'[\text{OH}^-]}))$  will be close to unity. Measurements of equilibrium optical densities indicate an apparent extinction coefficient of the spiro-complex of  $2.2 \times 10^4 \text{ l.mol}^{-1} \text{ cm}^{-1}$ . By comparison with similar complexes an extinction coefficient in the range  $2-3 \times 10^4 \text{ l.mol}^{-1} \text{ cm}^{-1}$  <sup>6,8</sup> would be expected. It is therefore possible to achieve a minimum conversion of ca. 80% of the total substrate to spiro-complex

in solutions of high pH. This sets a lower limit of 4 for the value of  $K_2$ . The value of  $K'$ , the equilibrium constant which governs proton loss from the thiol group to hydroxide, is likely to be in the range  $10^4$  to  $10^5$ . For comparison the  $pK_a$  value for 2-ethoxyethanethiol is 9.38.<sup>260</sup> With the stated values of  $K_2$  and  $K'$  then the value of the constant will be close to unity so that equation 9.13 will apply.

$$k_{obs} = k_1 K [OH^-] + k_{-1} \quad 9.13$$

A plot of  $k_{obs}$  versus  $[OH^-]$  gives a straight line with intercept ( $k_{-1}$ )  $2.2 \pm 2 \text{ sec}^{-1}$  and slope ( $k_1 K$ )  $(1.4 \pm 0.2) \times 10^4 \text{ l.mol}^{-1} \text{ sec}^{-1}$ . Combination of  $k_1 K$  and  $k_{-1}$  gives a value of  $(6.2 \pm 1) \times 10^3 \text{ l.mol}^{-1}$  for  $K_1 K$ .

#### Second relaxation time

The derivation of the rate equation for the second relaxation time can be treated in two ways:

(i) Assuming  $k_d$  is the rate-determining step

$$\begin{aligned} \frac{d[\text{picrate}]}{dt} &= k_d [S^-] \\ &= \frac{k_d [\text{spiro}]}{K_2} \end{aligned} \quad 9.14$$

$$\frac{d[\text{picrate}]}{dt} = - \frac{d[\text{spiro}]}{dt} - \frac{d[\text{parent}]}{dt} \quad 9.15$$

$$= - \frac{d[\text{spiro}]}{dt} \left( 1 + \frac{1}{K_1 K [OH^-]} \right) \quad 9.16$$

$$k_{obs} = - \frac{d[\text{spiro}]}{dt} \cdot \frac{1}{[\text{spiro}]} \quad 9.17$$

From equations 9.14 and 9.16

$$\frac{k_d [\text{spiro}]}{K_2} = - \frac{d[\text{spiro}]}{dt} \left( 1 + \frac{1}{K_1 K [OH^-]} \right)$$

Using equation 9.17

$$\frac{k_d}{K_2} = k_{\text{obs}} \left( 1 + \frac{1}{K_1 K [\text{OH}^-]} \right)$$

Rearranging gives

$$\frac{1}{k_{\text{obs}}} = \frac{K_2}{k_d} + \frac{K_2}{k_d} \cdot \frac{1}{K_1 K [\text{OH}^-]} \quad 9.18$$

The same equation is obtained by considering the rate of picrate formation.

A plot of  $\frac{1}{k_{\text{obs}}}$  versus  $\frac{1}{[\text{OH}^-]}$  gives a straight line with intercept  $\left(\frac{K_2}{k_d} = 5 \pm 0.5 \text{ sec}\right)$  and slope  $\left(\frac{K_2}{k_d} \cdot \frac{1}{K_1 K} = (6 \pm 0.2) \times 10^{-4} \text{ sec.mol.l}^{-1}\right)$ .  
Combination of slope and intercept gives a value of  $(8 \pm 0.5) \times 10^3 \text{ l.mol}^{-1}$  for  $K_1 K$ , in good agreement with the value obtained from equilibrium measurements.

An estimate of the value of  $K_2$  and hence  $k_d$  can be made as follows.  
If  $K$  for (9.11) is ca.  $10^{-1} \text{ l.mol}^{-1}$  then  $K_1$  for the spiro-complex (9.5) is  $8 \times 10^4$ . Considering complexes (6.3) and (9.3)

$$\frac{K_1 (6.3)}{K_1 (9.3)} = \frac{1.8 \times 10^8}{1 \times 10^5}$$

Assuming that  $K_1$  and  $K_2$  for complex (9.5) are in the same ratio then

$$\frac{1.8 \times 10^8}{1 \times 10^5} = \frac{8 \times 10^4}{K_2}$$

$$\therefore K_2 = 45$$

$$\text{and hence } k_d = 9 \text{ sec}^{-1}.$$

(ii) Assuming  $k_{-2}$  is the rate-determining step

$$\frac{d[\text{picrate}]}{dt} = k_{-2}[\text{spiro}]$$

From equations 9.15 and 9.16

$$k_{-2}[\text{spiro}] = - \frac{d[\text{spiro}]}{dt} \left( 1 + \frac{1}{K_1 K [\text{OH}^-]} \right)$$

$$\therefore k_{-2} = k_{\text{obs}} \left( 1 + \frac{1}{K_1 K [\text{OH}^-]} \right)$$

Rearranging gives 
$$\frac{1}{k_{\text{obs}}} = \frac{1}{k_{-2}} + \frac{1}{k_{-2}K_1K[\text{OH}^-]}$$

In this case the intercept gives a value for  $\frac{1}{k_{-2}}$  and hence  $k_{-2}$  is  $0.2 \text{ sec}^{-1}$ . Again the slope leads to a value of  $8 \times 10^3 \text{ l.mol}^{-1}$  for  $K_1K$ .

1-(2-Hydroxythioethoxy)-2,4-dinitrobenzene

For comparison, rates of 2,4-dinitrophenol (2,4-DNP) formation were measured for the 2,4-dinitro analogue. Data are given in Table 9.11.

TABLE 9.11

Variation of the Rate of Reaction of 1-(2-Hydroxythioethoxy)-2,4-dinitrobenzene ( $4.2 \times 10^{-5} \text{ M}$ ) with Sodium Hydroxide Concentration at  $25^\circ\text{C}$

<u>[Sodium hydroxide]</u> (M)	$10^4 k_{\text{obs}}^a$ ( $\text{sec}^{-1}$ )
0.01	2.06
0.025	4.64
0.05	9.09
0.075	13.7
0.10	16.3

<sup>a</sup> Measurements made at 400 nm

In this case there was no evidence for spiro-complex formation in aqueous media although in DMSO solutions a transient red colour was observed. Therefore the species likely to be present in appreciable concentrations are the parent, the phenol and possibly  $\text{S}^-$ .

As before expressions for the observed first-order rate constant can be derived in two ways.

(i) Assuming  $k_d$  is the rate-determining step

$$k_{\text{obs}} = \frac{d[2,4\text{-DNP}]}{dt ([2,4\text{-DNP}]_{\infty} - [2,4\text{-DNP}])} \quad 9.19$$

$$[2,4\text{-DNP}]_{\infty} - [2,4\text{-DNP}] = [\text{parent}] + [\text{S}^-] \quad 9.20$$

But

$$\frac{[\text{O}^-]}{[\text{parent}][\text{OH}^-]} \cdot \frac{[\text{spiro}]}{[\text{O}^-]} \cdot \frac{[\text{S}^-]}{[\text{spiro}]} = K_1 K_2 \frac{1}{K_2}$$

$$\therefore [\text{S}^-] = [\text{parent}][\text{OH}^-] \frac{K_1 K_2}{K_2}$$

Substituting in equation 9.20 gives

$$[2,4\text{-DNP}]_{\infty} - [2,4\text{-DNP}] = [\text{S}^-] \left(1 + \frac{K_2}{K_1 K [\text{OH}^-]}\right) \quad 9.21$$

$$\frac{d[2,4\text{-DNP}]}{dt} = k_d [\text{S}^-] \quad 9.22$$

Using equations 9.19, 9.21 and 9.22 gives

$$k_{\text{obs}} = \frac{k_d}{1 + \frac{K_2}{K_1 K [\text{OH}^-]}}$$

$$\therefore \frac{1}{k_{\text{obs}}} = \frac{1}{k_d} + \frac{K_2}{K_1 K k_d [\text{OH}^-]}$$

A plot of  $\frac{1}{k_{\text{obs}}}$  versus  $\frac{1}{[\text{OH}^-]}$  is linear, the intercept giving  $k_d$  ca.  $5 \times 10^{-3} \text{ sec}^{-1}$ .

(ii) Assuming  $k_{-2}$  is the rate-determining step

$$\frac{d[2,4\text{-DNP}]}{dt} = k_{-2} [\text{spiro}]$$

Substitution in equation 9.19 gives

$$k_{\text{obs}} = \frac{k_{-2} [\text{spiro}]}{([2,4\text{-DNP}]_{\infty} - [2,4\text{-DNP}])}$$

Since the only species present in appreciable concentration will be the parent and 2,4-DNP

$$[2,4\text{-DNP}]_{\infty} - [2,4\text{-DNP}] = [\text{parent}]$$

$$\therefore k_{\text{obs}} = \frac{k_{-2}[\text{spiro}]}{[\text{parent}]} \quad \text{but} \quad \frac{[\text{spiro}]}{[\text{parent}]} = K_1 K [\text{OH}^-]$$

$$\therefore k_{\text{obs}} = k_{-2} K_1 K [\text{OH}^-]$$

Experimentally  $\frac{k_{\text{obs}}}{[\text{OH}^-]} = 1.8 \times 10^{-2} \text{ M}^{-1} \text{ sec}^{-1} (= k_{-2} K_1 K)$

Assuming that  $K_1 K$  values for complexes (6.5) and (9.8) are in the same ratio as observed for complexes (6.3) and (9.5) then

$$\frac{0.05}{K_1 K (9.8)} = \frac{1.8 \times 10^7}{8 \times 10^3}$$

Thus  $K_1 K (9.8) = 2.2 \times 10^{-5} \text{ M}^{-1}$  and  $k_{-2} = 8 \times 10^2 \text{ sec}^{-1}$ .

Although the results do not prove conclusively that either  $k_d$  or  $k_{-2}$  is the slow step governing the second relaxation time, it seems probable that  $k_d$  is rate-determining. There are a number of points which suggest that this is the case.

(a) If ring-opening of the spiro-complex (9.5) by cleavage of the carbon-sulphur bond is rate-determining, then the value of  $0.2 \text{ sec}^{-1}$  for  $k_{-2}$  is not consistent with a  $k_{-1}$  value of  $2 \text{ sec}^{-1}$  for carbon-oxygen bond-breaking when compared to the rates of ring-opening of complexes (6.3) and (9.3) (Table 9.4) where the rate for the sulphur analogue is some two-three orders of magnitude greater than for the dioxolan complex.

(b) For the 2,4-dinitrophenyl derivative there is no detectable red colouration indicating that there is no build-up of spiro-complex which might be expected if  $k_{-2}$  were rate-determining.

(c) It was shown<sup>194</sup> that decomposition of the 2,4-dinitrophenyl derivative in the presence of 2,4-dinitrochlorobenzene yielded 74% of 1-(2,4-dinitro-phenoxy)-2-(2,4-dinitrophenylthio)ethane. However attack of  $(\text{O}^-)$  on the 2,4-dinitrochlorobenzene results in the same product. Nevertheless present

results suggest that the rate of ring closure to give (9.5) will be several orders of magnitude greater than substitution of chlorine from 2,4-dinitrochlorobenzene. (Compare the rates of reaction of substituted thiophenoxide ions with the same substrate given in Chapter 3 together with the fact that sulphur nucleophiles have greater reactivity than oxygen nucleophiles). Thus production of the substituted ethane in high yield in the presence of 2,4-dinitrochlorobenzene would seem to indicate that  $k_d$  is rate-determining. The magnitude of the  $k_d$  values for the picryl and 2,4-dinitrophenyl compounds would seem to favour  $k_d$  as the slow step in that they reflect well the leaving-group ability of picrate and 2,4-dinitrophenoxide ions as indicated by their  $pK_a$  values.<sup>261</sup> Such correlations have been observed<sup>262</sup> with similar aryloxy leaving groups.

Kinetic and equilibrium data for complex (9.5), collected in Table 9.12

TABLE 9.12

Kinetic and Equilibrium Data for Complexes (6.3), (9.3) and (9.5) in Water at 25°C

<u>Complex</u>	$\frac{K_1 K}{(1.\text{mol}^{-1})}$	$K_1^a$	$\frac{k_1 K}{(1.\text{mol}^{-1}\text{sec}^{-1})}$	$\frac{k_1^a}{(\text{sec}^{-1})}$	$\frac{k_{-1}}{(\text{sec}^{-1})}$
(6.3)	$1.8 \times 10^7$	$1.8 \times 10^8$	$1.6 \times 10^6$	$1.6 \times 10^7$	.05 <sup>b</sup>
(9.3)	$1 \times 10^9$	$1 \times 10^5$	$4 \times 10^{10}$	$4 \times 10^6$	19.5 <sup>b</sup>
(9.5) (C-O	$(8 \pm 1) \times 10^3$	$(8 \pm 1) \times 10^4$	$(1.4 \pm .2) \times 10^4$	$1.4 \times 10^5$	$2.2 \pm .2$
(C-S	$4.5 \times 10^5$	45			>9

<sup>a</sup> Estimated assuming that K for the parent alcohol and thiol are  $10^{-1}$  and  $10^4$  respectively.

can be compared with those given for the dioxolan and dithiolan complexes (6.3) and (9.3). In considering the equilibrium  $K_1$  for complex (9.5) it is interesting to note that the  $K_1 K$  value indicates a somewhat lower stability for this complex than the di-oxygen analogue. The reduced stability, reflected in

a lower  $k_1K$  value and a correspondingly larger value for  $k_{-1}$ , can be accounted for in a number of ways. Replacement of oxygen by sulphur would be expected to introduce steric effects. In addition the polarisation ( $\overset{\delta+}{C}-\overset{\delta-}{O}$ ) of the ether linkage favouring attack by  $O^-$  at the ring carbon atom is considerably reduced in thioethers as a consequence of the smaller electronegativity of sulphur. Related to this is Bernasconi's<sup>40,168</sup> argument that 1,1-dialkoxy-Meisenheimer complexes owe some of their stability to the electronegative alkoxy substituents at the  $sp^3$  hybridised ring carbon atom.

Comparison between the equilibrium  $K_2$  and the dithiolan complex is not as easy since the data for (9.5) are estimated values only. However results seem to indicate that formation of the oxathiolan complex via the thiolate anion is much less preferred when compared to (9.3). One piece of evidence which supports this is the greater rate of irreversible decomposition of (9.5) indicating that the concentration of the thiolate is appreciable. This of course assumes that (9.3) decomposes in an analogous way to give thiopicrate and ethylene sulphide.

REFERENCES

1. P. Hepp, Annalen, 1882, 215, 344.
2. C.L. Jackson and F.H. Gazzolo, Amer.Chem. J., 1900, 23, 376.
3. J. Meisenheimer, Annalen, 1902, 323, 205.
4. R. Foster and C.A. Fyfe, Rev. Pure and Applied Chem., 1966, 16, 61.
5. E. Buncl, A.R. Norris and K.E. Russell, Quart. Rev. (London), 1968, 22, 123.
6. M.R. Crampton, Adv. Phys. Org. Chem., 1969, 7, 211.
7. P. Buck, Angew. Chem. (Int. Ed.), 1969, 8, 120.
8. M.J. Strauss, Chem. Rev., 1970, 70, 667.
9. C.A. Fyfe in 'The Chemistry of the Hydroxyl Group', ed. S. Patai, Wiley, 1971, Part 1, page 51.
10. T.N. Hall and C.F. Poranski in 'The Chemistry of the Nitro and Nitroso Groups', ed. H. Feuer, Wiley, 1970, Part 2, page 329.
11. R.S. Mulliken, J. Amer. Chem. Soc., 1952, 74, 811. For a general survey of charge-transfer complexes see for example R. Foster, 'Organic Charge-Transfer Complexes', Academic Press, 1969.
12. M.R. Crampton and V. Gold, J. Chem. Soc. (B), 1966, 498.
13. V. Gold and C.H. Rochester, ibid., 1964, 1692.
14. J.F. Bunnett and R.E. Zahler, Chem. Rev., 1951, 49, 273.
15. J.F. Bunnett, Quart. Rev. (London), 1958, 12, 1.
16. S.D. Ross, Progr. Phys. Org. Chem., 1963, 1, 31.
17. J. Miller, 'Aromatic Nucleophilic Substitution', Elsevier, 1968.
18. Th. J. de Boer and I.P. Dirkx in 'The Chemistry of the Nitro and Nitroso Groups', ed. H. Feuer, Wiley, 1969, Part 1, page 487.
19. C.F. Bernasconi, in M.T.P. Int. Rev. Sci. : Org. Chem., Ser. One, 1973, 3, 33.
20. G.S. Hammond and L.R. Parks, J. Amer. Chem. Soc., 1955, 77, 340.
21. N.B. Chapman and D.A. Russell-Hill, J. Chem. Soc., 1956, 1563.
22. R.E. Parker and T.O. Read, ibid., 1962, 3149.
23. R. Foster and D. Ll. Hammick, ibid., 1954, 2153.

24. L.K. Dyllal, ibid., 1960, 5160.
25. E.D. Bergmann and S. Pinchas, Rec. Trav. Chim., 1952, 71, 161.
26. R. Foster, Nature, 1955, 176, 746.
27. S.S. Gitis and A.I. Glaz, J. Gen. Chem. USSR, 1957, 27, 1960.
28. R. Foster and R.K. Mackie, J. Chem. Soc., 1963, 3796.
29. R. Destro, C.M. Gramaccioli, A. Mugnoli and M. Simonetta, Tetrahedron Letters, 1965, 2611.
30. R. Destro, C.M. Gramaccioli and M. Simonetta, Nature, 1967, 215, 389.
31. R. Destro, C.M. Gramaccioli and M. Simonetta, Acta Cryst., 1968, B24, 1369.
32. H. Ueda, N. Sakabe, J. Tanaka and A. Furusaki, Nature, 1967, 215, 956.
33. M.R. Crampton and V. Gold, J. Chem. Soc., 1964, 4293.
34. H. Zollinger, P. Caveng, P.B. Fischer, E. Heilbronner and A.L. Miller, Helv. Chim. Acta, 1967, 50, 848.
35. H. Hosoya, S. Hosoya and S. Nagakura, Theor. Chim. Acta, 1968, 12, 117.
36. K.L. Servis, J. Amer. Chem. Soc., 1965, 87, 5495.
37. R. Foster and C.A. Fyfe, Tetrahedron, 1965, 21, 3363.
38. J.B. Ainscough and E.F. Caldin, J. Chem. Soc., 1956, 2528.
39. M.R. Crampton and V. Gold, J. Chem. Soc. (B), 1966, 893.
40. C.F. Bernasconi, J. Amer. Chem. Soc., 1971, 93, 6975.
41. V. Gold and C.H. Rochester, J. Chem. Soc., 1964, 1967.
42. K.L. Servis, J. Amer. Chem. Soc., 1967, 89, 1508.
43. C.H. Rochester, J. Chem. Soc., 1965, 2404.
44. T. Abe, Bull. Chem. Soc. Japan, 1966, 627.
45. J. Murto, Suomen Kemistilehti, 1965, B38, 255.
46. R. Foster, C.A. Fyfe and J.W. Morris, Rec. Trav. Chim., 1965, 84, 516.
47. R.J. Pollitt and B.C. Saunders, J. Chem. Soc., 1964, 1132.
48. M.R. Crampton and V. Gold, Chem. Commun., 1965, 256.
49. R. Foster, C.A. Fyfe, P.H. Emslie and M.I. Foreman, Tetrahedron, 1967, 23, 227.
50. S.S. Gitis and A.Y. Kaminskii, J. Gen. Chem. USSR, 1960, 30, 3771.

51. C.E. Griffin, E.J. Fendler, J.H. Fendler and W.E. Byrne, Tetrahedron Letters, 1967, 45, 4473.
52. E.J. Fendler, J.H. Fendler, W.E. Byrne and C.E. Griffin, J. Org. Chem., 1968, 33, 4141.
53. F. Terrier and F. Millot, Compt. Rend. C, 1969, 268, 808.
54. F. Millot and F. Terrier, Bull. Soc. Chim. France, 1969, 2692.
55. F. Terrier, F. Millot and P. Letellier, ibid., 1970, 1743.
56. C. Dearing, F. Terrier and R. Schaal, Compt. Rend. C, 1970, 271, 349.
57. F. Terrier, J.C. Halle, M.P. Simonnin and M.J. Lecourt, Organic Mag. Resonance, 1971, 3, 361.
58. F. Terrier and M.P. Simonnin, Bull. Soc. Chim. France, 1971, 677.
59. F. Millot, J. Morel and F. Terrier, Compt. Rend. C, 1972, 274, 23.
60. F. Terrier, F. Millot and R. Schaal, J.C.S. Perkin II, 1972, 1192.
61. M.P. Simonnin, M.J. Lecourt, F. Terrier and C.A. Dearing, Can. J. Chem., 1972, 50, 3558.
62. J.E. Dickeson, L.K. Dyall and V.A. Pickles, Aust. J. Chem., 1968, 21, 1267.
63. J.H. Fendler, E.J. Fendler and C.E. Griffin, Tetrahedron Letters, 1968, 5631.
64. J.H. Fendler, E.J. Fendler and C.E. Griffin, J. Org. Chem., 1969, 34, 689.
65. E.J. Fendler, J.H. Fendler, C.E. Griffin and J.W. Larsen, ibid., 1970, 35, 287.
66. E.J. Fendler, J.H. Fendler and W. Ernsberger, ibid., 1971, 36, 2333.
67. R.J. Pollitt and B.C. Saunders, J. Chem. Soc., 1965, 4615.
68. M.I. Foreman and R. Foster, Can. J. Chem., 1969, 47, 729.
69. F. Terrier, F. Millot and M.P. Simonnin, Tetrahedron Letters, 1971, 2933.
70. M.R. Crampton and H.A. Khan, J.C.S. Perkin II, 1972, 733.
71. C.A. Fyfe, M. Cocivera and S.W.H. Damji, Chem. Commun., 1973, 743.
72. M.R. Crampton and H.A. Khan, J.C.S. Perkin II, 1973, 710.
73. A.G. Green and F.M. Rowe, J. Chem. Soc., 1913, 508.

74. M. Busch and W. Kogel, Ber., 1910, 43, 1549.
75. R.C. Farmer, J. Chem. Soc., 1959, 3433.
76. V. Gold and C.H. Rochester, J. Chem. Soc., 1964, 1697, 1727.
77. M.R. Crampton and V. Gold, Proc. Chem. Soc., 1964, 298.
78. E. Bergman, N.R. McFarlane and J.J.K. Boulton, Chem. Commun., 1970, 511.
79. J.J.K. Boulton, P.J. Jewess and N.R. McFarlane, J. Chem. Soc. (B), 1971, 928.
80. S. Sekiguchi and T. Shiojima, Bull. Chem. Soc. Japan, 1973, 46, 693.
81. C.F. Bernasconi and R.H. de Rossi, J. Org. Chem., 1973, 38, 500.
82. C.F. Bernasconi, R.H. de Rossi and C.L. Gehriger, ibid., 1973, 38, 2838.
83. S. Sekiguchi, K. Shinozaki, T. Hirose, K. Matsui and T. Itagaki,  
Tetrahedron Letters, 1974, 1745.
84. S. Sekiguchi, K. Shinozaki, T. Hirose, K. Matsui and K. Sekine, Bull. Chem. Soc. Japan, 1974, 47, 2264.
85. G. Biggi, C.A. Veracini and F. Pietra, Chem. Commun., 1973, 523.
86. T. Abe and T. Asao, Tetrahedron Letters, 1973, 1327.
87. F. Pietra, Chem. Commun., 1974, 544.
88. C.L. Lok, M.E. DenBoer and J. Cornelisse, Rec. Trav. Chim., 1973, 92, 340
89. G. Illuminati, Adv. in Heterocyclic Chem., 1964, 3, 285.
90. R.P. Mariella, J.J. Callahan and A.O. Jibril, J. Org. Chem., 1955, 20, 1721.
91. C.A. Fyfe, Tetrahedron Letters, 1968, 659.
92. M.E.C. Biffin, J. Miller, A.G. Moritz and D.B. Paul, Aust. J. Chem., 1970,  
23, 963.
93. P. Bemporad, G. Illuminati and F. Stegel, J. Amer. Chem. Soc., 1969, 91,  
6742.
94. M.E.C. Biffin, J. Miller, A.G. Moritz and D.B. Paul, Aust. J. Chem., 1970,  
23, 957.
95. F. Terrier, A.P. Chatrousse and R. Schaal, J. Org. Chem., 1972, 37, 3010.
96. C. Abbolito, C. Iavarone, G. Illuminati, F. Stegel and A. Vazzoler,  
J. Amer. Chem. Soc., 1969, 91, 6746.

97. M.E.C. Biffin, J. Miller, A.G. Moritz and D.B. Paul, Aust. J. Chem., 1969, 22, 2561.
98. G. Doddi, G. Illuminati and F. Stegel, Chem. Commun., 1969, 953; J. Org. Chem., 1971, 36, 1918.
99. G. Doddi, G. Illuminati and F. Stegel, Chem. Commun., 1972, 1143.
100. M.P. Simonnin, F. Terrier and C. Paulmier, Tetrahedron Letters, 1973, 2803.
101. C. Paulmier, M.P. Simonnin, A.P. Chatrousse and F. Terrier, ibid., 1973, 1123.
102. G. Doddi, G. Illuminati and F. Stegel, ibid., 1973, 3221.
103. C. Dell'Erba, M. Novi, G. Guanti and D. Spinelli, J. Heterocyclic Chem., 1975, 12, 327,
104. V. Gold and C.H. Rochester, J. Chem. Soc., 1964, 1710.
105. R. Gaboriand, R. Schaal and P. Letellier, Bull. Soc. Chim. France, 1969, 8, 2683.
106. K. Bowden and R.S. Cook, J. Chem. Soc. (B), 1971, 1771.
107. M.R. Crampton, M.A. El Ghariani and H.A. Khan, Tetrahedron, 1972, 28, 3299.
108. M.R. Crampton and M.A. El Ghariani, J. Chem. Soc. (B), 1970, 391.
109. (a) T. Abe and Y. Hasegawa, Chem. Letters (Tokyo), 1972, 985;  
(b) T. Abe and Y. Hasegawa, Bull. Chem. Soc. Japan, 1973, 46, 2756.
110. Y. Hasegawa, ibid., 1974, 47, 2186.
111. J.V. Janovsky and L. Erb, Ber., 1836, 19, 2155.
112. R. Canback, Svensk. Farm. Tidskr., 1949, 53, 151.
113. W. Zimmerman, Z. Physiol. Chem., 1935, 233, 257; 1937, 245, 47.
114. T.J. King and C.E. Newall, J. Chem. Soc., 1962, 367.
115. R. Foster and C.A. Fyfe, ibid., 1966, 53.
116. C.A. Fyfe, Can. J. Chem., 1968, 46, 3047.
117. S.S. Gitis, Y.D. Grudtsyn, E.A. Bronshtein, E.E. Gol'teuzen and A.Y. Kaminskii, Dokl. Akad. Nauk. USSR, 1972, 203, 1063.

118. J. Kavalek, V. Machacek, V. Sterba and J. Subert, Collect. Czech. Chem. Commun., 1974, 39, 2063.
119. R. Foster and C.A. Fyfe, Tetrahedron, 1966, 22, 1831.
120. J. Osugi and S. Muneo, Rev. Phys. Chem. Japan, 1967, 37, 43.
121. T. Abe, Bull. Chem. Soc. Japan, 1959, 32, 778.
122. M.J. Strauss and H. Schran, J. Amer. Chem. Soc., 1969, 91, 3974.
123. R. Foster, M.I. Foreman and M.J. Strauss, Tetrahedron Letters, 1968, 4949.
124. M.J. Strauss, T.C. Jensen, H. Schran and K. O'Conner, J. Org. Chem., 1970, 35, 383.
125. M.I. Foreman, R. Foster and M.J. Strauss, J. Chem. Soc. (C), 1969, 2112.
126. M.J. Strauss, Accounts Chem. Res., 1974, 7, 181.
127. C.F. Bernasconi, J. Org. Chem., 1971, 36, 1671.
128. E. Buncl and J.G.K. Webb, J. Amer. Chem. Soc., 1973, 95, 8470.
129. R. Wahren and O. Wennerstrom, Acta Chem. Scand., 1970, 24, 3064.
130. M. Nilsson, C. Ullenius and O. Wennerstrom, Tetrahedron Letters, 1971, 2713.
131. O. Wennerstrom, Acta Chem. Scand., 1971, 25, 789.
132. O. Wennerstrom. ibid., 2341.
133. I.P. Beletskaya, G.A. Artamkina and O.A. Reutov, Bull. Acad. Sci. USSR, 1973, 22, 1876.
134. F. Cuta and E. Beranek, Collect. Czech. Chem. Commun., 1958, 23, 1501.
135. F. Cuta and M. Sevela, Chem. Listy., 1943, 37, 1.
136. A.R. Norris, Can. J. Chem., 1967, 45, 2703.
137. B. Vickery, Chem. Ind. (London), 1967, 1523.
138. E. Buncl, A.R. Norris and W. Proudlock, Can. J. Chem., 1968, 46, 2759.
139. A.R. Norris, J. Org. Chem., 1969, 34, 1486.
140. A.R. Norris, Can. J. Chem., 1969, 47, 2895.
141. A.R. Norris and H.F. Schurvell, Can. J. Chem., 1969, 47, 4267.
142. G.N. Lewis and G.T. Seaborg, J. Amer. Chem. Soc., 1940, 62, 2122.
143. R. Foster, J. Chem. Soc., 1959, 3508.

144. R. Foster and R.K. Mackie, Tetrahedron, 1962, 16, 119.
145. G. Briegleb, W. Liptay and M. Cantner, Z. Phys. Chem. (Frankfurt), 1960, 26, 55.
146. M.R. Crampton and V. Gold, J. Chem. Soc. (B), 1967, 23.
147. M.J. Strauss and R.G. Johanson, Chem. Ind. (London), 1969, 242.
148. M.J. Strauss, Chem. Commun., 1970, 76.
149. L.B. Clapp, H. Lacey, C.G. Beckwith, R.M. Srivastava and N. Muhammad, J. Org. Chem., 1968, 33, 4262.
150. R.E. Miller and W.F.K. Wynne-Jones, J. Chem. Soc., 1959, 2375.
151. R. Foster and J.W. Morris, J. Chem. Soc. (B), 1970, 703.
152. E. Buncl and J.G.K. Webb, Can. J. Chem., 1972, 50, 129.
153. E. Buncl, H. Jarrell, H.W. Leung and J.G.K. Webb, J. Org. Chem., 1974, 39, 272.
154. E. Buncl and J.G.K. Webb, Can. J. Chem., 1974, 52, 630.
155. E. Buncl and H.W. Leung, Chem. Commun., 1975, 19.
156. H. Muraour, Bull. Soc. Chim. France, 1924, 35, 367.
157. R.A. Henry, J. Org. Chem., 1962, 27, 2637.
158. A.R. Norris, Can. J. Chem., 1967, 45, 175.
159. M.R. Crampton, J. Chem. Soc. (B), 1967, 1341.
160. M.R. Crampton, ibid., 1968, 1208.
161. F. Pietra and G. Biggi, J.C.S. Perkin I, 1973, 1980.
162. F. Pietra and C.A. Veracini, Chem. Commun., 1974, 623.
163. H.A. Benesi and J.H. Hildebrand, J. Amer. Chem. Soc., 1949, 71, 2703.
164. For reviews see for example (a) M.A. Paul and F.A. Long, Chem. Rev., 1957, 57, 1 and (b) C.H. Rochester, 'Acidity Functions', Academic Press, 1970.
165. L.P. Hammett and A.J. Deyrup, J. Amer. Chem. Soc., 1932, 54, 2721.
166. M.R. Crampton and H.A. Khan, J.C.S. Perkin II, 1972, 1178.
167. C.F. Bernasconi, J. Amer. Chem. Soc., 1968, 90, 4982.
168. C.F. Bernasconi, ibid., 1970, 92, 4682.

169. J. Hine, ibid., 1963, 85, 3239.
170. J. Hine, L.G. Mahone and C.L. Liotta, ibid., 1967, 89, 5911.
171. J. Miller, ibid., 1963, 85, 1628.
172. E. Buncl, A.R. Norris, W. Proudlock and K.E. Russell, Can. J. Chem., 1969, 47, 4129.
173. (a) A.J. Parker, Proc. Chem. Soc., 1961, 371;  
(b) J.F. Bunnett, Ann. Rev. Phys. Chem., 1963, 14, 271.
174. A.J. Parker, Quart. Rev. (London), 1962, 163; Adv. Phys. Org. Chem., 1967, 5, 173.
175. M.E.C. Biffin and D.B. Paul, Aust. J. Chem., 1974, 27, 777.
176. J.W. Larsen, K. Amin and J.H. Fendler, J. Amer. Chem. Soc., 1971, 93, 2910.
177. J.W. Larsen, K. Amin, S. Ewing and L.L. Magid, J. Org. Chem., 1972, 37, 3857.
178. E.J. Fendler and J.H. Fendler, Adv. Phys. Org. Chem., 1970, 8, 271.
179. L.M. Casilio, E.J. Fendler and J.H. Fendler, J. Chem. Soc. (B), 1971, 1377.
180. J.H. Fendler, E.J. Fendler and M.V. Merritt, J. Org. Chem., 1971, 36, 2172.
181. M.R. Crampton and H.A. Khan, J.C.S. Perkin II, 1972, 1173.
182. M.R. Crampton and H.A. Khan, ibid., 2286.
183. M.R. Crampton and H.A. Khan, ibid., 1873, 1103.
184. M.R. Crampton, ibid., 1973, 2157.
185. M.R. Crampton, ibid., 1975, 825.
186. H.K. Frensdorff, J. Amer. Chem. Soc., 1971, 93, 600.
187. R.A. Robinson and R.H. Stokes, 'Electrolyte Solutions' Butterworths, Second edition, 1970, page 547.
188. (a) R. Leukart, J. Prakt. Chem., 1890 [2], 41, 179;  
(b) J.R. Cox, C.L. Gladys, L. Field and D.E. Pearson, J. Org. Chem., 1960, 25, 1083.
189. M.R. Crampton, J. Chem. Soc. (B), 1971, 2112.

190. 'Dictionary of Organic Compounds', Fourth Edition, Eyre and Spottiswoode, 1964.
191. J. Glazer, E.D. Hughes, C.K. Ingold, A.T. James, G.T. Jones and E. Roberts, J. Chem. Soc., 1950, 2674.
192. H.H. Hodgson and E.W. Smith, J. Soc. Chem. Ind., 1930, 49, 408T.
193. J.J. Blanksma and P.G. Fohr, Rec. Trav. Chim., 1946, 65, 711.
194. C.C. Culvenor, W. Davies and W.E. Savige, J. Chem. Soc., 1952, 4480.
195. E. Farina, F. Pietra and C.A. Veracini, Chem. Commun., 1974, 672.
196. E.F. Caldin, J.E. Crooks and A. Queen, J. Phys. E. (Sci. Instr.), 1973, 6, 930.
197. E.A. Guggenheim, Phil. Mag., 1926, 2, 538.
198. G.F. Smith, J. Chem. Soc., 1943, 521.
199. J. Hine 'Physical Organic Chemistry', Second Edition, McGraw-Hill, 1962, page 160.
200. C.G. Swain and C.B. Scott, J. Amer. Chem. Soc., 1933, 75, 141.
201. R.G. Pearson, ibid., 1963, 85, 3533.
202. G. Capozzi and G. Modena in 'The Chemistry of the Thiol Group', ed. S. Patai, Wiley, 1974, Part 2, page 785.
203. G. Leandri and A. Tundo, Ann. Chim. (Rome), 1955, 45, 832.
204. J.F. Bunnett and W.D. Merritt, J. Amer. Chem. Soc., 1957, 79, 5967.
205. J.F. Bunnett and N.S. Nudelman, J. Org. Chem., 1969, 34, 2038.
206. D. Semenov-Garwood, ibid., 1972, 37, 3797.
207. G. Bartoli, L. di Nunno, L. Forlani and P.E. Todesco, Internat. J. Sulphur Chem. C, 1971, 77.
208. G. Guanti, C. Dell'Erba, F. Pero and G. Leandri, J.C.S. Perkin II, 1975, 212.
209. P. De Maria, A. Fini and F.M. Hall, Chim. Ind. (Milan), 1973, 55, 808.
210. G. Guanti, C. Dell'Erba and P. Macera, J. Heterocyclic Chem., 1973, 10, 1007.

211. R.F. Hudson and G. Klopman, J. Chem. Soc., 1962, 1062.
212. G.S. Krishnamurthy and S.I. Miller, J. Amer. Chem. Soc., 1961; 83, 3961.
213. (a) F.G. Bordwell and W.J. Boyle, ibid., 1972, 94, 3907;  
(b) C.D. Johnson and K. Schofield, ibid., 1973, 95, 270.
214. H. van Bekkum, P.E. Verkade and B.M. Wepster, Rec. Trav. Chim., 1959, 78, 815.
215. Y. Ogata and A. Kawasaki in 'The Chemistry of the Carbonyl Group', ed. S. Patai, Wiley, 1970, Part 2, page 1.
216. R.P. Bell, Adv. Phys. Org. Chem., 1966, 4, 1.
217. (a) J.F. Bunnett, J.H. Miles and K.V. Nahabedian, J. Amer. Chem. Soc., 1961, 83, 2512;  
(b) E.J. Forbes and M.J. Gregory, J. Chem. Soc. (B), 1968, 205.
218. (a) W.J. Bover and P. Zuman, J.C.S. Perkin II, 1973, 786;  
(b) P. Greenzaid, J. Org. Chem., 1973, 38, 3164.
219. (a) J. Miller, J. Amer. Chem. Soc., 1954, 76, 448;  
(b) R.L. Heppolette, J. Miller and V.A. Williams, ibid., 1956, 78, 1975;  
(c) N.S. Bayliss, R.L. Heppolette, L.H. Little and J. Miller, ibid., 1978.
220. M.R. Crampton, J.C.S. Perkin II, 1975, 185.
221. N. Marendic and A.R. Norris, Can. J. Chem., 1973, 51, 3927.
222. C.F. Bernasconi and R.G. Bergstrom, J. Amer. Chem. Soc., 1973, 95, 3603.
223. M.J. Strauss and S.P.B. Taylor, ibid., 3813.
224. E. Buncel, A.R. Norris, K.E. Russell and P.J. Sheridan, Can. J. Chem., 1974, 52, 25.
225. M. Eigen and L. De Maeyer in 'Technique of Organic Chemistry', ed. A. Weissberger, Interscience, 1963, Vol. VIII, Part 2, page 895.
226. Reference 187, page 230.
227. S. Glasstone, K.J. Laidler and H. Eyring, 'The Theory of Rate Processes' McGraw-Hill, First edition, 1941, page 404.
228. C.F. Bernasconi and R.G. Bergstrom, J. Amer. Chem. Soc., 1974, 96, 2397.

229. C.F. Bernasconi and C.L. Gehriger, J. Amer. Chem. Soc., 1974, 96, 1092.
230. C.F. Bernasconi and H.S. Cross, J. Org. Chem., 1974, 39, 1054.
231. P. Ballinger and F.A. Long, J. Amer. Chem. Soc., 1960, 82, 795.
232. J. Murto and J. Vainionpaa, Suomen Kemistilehti, 1966, B39, 133.
233. S.S. Gitis, A.J. Kaminskii, A.J. Glaz and Z.A. Kosina, Reakts. spos org. Soedinenii, 1967, 4, 625.
234. J.H. Fendler, E.J. Fendler, W.E. Byrne and C.E. Griffin, J. Org. Chem., 1968, 33, 977.
235. J. Murto in 'The Chemistry of the Hydroxyl Group', ed. S. Patai, Wiley, 1971, part 2, page 1087.
236. M.R. Crampton and M.A. El Ghariani, J. Chem. Soc. (B), 1969, 330.
237. M.R. Crampton and M.A. El Ghariani, ibid., 1971, 1043.
238. P.K. Glasoe and F.A. Long, J. Phys. Chem., 1960, 64, 188.
239. J.N. Brønsted and K.J. Pedersen, Z. Phys. Chem., 1924, 108, 185.
240. (a) E.H. Cordes, Progr. Phys. Org. Chem., 1967, 4, 1;  
(b) E.H. Cordes and H.G. Bull, Chem. Rev., 1974, 74, 581.
241. (a) T.H. Fife, Accounts Chem. Res., 1972, 5, 264;  
(b) E. Anderson and B. Capon, J. Chem. Soc. (B), 1969, 1033;  
(c) R.F. Atkinson and T.C. Bruice, J. Amer. Chem. Soc., 1974, 96, 819.
242. E.M. Arnett, Progr. Phys. Org. Chem., 1963, 1, 223.
243. J.E. Leffler and E. Grunwald, 'Rates and Equilibria of Organic Reactions', Wiley, 1963, page 73.
244. B. Capon in 'Organic Reaction Mechanisms', eds. B. Capon and C.W. Rees, Interscience, 1972, page 389.
245. J. Murto and A. Viitala, Suomen Kemistilehti, 1966, B39, 138.
246. J.F. Bunnett, quoted in reference 230.
247. J.H. Fendler and E.J. Fendler, J. Org. Chem., 1970, 35, 3378.
248. J.B. Ainscough and E.F. Caldin, J. Chem. Soc., 1956, 2540.

249. (a) J.H. Fendler, E.J. Fendler and L.M. Casilio, J. Org. Chem., 1971, 36, 1749;  
(b) J.W. Bunting and W.G. Meathrel, Can. J. Chem., 1973, 51, 1965.
250. A.A. Bothner-By, Adv. Magn. Res., 1965, 1, 195.
251. M. Karplus, J. Amer. Chem. Soc., 1963, 85, 2870.
252. C.F. Bernasconi and R.G. Bergstrom, J. Org. Chem., 1971, 36, 1325.
253. B. Capon, Quart. Rev. (London), 1964, 18, 45 and references therein.
254. A. Ya. Kaminskii, S.S. Gitis, Yu. D. Grudtsyn, L.I. Khabarova, E.G. Kaminskaya and V. Sh. Golubchik, Zh. Org. Khim., 1974, 10, 1736  
CA 81, 151685.
255. R.P. Bell, 'The Proton in Chemistry', second edition, Chapman and Hall, 1973, page 111.
256. M.R. Crampton in 'The Chemistry of the Thiol Group', ed. S. Patai, Wiley, part 1, page 379.
257. E. Campaigne in 'Organic Sulphur Compounds', ed N. Kharasch, vol. 1, Pergammon Press, 1961, page 134.
258. (a) N.C. De and L.R. Fedor, J. Amer. Chem. Soc., 1968, 90, 7266, ref. 29;  
(b) K. Pihlaja, ibid., 1972, 94, 3330.
259. D. Seebach, Synthesis, 1969, 17 and references therein.
260. M.M. Kreevoy, E.T. Harper, R.E. Duvall, H.S. Wilgus and L.T. Ditsch, J. Amer. Chem. Soc., 1960, 82, 4899.
261. Reference 235, page 1106, Table 3.
262. Reference 14, page 333, Table 24.